Development of a Rapid Point of Care Diagnostic Immunoassay for the Detection of *P. aeruginosa* Infections in Cystic Fibrosis Patients

2019

Andrew Martin

A thesis submitted to the University of Kent for the degree of Doctor of Philosophy in Biochemistry

University of Kent

School of Biosciences

Declaration

No part of this thesis has been submitted in support of an application for any degree or other qualification of the University of Kent, or any other University or institution of learning.

Andrew Martin **Date: 10/07/19**

Abstract

Pseudomonas aeruginosa infections are the leading cause of morbidity and mortality in cystic fibrosis (CF) patients and it is the predominant pathogen found in patients by adulthood. During the initial stages of infection, isolates are mostly planktonic, express high levels of virulence factors, and can often be eradicated via aggressive antibiotic treatment. However, once chronic infection is established, *P. aeruginosa* may develop a mucoid phenotype, leading to development of a bacterial biofilm, the emergence of antibiotic resistance, a worsening of symptoms and an increased frequency of pulmonary exacerbations. There is therefore an urgent need for a reliable biomarker of initial *P. aeruginosa* infection that will allow early intervention/application of antibiotics in CF patients and monitoring of treatment. In the work described here, a potential biomarker of early infection has been identified as elastase, a secreted protease encoded by the *lasB* structural gene under regulation of the las quorum sensing pathway, which plays a key role in virulence and infection via digestion of a wide range of substrates including collagen and elastin. Development of a rapid point of care diagnostic assay targeting elastase in CF patient samples, such as sputum, may allow for early identification of acute *P. aeruginosa* infection and thus earlier treatment. A recombinant form of elastase was produced in the *E. coli* strain BL21*(DE3)pLysS and subsequently purified and characterised to assess its conformational stability and specific activity. This recombinant material was used to immunise rabbits and sheep, and elastase-specific polyclonal antibodies were purified from the resulting antisera. Attempts were made to generate high affinity monoclonal antibody fragments from peripheral blood lymphocytes of the immunised animals via antibody phage display, but were unsuccessful. Prototype sandwich ELISA and lateral flow format immunoassays (LFIAs) were developed incorporating purified polyclonal antibodies, with lower limits of detection of 27 pg/mL (rabbit polyclonal ELISA) and 1 ng/mL (rabbit polyclonal LFIA). Specificity of the assay was assessed via application of culture supernatants from clinical isolates of *P. aeruginosa* and other bacterial strains commonly associated with CF. When the assay was used to analyse CF patient isolates, 29/31 first isolates and 12/17 chronic isolates returned a positive test, whereas 0/20 non-*Pseudomonas* strains returned a positive test, demonstrating the highly specific nature of the assay and its utility as an indicator of early infection. In conclusion, the work presented here demonstrates the proof of concept development of a highly specific and sensitive point of care diagnostic assay for the detection of acute *P. aeruginosa* infection in CF patients, with scope for further development via generation of monoclonal antibodies and signal enhancement techniques.

Acknowledgements

I would first like to express my utmost gratitude to Professor Mark Smales for the opportunity to work within the Smales Lab, and for his constant guidance, encouragement and supervision on a research project from which I have gained valuable experience and have greatly enjoyed. I would also like to thank Dr Paul Davis for his assistance and support, as well as for providing the opportunity to work with the team at Mologic Ltd when necessary. Specifically, I would like to extend thanks to Steve Eida, Matthew Tyreman and Michael Johnson for providing their technical expertise and for training me in a number of techniques. I would also like to express thanks to Professor Jane Davies of the National Heart and Lung Institute at Imperial College for providing valuable clinical isolates. To all members of the Smales Lab, old and new, I am incredibly thankful for the past four years of exceptional company. It has been an absolute joy to work in an environment full of such wonderful and talented people, and I am infinitely grateful for every one of the relationships I have made. I would especially like to thank Dr James Budge and Dr Tanya Knight for acting as mentors to me throughout the project and for inspiring me from the very beginning, both in and outside of work. I would also like to express my sincerest appreciation for my fellow PhD students Joanna Bird and Natalie Talbot for their continued support throughout the past four years, without which I would never have made it this far. I would also like to thank the BBSRC for providing the funding to make this project possible. Finally, I would like to thank my parents and my two brothers, who have continued to support me unconditionally throughout the most stressful times; I am eternally grateful for all that you do for me.

Table of Contents

List of Abbreviations

AI	autoinducer
AP	alkaline phosphatase
AuNP	gold nanoparticle
bp	base pairs
BSA	bovine serum albumin
cDNA	complementary DNA
CF	cystic fibrosis
CFU	colony forming units
CHO	Chinese Hamster Ovary
COPD	chronic obstructive pulmonary disorder
DMSO	dimethyl sulfoxide
DNA	deoxyribonucleic acid
DTT	dithiothreitol
E. coli	*Escherichia coli*
EDTA	ethylenediaminetetraacetic acid
ELISA	enzyme linked immunosorbent assay
Fab	fragment antigen binding
GuHCl	guanidine hydrochloride
HRP	horseradish peroxidase
IEC	ion exchange chromatography
IPTG	isopropyl β-D-1-thiogalactopyranoside
IgG	immunoglobulin G
IMAC	immobilised metal affinity chromatography
kDa	kilodaltons

LB	lysogeny broth
LFIA	lateral flow immunoassay
mAb	monoclonal antibody
MALDI-TOF	matrix assisted laser desorption ionisation time of flight
MBP	eosinophilic major basic protein
MMP9	matrix metalloproteinase 9
mRNA	messenger RNA
MS	mass spectrometry
P. aeruginosa	*Pseudomonas aeruginosa*
pAb	polyclonal antibody
PAGE	polyacrylamide gel electrophoresis
PBL	peripheral blood lymphocyte
PBS	phosphate buffered saline
PCR	polymerase chain reaction
PEG	poly(ethylene glycol)
pNPP	para-nitrophenylphosphate
POC	point of care
QS	quorum sensing
RAGE	receptor for advanced glycation end-products
RNA	ribonucleic acid
rcf	relative centrifugal force
rpm	revolutions per minute
scFv	single chain variable fragment
SDS	sodium dodecyl sulfate
SEC	size exclusion chromatography

SOB	super optimal broth
SOC	super optimal broth with catabolite repression
TB	terrific broth
TEM	transmission electron microscopy
TMB	tetramethylbenzidine
TSAP	thermosensitive alkaline phosphatase

List of Figures

List of Tables

Chapter 1

Introduction

1.1 General Introduction

The body of work in this thesis describes the development and validation of a rapid point of care diagnostic test to detect the opportunistic bacterial pathogen *Pseudomonas aeruginosa* in the lungs and airways of cystic fibrosis (CF) patients. This was achieved through the generation of polyclonal antibodies to a recombinant form of the *P. aeruginosa* major virulence factor elastase, encoded by the *lasB* structural gene (the recombinant form generated as part of the work in this study). This chapter reviews the mechanisms of *Pseudomonas* pathogenicity, available diagnostic assays and treatments in the context of cystic fibrosis, and current challenges to the development of new diagnostic assays, whilst outlining the overall aims of the study.

1.2 Biology of *Pseudomonas aeruginosa*

1.2.1 *Pseudomonas aeruginosa* and its Virulence Factors

Pseudomonas aeruginosa is a Gram negative, opportunistic bacterial pathogen commonly associated with nosocomial infections, most often in immunocompromised individuals, and particularly in the case of chronic wounds, neutropenia and cystic fibrosis (Lyczak, Cannon, & Pier, 2000). The bacterium is able to adapt to a wide range of environments and displays a high level of intrinsic antibiotic resistance, making it particularly challenging to treat. *P. aeruginosa* cells possess a single polar flagellum surrounded by a number of type 4 pili, important for cell motility as well as initiation of infection (Gellatly & Hancock, 2013). *P. aeruginosa* is able to adhere to the host epithelium via binding of its flagellum to asialoGM1, an asialyated glycolipid, initiating inflammatory responses mediated both by nuclear factor kappa B and caspase 1 (Miao, Andersen-Nissen, Warren, & Aderem, 2007). In mutant strains lacking flagella, a deficiency in acute infection can be observed (Feldman et al., 1998). The type 4 pili act as adhesins, contributing to formation of the bacterial biofilm via aggregation and formation of microcolonies, and thus are commonly investigated as targets for anti-pseudomonal therapies such as vaccine development, although variation in surface antigens can pose an issue if looking to develop vaccines and therapies directly to these (Kipnis, Sawa, & Wiener-Kronish, 2006).

There are several proteases secreted by *P. aeruginosa* that contribute to destruction of tissue and immune system components. The structural genes *lasA* and *lasB* encode for staphylolysin

and elastase respectively, two proteases that work in concert to digest a wide range of substrates. Staphylolysin is a serine protease which enhances the elastolytic activity of elastase, as well as hydrolysing pentaglcyine bridges in Staphylococcal peptidoglycans, causing cell lysis and contributing to *P. aeruginosa*'s opportunistic ability (Matsumoto, 2004). Staphylolysin is believed to enhance elastolytic activity via modifying elastin to expose alanine-rich segments for which elastase has a strong preference (Peters & Galloway, 1990). Elastase, meanwhile, is an autocatalytic, elastolytic zinc metalloprotease with a broad substrate specificity described in further detail in **Section 1.4**. Alkaline protease, encoded by the structural gene *AprA* is a zinc metalloprotease which digests host complement components and fibronectin (Laarman et al., 2012). Protease IV is a serine protease known to digest complement components, fibrinogen and immunoglobulins, as well as surfactant proteins A and D, which can assist *P. aeruginosa* with survival via avoidance of macrophages (Malloy et al., 2005). These proteases are important virulence factors of *P. aeruginosa*, and as such have become targets of great interest for the development of diagnostic assays, specifically for early detection of this bacterium. The *P. aeruginosa* quorum sensing pathways described in **Section 1.2.2** regulate expression of these genes in a hierarchical manner, based on population density.

1.2.2 Quorum Sensing in *P. aeruginosa*; The las, rhl and pqs Systems

As *P. aeruginosa* colonises an area, cell-population density fluctuates. In order to regulate this, the bacteria make use of quorum sensing (**Figure 1.1**), a cell signalling mechanism that regulates gene expression in response to fluctuations in cell population density. Quorum sensing is driven by autoinducers; small, membrane diffusible signalling molecules, which can control adaptation of *P. aeruginosa*, among other bacteria, to changes in the environment such as the pro-inflammatory microenvironment of the cystic fibrosis lung. Once a threshold concentration of autoinducers is reached, brought about by a sufficiently high population of bacteria, these molecules bind to a transcriptional activator protein, acting as cofactors of transcriptional regulators that coordinate traits such as virulence or the shift to a mucoid phenotype through expression of a target gene(s) (Gellatly & Hancock, 2013).

In *P. aeruginosa*, there are 3 quorum sensing systems that work hierarchically to coordinate transcription of many genes **(Figure 1.1)**, including those involved in virulence, and it has been widely reported that deficiency in any one of these three quorum sensing systems leads to impaired pathogenicity and an inability to form bacterial biofilms (Kipnis et al., 2000). The *las* system positively regulates the two other systems, *rhl* and *pqs* (Wilder, Diggle, & Schuster, 2011), and controls expression of virulence factors involved in infection and colonisation. This system

is coordinated by the autoinducer 3-oxo-dodecanoyl homoserine lactone (3-oxo-C12-HSL) produced by the *lasI* acyl homoserine lactone synthase. This acts on the transcriptional activator LasR (Deep, Chaudhary, & Gupta, 2011) to induce *lasB*, the structural gene encoding the major extracellular virulence factor elastase, as well as a number of other virulence factor genes including *lasA, aprA* and *toxA* (Kiratisin, Tucker, & Passador, 2002). 3-oxo-C12-HSL-LasR complexes may also bind to the promoter region of *rhlR,* encoding the transcriptional regulator for the rhl pathway, which binds the autoinducer molecule N-butanoyl-L-homoserine lactone synthase (C4-HSL) to induce another set of virulence factors also including the *lasB* structural gene.

The third quorum sensing pathway, the *pqs* system, is modulated by the signal molecule 2-heptyl-3-hydroxy-4-quinolone and acts not only to control the expression of multiple virulence factors including *lasB*, but additionally as a regulator of both the *las* and *rhl* quorum sensing systems (Pesci et al., 1999). Synthesis of the *Pseudomonas* Quinolone Signal (PQS) is under the control of three operons: *pqsABCDE*, *phnAB*, and *pqsH,* and srequires the PqsR transcriptional regulator for synthesis (Gallagher et al., 2002). Transcription of the *pqsABCDE* promoter is regulated positively by the *las* system regulator LasR-3-oxo-C12-HSL and regulated negatively by the *rhl* system autoinducer RhlR-C4-HSL, both via the *pqs* regulator PqsR (Pesci et al., 1999).

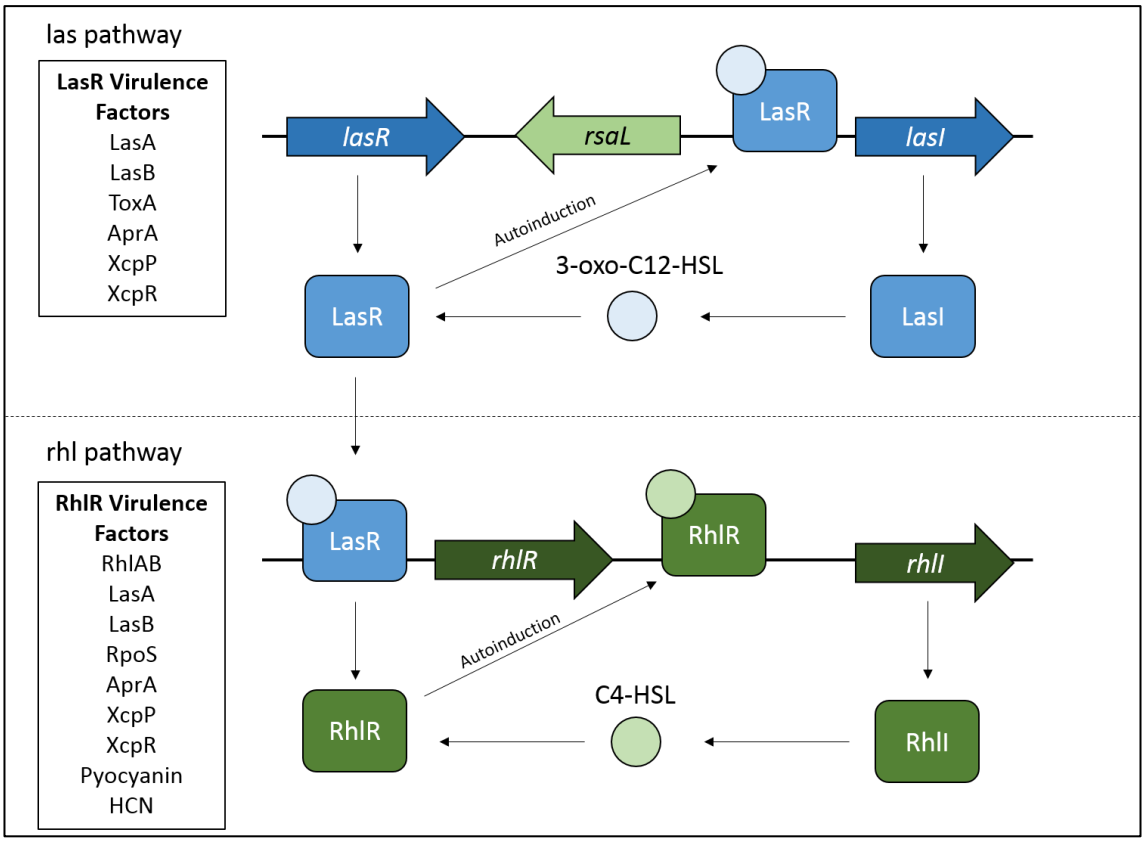

Figure 1.1 | The las and rhl quorum sensing pathways in *P. aeruginosa*. Upregulation of *lasI* promotes production of the autoinducer 3-oxo-C12-HSL which binds the las response regulator LasR. 3-oxo-C12-HSL-LasR complexes bind to the promoter region of many virulence factor structural genes, as well as *rhlR*, activating its transcription and leading to production of the autoinducer C4-HSL. In this way, the systems are arranged in a hierarchical manner. Adapted from Nadal Jimenez *et al.* (Nadal Jimenez et al., 2012).

1.2.3 The Mucoid Phenotype of *P. aeruginosa*

As *P. aeruginosa* colonises an area such as the lung (as in cystic fibrosis patients) or a chronic wound, the inflammatory response recruits polymorphonuclear leukocytes for phagocytosis. Once activated, these polymorphonuclear leukocytes are able to induce a mutation in the *mucA* gene, leading to the generation of a mucoid phenotype (Mathee et al., 1999). This phenotype is characterised by the formation of a bacterial biofilm via alginate synthesis, enhanced antibiotic resistance, and resistance to immune responses such as opsonisation and phagocytosis (Pritt, O'Brien, & Winn, 2007). The alginate produced enables *P. aeruginosa* to withstand the inflammatory response via scavenging of oxygen radicals (Høiby, Ciofu, & Bjarnsholt, 2010), protecting bacterial microcolonies in a contained matrix known as a biofilm.

1.2.3.1 *P. aeruginosa* Biofilms

P. aeruginosa biofilms are commonly found in sputum from the conductive zone of the cystic fibrosis lung and pose a significant challenge to eradication of infection. Biofilms are highly

organised communities of bacteria encased in a matrix of extracellular polysaccharides, lipids and proteins, which comprise up to 90% of the biofilm volume and provide structural integrity and resistance to antimicrobials and components of the host immune response (Hall-Stoodley & Stoodley, 2009).

Worlitzsch *et al.* elucidated that biofilm growth frequently occurs at the intraluminal airway where it binds to mucus, rather than the epithelial surface compartment, through the morphometric analysis of freshly excised lung tissue from CF patients (Worlitzsch et al., 2002). It has been suggested that the resulting extreme hypoxic conditions allow mucoid *P. aeruginosa* to thrive, likely through the upregulation of alginate production, as well as availability of nitrate in the airway surface liquid, which is able to act as a terminal electron acceptor. The outer membrane protein OprF was found to be upregulated as much as 40-fold in anaerobic biofilms as opposed to their aerobically growing counterparts (Yoon et al., 2002), suggesting a potential role in the denitrification process and ability for *P. aeruginosa* to thrive in an anaerobic environment. This preference for a hypoxic environment further perpetuates anaerobic conditions within the CF lung, which in turn encourages further proliferation.

1.2.3.2 Antibiotic Resistance in Mucoid *P. aeruginosa*

The mucoid phenotype confers antibiotic resistance to *P. aeruginosa* through a variety of mechanisms. One such contributing factor towards the observed antibiotic resistance is the upregulation of rpoS, the RNA polymerase sigma factor, which regulates a general stress response resulting in protective physiological changes to the cell (Mah & O'Toole, 2001). The protection of *P. aeruginosa* microcolonies provided by the formation of a biofilm naturally reduces outer membrane permeability, resulting in reduced drug uptake and lower overall susceptibility to antibiotic treatments. This is compounded by *P. aeruginosa*'s already substantially lower outer membrane permeability when compared to other Gram-negative bacteria such as *E. coli*, providing it intrinsic resistance via a selective barrier to many drugs (Hancock, 1998).

Another biofilm-induced mechanism of adaptive resistance by *P. aeruginosa* is related to the differences in nutrient access within the biofilm. This results in a wide range of metabolic activity across the bacterial population, which in turn affects growth rate. As a result, different antibiotics may be less effective depending on whether they are designed to target growing cells, such as β-lactams and aminoglycosides, or more slowly growing bacteria such as polymyxins (Fuente-nu & Breidenstein, 2011). Slow-growing or non-dividing cells are more prevalent within *P. aeruginosa* biofilms, and are known to be more capable of surviving stressful

environments such as those brought about by antibiotic treatment. Such cells are known as 'persisters' and are thought to be linked to mutations in several genes including, but not limited to, *algR*, *rpoS*, and *relA*, which may provide further insight into this antibiotic resistance (Fuente-nu & Breidenstein, 2011).

1.3 Cystic Fibrosis and *P. aeruginosa* Infection

1.3.1 Cystic Fibrosis

1.3.1.1 Causes of Cystic Fibrosis

Cystic fibrosis (CF) is an autosomal recessive genetic condition caused by a mutation in the cystic fibrosis transmembrane regulator gene (CTFR), with the most common mutation being Phe508del (Castellani et al., 2008), which impairs transport of chloride ions, leading to reduced mucociliary transport in the lungs of CF patients (Riordan et al., 1989). The CFTR gene encodes a 168 kDa, multi-domain ATP-binding cassette transporter protein which functions as an ion channel, transporting bicarbonate anions (Quinton, 2008). CFTR mutants can be split into 6 distinct classes based on their resultant phenotype (**Table 1.1** & **Figure 1.2**). Class 1 mutants produce no CFTR protein, class 2 mutants result in the retention of misfolded CFTR in the ER and subsequent proteasomal degradation, which includes Phe508del, and class 3 mutants impair the opening of the ion channel. All three of these types of mutation lead to a severe phenotype and loss of CFTR function. Class 4, 5 and 6 mutations result in a milder phenotype, retaining some residual CFTR function. As an example, class 4 mutations cause reduced ion flow, class 5 mutants substantially reduce the amount of transcribed mRNA and thus protein synthesised, and class 6 mutants lead to plasma membrane instability (Boyle & De Boeck, 2013). Mutations of the CFTR gene are also thought to result in dehydration of the lung mucous layer, resulting in unfolding of mucin carbohydrate side-chains and causing them to bind cell-tethered MUC1 and MUC4 mucins. As a result, the mucous layer may attach to the lung epithelium, inhibiting mucociliary clearance (Knowles & Boucher, 2002).

Table 1.1 | Example CFTR mutations and their resultant phenotypes. Reproduced from Boyle & DeBoeck (Boyle & De Boeck, 2013). Incidence was taken from the most recent Cystic Fibrosis Foundation Patient Registry Annual Data Report (https://www.cff.org/Research/Researcher-Resources/Patient-Registry/2017-Patient-Registry-Annual-Data-Report.pdf).

Mutation Class	Resultant Phenotype	Mutation Type	Examples & Incidence (Where available) (%)
I	No functional CFTR	Nonsense; frameshift; canonical splice	Gly542X **(4.6)** Trp1282X **(2.3)** Arg553X **(1.8)** 621+1G→T **(1.6)**
II	No functional CFTR	Missense; amino acid deletion	Phe508del **(85.8)** Asn1303Lys **(2.4)** Ile507del **(0.8)** Arg560Thr
III	Impaired Ion Channel regulation	Missense; amino acid change	Gly551Asp **(4.5)** Gly178Arg Gly551Ser Ser549Asn
IV	Impaired CFTR conductance	Missense; amino acid change	Arg117His **(2.9)** Arg347Pro **(0.6)** Arg117Cys Arg334Trp **(0.6)**
V	Reduced CFTR synthesis	Splicing defect; missense	3849+10kbC→T **(1.7)** 2789+5G→A **(1.4)** 3120+1G→A **(1.1)** 5T **(0.8)**
VI	Reduced CFTR membrane stability	Missense; amino acid change	4326delTC Gln1412X 4279insA

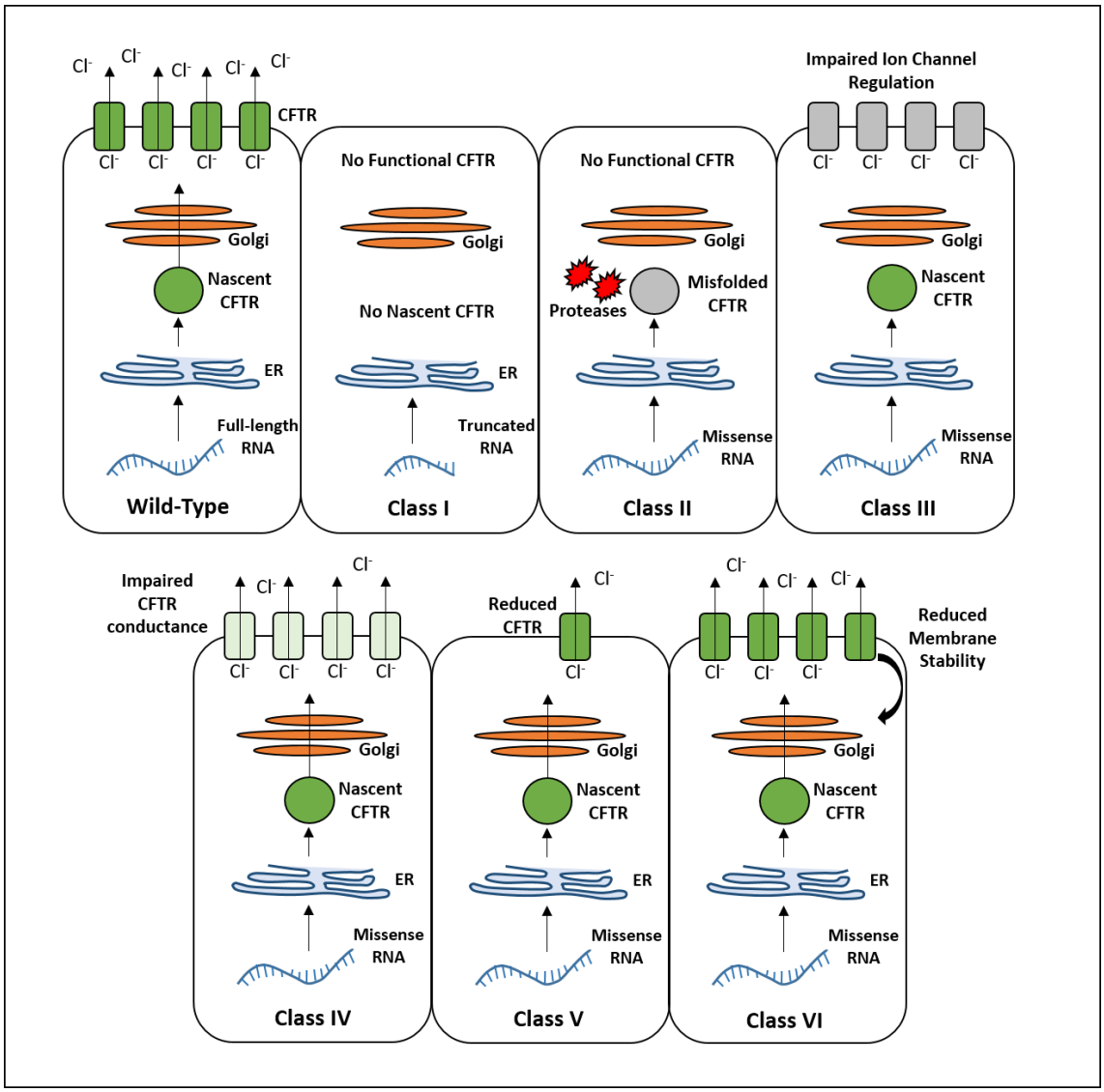

Figure 1.2 | The 6 classes of CFTR mutations resulting in Cystic Fibrosis and the mode of action by which these mutants impact the transporter and/or cell. Adapted from Boyle & De Boeck (Boyle & De Boeck, 2013).

1.3.1.2 Symptoms of Cystic Fibrosis (CF)

Patients with CF typically present with bronchiectasis, an abnormal widening of the airways, and severe neutrophil-driven inflammation of the lungs and airways, which leaves them vulnerable to bacterial infection and results in accumulation of viscous mucous which causes obstructions (Cohen & Prince, 2012). Failure to clear these bacterial infections results in a pro-inflammatory microenvironment which opportunistic pathogens such as *Pseudomonas aeruginosa* may take advantage of by developing a mucoid phenotype, as discussed in **Section 1.2.3** above (Mathee et al., 1999). Dysfunction of CFTR also alters the pH of airway surface liquid, due to its role in conducting bicarbonate ions. This leads to an impairment of innate immunity by limiting the function of antimicrobial peptides, as demonstrated in a ferret CF lung model in which an

increase in the pH of bronchoalveolar lavage fluid reduced bacterial killing by approximately 10-fold (Keiser et al., 2015).

According to the most recently available Cystic Fibrosis Foundation Patient Registry Annual Data Report at the time of writing, (Available from: https://www.cff.org/Research/Researcher-Resources/Patient-Registry/2017-Patient-Registry-Annual-Data-Report.pdf), CF affects almost 30,000 people worldwide. CF is considered to be a lifelong illness, and the median predicted survival age of CF patients has continued to improve over time. As of 2017 the predicted median survival of CF patients is 43.6 years, increasing from 42.4 years in 2016, and from 32.7 in the past 15 years, likely due to advances in both antibiotic treatment, sputum clearance and early detection of infection.

1.3.1.3 Pulmonary Exacerbations

Pulmonary exacerbations in cystic fibrosis are loosely defined as intermittent episodes of acute worsening of symptoms. Generally speaking, pulmonary exacerbations are characterised by a decline in lung function, increased sputum production, chest pain, frequent coughing, weight loss and loss of appetite (Goss & Burns, 2007), although no firm definition has been universally accepted. The classical definition of a pulmonary exacerbation is based on the Fuch's criteria, in which 4 symptoms from a select list must be present in order to identify an exacerbation. These symptoms include malaise, fatigue, a decrease in >10% forced expiratory volume in 1 second (FEV1s), increased cough, increased dyspnoea, a temperature above 38°C and an increase in sputum production or decrease in clearance (Fuchs et al., 1994). Although considered to be an acute worsening of symptoms, severe exacerbations can result in a permanent decline in lung function (Sanders et al., 2010) and the onset of CF-related diabetes (Marshall et al., 2005), and so the early prediction of such events is key to improving the quality of life of CF patients.

1.3.2 *P. aeruginosa* Infections in the Lungs of Cystic Fibrosis Patients

1.3.2.1 Acute *P. aeruginosa* Infections

Common lung infections and their incidence by age in CF patients are shown in Figure 1.3. *Pseudomonas aeruginosa* is the dominant pathogen found in the lungs of cystic fibrosis patients **(Figure 1.3)**, with approximately 40% of child CF patients and 70% of adults infected according to the most recent Cystic Fibrosis Foundation Patient Registry Annual Data Report available at the time of writing (available at the link in **Section 1.3.1.2**). The pathogen is a major bacterium of nosocomial infections, known to be involved not only in colonisation of the cystic fibrosis lung, but also frequently in hospital-acquired pneumonia and chronic wound sepsis. Infection with *P.*

aeruginosa in CF patients is the leading cause of morbidity and mortality (Bhagirath et al., 2016), attributable to its ability to adapt to the environment of the CF lung and its innate antibiotic resistance. In acute infections, the pathogen secretes tissue-damaging exotoxins into the environment, as well as directly injecting them into host cells via the type III secretion system (Kazmierczak & Murray, 2013). Prior to chronic infection, lung function may only be slightly impaired. Patients may present with poorer chest radiographs but it is not until the later stages of infection that lung function begins to decline considerably (Burns et al., 2001). During the acute phase of infection, the bacterium is predominantly non-mucoid and responds to antibiotic treatment (West et al., 2002). At these early stages of infection, planktonic isolates can be detected in sputum samples (Høiby et al., 2010), although their lower population density presents challenges to diagnostic sensitivity. However, the importance of early diagnosis cannot be overstated, as early clearance of planktonic *P. aeruginosa*, facilitated by antibiotic treatment, is widely known to improve patient lung function through prevention of chronic colonisation by mucoid isolates (Stuart, Lin, & Mogayzel, 2010).

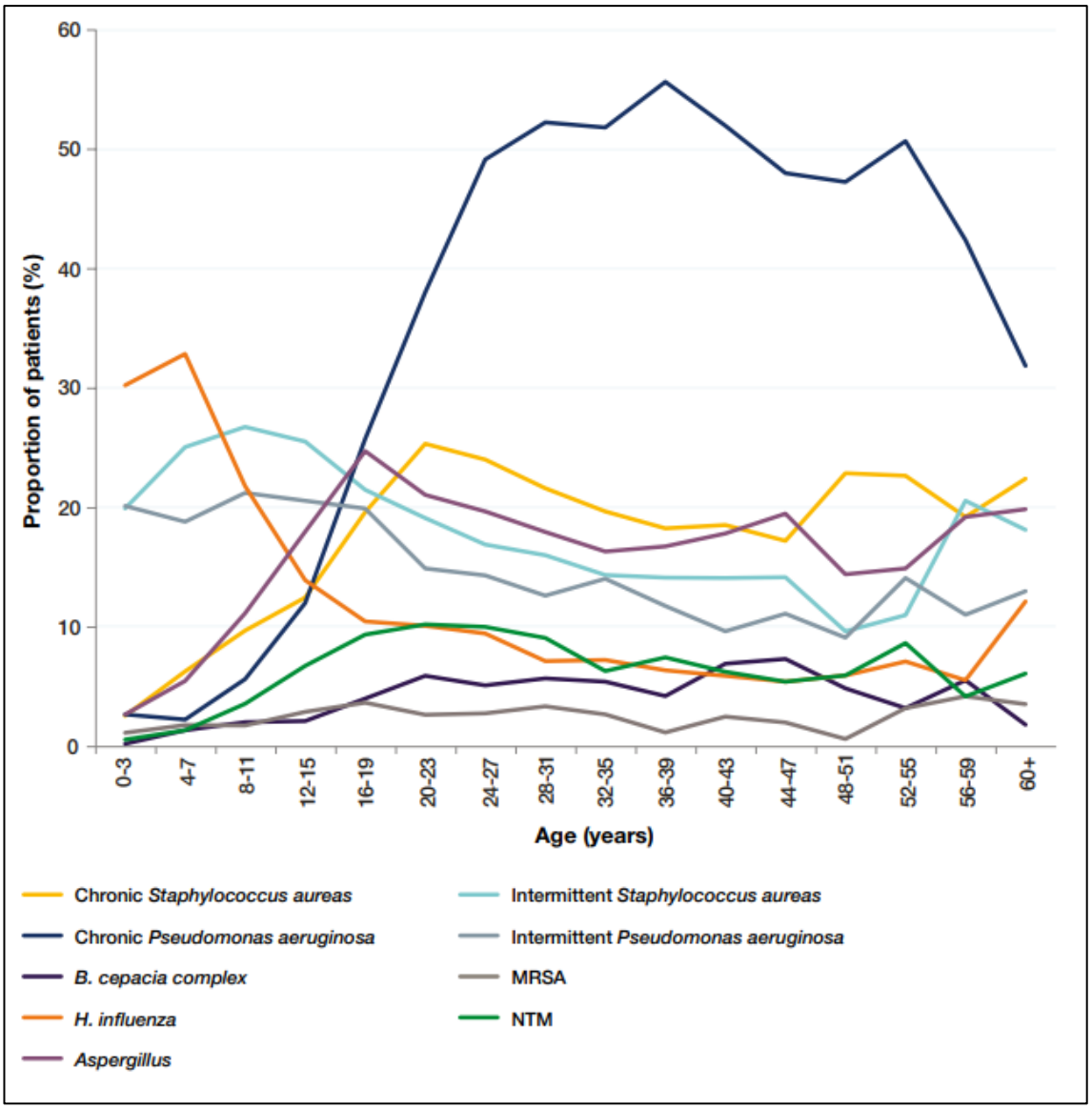

Figure 1.3 | Incidence of lung infections recorded in cystic fibrosis patients in 2017 as reported in the UK Cystic Fibrosis Registry's Annual Data Report 2017, published August 2018. Shown above are the most frequently encountered infections in CF correlated with patient age. Chronic *P. aeruginosa* infections are observed to impact the highest proportion of patients by early adulthood, with over 50% of all patients studied testing positive for chronic infection by age 24-27. MRSA: Methicillin Resistant *Staphylococcus aureus.* NTM: Non-tuberculosis mycobacteria

1.3.2.2 Chronic *P. aeruginosa* Infections

As *Pseudomonas aeruginosa* infections progress, the bacterium adapts to the environmental conditions of the CF lung and may develop a mucoid phenotype, characterised by formation of a bacterial biofilm and emergence of resistance to a multitude of antibiotics (Marvig et al., 2015), as discussed previously in **Section 1.2.3**. This typically leads to a rapid decline in lung function and an increased frequency of pulmonary exacerbations, which ultimately results in a rise in mortality for infected patients (Emerson et al., 2002). During these exacerbations, *P. aeruginosa* may express virulence factors mainly involved in the acute infection stage (Woo et al., 2012).

Chronic *P. aeruginosa* infections can most commonly be detected in biofilms found inside sputum within the conductive zone. Mucoid *P. aeruginosa* thrives in anaerobic conditions caused by the metabolic burst brought about via phagocytosis of pathogens by polymorphonuclear leukocytes in the inflammatory response (Worlitzsch et al., 2002). It is thought that up to 90% of *P. aeruginosa* isolates from chronically infected CF airways are mucoid variants, posing a significant challenge to eradication therapies (Govan & Deretic, 1996). Chronic *P. aeruginosa* infections often persist long-term due to their acquired antibiotic resistance, and so it is crucial to detect infection as early as possible, whilst the pathogen is non-mucoid and receptive to antibiotic treatment.

1.3.3 Diagnosing and Treating *P. aeruginosa* Infections in Cystic Fibrosis Patients

1.3.3.1 Existing Diagnostic Assays for Detection of *P. aeruginosa*

Detection of *P. aeruginosa* in the sputum of infected patients has often been performed via sputum culture, in which instance the bacterium may be detected some time before symptoms of infection begin to develop (Hoiby et al., 1977). This method is currently considered the "gold standard" in the diagnosis of *P. aeruginosa* infection among CF patients, and is recommended to be performed at least once every three months (Smyth et al., 2014). Sampling is most commonly performed via bronchoalveolar lavage, an invasive procedure in which saline is squirted into a small subsection of the lung and aspirated for analysis (Connett, 2000), although expectorated sputum samples and oropharyngeal swabs are also used due to their less invasive nature. Bacterial sampling is currently the most reliable method of detecting bacterial infections in the CF airway. However, sampling and culturing is time consuming and often invasive, and conflicting reports around negative cultures not ruling out *P. aeruginosa* infection and positive cultures not necessarily indicating infection suggest that bacterial culture sampling alone is not an ideal diagnostic approach (Doumit et al., 2016; Ramsey et al., 1991; Rosenfeld et al., 1999).

Among the most common methods of detection are also PCR based assays, in which specific primers are designed to genes unique to *P. aeruginosa*, such as the O-antigen acetylase gene (Choi et al., 2013). Another, more recent PCR based assay involves the use of DNA-binding magnetic nanoparticles to measure chemiluminescence of amplified target genes (Tang et al., 2013). Whilst these assays have been demonstrated to be highly sensitive, in some cases detecting as low as 10 CFU/mL *P. aeruginosa* (Hummel et al. 1998), they typically require highly trained staff and specialist equipment to operate, and are easily susceptible to contaminants, resulting in the emergence of false positive results.

The use of crossed immunoelectrophoresis as a diagnostic tool has also been implemented, in which serum from patients is separated first via agarose gel electrophoresis, followed by precipitation of anti-pseudomonal antibodies via electrophoresis in the same gel containing an anti-human IgG antibody (Hoiby, 1977; Hoiby et al., 1977). Other serological tests for the presence of *P. aeruginosa* have also been explored, with multiple existing ELISAs measuring various anti-pseudomonal antibodies in the serum of infected patients (Pedersen, Espersen, & Høiby, 1987; Shand et al., 1991; Tramper-Stranders et al., 2006). However, the use of serology alone to detect early *P. aeruginosa* infections is unreliable, as prior studies have shown that host responses are varied in cystic fibrosis patients. Not all infected patients elicit a strong serologic response despite conflicting culture data, whereas the reverse can also be true. Some patients elicit a detectable serologic response despite an absence of *P. aeruginosa* following culture from oropharyngeal swabs (Anstead et al., 2013). Sandwich ELISAs to detect *P. aeruginosa* virulence factors have also been briefly explored, such as the anti-elastase sandwich ELISA (Jaffar-Bandjee et al., 1993), which incorporated anti-elastase polyclonal antibodies, and was capable of detecting elastase to a detection limit of 0.26 ng/mL. However, this assay has not been tested with clinically relevant isolates or samples from infected CF patients. Though highly specific and sensitive methods of detecting *P. aeruginosa*, such assays can often be invasive, sometimes requiring that blood samples be taken from patients at regular intervals. These techniques are also time consuming, often taking hours to obtain a conclusive result and requiring the use of specialist equipment, external labs and expensive reagents to analyse samples, which may not always be feasible or cost-effective, particularly in less developed areas of the world. There is thus an urgent need for less invasive and more rapid, sensitive, specific and cost effective diagnostics that can be used at the point of care for *P. aeruginosa* infection in CF patients. Development of a lateral flow based assay therefore represents an ideal alternative assay for the early detection of *P. aeruginosa* due to its simple interface, rapid turnaround time (< 10 minutes), low cost of manufacturing and straightforward interpretation of results. If a sufficiently high sensitivity can be achieved, it may be possible to detect *P. aeruginosa* secreted antigens in patient saliva, overcoming another key shortcoming of the current gold standard of bacterial sampling: invasiveness of sample acquisition.

There are a vast range of detection methodologies implemented for *P. aeruginosa* identification, encompassing microbiological methods, molecular biology based methods, immunological approaches, electrochemical assays and the use of mass spectrometry. A comprehensive review of such assays conducted by Tang et al. concluded that direct detection of the pathogen in clinical samples is critical to reducing the risk of false results and shortening diagnostic

turnaround time (Tang et al., 2017). Thus, the targeting of specific virulence factors such as elastase over patient immunological markers presents the opportunity to develop a diagnostic assay which is both highly specific and highly sensitive.

1.3.3.2 Available Treatments for Cystic Fibrosis Patients with *P. aeruginosa* Infections

Once acquired, chronic *P. aeruginosa* lung infections are a lifelong condition. For this reason, early detection is a vital tool for the eradication of acute infections. Eradication therapy is the recommended course of action upon detection of *P. aeruginosa* in the cystic fibrosis lung, most often involving aggressive antibiotic treatment. Currently, the inhaled aminoglycoside antibiotic tobramycin is recommended by EU guidelines for this purpose (Smyth et al., 2014), but there is insufficient evidence to support its efficacy. More recently, antibiotics such as such as the inhaled monobactam aztreonam, the polymyxin colistin and the fluoroquinolone levofloxacin have been investigated, though such studies have failed to provide a convincing case for total eradication due to limited follow-up studies and a lack of change in lung function between patients undergoing eradication therapy and those left untreated (Mayer-Hamblett et al., 2015). The most notable effect of eradication therapy is the delay in *P. aeruginosa* recurrence reported by Mayer-Hamblett et al. in which a 5 year follow-up study found a median *P. aeruginosa* recurrence time of 3.5 years in patients treated with sustained antibiotics compared to just 1 year in the untreated group (Mayer-Hamblett et al., 2015). In the instances that eradication therapy fails, chronic infections develop and must be managed. At the time of writing, inhaled tobramycin appears to be the most well-studied and effective at reducing acute pulmonary exacerbation frequency and maintaining lung function (Ryan, Singh, & Dwan, 2011).

Table 1.2 | Inhaled antibiotic use among cystic fibrosis patients with chronic *Pseudomonas aeruginosa* infections. Data obtained from the UK Cystic Fibrosis Registry Annual Data Report 2017, published August 2018.

Patients/Antibiotic	Total	< 16 Years Old	≥ 16 Years Old
Patients with chronic *P. aeruginosa*	2749	209	2540
Tobramycin Solution; n **(%)**	626 **(22.8)**	72 **(34.4)**	554 **(21.8)**
Other aminoglycoside; n **(%)**	52 **(1.9)**	< 5	52 **(2.0)**
Colistin; n **(%)**	680 **(24.7)**	79 **(37.8)**	601 **(23.7)**
Promixin; n **(%)**	859 **(31.2)**	98 **(46.9)**	761 **(30.0)**
Aztreonam; n **(%)**	628 **(22.8)**	10 **(4.8)**	618 **(24.3)**
Colistimethate (DPI); n **(%)**	531 **(19.3)**	15 **(7.2)**	516 **(20.3)**
Tobramycin Inhalation Powder; n **(%)**	782 **(28.4)**	26 **(12.4)**	756 **(29.8)**
At least one of the above; n **(%)**	2469 **(89.8)**	191 **(91.4)**	2278 **(89.7)**

1.4 *Pseudomonas aeruginosa* Elastase

1.4.1 Structure and Function of Elastase

Elastase, encoded by the *lasB* structural gene of *P. aeruginosa*, is a secreted 33 kDa zinc metalloproteinase (Morihara, 1964) of the thermolysin family. The protease has a broad substrate specificity and is a key virulence factor involved in both initial infection and formation of the bacterial biofilm (Yu et al., 2014). Elastase is synthesised as a preproenzyme incorporating a short signal sequence and inhibitory propeptide which is processed autoproteolytically prior to secretion (McIver, Kessler, & Ohman, 1991a). Expression of *lasB* is regulated via the *las* quorum sensing pathway as described above, under control of the transcriptional regulator *lasR* which, when deleted in mutant strains, leads to absence of elastolytic activity and elastase protease (Gambello & Iglewski, 1991). There is substantial evidence for the idea that elastase may promote biofilm formation, possibly via rhamnolipid-mediated regulation. For instance, it is known that deletion of *lasB* in the laboratory strain PA01 results in reduced bacterial attachment and impaired ability to form microcolonies (Yu et al., 2014), and that inhibition of elastase with the novel inhibitor N-mercaptoethyl-Phe-Tyr-amide impairs growth of bacterial biofilms (Cathcart et al., 2011). In addition to its contribution to biofilm formation, elastase acts to destroy host tissue, particularly in chronic wounds and the cystic fibrosis lung. The protease also hydrolyses immune system components (Tamura et al., 1992), stimulating a prolonged inflammatory response and creating a nutrient-poor, hypoxic environment which *P. aeruginosa* can adapt to and thrive in via the generation of a mucoid phenotype.

1.4.2 The Role of Elastase in Infection and Virulence

Elastase plays a key role in the initial infection of *P. aeruginosa*, primarily by solubilising elastin in human tissues (Wretlind & Pavlovskis, 1983) for which the exact mechanism has recently been elucidated. Studies examining synthetic peptide substrates have shown that elastase has a preference for aromatic and large aliphatic hydrophobic amino acid residues at the P1 position (Cathcart et al., 2011). More recently, it was determined that elastase binds the hydrophobic domains of elastin fibres and hydrolyses the peptide bonds of hydrophobic amino acid residues, creating cavities on the fibres which cause them to weaken and break up into smaller fragments which are then degraded into peptides and free amino acids (J. Yang et al., 2015).

Elastase is also capable of damaging and degrading several components of the immune system, the extracellular matrix and tight junctions of lung epithelia. It has been shown that degradation of pulmonary surfactant protein A by elastase results in impaired phagocytosis of *P. aeruginosa* in a mouse lung model via reduced opsonisation and membrane permeabilisation of the bacteria, and that deletion of the *lasB* structural gene enhances pathogen clearance via opsonisation (Kuang et al., 2011).

1.4.3 The Role of Elastase in Biofilm Formation

Elastase is believed to contribute to biofilm formation via generation of GTP required for the synthesis of alginate, an exopolysaccharide virulence factor which enhances cell adhesion and protects *P. aeruginosa* from its environment (Boyd & Chakrabarty, 1995). Elastase cleaves the 16 kDa form of nucleoside diphosphate kinase, releasing a 12 kDa protein which can form complexes with pyruvate kinase to generate GTP, leading to the synthesis of GDP-mannose, an important intermediate in alginate synthesis (Kamath, Kapatral, & Chakrabarty, 1998). Deletion of *lasB* in *P. aeruginosa* lab strain PAO1 results in reduced expression of the rhamnolipid genes *rhlA* and *rhlB* through decreased synthesis of C4 homoserine lactones, resulting in flatter, weaker biofilm formation (Yu et al., 2014). This evidence suggests elastase promotes formation of the bacterial biofilm via the *Rhl* quorum sensing pathway, though the exact mechanism by which this occurs remains unclear.

1.4.4 Rationale for Elastase as a Predictive Biomarker of Early Infection

Whilst there are currently a range of diagnostic approaches to the detection of *P. aeruginosa*, as outlined in **Section 1.3.3.1**, there continues to be an urgent requirement for diagnostic tools which have the ability to detect acute stage infections, prior to the formation of the bacterial biofilm. **Section 1.4** details the role that the secreted protease elastase plays in the early stages

of infection and in the transition to a mucoid phenotype. As such, the virulence factor holds great potential as a clinical biomarker. Rapid detection of secreted elastase may be an indicator of ongoing acute *P. aeruginosa* infections, which are readily treatable via antibiotics. Furthermore, the targeting of secreted virulence factors allows for a more reliable assay by avoiding the pitfalls of an immune response based assay which can often provide false positives due to the presence of anti-*pseudomonas* antibodies long after an infection has subsided. By selecting highly specific monoclonal antibodies via robust *in vitro* display methods, the hurdle of low specificity may be overcome in order to provide a reliable and robust diagnostic assay which meets the high sensitivity requirements characteristic of a typical ELISA test. **Section 1.3.3.1** further details the key shortcomings of the current "gold standard" detection methods, primarily centred around bacterial culture and tracking of the immune response. By developing a sensitive assay specific to a well characterised virulence factor known to play a critical role in early stage infection, it is believed that *P. aeruginosa* infections can be more rapidly identified prior to their conversion to a mucoid phenotype, facilitating the rapid eradication of the pathogen via antibiotic treatment and a potential substantial decrease in nosocomial infections due to early clearance.

1.5 Point of Care Diagnostic Assays

1.5.1 Point of Care Diagnostics; An Overview

Point of care (POC) diagnostic assays are a rapidly expanding class of diagnostic tools introduced into practice over the last 50 years. Such assays are intended to provide low cost medical care to patients away from the clinic, particularly in less developed regions without specialised laboratories, but also in more developed areas in order to alleviate the economic burden on healthcare services. In 2006, the World Health Organisation outlined the **ASSURED** criteria; a set of characteristics by which POC diagnostic assays should abide (Peeling, Holmes, Mabey, & Ronald, 2006). An ideal assay should first be **A**ffordable for the patient, **S**ensitive enough to detect the target analyte and minimise false negatives, **S**pecific enough to minimise chances of a false positive result, **U**ser-friendly in that tests can be carried out without the need for a trained technician, **R**apid & robust with a short turnaround for results and ideally stable across a range of conditions, **E**quipment-free and **D**eliverable to end users. It is not always possible for a POC diagnostic device to meet every one of these requirements, so some flexibility is expected. For example, for many lateral flow assays a dedicated reader device may sometimes be used with the provision that it is easy to operate and can be provided to the end user.

POC assays exist in a variety of formats, from simple handheld dipstick assays and lateral flow devices to larger benchtop devices, which are usually scaled down, easier to use versions of typical lab equipment. Many of the earliest commercial point of care diagnostics to reach the market were blood glucose monitoring tests for the monitoring of glucose in diabetic patients. The DextroStix® reagent strip released in 1964 utilised the glucose oxidase reaction with a chromagen system for visualisation of results. Blood samples were incubated on a semi-permeable reagent pad containing glucose oxidase, peroxidase and a chromagen, and after 1 minute the blue colour change was compared to a series of standards. Soon after, a reflectance meter was developed in order to provide more accurate quantitative readouts, though these readers were expensive and bulky, weighing 1.2 kg (Free & Flee, 1984). In the present day, typical blood-glucose readers weigh as little as 9 g, require microlitre volumes of blood for analysis and on average cost less than $5, with a turnaround time of under 5 minutes (Rajendran & Rayman, 2014).

Benchtop POC devices are typically smaller, simplified versions of common laboratory equipment. One example is the GeneXpert system from Cepheid, which uses automated real-time PCR to perform rapid molecular testing without a need for sample preparation and with minimal operation. Reagents are stored in a single-use cartridge which is inserted into the device containing a syringe body which allows for movement of sample and prevention of contamination (Raja, 2005) . The Siemens DCA Vantage Analyzer is another benchtop analyser device used to monitor glycaemic control and detect kidney disease at the point of care via measurement of haemoglobin A1c (Pope et al., 1993).

While POC assays are becoming more and more prevalent in the health care sector, there are still many challenges that must be overcome. Such assays are becoming increasingly important in developing areas of the world and as such, harsher climates can pose a problem. Many POC diagnostics incorporate heat-sensitive reagents which may denature at higher temperatures, and so must be refrigerated, requiring a certain level of infrastructure. From a financial standpoint, although many POC assays such as the paper based lateral flow immunoassay are very cheap to produce, more complex diagnostics are still too expensive in some areas of the world. Private healthcare organisations may also consider traditional laboratories to be more profitable and steer their patients towards this approach (Zarei, 2018).

1.5.2 Lateral Flow Immunoassays

Lateral flow assays are rapid, typically paper-based point of care diagnostics used to detect specific analytes in mixtures such as blood, saliva, sputum and urine. Such devices can detect a

target antigen (Gates-Hollingsworth & Kozel, 2013), antibody (Vrublevskaya et al., 2017) or amplicon (Pöhlmann, Dieser, & Sprinzl, 2014) qualitatively (i.e. by presence of a visible marker) or quantitatively through the use of a dedicated reader device. Lateral flow immunoassays (LFIAs) are antibody-based assays which fall into two main device formats: The sandwich assay and the competitive assay. In the sandwich assay format, conjugated antibodies bind to a target analyte to form labelled antibody-antigen complexes which migrate via capillary flow through the membrane towards the test line, where they bind to complementary immobilised antibodies. An excess of these complexes bind to anti-species antibodies located on the control line to confirm the sample has reached the end of the membrane. A common example of a commercial sandwich assay is the home pregnancy test, which detects elevated levels of human chorionic gonadotrophin (hCG) in the urine of pregnant women via antibodies specific to the β-subunit of hCG, as well as anti-human IgG antibodies (Butler, Khanlian, & Cole, 2001). In competitive assays, conjugated particles are bound to capture antibodies located at the test and control lines. The applied analyte then competes with the test line binding sites, causing dissociation of conjugated particles. In this instance, the lack of a test line indicates a positive result (Wong & Tse, 2009).

Lateral flow assays are composed of multiple key components (**Figure 1.4**). The strip itself is a combination of different membrane materials mounted on a backing card for support. The sample pad is typically made of a cellulose matrix or similar material, and functions to absorb the sample and transport it to the conjugate pad. In some instances this pad may act to adjust the sample in some way, such as adjusting pH, separating blood components or filtering out any solids. The conjugate pad is typically a glass fibre or polyester membrane containing dried conjugate, which is released upon sample flow for transfer to the nitrocellulose membrane. This membrane is the main reaction site of the assay, bearing both the test and control lines, and so it is crucial in the determination of a lateral flow assay's sensitivity. Typically a slower capillary flow rate will improve the sensitivity of the assay as it allows more time for the conjugate-analyte complex to bind to the immobilised antibodies. Nitrocellulose membranes must also have a high affinity for antibody adsorption in order to allow for test and control lines to be properly dispensed, but also low non-specific adsorption as this will affect the outcome of the test (Sajid, Kawde, & Daud, 2015). Finally, the absorbent pad acts as a sink to absorb excess sample and maintain capillary flow throughout the test strip.

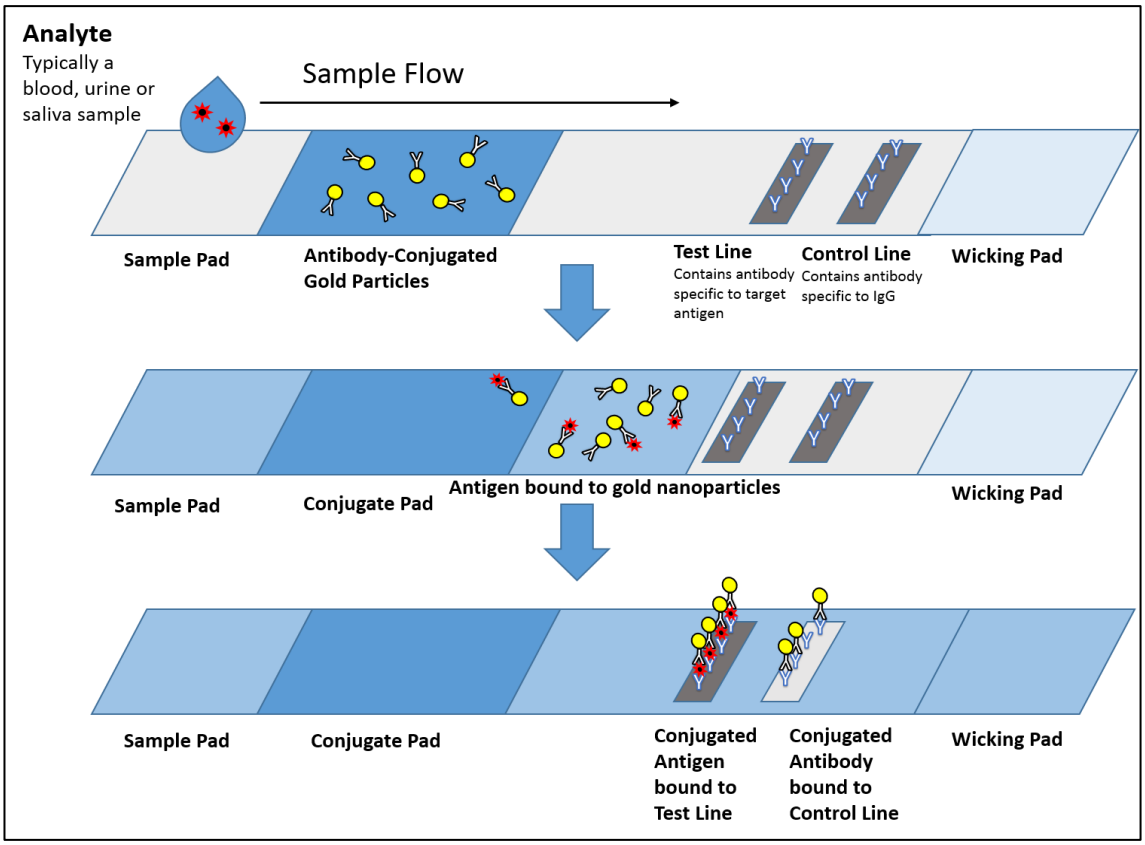

Figure 1.4 | Schematic depicting a typical lateral flow immunoassay diagnostic test. The sample is applied to the sample pad and travels via capillary flow along the membrane. Antibodies conjugated to gold nanoparticles bind the target antigen and subsequently are bound to immobilised antibodies without gold particles, creating a positive test line. A control line containing antibodies complementary to IgG verifies that the sample has reached the end of the membrane.

There are many advantages to lateral flow assays over other diagnostic assays. An important factor is the cost and availability of such devices. Paper-based LFIAs are relatively inexpensive and easy to produce in large quantities compared to other assay formats, meaning diagnostics can be made more readily available to less economically developed areas of the world as well as reducing the economic burden on healthcare services such as the NHS. These assays are also able to be performed at the point of care (e.g. in the home or field) and without the use of specialised equipment, meaning results are obtained quickly and easily and do not require processing through an external lab, which ultimately leads to faster treatment and fewer trips to the GP or hospital as patients can often keep track of their conditions independently.

Low sensitivity is a common constraint of paper-based lateral flow assays, which can limit their viability for certain analytes, particularly those found in low concentrations in bodily fluids. There have been several attempts to address the issue of low sensitivity in recent years, such as enhancement of visual signal via labelling of detector antibodies with enzymes and coating of gold nanoparticles. The labelling of antibodies with horseradish peroxidase has been reported

to enhance signal detection 10-fold in some cases (Parolo, de la Escosura-Muñiz, & Merkoçi, 2013), however this approach is not without its own set of limitations. In exchange for an increase in sensitivity, the background signal appears to be amplified. The assays also take longer to perform as strips must be washed and incubated in a chromogenic substrate such as 3,3',5,5'-tetramethylbenzidine (TMB) following sample application in order for the test line to develop. A further development to enzyme-enhanced LFIAs that has been explored more recently is the coating of gold nanoparticles with platinum, which has been demonstrated to improve detection sensitivity 100-fold via the improved peroxidase-like catalytic properties of platinum shells, however at an additional cost (Gao et al., 2017).

1.5.3 Enzyme Linked Immunosorbent Assays

The enzyme linked immunosorbent assay (ELISA) is an immunoassay method originally described in 1971 by two research groups (Engvall & Perlmann, 1971; Van Weemen & Schuurs, 1971), used frequently at the point of care. The assay utilises the binding of a labelled specific antibody to an antigen to allow detection of small quantities of proteins, peptides and small molecules in a fluid phase (**Figure 1.5** and **Figure 1.6**). Antibodies for detection are typically labelled with an enzyme such as horseradish peroxidase (HRP) or alkaline phosphatase (AP) and a chromogenic substrate such as 3,3',5,5'-tetramethylbenzidine (TMB) or p-nitrophenyl phosphate (pNPP) is used to indicate the presence of a specific analyte following antibody binding. Fluorogenic substrates may also be used, and are often able to provide a more sensitive quantitative measure of the target analyte. ELISA format assays can be classed as direct, indirect, sandwich or competitive assays, each with their own distinct advantages and disadvantages depending on the nature of the target analyte or sample.

Direct ELISAs are the simplest form of ELISA, in which an antigen-containing sample is immobilised on the surface of, for example, a 96 well plate, and an enzyme-labelled specific antibody binds directly to the antigen of interest present in the sample prior to addition of substrate (**Figure 1.5**). Similarly, an indirect ELISA also involves the direct binding of an antigen to the well surface (**Figure 1.5**). However, the main difference in these assays is in the binding of an unlabelled specific antibody, followed by the binding of an enzyme-labelled secondary antibody. A key advantage of this approach over a direct ELISA is that the specific primary antibody does not need to be enzyme labelled, as an anti-species labelled secondary antibody is used instead, which is often commercially available. However, in both techniques the direct binding of antigen to the well surface may be a limitation as in complex samples many different proteins will adhere non-specifically. To overcome this, a sandwich ELISA format may be

implemented. In a sandwich ELISA, the well surface is coated with an unlabelled antibody specific to the target analyte, and the sample is applied to the plate. In this way, only the target antigen will bind and other components of the sample will be washed away. After the antigen is bound, a secondary enzyme-labelled specific antibody is bound to the antigen followed by substrate addition. These assays are often highly sensitive and do not require the sample to be purified prior to assay, but are typically less cost effective and take longer to develop due to the requirement of at least two antibodies with different binding modes to a target analyte if monoclonal antibodies are desired. Competitive ELISAs follow the same principle of a specific antibody binding a target antigen, but with an additional step (**Figure 1.6**). The analyte mixture is pre-incubated with a specific antibody and the resulting complexes are added to a 96 well plate that has been coated with the target antigen. Following incubation, unbound antibody is washed from the plate and a secondary antibody is added. Absence of colour following development with a chromogenic substrate indicates the presence of the analyte of interest in the sample.

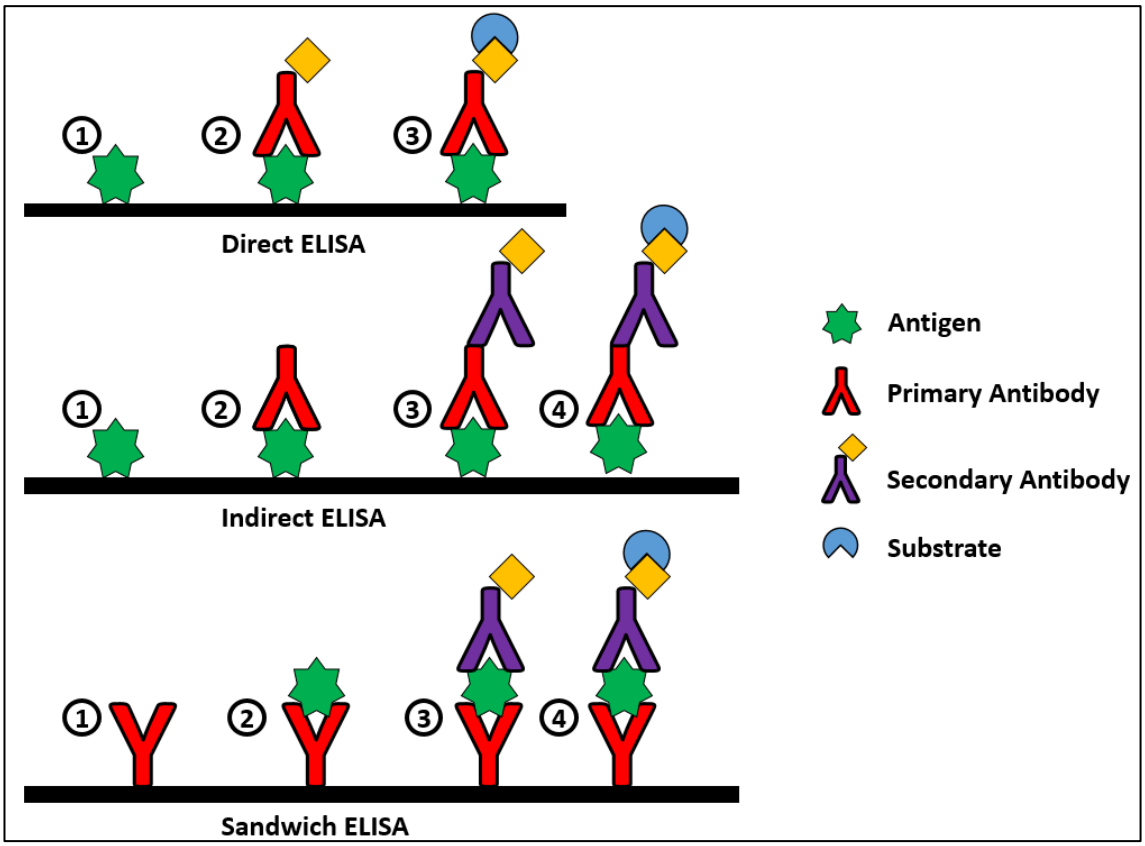

Figure 1.5 | Schematic depicting the three main types of Enzyme Linked Immunosorbent Assay (ELISA) format. In direct ELISA, a single antigen-specific labelled antibody binds directly to the immobilised antigen of interest, and a signal is generated upon addition of substrate. In indirect ELISA, the antigen-specific primary antibody is unlabelled, and a signal is generated indirectly via the binding of a species-specific enzyme-labelled secondary antibody, followed by substrate development. In sandwich ELISA, the unlabelled primary antibody is immobilised and the antigen-containing sample is captured, followed by detection with a second antigen-specific enzyme-labelled antibody. Sandwich ELISA is the most specific, but requires two antigen-specific antibodies with differing epitope specificities.

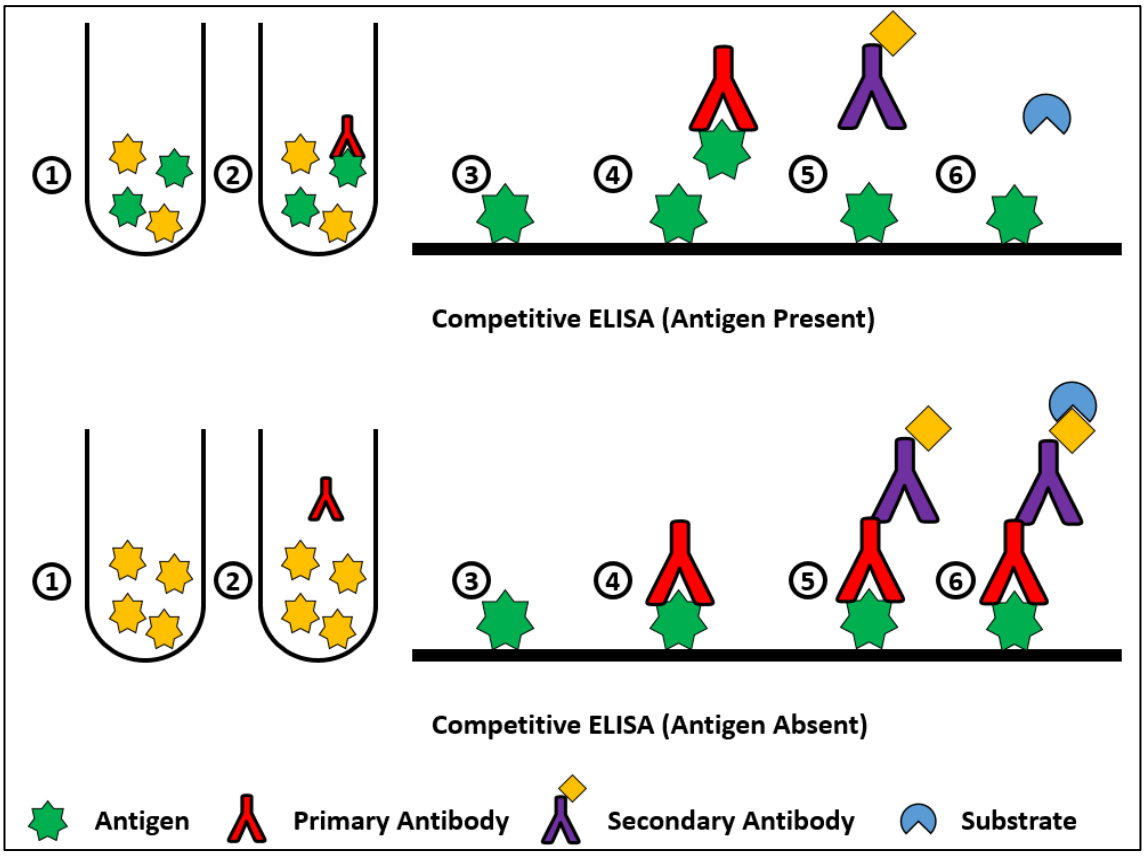

Figure 1.6 | Schematic depicting the mechanisms of competitive ELISA in both the presence and absence of a target analyte. Specific antigen of interest is denoted in green, whereas non-specific antigens are denoted in yellow. In the presence of specific antigen, antibody binding to the ELISA surface is blocked as the binding site is occupied, resulting in an absence of signal. In the absence of specific antigen, the primary antibody binding site is free and able to bind to the immobilised antigen, generating a signal via the subsequent binding of labelled secondary antibody and substrate development.

1.6 Antibody Phage Display

1.6.1 Phage Display Technology

The process of phage display was initially described in 1985, in which small peptides of the EcoRI endonuclease were fused to the pIII minor capsid protein of filamentous bacteriophage f1 (G. P. Smith, 1985). It was discovered that by inserting foreign DNA within the sequence of gene III, the structural gene encoding pIII, the foreign sequence can be displayed in an immunologically accessible form, fused to pIII on the phage surface. In modern phage display methodology, a phagemid is used to fuse a target peptide or protein to either the pIII minor capsid protein or the pVIII major capsid protein for display (**Figure 1.7**). Phagemids are specialised cloning vectors containing the phage origin of replication and packaging signal, as well as the plasmid origin of replication and tools for gene expression. Upon infection with a filamentous helper phage, such as strain M13KO7, the phage origin of replication is activated and the resulting phage ssDNA is packaged into phage-like particles on the surface of infected *E. coli* cells (Kay, Winter, & McCafferty, 1996). Since its inception, phage display has been used to produce monoclonal

antibodies, investigate protein-protein interactions and determine enzyme-substrate specificity, as well as to map epitopes of specific antigens and identify G-protein coupled receptor agonists and antagonists (Pande, Szewczyk, & Grover, 2010).

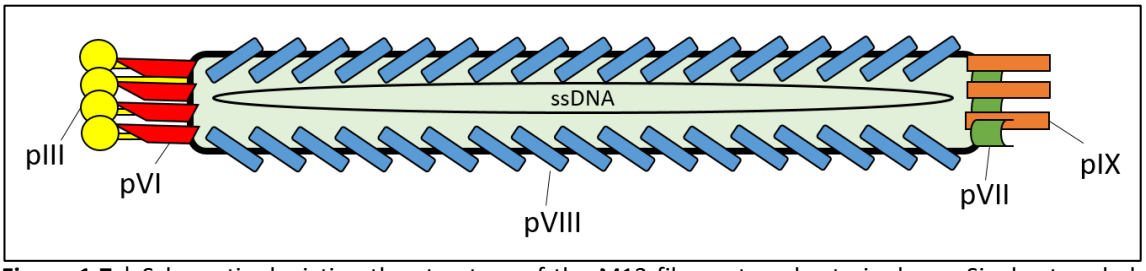

Figure 1.7 | Schematic depicting the structure of the M13 filamentous bacteriophage. Single stranded DNA encoding the bacteriophage genome is encapsulated within a series of coat proteins. Inserting foreign DNA within the coat protein genes allows for protein or peptide display via formation of a coat protein-fusion on the surface of the bacteriophage. Recombinant protein/peptide fusion is most often linked to the pIII capsid protein for monovalent display, of which there are typically 5 copies, and to the pVIII capsid protein for multivalent display, of which there are approximately 2700 copies.

1.6.2 Application of Phage Display to Generate High Affinity Monoclonal Antibodies

The production of antibodies and antibody fragments via phage display technology was first described by Clackson *et al.* in order to bypass hybridoma technology, by generating an scFv library prepared from mice immune to 2-phenyloxazol-5-one to be displayed on the surface of fd phage (Clackson et al., 1991). Since then, phage display has routinely been used to produce high affinity recombinant monoclonal antibody fragments through the genetic engineering of bacteriophage and antigen panning techniques (Barbas, 2001).

1.6.2.1 Generation of Antibody Libraries

The process of antibody phage display begins with the generation of antibody libraries, which are prepared from RNA extracted from the immune cells of a host animal, often previously immunised with a specific antigen of interest (**Figure 1.8**). cDNA is then generated via reverse transcription, and antibody heavy and light chain gene variants are amplified via PCR using specific primer sets, which can then be cloned into a defined phagemid vector (**Figure 1.8**). This generates a large, highly diverse library containing the immune repertoire of the host animal, which can be enriched in order to bias towards an antigen of interest or antibodies with high affinity. In the case of Fab fragments, heavy and light chain DNA fragments are often separately cloned into a single vector. Dual vector systems have also been utilised (Ostermeier & Benkovic, 2000), which can reduce the time spent in the cloning phase, but have not become common practice, likely due to the need to handle multiple phagemids. When scFv fragments are desired, variable heavy and light chain fragments are often joined by a short, flexible linker region via

pull-through PCR assembly and cloned into a phagemid vector in a single step. The phagemid vector is usually engineered to express antibody fragments as a fusion with the pIII minor capsid protein of M13 filamentous bacteriophage which, following infection with helper phage, provides antibody display on the surface of the phage with its respective nucleotide sequence contained within.

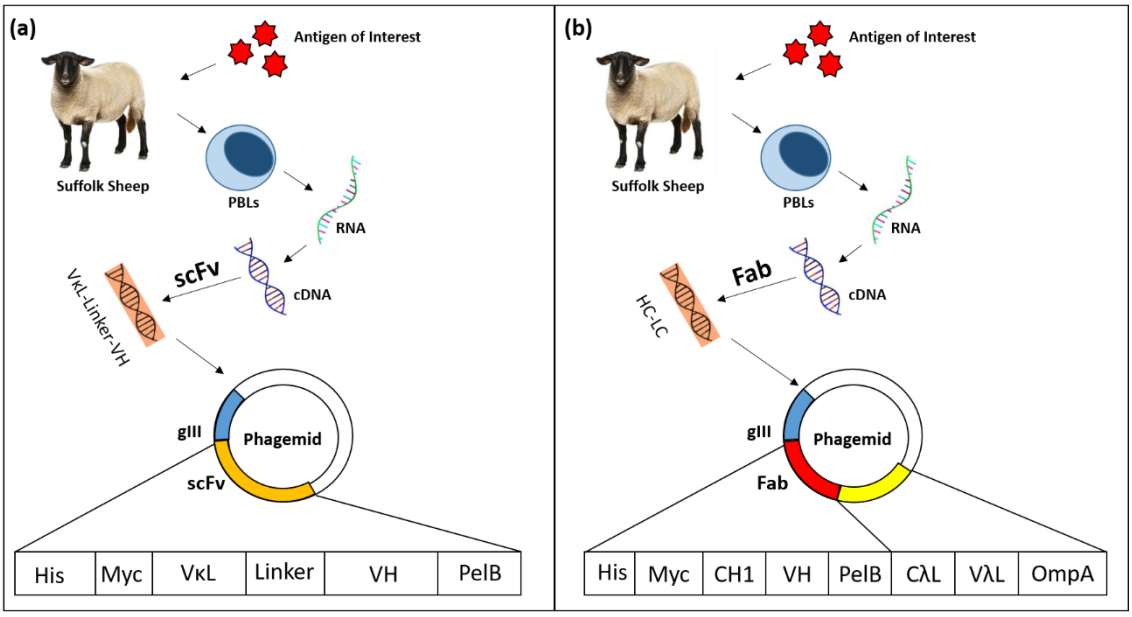

Figure 1.8 | Schematic outlining a standard restriction cloning procedure for the assembly of an immune library of **(a)** scFv fragments and **(b)** Fab fragments. The full scFv gene is denoted in orange, whereas the Fab sequence is divided into heavy chain (CH1 and VH domains) denoted in red, and light chain (CL and VL domains). The gene III sequence, encoding the p3 coat protein, is denoted in blue and is expressed as an antibody-fusion protein with the antibody fragment presented on the protein's C-terminus.

1.6.2.2 Enrichment of Antibody Libraries via Biopanning

Once a library is built, it is usually enriched against a particular antigen via phage biopanning (**Figure 1.9**), as a typical library contains approximately 10^8 independent transformants. This process consists of multiple rounds of phage binding to a specific antigen, often immobilised on an ELISA plate, immunotube, or biotinylated and bound to streptavidin coated magnetic particles. Non-binders, non-specific binders or binders of weak affinity are washed away and more specific and higher affinity binders are eluted for reinfection. Following three to four rounds of panning, highly specific clones are isolated and carried forward for expression. To confirm panning has isolated clones of the desired specificity and sensitivity, polyclonal phage ELISAs are routinely performed on antigen-coated plates, using an anti-M13 antibody to detect for bound phage.

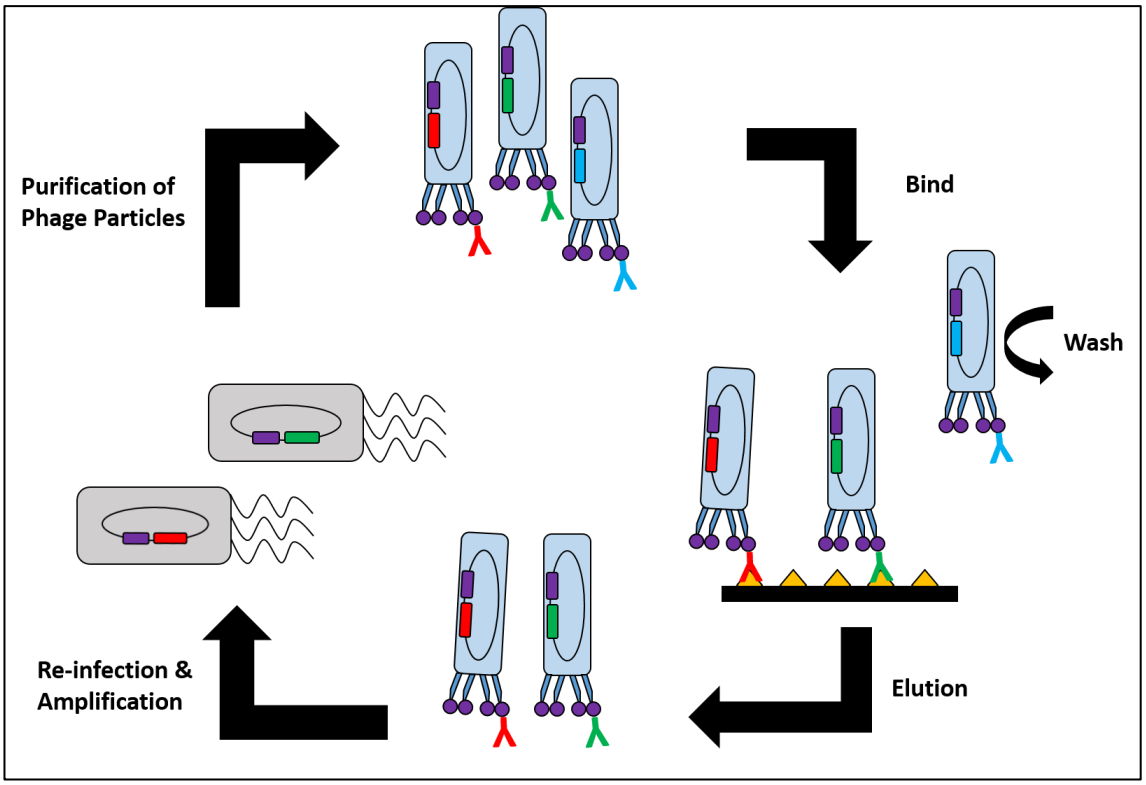

Figure 1.9 | Schematic depicting the phage display biopanning cycle. Typically, 3 to 4 rounds of biopanning are performed in order to bias a library towards a specific antigen and enrich for specific binding and high affinity binding antibodies before monoclonal selection. Gene III and its encoded coat protein pIII are indicated in purple, whereas the fusion antibody genes and their respective variants are indicated in red, green and blue.

1.6.2.3 Selection of Monoclonal Antibodies

Following enrichment across multiple rounds of panning, the infected library is re-plated and individual colonies are picked for monoclonal selection via monoclonal phage ELISA. Positive clones are re-grown and plasmid DNA is then purified and sequenced in order to be carried forward for subsequent expression and purification of the isolated monoclonal antibodies or fragments. In some instances, the antibody sequence is expressed in the phagemid vector used for enrichment following restriction cloning to remove gene III, although often the antibody sequence is sub-cloned into a dedicated expression vector for the host expression system of choice, such as pET (*E. coli*) or pcDNA 3.1 (CHO). These mAbs are usually then characterised in order to assess affinity, activity and stability, and the antibodies with the most desirable traits for a specific purpose are carried forward for application in therapeutics or immunoassays.

1.6.3 Advantages of Antibody Phage Display

There are many advantages to using phage display to develop monoclonal antibodies over previously used techniques such as hybridoma technology. The *in vitro* nature of the technique

allows for more specific epitope selection by biasing libraries towards specific regions of a target antigen (Parsons et al., 1996), as well as independent optimisation of binding affinity through stringing biopanning and selection (Lu et al., 2003). As antibody phage display is not reliant on the immune system, antibodies can be produced against targets with low immunogenicity, such as non-proteinaceous antigens. For example, antibodies against mycolic acid, a tuberculosis biomarker, have been generated from naïve phage display libraries through biopanning (Chan et al., 2013). Antibody phage display is also high throughput, with reports of libraries containing up to 10^{12} clones, which allows for a wide range of diversity and a greater representation of the immune repertoire of the host. A key aspect of antibody phage display is the ability to physically link antibody phenotype with genotype, as the phage particle presents the antibody or fragment on its surface whilst housing the nucleotide sequence within as ssDNA.

1.7 Aims of Thesis

The work described in this thesis is focused around the development of a rapid, highly sensitive point of care diagnostic assay for the early detection of *Pseudomonas aeruginosa* in the lungs and airways of cystic fibrosis patients. Whilst many early antibody-based diagnostic assays targeted host immune response to initial infection, the assay developed in this body of work focused primarily on detecting the secreted protease elastase, encoded by the structural gene *lasB*, a well-studied *P. aeruginosa* virulence factor. In order to generate antibodies specific to this virulence factor, recombinant elastase was first expressed in the periplasm of *Escherichia coli* and purified via nickel affinity chromatography. This recombinant product was briefly assessed to determine specific activity and conformational stability, before being used as an immunogen to raise anti-elastase polyclonal antibodies in rabbits and sheep. Affinity purified polyclonal antibodies were assessed in both ELISA and lateral flow format diagnostic assays, using purified recombinant elastase as a standard. Both assay formats were also assessed with frequently used *P. aeruginosa* laboratory strain supernatants, as well as clinically relevant strains isolated from patients in a cystic fibrosis paediatric clinic. Work was also undertaken on the development of high affinity monoclonal antibody fragments via antibody phage display, using RNA extracted from the peripheral blood lymphocytes derived from the spleens of immunised animals. The aims were therefore;

1. To clone and assess different systems for the expression of a number of potential antigens for development of various immunoassays with a particular focus upon the expression of the *lasB* elastase from *P. aeruginosa.*
2. To purify and characterise recombinant elastase.

3. To use the characterised and purified recombinant elastase protein to immunise rabbits and sheep to generate polyclonal anti-elastase antibodies.
4. To characterise the polyclonal anti-elastase antibodies and the titre/affinity of these.
5. To use peripheral blood lymphocytes from immunised animals and phage display to investigate generation of monoclonal anti-elastase antibodies.
6. To develop immunoassays for detection of elastase, and hence presence of *P. aeruginosa*, and then test/validate the assays on lab strains and clinical isolates.

The findings from the investigations into these aims are described in the following chapters.

Chapter 2

Materials & Methods

2.1 General Methods

All materials used in this study were of analytical grade or higher unless otherwise stated.

2.2 Molecular Biology

2.2.1 Purification of Plasmid DNA from *E. coli*

Following overnight incubation at 37°C, 200 rpm, 5 mL *E. coli* DH5α cultures grown in Lysogeny broth (LB) were pelleted via centrifugation at 2500 x g for 15 minutes. Plasmid DNA was purified from the resulting pellets via the QIAPrep© Spin Miniprep Kit (Qiagen) following the manufacturer's protocol. DNA was eluted in nuclease free water and subsequently quantified using a NanoDrop 1000 Spectrophotometer (ThermoFisher Scientific™) and the DNA stored at -20°C or kept on ice for immediate use. When larger quantities of DNA were required, 250 mL bacterial cultures were grown and pelleted as above, followed by purification via the HiSpeed™ Plasmid Maxi kit (Qiagen) following the manufacturer's protocols.

2.2.2 Amplification of Target Genes via the Polymerase Chain Reaction

Target genes were amplified from human cDNA templates (Origene Technologies, Inc.) using Phusion Hi-Fidelity DNA Polymerase (ThermoFisher Scientific™). Primers were designed based on the mRNA sequences of the genes of interest, incorporating NheI and KpnI restriction sites to facilitate cloning into expression vectors, and were synthesised by Eurofins Genomics (**Table 2.1**). Standard Phusion reaction components and conditions are outlined in **Tables 2.2** and **2.3**.

Table 2.1 | Primers used for the amplification of target antigen mRNA sequences from cDNA templates. Restriction sites are highlighted in red (NheI) and blue (KpnI).

Gene	Forward Primer Sequence (5' → 3')	Reverse Primer Sequence (5' → 3')
MMP-9	TAT**GCTAGC**ATGAGCCTCTGGCA	ATA**GGTACC**CTAGTCCTCAGGGCA
Siglec-8	TAT**GCTAGC**ATGCTGCTGCTGC	ATA**GGTACC**TCAGCCTCTGACTTCTTTGC
MBP	TAT**GCTAGC**ATGAAACTCCCCCTACTTCTG	ATA**GGTACC**TCAGTAGGAACAGATGAAAGGAAGT
RAGE	TAT**GCTAGC**ATGGCAGCCGG	ATA**GGTACC**TCAAGGCCCTCCAGTA
sRAGE		ATA**GGTACC**TCACATGTGTTGGGGGC

Table 2.2 | Reaction components used with Phusion Hi-Fidelity DNA Polymerase.

Component	Volume (µL)/reaction
cDNA Template	1
Forward Primer	2
Reverse Primer	2
5x HF Buffer	10
Phusion Polymerase	0.5
10 mM dNTP mix	1
nfH_2O	33.5
Total Volume	**50**

Table 2.3 | Conditions for PCR reactions with Phusion Hi-Fidelity DNA Polymerase.

Step	Time (min:s)	Temperature (°C)	
Initial Denaturation	0:30	98	
Denaturation	0:10	98	30 Cycles
Annealing	0:30	60	
Extension	1:00/kb	72	
Final Extension	7:00	72	
Hold	∞	4	

2.2.3 Generation of the *Pseudomonas aeruginosa lasB* Nucleotide Sequence

The mRNA sequence of the *P. aeruginosa* Elastase encoding gene *lasB* (Uniprot Accession: P14756) was codon optimised for expression in *E. coli* via the online codon optimisation tool (Integrated DNA Technologies), and the resulting DNA sequence was synthesised by GeneArt Gene Synthesis (ThermoFisher Scientific™) to include BamHI and XhoI restriction sites at the 5' and 3' ends respectively. The sequence also included a C-terminal 6x polyhistidine tag in order to facilitate purification of the recombinant product via nickel affinity chromatography and for western blotting. The requested gene was provided in a donor plasmid containing an ampicillin resistance gene.

2.2.4 Enzymatic Restriction Digests of DNA

Restriction digests for the cloning of antigen genes were performed using FastDigest™ restriction enzymes (ThermoFisher Scientific™), following manufacturer's protocols. Digested pDNA was separated via 1% agarose gel electrophoresis for 1 hour at 100 V with ethidium bromide staining to allow visualisation of DNA, and bands of interest were excised from the gel using a sterile razor blade under ultraviolet light. Purification of digested pDNA from agarose gel pieces or digested PCR product was performed via the Wizard® SV Gel and PCR Clean-Up system (Promega), following the manufacturer's instructions.

2.2.5 Dephosphorylation and Ligation of DNA

Linearised pDNA was dephosphorylated using thermosensitive alkaline phosphatase (Promega) via incubation at 37°C for 15 minutes followed by heat inactivation at 74°C for 15 minutes. Following dephosphorylation, DNA ligations were performed with T4 DNA ligase (Promega) at plasmid:insert ratios of 1:0, 1:3 and 1:5. Reactions were incubated at 4°C overnight prior to transformation into DH5α *E. coli*.

2.2.6 Transformation of Recombinant Plasmids in DH5α *E. coli*

Following ligation, recombinant pDNA constructs were amplified via transformation in DH5α *E. coli*. The entire ligation reaction mixture was added to a 100 µL aliquot of calcium competent cells and incubated on ice for 30 minutes. Cells were then subjected to heat-shock in a 42°C water bath for 90 seconds and allowed to recover on ice for 2 minutes. 900 µL of sterile SOC media was then added to the tube and cells were incubated at 37°C in a shaking incubator at 180 rpm for 1 hour. Following incubation, 100 µL of transformed bacterial culture was streaked on an LB agar plate containing 100 µg/mL ampicillin and incubated overnight at 37°C in a static incubator.

2.3 *E. coli* Recombinant Protein Expression and Purification

2.3.1 Expression of Target Genes in BL21*(DE3)pLysS *E. coli*

Recombinant pET-23b constructs were transformed in the *E. coli* protein expression strain BL21*(DE3)pLysS following the techniques described in **Section 2.2.5**. In order to select for cells containing the pLysS plasmid, 34 µg/mL chloramphenicol was included in the LB agar plates. From streaked plates, a single colony was picked and grown overnight in 10 mL LB media containing 100 µg/mL ampicillin and 34 µg/mL chloramphenicol. The following morning, cells

were harvested via centrifugation at 2500 x g for 15 minutes, and the resulting pellets were resuspended in 400 mL terrific broth containing the same antibiotics. Cultures were grown at 37°C in a shaking incubator at 200 rpm to an OD_{600} of approximately 0.5 and protein expression then induced via the addition of IPTG to a final concentration of 0.4 mM. Growth was continued at a range of temperatures from 19-37°C overnight and cultures harvested via centrifugation at 3000 x g for 20 minutes at 4°C.

2.3.2 Whole Cell Fractionation of *E. coli*

10 mL of an *E. coli* cell culture expressing proteins of interest was harvested via centrifugation following overnight induction with IPTG. Pellets were resuspended in 0.5 mL Buffer 1 (100 mM tris-acetate pH 8.2, 500 mM sucrose, 5 mM EDTA pH 8.0) and 0.5 mL ddH_2O, 40 µL 2 mg/mL lysozyme and 20 µL 1M $MgSO_4$ added. Resuspended cells were incubated on ice for 5 minutes and the periplasmic fraction was harvested via centrifugation at 20,000 x g for 2 minutes. To isolate the insoluble fraction, the resulting pellet was resuspended in 0.75 mL Buffer 2 (50 mM tris-acetate pH 8.2, 250 mM sucrose, 10 mM $MgSO_4$) and centrifuged for 5 minutes at 20,000 x g, followed by resuspension in Buffer 3 (50 mM tris-acetate pH 8.2, 2.5 mM EDTA pH 8.0) and sonication 5 times with 10 second pulses. Following further centrifugation at 20,000 x g for 15 minutes, the insoluble fraction was separated as the resulting pellet. The supernatant was centrifuged at 160,000 x g for 30 minutes in an ultracentrifuge to separate out the cytosolic fraction (supernatant) and membrane fraction (pellet), and the contents of each fraction were analysed via SDS-PAGE.

2.3.3 Embedding of Antigen-Expressing *E. coli* Strains for TEM Analysis

50 mL of LB media was inoculated with a single colony and grown at 37°C with shaking to an OD_{600} of approximately 0.4. Following harvesting of cells via centrifugation at 3000 x g for 10 minutes, pellets were resuspended in 2 mL 2.5% glutaraldehyde in a 100 mM sodium cacodylate buffer, pH 7.2 (CAB) and fixed for 2 hours with gentle rotation at 20 rpm. Cells were then pelleted via centrifugation at 6000 x g for 2 minutes and washed twice for 10 minutes with 100 mM CAB. Post-fixation was performed with 1% osmium tetroxide in 100 mM CAB for 2 hours, followed by two washes in dH_2O. Cells were then dehydrated by incubation in an ethanol gradient: 50% EtOH for 10 minutes, 70% EtOH overnight, 90% EtOH for 10 minutes, and 3 x 10 minute washes in 100% dry EtOH, followed by 2 washes with propylene oxide for 15 minutes. Pellets were embedded by resuspension in 1 mL of equal parts propylene oxide and agar LV resin, incubated for 30 minutes with rotation, and then infiltrated twice in 100% agar LV resin. Pellets were then resuspended in fresh resin and transferred to a 1 mL Beem embedding capsule, followed by

centrifugation at 3000 x g for 5 minutes to concentrate cells to the tip of the mould, and were then incubated for 20 hours at 60°C in order to polymerise.

2.3.4 Sectioning and Visualisation of Samples via Transmission Electron Microscopy

Samples were ultra-thin sectioned on a RMC MT-XL ultra-microtime using a diamond knife (Diatome 45°). 60-70 nm sections were collected on un-coated 300 mesh copper grids, which were then stained via incubation in 4.5% uranyl acetate in a 1% acetic acid solution for 45 minutes. The grids were subsequently washed in a stream of dH_2O and stained with Reynolds lead citrate for 7 minutes, followed by another wash in a stream of dH_2O. Electron microscopy was performed using a JEOL-1230 transmission electron microscope equipped with a Gatan multiscan digital camera, operated at an accelerating voltage of 80 kV.

2.3.5 Purification of His-Tagged Proteins via Nickel Affinity Chromatography

Expressed proteins containing a C-terminal 6xHis tag were purified via nickel affinity chromatography using a gravity flow column containing 1 mL Chelating Sepharose™ FastFlow (GE Healthcare) charged with 5 column volumes of 100 mM $NiSO_4$. The charged resin was equilibrated with 25 column volumes of equilibration buffer containing 20 mM Tris-HCl, 1 M NaCl and 5 mM Imidazole, pH 8. Samples to be purified were then loaded onto the column and allowed to flow through, and the resin was then washed with 20 column volumes of wash buffer containing 20 mM Tris-HCl, 1 M NaCl and 25-100 mM Imidazole. The concentration of imidazole in the wash buffer varied depending on the protein of interest. His-tagged proteins were eluted in 5 mL of elution buffer containing 20 mM Tris-HCl, 1 M NaCl and 400 mM Imidazole. At each stage of purification, samples were taken for analysis via SDS-PAGE. Elution fractions were pooled and buffer exchanged into PBS via overnight dialysis in visking dialysis membrane (Medicell) at 4°C. Dialysed material was then concentrated to a final concentration of 1 mg/mL using a VivaSpin concentrator column (Sartorius).

2.3.6 Purification of Anti-Elastase Polyclonal Antibodies from Antiserum

A 1 mL HiTrap NHS-Activated HP affinity column (GE Healthcare) was coupled with 1 mg recombinant elastase following the manufacturer's instructions. Purification of anti-elastase antibodies from the antiserum of immunised animals was performed using the following protocol:

1. Load 10 mL antiserum
2. Wash with 3 mL PBS
3. Wash with 3 mL 1 M NaCl
4. Wash with 3 mL PBS
5. Elute antibody with 3 mL 0.1 M Glycine-HCl, pH 2.5
6. Wash with 3 mL PBS

Absorbance at 280 nm was monitored for elution fractions, and antibody-containing fractions were pooled and buffer exchanged into 3.5 mL PBS via a PD-10 desalting column (GE Healthcare). Purified antibody was then concentrated to approximately 10 mg /mL using a VivaSpin 5000 30 kDa MWCO concentrator column (Sartorious).

2.3.7 HRP Labelling of Purified Antibodies

Labelling of antibodies with horseradish peroxidase was carried out using the Lightning-Link HRP antibody labelling system (Novus Biologicals), following the manufacturer's protocols.

2.4 Protein Analysis and Characterisation

2.4.1 Determination of Protein Concentration via Bradford Assay

The concentration of proteins in cell fractions, purification fractions and purified material was estimated using the Bradford assay (Bradford, 1976). Samples were diluted 1:25 in ddH_2O and 1 mL of filtered Bradford Reagent (50 mg Coomassie Brilliant Blue G250, 15 mL ethanol, 50 mL 85% phosphoric acid, 435 mL ddH_2O) was added and left to incubate at room temperature for 10 minutes. Absorbance was then read at 580 nm on a spectrophotometer and a standard curve generated using known amounts of BSA to determine protein concentration in µg/mL.

2.4.2 Separation of Proteins via SDS-PAGE

Protein samples were prepared for SDS-PAGE analysis in a 4x reducing Laemmli sample buffer containing 50 mM Tris-HCl pH 6.8, 2% SDS, 10% glycerol, 1% β-mercaptoethanol, 12.5 mM EDTA and 0.02% bromophenol blue and boiled for 10 minutes at 100°C. Prepared samples were

separated according to their molecular weight via electrophoresis on 8% SDS polyacrylamide gels at 85 V for 30 minutes, followed by 135 V for 1 hour in a 1X SDS running buffer prepared from a 10X stock (200 mM Glycine, 250 mM Tris, 1% SDS). Gels were run with the Precision Plus Protein™ Dual Colour Standard (Bio-Rad) for protein size estimation. Components of the polyacrylamide gels are described in **Table 2.4**. Polyacrylamide gels were then stained with a staining solution (1% Coomassie Brilliant Blue G250, 50% Methanol, 10% Glacial Acetic Acid) for 1 hour at room temperature and destained with a destaining solution (24% Methanol, 14% Glacial Acetic Acid) for 1 hour at room temperature.

Table 2.4 | Components of 8% polyacrylamide resolving gels made for SDS-PAGE analysis.

Component	Volume / gel (mL)	Conc. / gel
1.5 M Tris-HCl pH 8.8	1.6	400 mM
30% Acrylamide/Bis Solution 37.5:1	2.5	1.4% (w/v)
10% SDS	0.0625	0.004% (w/v)
400 mM Ammonium Persulphate	0.0625	4.2 mM
TEMED	0.0025	0.04% (v/v)
ddH_2O	1.8	N/A

2.4.3 Transfer of Proteins from Polyacrylamide to Nitrocellulose for Western Blot Analysis

Following SDS-PAGE, separated proteins were transferred to a 0.45 µm pore-size nitrocellulose membrane (Amersham™ ProTran™) for 1 hour at 750 mA in a 2051 Midget Multiblot Electrophoretic Transfer Unit at 4°C, immersed in a 1X transfer buffer prepared from a 10X stock (100 mM Glycine, 125 mM Tris, 0.5% SDS).

2.4.4 Identification of Recombinant Proteins by Tryptic Digestion and MALDI-ToF Mass Spectrometry

2.4.4.1 In-Gel Tryptic Digestion of Proteins and Sample Preparation for MALDI-ToF Mass Spectrometry

Following separation of proteins on an SDS polyacrylamide gel and staining, gels were washed with ddH_2O and protein bands of interest excised with a sterile blade. In-gel tryptic digestion and peptide extraction was then performed following the methods described by Shevchenko *et al.* (Shevchenko et al., 1996). Extracted peptides were spotted onto an MTP AnchorChip™

600/384 T F plate (Bruker) and allowed to air dry before overlaying with an equal volume of α-cyano-4-hydroxycinnamic acid matrix. An equal volume of peptide calibration standard II mix (Bruker) was spotted in between samples and allowed to air dry.

2.4.4.2 Identification of Recombinant Proteins by MALDI-ToF MS

Mass spectra were collected on an UltrafleXtreme MALDI-ToF Mass Spectrometer (Bruker) and the peptide mass fingerprints were compared against known fingerprints using the Mascot protein identification software (Matrix Science). Where no significant matches were found, subsequent MS/MS analysis was performed using the top five m/z ion peaks. The KentProt database, a modified form of SwissProt, was searched, accounting for the following conditions: Trypsin digestion, fixed modifications of carbomidomethyl cysteine, variable modifications of oxidation of methionine, and allowing for up to one missed cleavage. MS data scores over the Mascot significance threshold ($p < 0.05$) were confidently assigned to known proteins.

2.4.5 Measurement of Gelatinase Activity via Gelatin Zymography

Protein samples were prepared for SDS-PAGE in 4x reducing Laemmli sample buffer, but were not boiled. Prepared samples were run as standard on SDS-PAGE gels containing 1% gelatin at 4°C for 30 minutes at 100 V, followed by 1 hour at 150 V in 1X SDS running buffer. Following SDS-PAGE, gels were washed twice in a 2.5% Triton X-100 solution for 20 minutes, followed by 2 x 15 minute washes in assay buffer (20 mM Na_2HPO_4, 50 mM NaCl, pH 8.0). Gels were then left overnight in assay buffer at 37°C, before staining for 20 minutes in Coomassie blue staining solution and subsequent destaining for 1 hour in destain solution.

2.4.6 Assessment of Hydrolytic Activity via Fluorescent Peptide Assay

A fluorescent peptide specific for *Pseudomonas aeruginosa* elastase, with the sequence Ala-Ala-Phe-Ala, containing a dabsyl acceptor at the N-terminus and an edans donor fluorophore at the C-terminus, was synthesised via solid-phase peptide synthesis and solubilised in 1% DMSO. FRET-based activity assays were then carried out using the conditions described by Elston *et al.* (Elston, Wallach, & Saulnier, 2007) and a Cary Eclipse Fluorescence Spectrophotometer (Agilent) with data being collected using the built-in Kinetics program.

2.4.7 Determination of Protein Stability via Unfolding Assay

To measure protein unfolding and establish the $\Delta G^0(H_2O)$ of recombinant elastase, a denaturation curve experiment was performed in which 10 µM elastase was incubated with varying concentrations of guanidine hydrochloride for 10 minutes at room temperature,

followed by measurement of intrinsic fluorescence at an emission wavelength of 335 nm in a Cary Eclipse Fluorescence Spectrophotometer. This wavelength was determined by performing emission wavelength scans of recombinant elastase in the absence of guanidine hydrochloride and in the presence of 6 M guanidine hydrochloride following excitation at 280 nm.

2.4.8 Measurement of Serum Antibody Titre via Indirect ELISA

Each well of a 96 well Nunc-Immuno™ MaxiSorp™ plate was coated with 100 ng of recombinant elastase overnight at 4°C. The following morning, serum dilutions were prepared in assay buffer (1% BSA in 0.1% PBST), plates were washed 4 times with TBST and 100 µL of diluted antiserum was added to the wells. Following a 1 hour incubation at room temperature whilst shaking on a plate shaker, the plate was washed again 4 times with TBST and probed with 100 µL of a conjugated secondary antibody at the recommended dilution in 1% BSA and 0.1% PBST. Plates were then incubated for a further hour at room temperature on a plate shaker, before washing 4 times with TBST. 100 µL of pNPP or TMB substrate was added and the plate was incubated for 15 minutes at 37°C or room temperature respectively. Absorbance was then read at 405 nm for alkaline phosphatase conjugated antibodies, or 450 nm for horseradish peroxidase conjugated antibodies, using a FLUOstar® OPTIMA microplate reader (BMG Labtech).

2.4.9 Assessment of Antibody Sensitivity via Sandwich ELISA

A 96 well Nunc-Immuno™ MaxiSorp™ plate was sensitised with 100 µL dilutions of affinity purified anti-elastase polyclonal antibody overnight at 4°C. The following morning, the plate was washed 4 times with TBST, and 100 µL elastase dilutions were added to the wells, prepared in assay buffer (1% BSA in 0.1% PBST). Following a 1 hour room temperature incubation on a shaker, plates were again washed and 100 µL dilutions of HRP-labelled affinity purified anti-elastase polyclonal antibody were added to each well. The plate was again incubated for 1 hour at room temperature, shaking on a plate shaker, and washed 4 times with TBST. Colour was developed via the addition of 100 µL TMB Substrate Solution (Biopanda) and, after a 10 minute room temperature incubation, 100 µL of Stop Solution (Biopanda) was added to prevent further development. Absorbance was read at 450 nm on a FLUOstar® OPTIMA microplate reader (BMG Labtech).

2.4.10 Assessment of Patient-Derived Clinical Isolates via Sandwich ELISA

A variety of *Pseudomonas* and non-*Pseudomonas* clinical isolates cultured from patient sputum samples were provided by the laboratory of Dr Jane Davies at the National Heart and Lung Institute at Brompton Imperial College London. These samples comprised “first isolates”, the

earliest confirmed *Pseudomonas*-positive isolates from Cystic Fibrosis patients, "chronic isolates", isolates obtained following prolonged *Pseudomonas* infection, and "control isolates", a range of non-*Pseudomonas* but clinically relevant Cystic Fibrosis bacterial strains. Isolates were received as glycerol stocks and were revived by streaking overnight on LB-agar plates, incubated at 37°C overnight. 3 mL overnight cultures were then grown overnight at 37°C from a single colony, and supernatant for assessment was obtained via centrifugation at 4,000 x g for 10 minutes. Sandwich ELISAs were then performed as in **Section 2.4.9**, wherein 50 uL of culture supernatant was diluted ½ in 2% BSA and 0.2% PBST. Further information on isolates tested is available upon request to Dr Jane Davies.

Table 2.5 | Clinical Isolate Sample IDs provided by the National Heart & Lung Institute, Brompton Imperial College.

Sample ID	Isolate Classification
F1 – F31	*P. aeruginosa* - First Isolate
CH1 – CH10	*P. aeruginosa* - Chronic Isolate
C1 – C4	*Staphylococcus aureus*
C5 – C8	*Klebsiella pneumoniae*
C9 – C12	*Escherichia coli*
C13 – C16	*Stenotrophomonas maltophilia*
C17 – C20	*Serratia marcescens*

2.4.11 Mapping of Linear Epitopes of Polyclonal Antibodies via Peptide Array

To identify linear epitopes recognised by affinity purified antibodies, a synthetic peptide array was constructed. The array consisted of overlapping 15 amino acid residue long peptide "spots", comprising the full sequence of mature elastase. In order to probe the array, it was first washed with PBST 4 times for 5 minutes, followed by an hour of blocking in 5% skimmed milk in PBST. Following blocking, the array was probed with 20 mL of 100 ng/mL HRP-labelled antibody diluted in 5% skimmed milk and incubated for 1 hour at room temperature with shaking. The array was washed again with PBST and 5 mL of TMB Substrate Solution (Biopanda) was added to develop a signal. Once spots had developed, the array was washed thoroughly with water to stop the reaction.

2.5 Antibody Phage Display

2.5.1 Extraction of Total RNA from Peripheral Blood Lymphocytes

Peripheral blood lymphocytes (PBLs) were prepared by Orygen Antibodies from a New Zealand White rabbit immunised with recombinant LasB (RA528), resuspended in RNAlater (Ambion) and subsequently aliquoted in volumes of 200 µL. Four PBL aliquots were processed using the RNeasy RNA extraction kit (Qiagen) in order to purify total RNA following the manufacturer's protocols.

2.5.2 Generation of First Strand cDNA for the Heavy and Light Chain Antibody Fragments

cDNA synthesis from purified RNA was performed via reverse-transcription PCR using Superscript IV reverse transcriptase (Invitrogen) for and an oligonucleotide mix incorporating species-specific forward primers for the heavy and kappa light antibody chain variants provided by Alta Biosciences and prepared at a concentration of 2 pmol/µL. When working with material from immunised sheep, lambda light chain cDNA was also synthesised. The initial reaction mixture was incubated at 65°C for 5 minutes, followed by 1 minute of quenching on ice. Subsequently, 7 µL of reverse transcriptase master mix described in **Table 2.6** was added to each reaction and incubated at 55°C for 15 minutes, followed by heat inactivation at 80°C for 10 minutes. Reaction components are described in **Tables 2.6 and 2.7**.

Table 2.6 | Reaction components for initial stage of reverse transcription of cDNA from total RNA.

Reagent	Volume / reaction (µL)	Conc. / reaction
Forward Primer Mix	1	0.1 µM
RNA	5	30 ng/µL
dNTP Mix	1	0.5 mM each
nfH_2O	6	N/A

Table 2.7 | Reaction components for second stage of reverse transcription of cDNA from total RNA.

Reagent	Volume / reaction (µL)	Conc. / reaction
5x SSIV Buffer	4	1x
0.1 M DTT	1	5 mM
RNAse Out (Invitrogen)	1	40 U
SuperScript IV Reverse Transcriptase	1	200 U

2.5.3 Amplification of scFv and Fab Fragments via Polymerase Chain Reaction

2.5.3.1 Amplification of Fab Fragments

Amplification of antibody chain DNA variants was performed using Phusion Hi-Fidelity Polymerase (ThermoFisher Scientific™). Primer sets were provided by the industrial partner Mologic Ltd., and incorporated primers specific to the rabbit heavy and kappa light antibody chains of IgG, as well as sheep heavy chain, kappa and lambda light chain variants. Reaction components and conditions are described in **Table 2.8** and **Table 2.9**.

Table 2.8 | Reaction components used for PCR amplification of antibody chain DNA fragments.

Reagent	Volume / reaction (µL)	Conc. / reaction
5X GC Buffer	10	1x
Phusion Polymerase	0.5	1 U
Forward Primer	1.25	3 µM
Reverse Primer Set	1.25	3 µM
10 mM dNTPs	2	400 µM
DMSO	1.5	3% (v/v)
nfH_2O	28.5	N/A
cDNA Template	5	Not quantified

Table 2.9 | Reaction conditions used for PCR amplification of antibody chain DNA fragments.

Temperature (°C)	Time (s)	
98	120	
98	10	35 Cycles
58	30	
72	40	
72	600	

2.5.3.2 Amplification of scFv Fragments

25 separate PCR reactions were performed under the conditions described in **Section 2.5.3.1** using different combinations of 25 primers to amplify the variable rabbit heavy and kappa light chain repertoire. Following purification of PCR products, a second pull-through PCR reaction was performed incorporating equal amounts of heavy and light chain DNA as a template in order to assemble full-length scFv gene products. The primers used are listed in **Table 2.10**.

Table 2.10 | Primer sequences for the amplification and assembly of rabbit scFv fragments from PBLs.

Primer Name	**Primer Sequence (5' → 3')**
rVH5' SfiI Reverse 1	GCCCAGCCGGCCATGGCCCAGTCGGTGGAGGAGTCCRGG
rVH5' SfiI Reverse 2	GCCCAGCCGGCCATGGCCCAGTCGGTGAAGGAGTCCGAG
rVH5' SfiI Reverse 3	GCCCAGCCGGCCATGGCCCAGTCGYTGGAGGAGTCCGGG
rVH5' SfiI Reverse 4	GCCCAGCCGGCCATGGCCCAGSAGCAGCTGRTGGAGTCCGG
rVH5' SfiI Reverse 5	GCCCAGCCGGCCATGGCCCAGTCGCTGGAGGAGTCCGGGGGT
rVH3' Linker Forward 1	CTCAGAGCCAGAGCCAGAAGATTTACCTTCCGATGGGCCCTTGGT GGAGGCTGARGAGAYGGTGACCAGGGTGCC
rVH3' Linker Forward 2	CTCAGAGCCAGAGCCAGAAGATTTACCTTCGACTGAYGGAGCCTT AGGTTGC
rVL5' Linker Reverse 1	GGCTCTGGCTCTGAGTCTAAAGTGGATGACGAGCTCGTGMTGAC CCAGACTCCA
rVL5' Linker Reverse 2	GGCTCTGGCTCTGAGTCTAAAGTGGATGACGAGCTCGATMTGAC CCAG ACTCCA
rVL5' Linker Reverse 3	GGCTCTGGCTCTGAGTCTAAAGTGGATGACGAGCTCGTGATGACC CAG ACTGAA
rVL5' Linker Reverse 4	GGCTCTGGCTCTGAGTCTAAAGTGGATGACGCTCAAGTGCTGACC CAGA G
rVL5' Linker Reverse 5	GGCTCTGGCTCTGAGTCTAAAGTGGATGACGMCMYYGWKMTG ACCCAGACTCC
rVL3' NotI Forward 1	CAGTCATTCTCGACTTGCGGCCGCACGTTTGATTTCCACATTGGTG CC
rVL3' NotI Forward 2	CAGTCATTCTCGACTTGCGGCCGCACGTAGGATCTCCAGCTCGGT CCC
rVL3' NotI Forward 3	CAGTCATTCTCGACTTGCGGCCGCACGTTTGACSACCACCTCGGTC CC
Pullthrough Forward	CCTTTCTATGCGGCCCAGCCGGCCATGGCC
Pullthrough Reverse	CAGTCATTCTCGACTTGCGGCCGC

2.5.4 Agarose Gel Purification of Antibody Chain PCR Products

PCR products were combined for each reverse primer set and separated via gel electrophoresis on a 1% agarose gel for 1 hour at 150 V using an ethidium bromide stain. Following separation, the amplified bands were visualised under UV light, excised with a sterile disposable scalpel and purified via the PureLink™ Quick Gel Extraction kit (Invitrogen™) following the manufacturer's instructions.

2.5.5 Enzymatic Restriction Digests of PSFD Phagemid and Antibody Chain DNA

All digests for antibody libraries were performed with restriction endonucleases (New England Biolabs®), using hi-fidelity enzymes where available. Digests were performed for 20 hours at the temperatures recommended by the manufacturer. Following digestion, linearised pDNA was separated on a 1% agarose gel and purified as in **Section 2.5.4**, whereas digested antibody chain DNA was purified via the PureLink™ PCR Purification Kit (Invitrogen™) following the manufacturer's instructions.

2.5.6 Ligation and Concentration of Digested Antibody Chain DNA and Phagemid Vector

Ligations were performed using T4 DNA Ligase (New England Biolabs®) at a vector:insert ratio of 1:7, incubating reactions at 16°C for 16 hours, followed by a 10 minute heat inactivation at 80°C in a thermocycler. Following ligation, DNA was concentrated and buffer exchanged into nuclease free water via the GeneJET Gel Extraction and DNA Cleanup Micro Kit (ThermoFisher Scientific™) following the manufacturer's instructions.

2.5.7 Transformation of Antibody Libraries in TG-1 *E. coli* via Electroporation

10 transformation ligations were performed per antibody chain ligation in the phage display competent *E. coli* strain TG-1 (Lucigen). Cells were incubated with 2 µL of cleaned up ligation mixture for 30 minutes on ice before electroporation in 0.1 mm gene pulser cuvettes (Bio-Rad). Cells were electroporated at a pulse of 1.8 kV for 5 mS in an *E. coli* Pulser™ (Bio-Rad), followed by addition of 970 µL recovery medium (Lucigen) and incubation at 37°C, shaking at 225 rpm for 1 hour. Following incubation, 1 in 10 serial dilutions of the transformation reaction were made and plated on TYE agar plates containing 1% glucose and 100 µg/mL ampicillin and grown overnight at 37°C in a static incubator. The remaining transformation culture was centrifuged at 3,300 x g for 10 minutes and all but 2 mL of the supernatant was discarded. The resulting pellet was resuspended in the remaining media and streaked on a 250 mL TYE agar bioassay plate

containing 1% glucose and 100 µg/mL ampicillin to be grown overnight at 30°C. Library size was estimated the next day by counting the colonies on the dilution plates, and libraries were recovered by gently scraping colonies from the bioassay plates and resuspending in 2 mL 2xTY media containing 15% glycerol. 500 µL of resuspended cells was purified using the Zyppy® Plasmid Midiprep Kit (Zymo Research) and the remainder was stored as 120 µL aliquots at -80°C.

2.5.8 Screening of Antibody Libraries via Colony PCR and Restriction Digests

Libraries were screened via colony PCR with Taq polymerase (New England Biolabs™) using a species specific heavy chain forward primer and the universal M13 reverse primer. 18 bacterial colonies were picked from plates containing the transformed library and colony PCR was carried using the components described in **Table 2.11** and under the conditions described in **Table 2.12**. The resulting PCR product was run on a 1% agarose gel to identify successfully ligated clones.

Table 2.11 | Reaction components for colony PCR of antibody libraries

Reagent	Volume / reaction (µL)	Conc. / reaction
10x Standard Taq Buffer	3	1x
Taq Polymerase	0.3	1.5 U
Forward Primer	0.6	2 µM
Reverse Primer	0.6	2 µM
10 mM dNTP Mix	0.6	0.2 mM
nfH_2O	24.9	N/A

Table 2.12 | Reaction conditions for colony PCR of antibody libraries

Temperature (°C)	Time (s)	
95	120	
95	30	35 Cycles
58	30	
68	90	
68	600	

Successfully ligated clones were purified via the PureLink™ PCR Purification Kit (Invitrogen™) and digested with the FastDigest restriction endonucleases (ThermoFisher Scientific™) MvaI and

BsuRI, or their slow digest alternatives BstNI and HaeIII, known to cut frequently in the heavy and light chain regions respectively. Digests were performed following the manufacturer's protocols prior to separation on a 3% agarose gel.

2.5.9 Infection of Antibody Libraries with M13KO7 Helper Phage

A 500 mL baffled flask containing 50 mL 2xTY media with 100 µg/mL ampicillin and 2% glucose was inoculated with 20 µL of the library glycerol stock and incubated at 37°C in a shaking incubator until the cells reached an OD_{600} of approximately 0.5. Cells were then infected with 20 µL of M13K07 helper phage glycerol stock at a concentration of 2×10^{12} pfu/mL and incubated in a 37°C water bath for 30 minutes. Infected cells were harvested via centrifugation at 3,300 x g for 10 minutes and resuspended in 5 mL 2xTY media containing 100 µg/mL ampicillin and 50 µg/mL kanamycin. The resuspended cells were added to a 2 L baffled flask containing 500 mL 2xTY media with 100 µg/mL ampicillin and 50 µg/mL kanamycin and grown overnight at 30°C with shaking at 220 rpm.

2.5.10 Harvest of Antibody Fragment Presenting Phage Particles via PEG Precipitation

Overnight TG-1 cultures infected with M13KO7 helper phage were harvested via centrifugation at 11,000 x g for 10 minutes. To the phage-containing supernatant, 100 mL of precipitation buffer (20% poly(ethylene glycol) 6000, 2.5 M sodium chloride) was added and incubated at 4°C for 1 hour. Following incubation, the solution was centrifuged at 11,000 x g for 30 minutes and the supernatant was discarded. The phage pellet was resuspended in 20 mL chilled water and 8 mL of precipitation buffer and incubated for a further 20 minutes at 4°C, followed by a 30 minute centrifugation at 3,300 x g. The supernatant was again discarded and resulting pellets were resuspended in a total of 3 mL of PBS prior to centrifugation in a microcentrifuge at 3,300 x g for 10 minutes. The phage-containing supernatant was then recovered and used immediately for biopanning, or stored short-term at 4°C.

2.5.11 Enrichment of Antibody Libraries via Phage Display Biopanning

A 4 mL immunotube was coated with 4 mL of 10 µg/mL recombinant LasB in PBS overnight at 4°C. The following morning, the immunotube was washed 3 times with PBS and blocked for 2 hours at room temperature in 2% (w/v) skimmed milk in PBS (MPBS). After blocking, the tube was washed again three times with PBS and incubated with a 4 mL phage solution containing 10^{12} phage pfu in 2% MPBS for 30 minutes on an under-over rotating mixer, followed by 90 minutes standing at room temperature. The supernatant was then discarded and the tube was

washed 20 times with 0.1% PBST, followed by 20 PBS washes. Bound phage was eluted with 1 mL of 100 mM glycine, pH 3.0 on an under-over rotating mixer for 10 minutes, and neutralised via addition of 0.5 mL 1 M Tris-HCl pH 7.4. This eluted phage was then used to infect 10 mL of an exponentially growing culture of TG-1 *E. coli*, and from this culture 10-fold serial dilutions were made and plated on TYE agar plates containing 100 µg/mL ampicillin and 2% glucose and grown overnight at 37°C. The remaining culture was centrifuged at 3,300 x g for 10 minutes and the resulting pellet was resuspended in 1 mL TYE media. The resuspended pellet was plated on a large TYE bioassay plate containing 100 µg/mL ampicillin and 2% glucose and grown overnight at 30°C. Biopanning was performed 3 times per library at an antigen concentration of 10 µg/mL, followed by a final 4th pan at 1 µg/mL.

2.5.12 Assessment of Harvested Phage via Polyclonal Phage ELISA

Recombinant antigen dilutions were made in PBS at concentrations of 1 µg/mL, 100 ng/mL and 10 ng/mL. A 96 well Nunc Maxisorp™ plate (ThermoFisher Scientific™) was sensitised with 100 µL of each LasB dilution, including blank wells containing only PBS, and incubated overnight at 4°C. The following morning, the plate was washed 3 times with PBS and each well was blocked with 300 µL of 2% MPBS for 1 hour at room temperature. The wells were subsequently washed again three times with PBS and 100 µL of each PEG-harvested phage sample was added to their respective wells at a dilution of 1:9 in 2% MPBS. Following a 90 minute incubation at room temperature, the plate was washed 3 times with PBST, followed by 3 PBS washes. 100 µL of 0.1 µg/mL anti-M13 HRP-conjugated primary antibody (Sino Biological) was added to each well and the plate was incubated for an additional 90 minutes at room temperature. The plate was then washed 3 times with PBST and 3 times with PBS, and 100 µL of TMB substrate solution was added to each well. Colour was allowed to develop for 20 minutes before the reaction was halted by addition of 100 µL 1 M hydrochloric acid to each well, and the absorbance at 450 nm was read on a plate reader.

2.5.13 Periplasmic Extraction of Individual Clones for Screening

96 colonies were picked from dilution plates streaked with the enriched library and grown in 100 µL 2-YT containing 100 µg/mL ampicillin and 1% glucose in a sterile 96-well cell culture plate (Corning), incubated overnight at 30°C and shaking at 230 rpm. The following morning, 2 µL of culture from each well was transferred to a new 96-well cell culture plate with 200 µL of 2-YT containing 100 µg/mL ampicillin and 0.1% glucose, which was then incubated at 37°C for a further 3 hours or until an OD_{600} of 0.9 was reached. IPTG was then added to each well to a final concentration of 1 mM and the plate was incubated overnight at 30 °C, shaking at 230 rpm. Cells

were then harvested via centrifugation at 1,800 x g for 10 minutes and the supernatant was discarded. Cell pellets were then resuspended in 100 µL of ice-cold lysis buffer (20% sucrose, 200 mM tris pH 7.5, 1mM EDTA, 500 µg/mL lysozyme). The resuspended cell pellets were incubated on a shaking platform at 4°C for 10 minutes followed by addition of 2 µL 250 mM $MgSO_4$ and further incubation for 10 minutes on a shaking platform at 4°C. The culture plate was then centrifuged at 1,800 x g for 10 minutes and the periplasmic supernatant aspirated for analysis via ELISA.

2.5.14 Assessment of Individual Clones via Monoclonal Expression ELISA

Each well of a 96 well Nunc Maxisorp™ plate (ThermoFisher Scientific™) was coated with 1 µg/mL recombinant antigen overnight at 4°C. The following morning, the plate was washed three times with PBS and blocked in 300 µg/mL 1% BSA-PBS for 1 hour at room temperature, followed by three further washes with PBS. Periplasmic samples extracted in section 2.5.13 were diluted 1:9 in 10% BSA-PBS and 90 µL was added to each well. The plate was incubated for 90 minutes at room temperature, followed by 3 PBST washes and 3 PBS washes. 100 µL of 1 µg/mL HRP conjugated anti-Myc tag antibody (Abcam) was added to each well, followed by a 90 minute room temperature incubation, and the plate was again washed 3 times with PBST and 3 times with PBS. Signal was developed using 100 µL of TMB substrate solution and the reaction was stopped after 10 minutes with 100 µL 1M hydrochloric acid. The absorbance in each well was then read at 450 nm on a plate reader.

2.6 Lateral Flow Development and Assessment

2.6.1 Conjugation of Detector Antibody to Colloidal Gold Nanoparticles

In order to determine the appropriate pH for conjugation of affinity purified antibody to gold nanoparticles, a variety of conjugation buffers ranging from pH 5.0 to pH 9.3 were assessed. 100 µL of 40 nm colloidal gold nanoparticles (BBI) were added to 10 wells of a 96-well polystyrene plate (StarLab) containing 1.5 µL 1 mg/mL antibody and 5 µL of each conjugation buffer. Electrostatic conjugation was allowed to occur during a 10 minute incubation period at room temperature, and 5 µL of 1 M NaCl was then added to each well. If the solution's colour changed from red to purple, the conjugate was deemed unstable and the buffer unfit for conjugation in a lateral flow device. If the solution maintained its red colour, the conjugate was considered stable. Once an appropriate buffer was selected, a large-scale conjugation was performed containing 50 µL conjugation buffer, 15 µL antibody and 1 mL colloidal gold. After a 10 minute incubation at room temperature, 10 µL of 200 mg/mL BSA was added to occupy any remaining

binding sites. After 30 minutes, the gold nanoparticles were pelleted at 4000 x g for 10 minutes and resuspended in 1 mL drying buffer (100 mM Tris-HCl, pH 9.4, 1% Tween-20, 3% BSA, 5% sucrose).

2.6.2 Assembly of Lateral Flow Wet Strips

1 mg/mL affinity purified antibody was plotted on 30 cm x 25 mm UniSart® CN140 membrane bands (Sartorious) in 1% sucrose using an IsoFlow Dispenser (Imagene Technology) at a rate of 0.1 µL/mm. Bands were then dried using an industrial oven (Hedinair) at a temperature of 60°C and a rate of 10 mm/sec before being mounted on backing card with a 22 mm layer of grade 222 thick chromatography paper (Ahlstrom) at the top end, and cut into 5 mm strips using a Matrix 2360 programmable shear (Kinematic Automation).

2.6.3 Lateral Flow Immunoassay Wet Testing

Anti-LasB wet strips were incubated for 10 minutes in a solution containing 4 µL of gold-conjugated detector antibody and 36 µL of recombinant elastase at 1/10 serial dilutions from 1 µg/mL to 100 pg/mL. After all solution was absorbed by the strip, the test line intensity was read using a cube reader, a handheld device provided by the industrial partner Mologic Ltd.

2.6.4 Enzyme Enhanced Lateral Flow Immunoassay Wet Tests

Anti-elastase wet strips were incubated for 10 minutes in a solution containing 36 µL recombinant elastase at a concentration of 10 ng/mL and 4 µL of HRP-labelled detector antibody at serial dilutions from 1/500 to 1/64000. Once all solution was absorbed by the strip, the test line intensity was read using a cube reader. Once an appropriate detector antibody dilution was determined, wet tests were repeated at a constant antibody dilution and variable elastase concentration to generate a standard curve.

2.6.5 Assembly of Lateral Flow Immunoassay Devices

Capture antibody was plotted and dried as in **Section 2.5.2**. 100 µL gold-conjugated antibody was sprayed on 8951 cotton linters (Ahlstrom) using an IsoFlow Dispenser air-pump attachment and dried at a rate of 5 mm/sec. Lateral flow strips were assembled on a backing card, including a layer of FR1 blood separation membrane (Advanced Microdevices) acting as a sample pad and 222 chromatography paper (Ahlstrom) acting as an absorbent pad, with each layer overlapping as in **Figure 2.1** and cut into 5 mm strips as in **Section 2.5.2**. Strips were then secured in a plastic housing and crushed together to tighten.

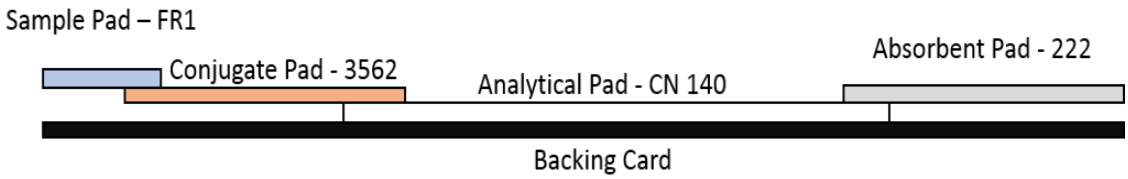

Figure 2.1 | Schematic depicting the overlapping membrane layers of a paper based lateral flow immunoassay.

2.6.6 Lateral Flow Immunoassay Dry Testing

80 µL of prepared sample was applied to the sample pad of the assembled lateral flow immunoassay devices and, following a 10 minute incubation at room temperature, test line intensities were read using a cube reader.

2.7 Calculations

The equations mentioned in this section were used for protein characterisation and assay parameters throughout this thesis.

2.7.1 Equilibrium Constant

K_{eq} = Fraction unfolded / (1 – fraction unfolded)

2.7.2 Standard State Free Energy Change

ΔG^0 = (-R*T*ln(keq)) Where R = 8.314 and T = 298 K

2.7.3 Lower Limit of Detection

LLOD = Mean absorbance of negative control * 3 standard deviations of the mean

2.8 Statistical Analysis

Statistical analysis was conducted for ELISAs where clinical isolates were analysed with at least three technical replicates.

2.8.1 One Way Analysis of Variance and Tukey Grouping

The software Minitab 18 was used to complete one-way analysis of variance (ANOVA) in order to determine statistically significant differences between the means of clinical isolates and control samples. Tukey grouping was used to sort data into statistically significant groups and the significance was determined to a 95% confidence level.

2.8.2 Receiver Operator Characteristic Curve Generation

Receiver operator characteristic (ROC) curves were generated using the software MedCalc in order to plot the true positive rate and false positive rate of a diagnostic assay. The area under the curve was calculated to measure how well the assay can distinguish between diagnostic groups.

Chapter 3

Generation and Characterisation of Recombinant Antigens in *Escherichia coli*

3.1 Introduction to the Work Described in this Chapter

This chapter describes the cloning and expression of target biomarker genes in a bacterial expression system. Originally, the scope of this project covered not only expression of potential antigens from *P. aeruginosa* infections in Cystic Fibrosis patients, but also a range of human biomarkers of inflammation, particularly those concerning inflammatory lung disease. Genes of interest were either amplified via the polymerase chain reaction using cDNA clones purchased from Origene as template DNA, or synthesised via GeneArt®'s gene synthesis service (Invitrogen) and cloned into a bacterial expression vector to be expressed in the *Escherichia coli* strain BL21*(DE3)pLysS. Following successful expression, recombinant antigens were to be purified via nickel affinity chromatography and subsequently characterised prior to immunisation to ensure a high quality, highly pure immunogen.

A range of human antigens were initially investigated as biomarkers of inflammation, including the Receptor for Advanced Glycation End-Products (RAGE) (UniProt Accession: **Q15109**) and its soluble form (sRAGE), the eosinophilic Major Basic Protein (MBP) (UniProt Accession: **P13727**), Matrix Metalloproteinase 9 (MMP9) (UniProt Accession: **P14780**) and the Sialic acid-binding Ig-like Lectin 8 (Siglec-8) (UniProt Accession: **Q9NYZ4**), with the intention of investigating the expression of these and then subsequently using these to develop ELISA-based and lateral flow diagnostic assays for inflammatory lung diseases such as chronic obstructive pulmonary disorder (COPD) or, in the case of MMP9, chronic wounds.

In addition to these human protein targets, two secreted proteases of the bacterium *Pseudomonas aeruginosa* were also investigated. Staphylolysin, encoded by the *lasA* structural gene (UniProt Accession: **P14789**), a staphylolytic endopeptidase involved in the breakdown of *Staphylococcus aureus* to facilitate opportunistic infection by *P. aeruginosa*, and elastase, encoded by the *lasB* structural gene (UniProt Accession: **P14756**), a protease with a broad substrate specificity known to break down components of the extracellular matrix and immune system. These two proteases were investigated with the intention of developing lateral flow diagnostic assays for the early detection of *P. aeruginosa* in the lungs of cystic fibrosis patients and prediction of pulmonary exacerbations.

Characterisation of elastase was performed via a variety of analytical techniques, including SDS-PAGE, western blot analysis, matrix assisted laser desorption ionisation time of flight mass spectrometry (MALDI-ToF-MS), fluorescence resonance energy transfer (FRET) assays, gelatin zymography, and refolding assays in order to assess specific activity and conformational stability prior to animal immunisation as a means to raise specific polyclonal antibodies.

The aim of the work described in this chapter was initially to generate a panel of plasmid constructs containing the above genes for expression in *E. coli*, Chinese hamster ovary (CHO) cell and *L. tarentolae* expression systems. It is noted that it was never the intention of this project to develop all of the targets described above; this being beyond the scope or capabilities of a single PhD project. However, by selecting a range of targets most promising in terms of expression and characterisation, the assay requirements of the industrial partner at the time would be assessed to then allow a focus on a single or small number of targets. Thus, following successful cloning and trial expressions in *E. coli*, the focus of the project quickly shifted to the expression, purification and characterisation of recombinant *Pseudomonas aeruginosa* elastase produced in *E. coli*, with the ultimate goal of generating highly sensitive and specific antibodies to recombinant elastase for incorporation into ELISA and lateral flow based diagnostic immunoassays, at the behest of the industrial partner Mologic Ltd. The primary rationale for the focus on elastase was two-fold; (1) the partner company's desire to develop a rapid diagnostic test for the presence of elastase which had good potential for the diagnosis of chronic wounds and early-stage Cystic Fibrosis infections, and (2) early results showed that of the chosen panel of candidate proteins, elastase expressed well and was able to be purified and characterised whilst the majority of the other candidate proteins were either not well expressed or their expression not assessed (e.g. the mammalian expression plasmids were used to make stable expressing CHO cells but due to the decision to forward the development of an elastase assay these were never assessed for expression). As such, there was a collective agreement to focus on elastase as there was not the capacity to assess all of the originally proposed candidates. As described in the introduction section, *P. aeruginosa* virulence factors are of great clinical interest for the detection of early *P. aeruginosa* infection in the lungs and airways of cystic fibrosis patients, as well as the prediction of pulmonary exacerbations.

3.2 Generation of Plasmid Constructs for the Expression of Target Genes

3.2.1 Generation of Modified Plasmids to Facilitate Tagging of Recombinant Proteins and Sub-cloning between Three Expression Vectors

To allow for easy identification and purification of recombinant antigen targets following expression, a small oligonucleotide fragment was designed and synthesised via the GeneArt® Gene Synthesis service (Invitrogen). This oligonucleotide incorporated a polyhistidine tag that would be C-terminal of the cloned target open reading frame (**Figure 3.1**) for purification via nickel affinity chromatography and a v5 viral epitope for identification of the recombinant product via western blotting, preceded by a prothrombin cleavage sequence to facilitate easy removal of these tags prior to immunisation. Relevant restriction sites were also incorporated in order to sub-clone this oligonucleotide into three different expression vectors: pET-23b (Novagen) for expression in *E. coli*, pcDNA™ 3.1/V5-His TOPO™ (ThermoFisher) for expression in CHO-S cells, and pLEXSY-neo2 (Jena Bioscience) for expression in *L. tarentolae*.

Figure 3.1 | Schematic of the restriction sites and tags incorporated into the oligonucleotide sequence synthesised via GeneArt® Gene Synthesis.

3.2.2 Generation of Plasmid Constructs for Expression in BL21*(DE3)pLysS *E. coli*

In order to express the target antigens in *Escherichia coli*, the genes of interest were cloned into the pET 23b (+) bacterial expression plasmid (Novagen). For the human-derived target antigens RAGE, MBP, MMP-9 and Siglec 8, human cDNA clones obtained from Origene Technologies, Inc. were used as templates to amplify their respective DNA sequences via polymerase chain reaction, which were subsequently cloned into a modified version of the pET 23b plasmid containing a C-terminal thrombin cleavage site, v5 epitope and 6x polyhistidine tag. A list of primers used for PCR amplification are reported in **Table 2.1**. The sequences for the *Pseudomonas aeruginosa*-derived antigens staphylolysin (*lasA*) and elastase (*lasB*) were codon optimised for expression in *E. coli* and synthesised commercially via the GeneArt® Gene Synthesis service (Invitrogen), and included both a C-terminal thrombin cleavage site and 6x polyhistidine tag, which was subsequently cloned into the commercially available pET 23b (+) plasmid. Genes cloned into the modified pET 23b (+) vector were digested with the restriction endonucleases NheI and KpnI, whereas genes cloned into the commercial pET 23b (+) vector were digested with the restriction endonucleases BamHI and XhoI. Following ligation with T4 ligase, recombinant plasmid constructs were transformed into the *E. coli* cloning strain DH5α and clones were screened via restriction digest followed by analysis on a 1% agarose gel (**Figure 3.2**). Successful clones were identified by the presence of a dropout band at the expected size

of 1224 bp for RAGE, 1005 bp for sRAGE, 678 bp for MBP, 2113 bp for MMP9, 1509 bp for Siglec 8, 1317 bp for LasA and 1557 bp for LasB. (**Figure 3.2**). Plasmid DNA from successful clones was amplified via MiniPrep (Qiagen) and transformed in the *E. coli* protein expression strain BL21*(DE3)pLysS for trial expression and purification.

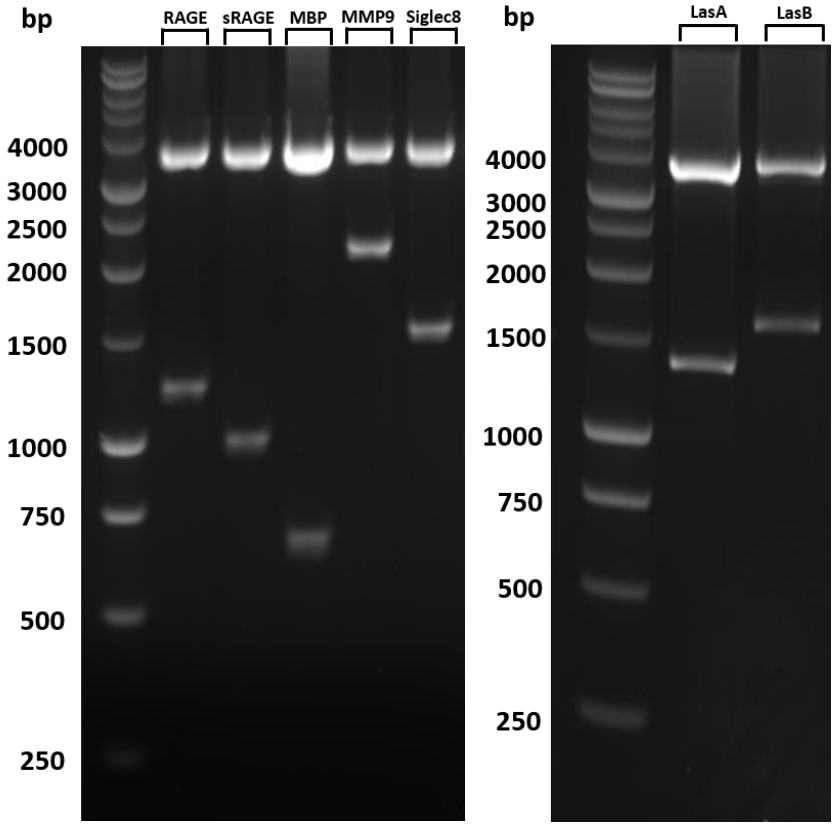

Figure 3.2 | Analytical 1% agarose gels containing pET 23b – antigen constructs, showing release of the genes of interest from the expression vector upon restriction digest with NheI/KpnI (Left) or BamHI/XhoI (right). The antigen of interest is denoted at the top of each lane. Expected band sizes were as follows: RAGE: 1224 bp; sRAGE: 1005 bp; MBP: 678 bp; MMP9: 2113 bp; Siglec 8: 1509 bp; LasA: 1317 bp; LasB: 1557 bp.

3.2.3 Generation of Plasmid Constructs for Expression in Chinese Hamster Ovary Cells

For stable expression in a suspension CHO cell line, the PCR amplified genes were cloned into a modified form of the commercially available pcDNA™ 3.1 v5-His TOPO™ mammalian expression vector (Invitrogen), incorporating the oligonucleotide sequence described in **Section 3.2.1**. The vector and amplified PCR products were digested with the restriction endonucleases NheI and KpnI and, following overnight ligation, reactions were transformed in the *E. coli* cloning strain DH5α. Clones were once again screened via restriction digest and analysed on 1% agarose (**Figure 3.3** Successful clones were identified by the presence of a dropout band at the expected

size of 1224 bp for RAGE, 1005 bp for sRAGE, 678 bp for MBP, 2113 bp for MMP9 and 1509 bp for Siglec 8 (**Figure 3.3**). Plasmid DNA from successful clones was amplified via MaxiPrep (Qiagen) to provide a sufficient quantity of recombinant plasmid for linearization and stable transfection into CHO-S.

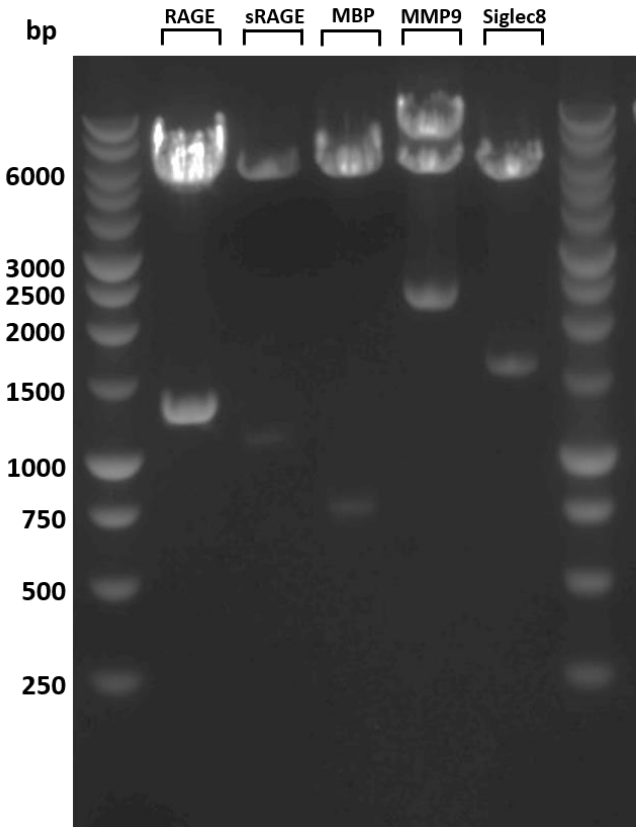

Figure 3.3 | Analytical 1% agarose gel containing pcDNA 3.1 – antigen constructs, showing release of the genes of interest from the expression vector upon restriction digest with NheI and KpnI. The antigen of interest is denoted at the top of each lane. Expected band sizes were as follows: RAGE: 1224 bp; sRAGE: 1005 bp; MBP: 678 bp; MMP9: 2113 bp; Siglec 8: 1509 bp.

3.2.4 Generation of Plasmid Constructs for Expression in *Leishmania tarentolae*

Target antigen genes were also cloned into the pLEXSY-neo2 expression vector, with the intention to express them in *Leishmania tarentolae*, a eukaryotic parasite expression system. This vector was also modified to include the tagged oligonucleotide depicted in **Figure 3.1** for ease of purification and subsequent identification of recombinant products following expression. The restriction endonucleases NheI and KpnI were once again used to clone amplified PCR products into the modified vector, which was then transformed in DH5α *E. coli*, and screened via restriction digest and separation on 1 % agarose (**Figure 3.4**). Successful clones were again identified by the presence of a dropout band at the expected size of 1224 bp for

RAGE, 1005 bp for sRAGE, 678 bp for MBP, 2113 bp for MMP9 and 1509 bp for Siglec 8 (**Figure 3.4**).

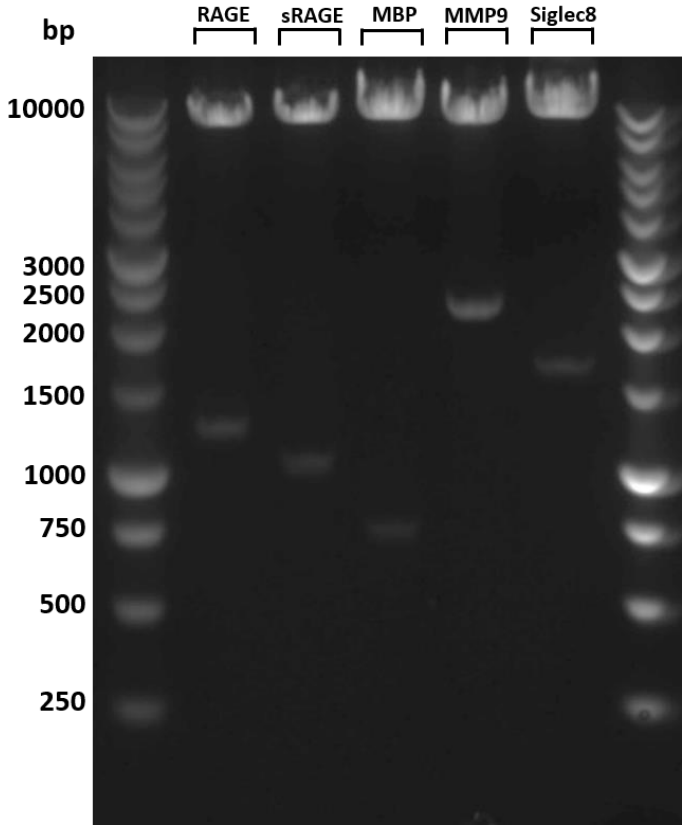

Figure 3.4 | Analytical 1% agarose gel containing pLEXSY neo-2 – antigen constructs, showing release of the genes of interest from the expression vector upon restriction digest with NheI and KpnI. The antigen of interest is denoted at the top of each lane. Expected band sizes were as follows: RAGE: 1224 bp; sRAGE: 1005 bp; MBP: 678 bp; MMP9: 2113 bp; Siglec 8: 1509 bp.

3.3 Expression of Target Antigen Genes in BL21*(DE3)pLysS *Escherichia coli*

3.3.1 Expression of Human Biomarkers of Inflammation in *E. coli*

Trial expression of the human biomarkers of inflammation was performed in the *E. coli* protein expression strain BL21*(DE3)pLysS. Cells were grown in 50 mL LB medium to an OD_{600} of 0.4 followed by induction of expression with 400 μM IPTG. Cell pellets were sampled prior to induction and following a 4 hour incubation at 25°C for assessment via transmission electron microscopy. Thin sections were prepared following the methods outlined in **Section 2.3.3** and **Section 2.3.4** and analysed on a JEOL-1230 transmission electron microscope, as it was predicted that expression of these complex human proteins in *E. coli* would result in the formation of aggregated material in the form of inclusion bodies, rather than a soluble product. A negative control was included consisting of BL21*(DE3)pLysS cells containing the empty modified pET23b

vector. The images generated (**Figure 3.5**) show formation of inclusion bodies in cells expressing MMP9, MBP, Siglec-8 and RAGE, observed as darkened areas at the poles of "Post-IPTG" cells. No inclusion bodies were visible in the cells expressing sRAGE (suggesting that this was either not expressed or expressed as a soluble protein) or, as to be expected, in the empty vector control cells.

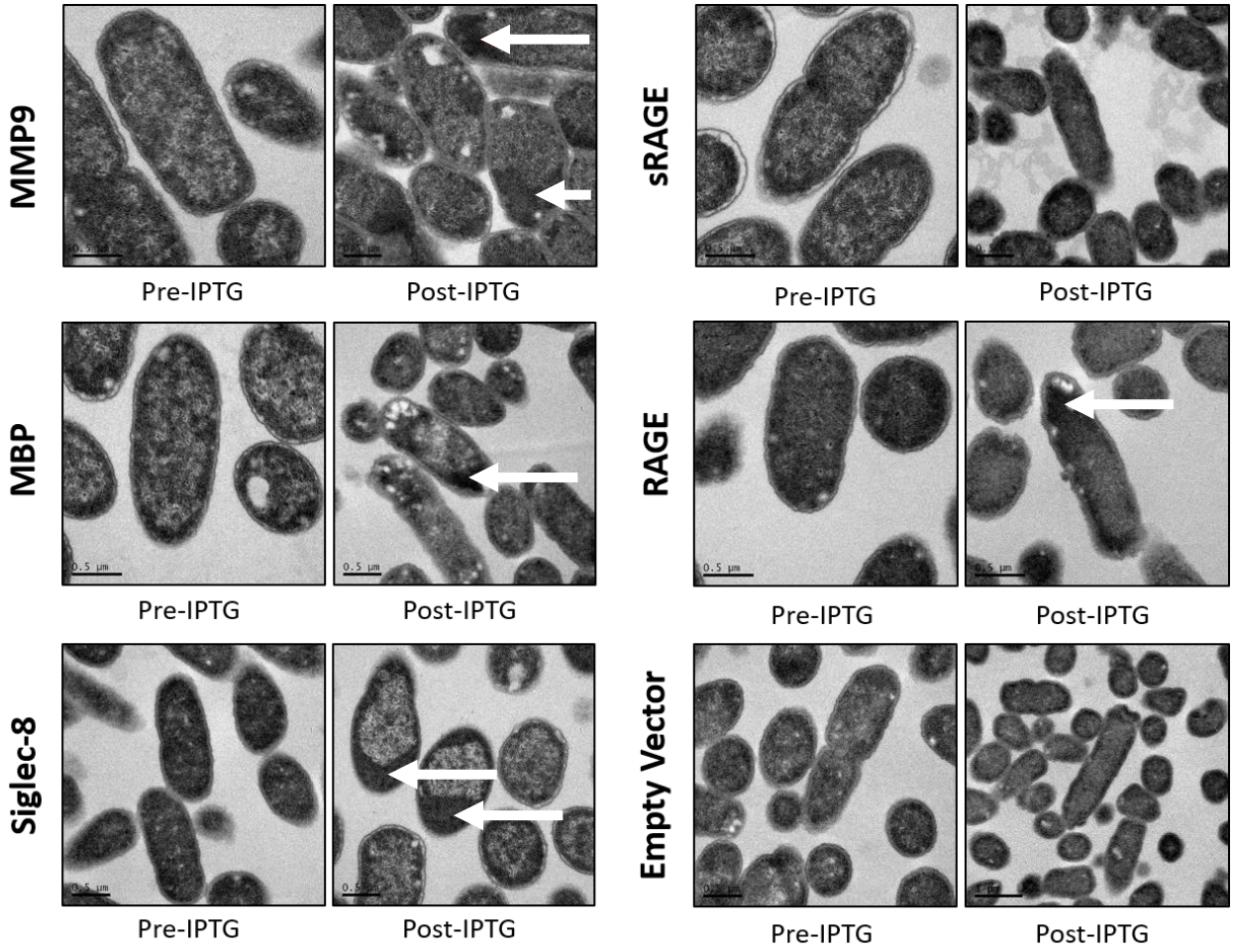

Figure 3.5 | Transmission electron microscopy of BL21*(DE3)pLysS cells expressing human targets of inflammation prior to and following induction with IPTG. Areas where inclusion bodies can be observed are highlighted by a white arrow.

3.3.2 Comparing the Effects of Time, Temperature and IPTG Concentration on Elastase Production in *Escherichia coli*

Prokaryotic expression of recombinant antigen genes was performed in the *E. coli* expression strain BL21*(DE3)pLysS via induction with the allolactose analogue isopropyl β-D1-thiogalactopyranoside (IPTG). Terrific Broth media was used for growth in order to achieve higher cell densities. From an overnight 10 mL culture, a 2 L baffled flask containing 400 mL of Terrific Broth media was inoculated to an OD_{600} of 0.1 and cells were allowed to grow to an OD_{600} of approximately 0.4 at 37°C. IPTG was then added to a final concentration of 400 µM to induce protein expression. In order to optimise expression, induction was performed overnight at 4 different temperatures: 19, 25, 30 and 37°C. Anti-his tag western blots were performed on whole cell lysates of induced cells at each induction temperature (**Figure 3.6**). At 37°C, processing of the propeptide appears to be inhibited, as there was an abundance of the 54 kDa preproelastase observed on the blot. At temperatures lower than 30°C some processing and/or degradation of the mature protease was evident (**Figure 3.6**). These fragments must still contain the C-terminus of the protein as this is where the His-tag that the antibody recognises resides, suggesting degradation from the N-termini. Induced cells growing at 30°C appeared to produce the most soluble 33 kDa processed product without degradation, so this temperature was used for future production of recombinant elastase.

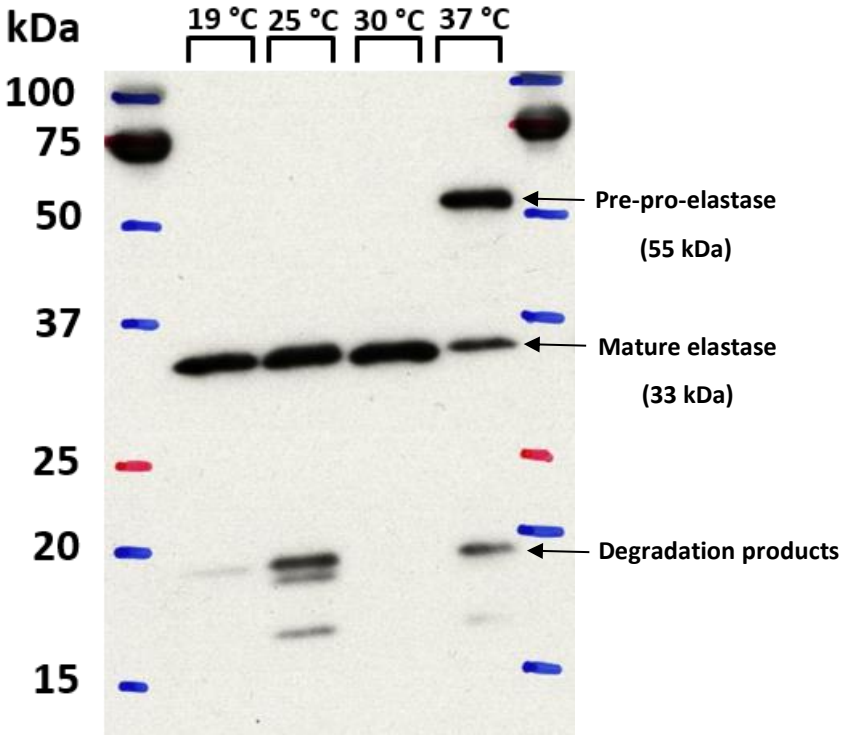

Figure 3.6 | Western blot analysis of *lasB* expressing BL21*(DE3)pLysS *E. coli* lysates induced with IPTG at 4 different temperatures. A HRP labelled anti-His tag primary antibody was used to detect recombinant elastase. Marker bands have been drawn on by hand as this blot was produced via overlay with chemiluminescent detection film rather than development on the direct transfer membrane.

3.3.3 Whole Cell Fractionation of Cells to Isolate Recombinant Elastase

To confirm secretion of recombinant elastase into the periplasm of *E. coli*, whole cell fractionations were performed to separate the cells into periplasmic, cytosolic, membranous and insoluble fractions (**Figure 3.7**). Fractionation was performed as described in **Section 2.3.2** following induction at 30°C. The majority of recombinantly expressed elastase was found in the periplasmic fraction, as determined via western blot analysis (**Figure 3.8**), suggesting a soluble, folded product due to the oxidising nature of the periplasm. A small amount of recombinant material also was found in both the insoluble and cytoplasmic fractions, likely as a result of the strong T7 promoter saturating the *sec* pathway of *E. coli*. From the Coomassie-stained SDS gel (**Figure 3.7**), no clear 33 kDa band was obvious, suggesting a low level of expression overall.

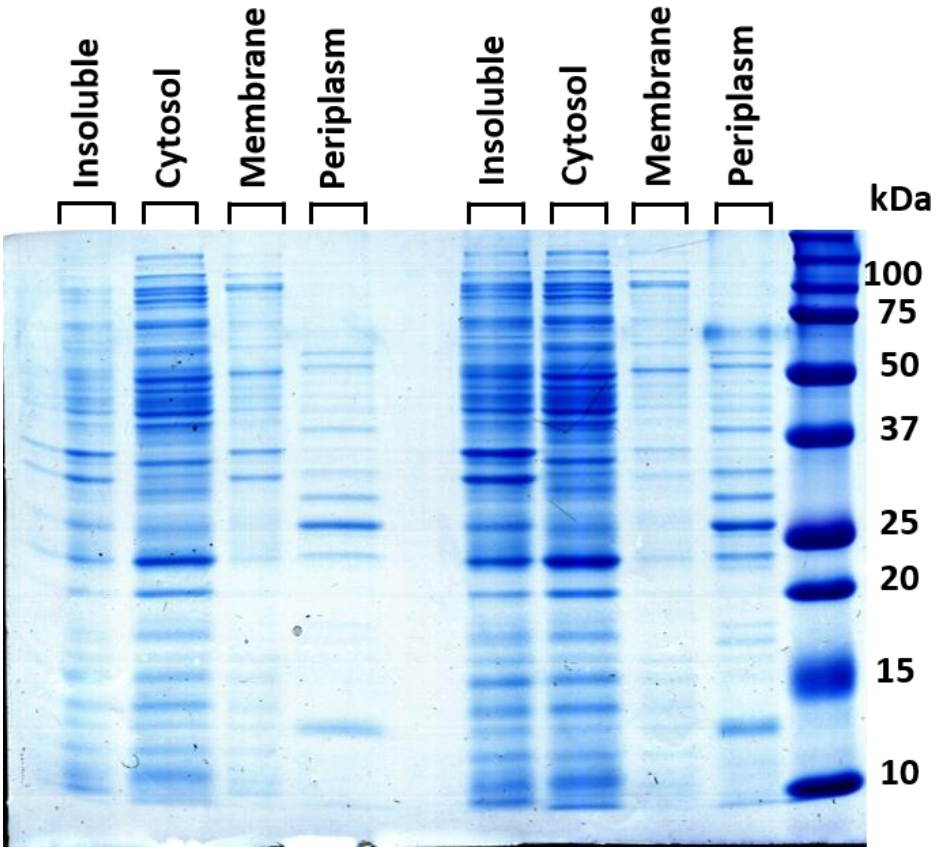

Figure 3.7 | Coomassie-stained SDS-PAGE analysis of 2 different BL21*(DE3)pLysS *E. coli* clones expressing recombinant elastase, separated into insoluble, cytosolic, periplasmic and membrane protein fractions. Processed elastase would be expected to be observed around 33 kDa.

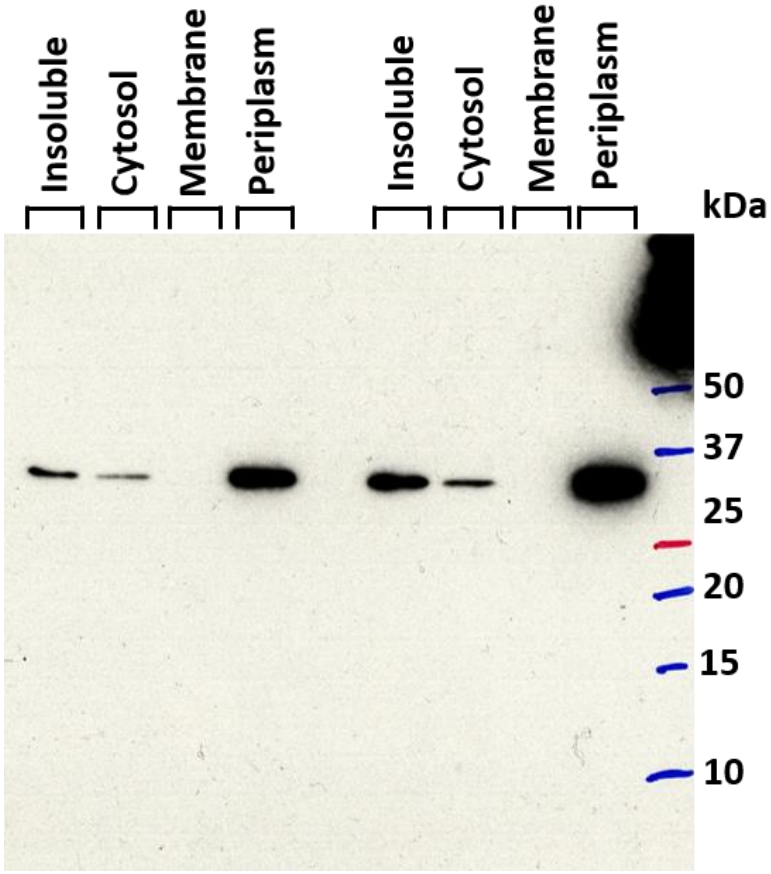

Figure 3.8 | Anti-His tag western blot analysis of 2 different BL21*(DE3)pLysS *E. coli* clones expressing recombinant elastase, separated into insoluble, cytosolic, periplasmic and membrane protein fractions. As anticipated, the majority of his-tagged recombinant elastase was detected in the periplasm, with a small proportion found in the cytosol or insoluble fraction, likely as a result of the strong T7 promoter outpacing the sec pathway secretion machinery. Marker bands have been drawn on by hand as this blot was produced via overlay with chemiluminescent detection film rather than development on the direct transfer membrane.

3.4 Purification of Recombinant Elastase from the Periplasm of *E. coli*

3.4.1 Nickel Affinity Purification of Recombinant Elastase

Recombinant elastase was purified from the periplasm of *lasB*-expressing BL21*(DE3)pLysS *E. coli* cells via nickel affinity chromatography on a gravity flow column containing 1 mL bed volume Chelating Sepharose® Fast Flow (GE Healthcare). Purification was performed as described in **Section 2.3.5** and the elution fractions obtained were pooled and buffer exchanged into PBS via overnight dialysis at 4°C. Following buffer exchange, the purified protein was concentrated to a final concentration of approximately 1 mg/mL using a VivaSpin 20 30-kDa MWCO concentrator column (Sartorious). Samples of each purification fraction were then analysed via SDS-PAGE on a 12% polyacrylamide gel followed by staining with Coomassie brilliant blue (**Figure 3.9**) and

transfer to nitrocellulose membrane for western blot analysis using an anti-his tag antibody (**Figure 3.10**). A 33 kDa band was observed as the major band in the 5 elution fractions, the apparent size of which was reduced following dialysis into PBS and spin concentration (**Figure 3.9**). The small reduction in size observed is likely a result of the degradation or cleavage of the C-terminal histidine tag and preceding prothrombin cleavage site. Disappearance of the 33 kDa band on an anti-his tag western blot following protein concentration further supports this idea (**Figure 3.10**). Some degradation of the unprocessed protein was also observed, particularly in the 2nd elution fraction. Larger bands observed in the elution fractions may indicate the full size 54 kDa prepro-elastase, whilst the smaller, sub-20 kDa band is most likely the cleaved propeptide (**Figure 3.9**). Subsequent purification attempts were unable to separate this smaller product from the 33 kDa elastase, suggesting some interaction between the two domains. Approximately 1 mg of recombinant elastase was successfully purified from the periplasm of 3 400 mL shake flask cultures, as determined via Bradford assay.

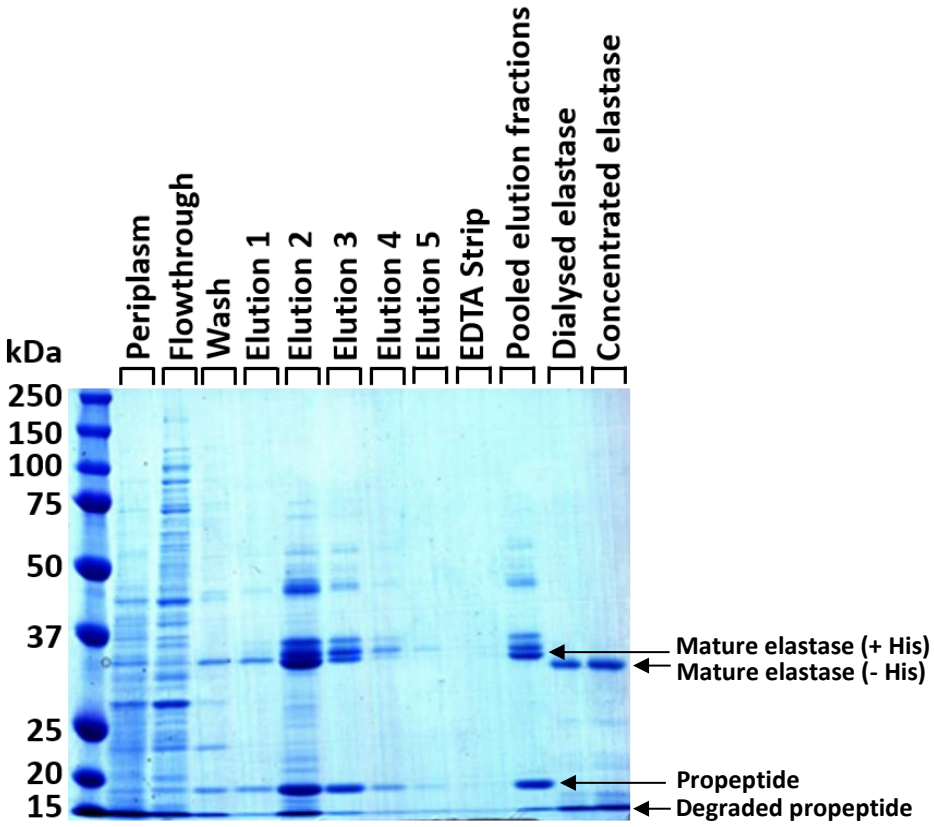

Figure 3.9 | SDS-PAGE analysis of purification fractions obtained via nickel affinity purification of recombinant elastase. Samples were prepared in a 4x reducing Laemmli sample buffer and incubated at 95°C for 10 minutes prior to loading.

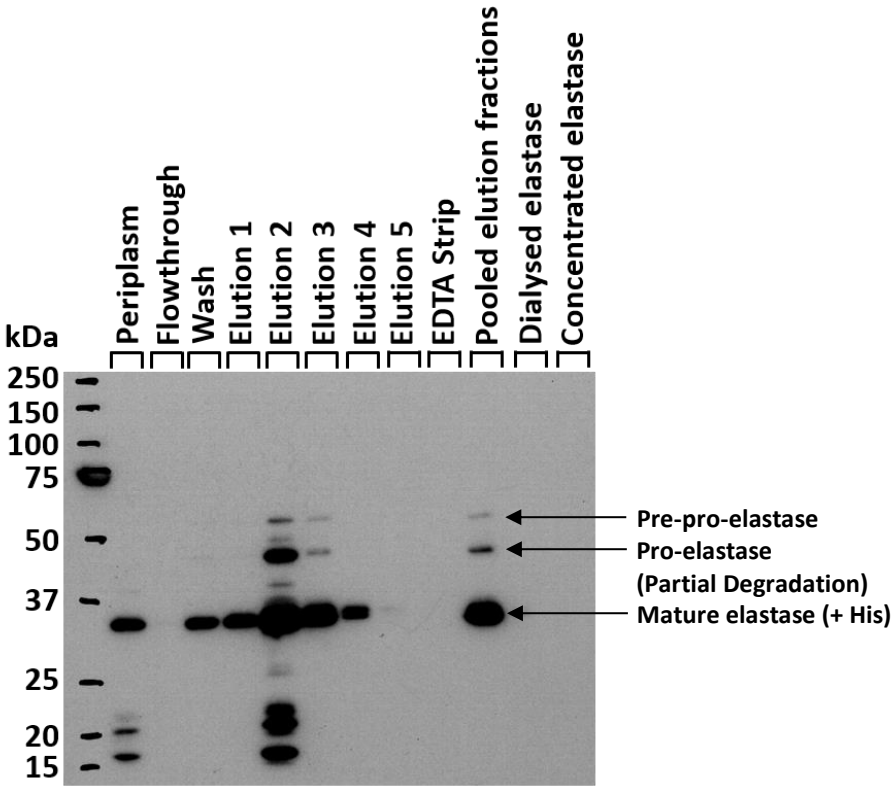

Figure 3.10 | Western blot analysis of purification fractions obtained via nickel affinity purification of recombinant elastase. Samples are the same as those in **Figure 3.9**. Detection was performed using a horseradish peroxidase labelled anti-his tag polyclonal antibody. Marker bands have been drawn on by hand as this blot was produced via overlay with chemiluminescent detection film rather than development on the direct transfer membrane.

3.5 Characterisation of Affinity Purified Recombinant Elastase

3.5.1 Identification and Confirmation of Elastase Expression and Purification using MALDI-ToF Mass Spectrometry

To ensure that the nickel affinity purified 33 kDa auto-processed protein was the desired elastase, the band was excised from a Coomassie stained SDS polyacrylamide gel and subjected to tryptic digestion following the methods outlined by Shevchenko *et al*. (Shevchenko et al., 1996). The digested sample was spotted onto an MTP Anchorchip™ 600/384 TF MALDI-ToF plate (Bruker) as outlined in **Section 2.4.4.1**, and MALDI-ToF mass spectrometry was performed as described in **Section 2.4.4.2**. The obtained peptide mass fingerprint (**Figure 3.11**) was compared to known fingerprints via the MASCOT protein identification software and sequence coverage was determined. 31% total sequence coverage was achieved, accounting for 51% of the processed 33 kDa protease, and included no sequence coverage of the propeptide domain (**Figure 3.12**). This method was repeated following excision of the 15 kDa protein band,

confirming the presence of the elastase propeptide, albeit with only one peptide matched and 1% total sequence coverage, accounting for 5% of the propeptide domain (**Figure 3.13**).

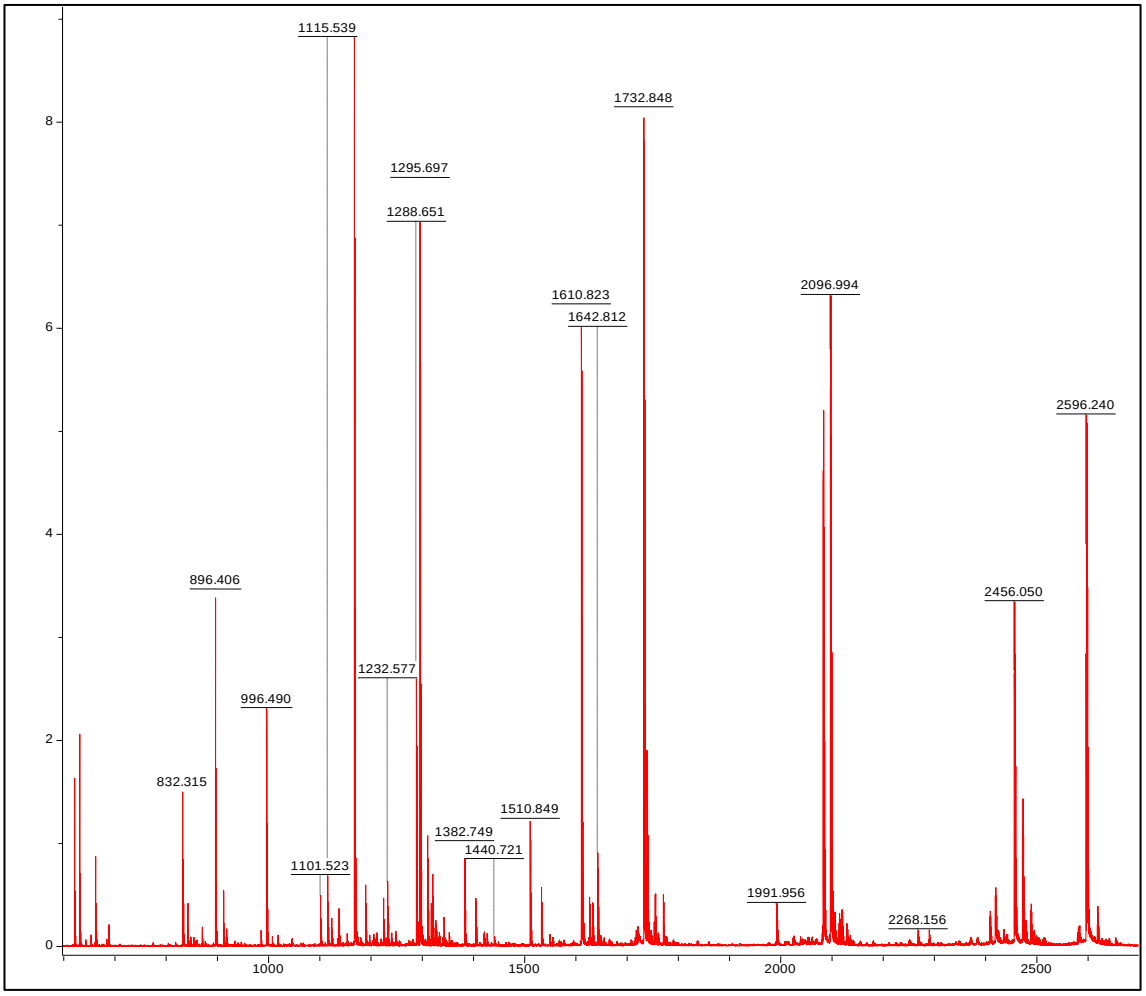

Figure 3.11 | MALDI-ToF mass spectrum for the excised 33 kDa elastase band, separated via SDS-PAGE and digested with trypsin. m/z (Da) is shown on the x-axis and ion intensity on the y-axis.

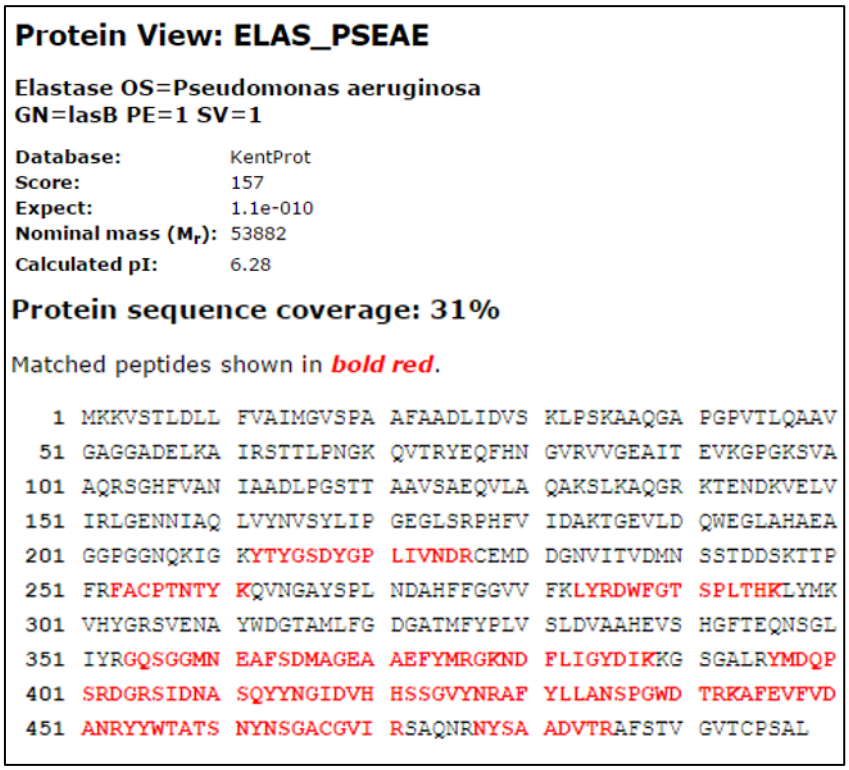

Protein View: ELAS_PSEAE

Elastase OS=Pseudomonas aeruginosa GN=lasB PE=1 SV=1

Database:	KentProt
Score:	157
Expect:	1.1e-010
Nominal mass (M_r):	53882
Calculated pI:	6.28

Protein sequence coverage: 31%

Matched peptides shown in ***bold red***.

```
  1 MKKVSTLDLL FVAIMGVSPA AFAADLIDVS KLPSKAAQGA PGPVTLQAAV
 51 GAGGADELKA IRSTTLPNGK QVTRYEQFHN GVRVVGEAIT EVKGPGKSVA
101 AQRSGHFVAN IAADLPGSTT AAVSAEQVLA QAKSLKAQGR KTENDKVELV
151 IRLGENNIAQ LVYNVSYLIP GEGLSRPHFV IDAKTGEVLD QWEGLAHAEA
201 GGPGGNQKIG KYTYGSDYGP LIVNDRCEMD DGNVITVDMN SSTDDSKTTP
251 FRFACPTNTY KQVNGAYSPL NDAHFFGGVV FKLYRDWFGT SPLTHKLYMK
301 VHYGRSVENA YWDGTAMLFG DGATMFYPLV SLDVAAHEVS HGFTEQNSGL
351 IYRGQSGGMN EAFSDMAGEA AEFYMRGKND FLIGYDIKKG SGALRYMDQP
401 SRDGRSIDNA SQYYNGIDVH HSSGVYNRAF YLLANSPGWD TRKAFEVFVD
451 ANRYYWTATS NYNSGACGVI RSAQNRNYSA ADVTRAFSTV GVTCPSAL
```

Figure 3.12 | Protein sequence coverage for 33 kDa elastase, obtained via comparison of mass spectra to a modified SwissProt MASCOT database. The 33 kDa processed elastase starts at amino acid A198. If just the sequence from this amino acid is considered, the coverage of the processed elastase increases to 51%.

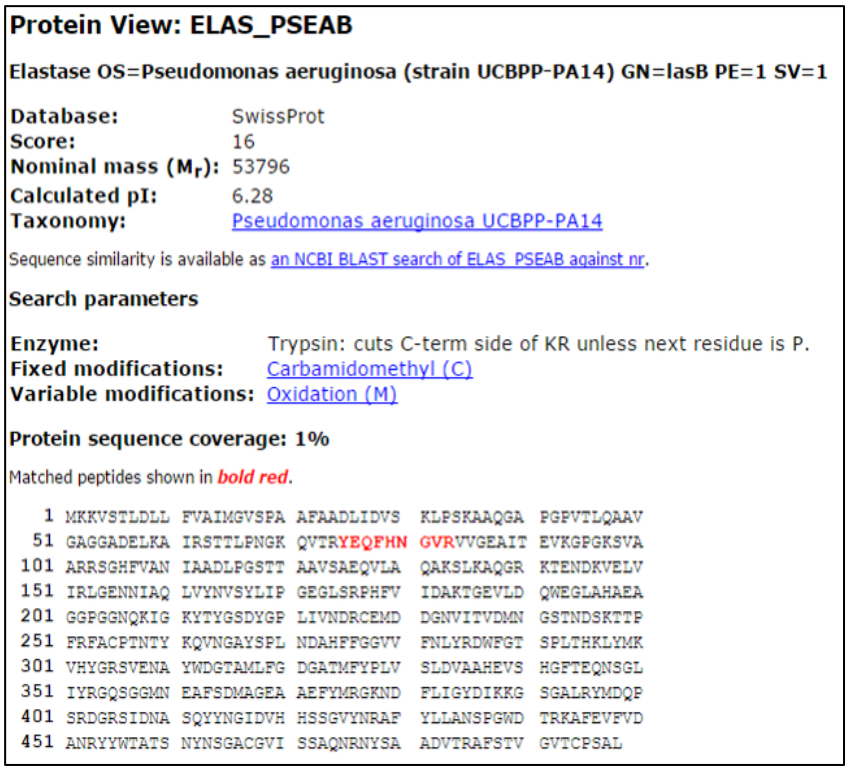

Protein View: ELAS_PSEAB

Elastase OS=Pseudomonas aeruginosa (strain UCBPP-PA14) GN=lasB PE=1 SV=1

Database: SwissProt
Score: 16
Nominal mass (M_r): 53796
Calculated pI: 6.28
Taxonomy: Pseudomonas aeruginosa UCBPP-PA14

Sequence similarity is available as an NCBI BLAST search of ELAS_PSEAB against nr.

Search parameters

Enzyme: Trypsin: cuts C-term side of KR unless next residue is P.
Fixed modifications: Carbamidomethyl (C)
Variable modifications: Oxidation (M)

Protein sequence coverage: 1%

Matched peptides shown in ***bold red***.

```
  1 MKKVSTLDLL FVAIMGVSPA AFAADLIDVS  KLPSKAAQGA  PGPVTLQAAV
 51 GAGGADELKA IRSTTLPNGK QVTRYEQFHN GVRVVGEAIT EVKGPGKSVA
101 ARRSGHFVAN IAADLPGSTT AAVSAEQVLA  QAKSLKAQGR  KTENDKVELV
151 IRLGENNIAQ LVYNVSYLIP GEGLSRPHFV  IDAKTGEVLD  QWEGLAHAEA
201 GGPGGNQKIG KYTYGSDYGP LIVNDRCEMD  DGNVITVDMN  GSTNDSKTTP
251 FRFACPTNTY KQVNGAYSPL NDAHFFGGVV  FNLYRDWFGT  SPLTHKLYMK
301 VHYGRSVENA YWDGTAMLFG DGATMFYPLV  SLDVAAHEVS  HGFTEQNSGL
351 IYRGQSGGMN EAFSDMAGEA AEFYMRGKND  FLIGYDIKKG  SGALRYMDQP
401 SRDGRSIDNA SQYYNGIDVH HSSGVYNRAF  YLLANSPGWD  TRKAFEVFVD
451 ANRYYWTATS NYNSGACGVI SSAQNRNYSA  ADVTRAFSTV  GVTCPSAL
```

Figure 3.13 | Protein sequence coverage for 15 kDa elastase, obtained via comparison of mass spectra to a modified SwissProt MASCOT database. The 15 kDa processed elastase fragment finishes at amino acid H197 If just the sequence from this amino acid is considered, the coverage of the 15 kDa elastase fragment increases to 5%.

3.5.2 Assessment of Elastase Gelatinase Activity via Gelatin Zymography

Hydrolytic activity of recombinant elastase was evaluated qualitatively via gelatin zymography. 20 µL of purified recombinant 1 mg/mL elastase was run alongside 20 µL of periplasm extracted from BL21*(DE3)pLysS *E. coli* cells expressing elastase, following the procedure described in **Section 2.4.5**. Following staining with Coomassie brilliant blue, active elastase was observed as a region devoid of blue stain, representing degradation of gelatin within the gel, at a molecular weight of approximately 33 kDa (**Figure 3.14**). This was anticipated to be a single, clear band visible only at the predicted molecular weight, but instead presented as a smear from the wells of the gel through to this molecular weight, suggesting that even when partially unfolded the enzyme may retain some level of hydrolytic activity both prior to, and following, purification.

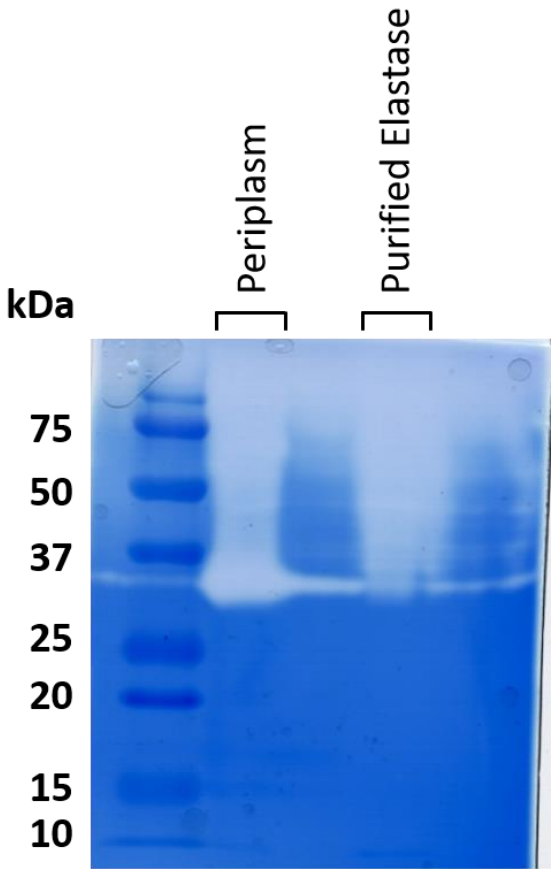

Figure 3.14 | Gelatin zymogram analysis to monitor the activity of 1 mg/mL recombinant elastase and 20 µL of extracted periplasm from elastase-expression BL21*(DE3)pLysS *E. coli*.

3.5.3 Assessment of Recombinant Elastase Hydrolytic Activity via a FRET-based Peptide Assay

To quantitatively investigate the hydrolytic activity of purified recombinant elastase, a 4-amino acid long internally quenched, fluorogenic peptide substrate was synthesised with the sequence Dabsyl-Ala-Ala-Phe-Ala-Edans, in order to replicate the highly sensitive FRET assay described by Elston *et al.* (Elston et al., 2007). Initially, 50 µM of peptide was incubated with 2, 4 and 8 nM recombinant elastase in a 1 mL reaction volume, and the change in fluorescence intensity measured over a 20 minute period. A fourth reaction containing 4 nM chymotrypsin in place of elastase was included in order to ensure the specificity of the assay (**Figure 3.15**). Following this, 10 µM peptide was incubated with 1-8 nM recombinant elastase in a 1 mL reaction volume and the assay undertaken as described in **Section 2.4.6** (**Figure 3.16**). Fluorescence was measured using an excitation wavelength of 340 nm and an emission wavelength of 460 nm. Initial rates were calculated for each concentration of elastase and a linear relationship was established between the concentration of elastase and the amount of substrate hydrolysed per minute

(**Figure 3.17**). This assay confirmed that the purified elastase was hydrolytically active. From these data the initial rate of hydrolysis was calculated as $V = 0.8818$ [elastase (nM)] – 0.2185, where V is the initial rate of hydrolysis of fluorescent peptide in µmol/min.

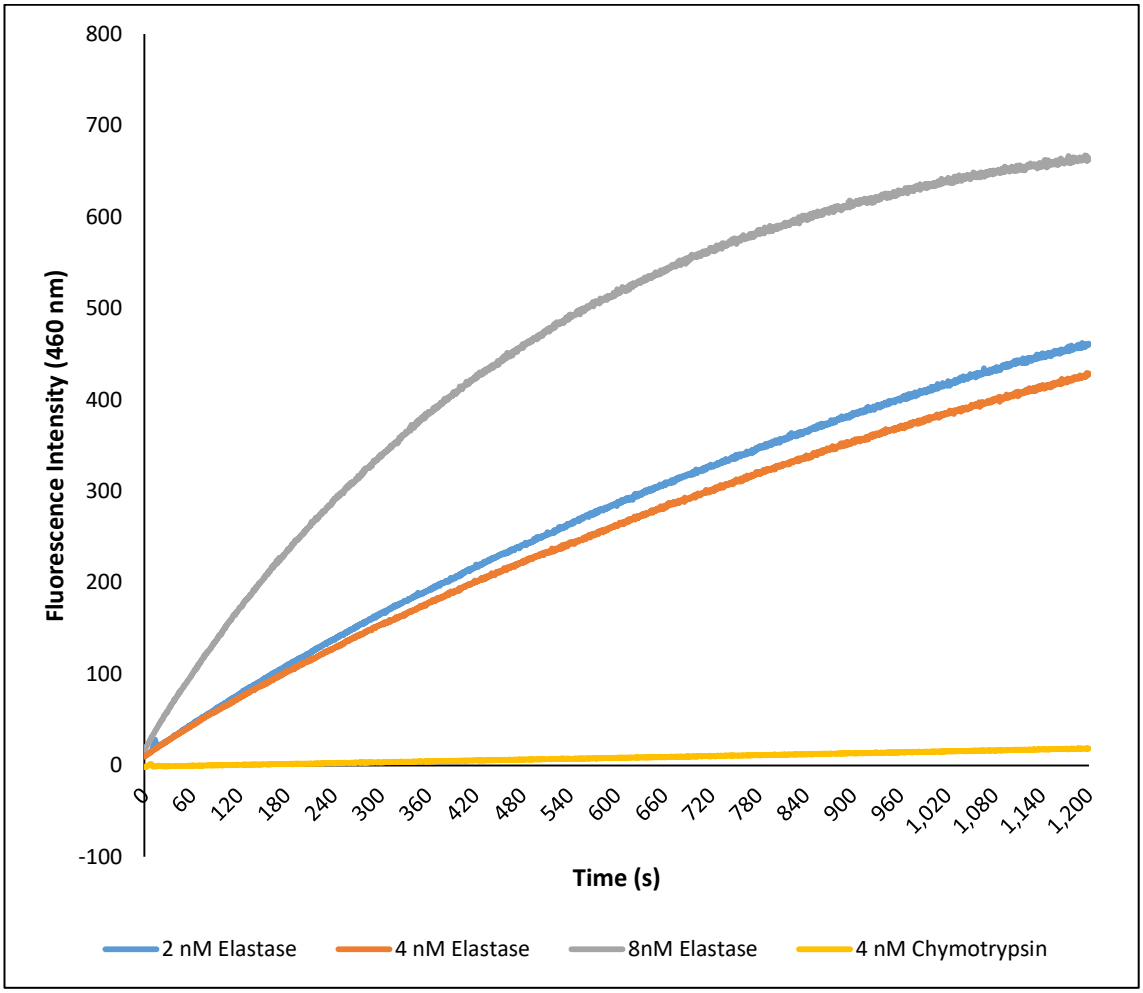

Figure 3.15 | Reaction progress curves for the hydrolysis of 50 µM Dabsyl-AAFA-Edans by recombinant elastase at various nanomolar concentrations. 4 nM chymotrypsin was also included to demonstrate the specificity of the assay.

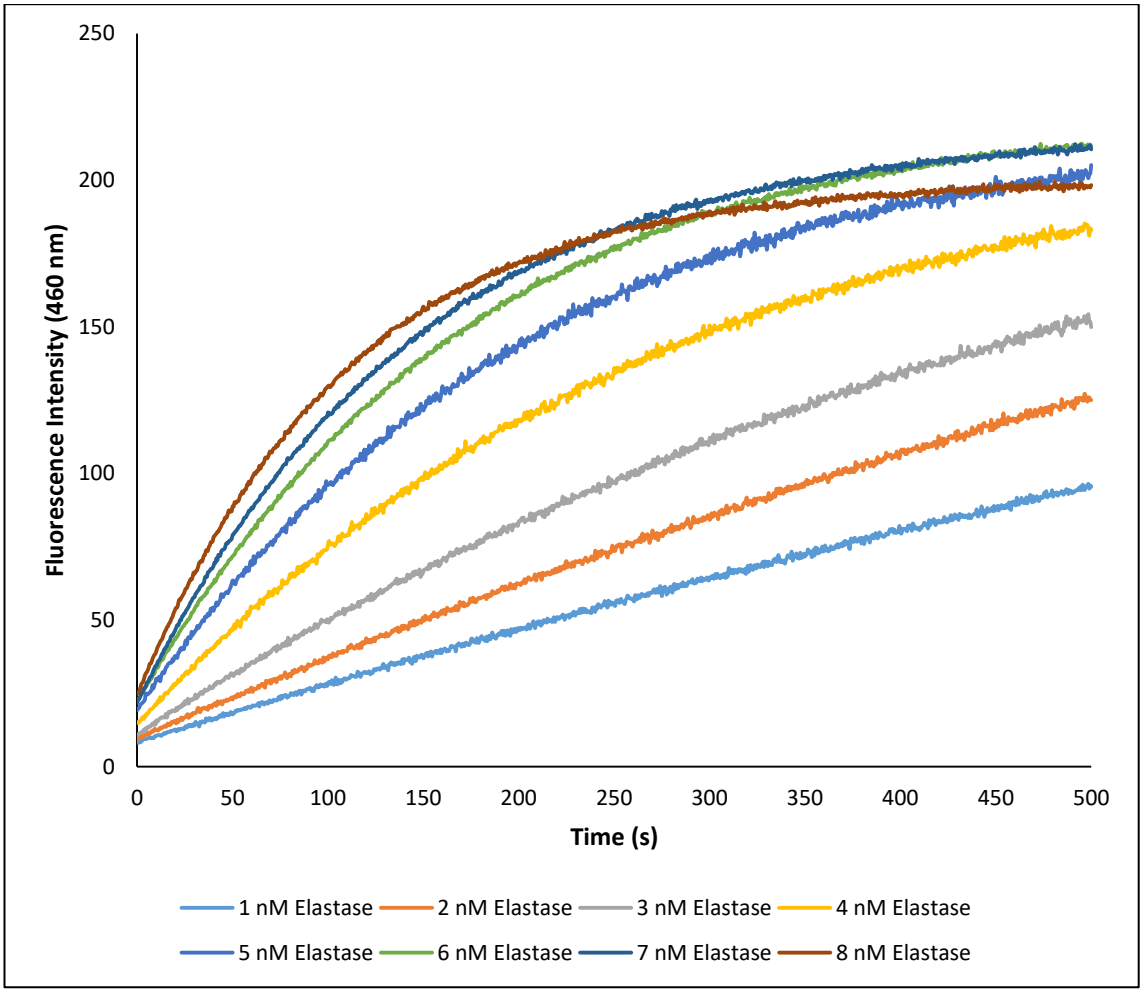

Figure 3.16 | Reaction progress curves for the hydrolysis of 10 µM Dabsyl-AAFA-Edans by recombinant elastase at different nanomolar concentrations.

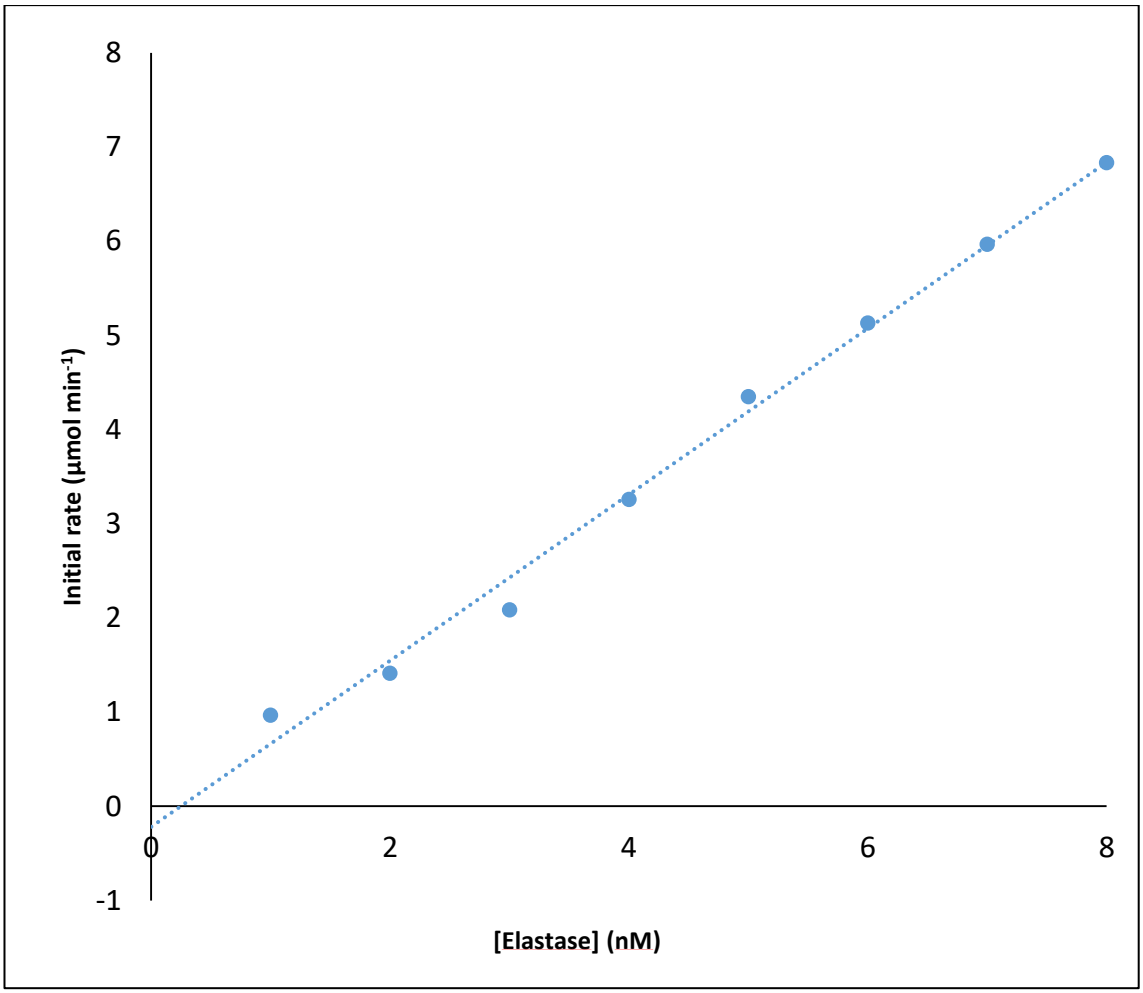

Figure 3.17 | Linear relationship between concentration of recombinant elastase and the initial rate at which the fluorescent peptide Dabsyl-AAFA-Edans was hydrolysed. $R^2 = 0.9921$.

3.5.4 Determination of the Conformational Stability of Recombinant Elastase

In order to assess the conformational stability of recombinant elastase, the purified protein was unfolded in the presence of guanidine hydrochloride (GuHCl). An emission wavelength scan was performed on a 10 μM sample of pure elastase in the presence and absence of 6 M GuHCl following excitation at 280 nm (**Figure 3.18**). The wavelength at which the resulting measured absorbance differed the most was identified as 335 nm, and therefore this wavelength of maximum emission was used for the measurements required for the generation of an elastase denaturation curve following the protocol described in **Section 2.4.7**. Recombinant elastase was allowed to incubate with GuHCl at concentrations of 1-6 M at 1 M intervals, and the absorbance of the resulting solution then read at an emission wavelength of 335 nm. Unfolding of recombinant elastase was determined to begin at a GuHCl concentration of 2 M, with full unfolding observed at a concentration of 3 M (**Figure 3.19**). Following this observation, further data points were added in this transition region by unfolding recombinant elastase at 0.2 M increments of GuHCl between 2 and 3 M. Using the absorbances recorded, the fraction of elastase folded and unfolded at each concentration of GuHCl was determined (**Figure 3.20**). The sigmoidal shape of the curve demonstrates a clear co-operative unfolding of recombinant elastase, suggesting a conformationally stable single-domain protein.

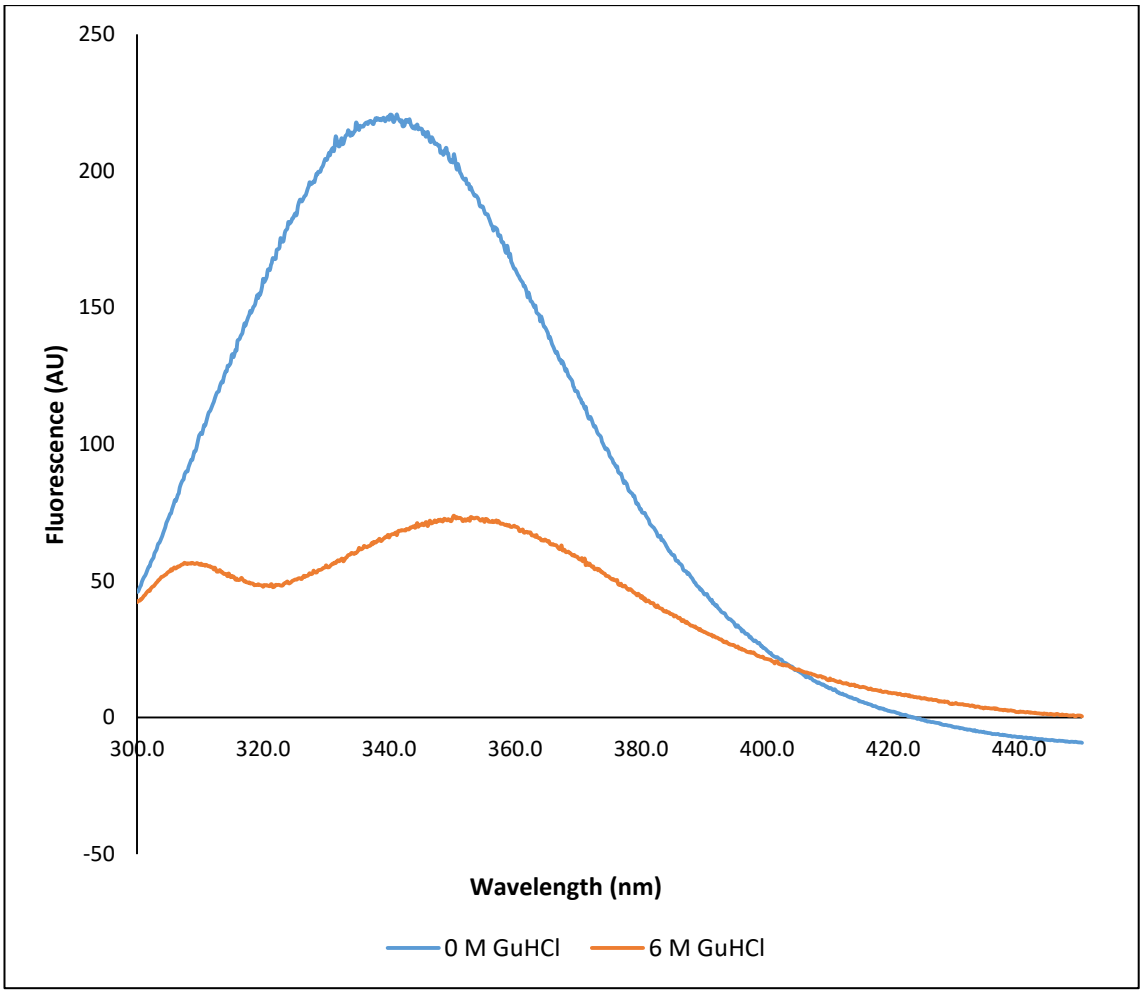

Figure 3.18 | Emission wavelength scan of recombinant elastase excited at 280 nm in both fully folded and fully unfolded states, assuming that the protein will be completely unfolded in 6 M GuHCl.

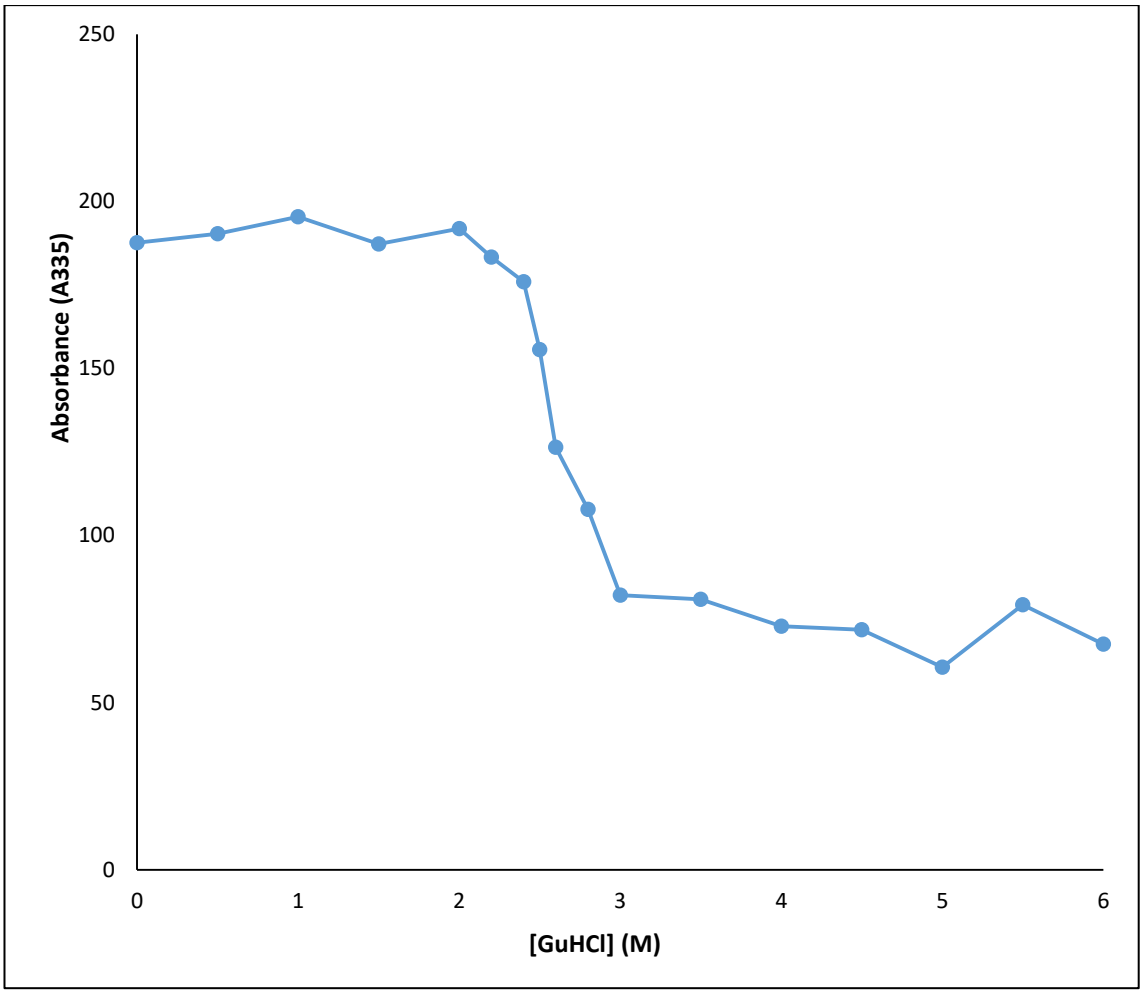

Figure 3.19 | Denaturation curve for recombinant elastase in the presence of increasing concentrations of guanidine hydrochloride, measured at an emission wavelength of 335 nm, as established in **Figure 3.18**, following excitation at 280 nm.

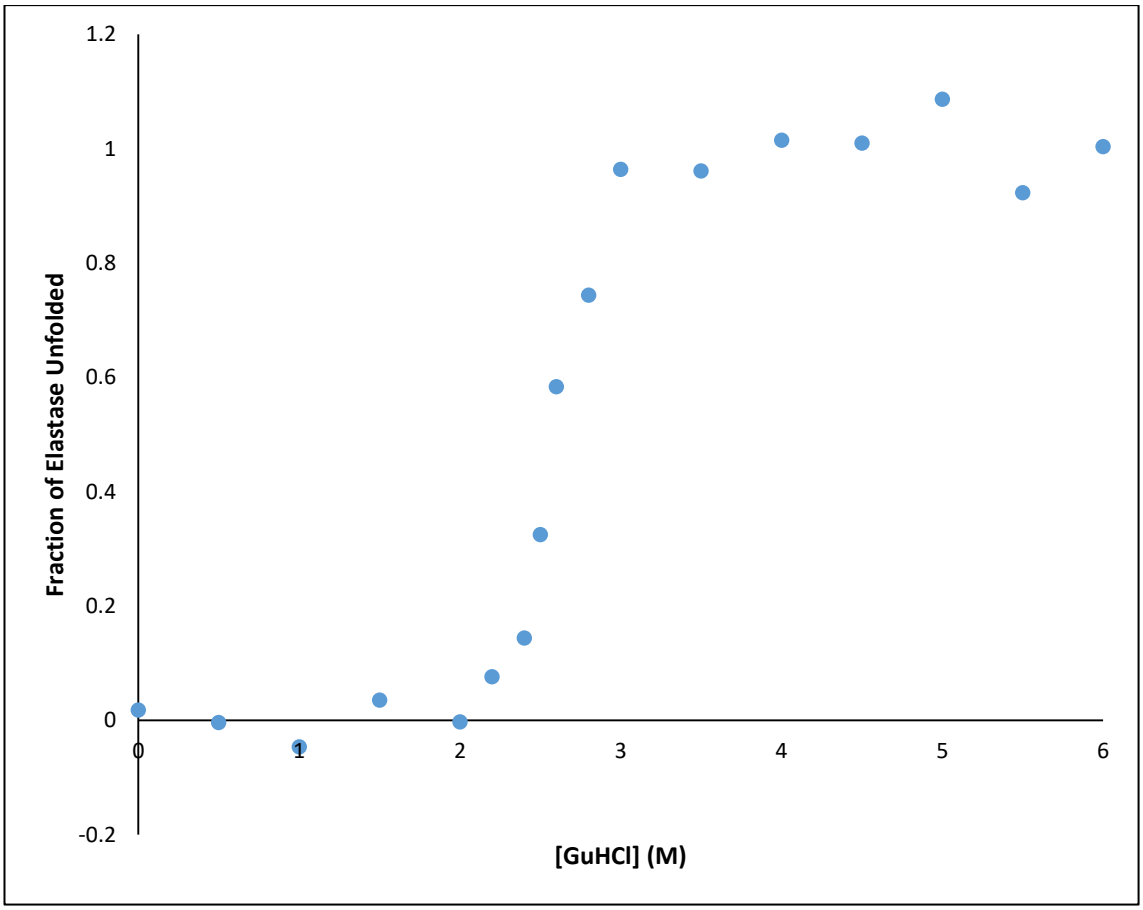

Figure 3.20 | Unfolding of recombinant elastase as a ratio of unfolded:folded material in the presence of increasing concentrations of guanidine hydrochloride.

3.6 Discussion

The original aim of the work described in this chapter was to generate a panel of plasmid constructs for the expression of a range of human biomarkers of inflammation across three different expression systems: *Escherichia coli*, *Leishmania tarentolae* and Chinese hamster ovary (CHO) cells. Each expression system has its own distinct benefits and limitations, and by directly comparing soluble protein yields, as well as the folding and activity of the resulting products, it would be possible to establish optimised protocols for the mass production of these recombinant antigens.

For instance, while an *E. coli* expression system allows for rapid growth and high-yield protein expression in a low-cost setting, the machinery of the cell is unable to cope with post-translational modifications or complex folding, particularly of eukaryotic proteins, often resulting in the formation of insoluble aggregated or misfolded material known as inclusion bodies (Mitraki & King, 1989). These can often be refolded following purification and denaturation, but this process can be time consuming and recovery of soluble material may be inefficient (Vallejo & Rinas, 2004). A mammalian cell line such as CHO cells, however, contains more sophisticated cellular machinery and organelles for protein folding and undertaking specific PTMs (e.g. glycosylation) and is therefore able to produce authentic fully-folded eukaryotic proteins (Kim, Kim, & Lee, 2012). CHO cells are able to achieve human-like glycosylation among other important post-translational modifications, making them an ideal platform for the production of complex eukaryotic proteins. The major drawback of a CHO cell expression system comes with its relatively high cost (compared to prokaryotic systems that use much more cost effective media), as well as a longer, more involved cell culture process in comparison with a bacterial expression system. *L. tarentolae*, on the other hand, is essentially a "middle-ground" expression system, capable of glycosylation, though not quite to the extent of a mammalian expression system. As such, it is important to weigh up the costs and benefits of each expression system for each target of interest, in order to ensure a good balance between the quantity and quality of the recombinant product, as well as the monetary and time costs involved. By generating a panel of plasmid constructs (**Figure 3.2, Figure 3.3** and **Figure 3.4**) to facilitate the expression of each antigen of interest in each expression system, a platform has been developed by which to screen protein expression systems and select the 'best', tailored specifically towards each individual antigen.

Initial trial expressions of the proteins of interest in BL21*(DE3)pLysS *E. coli* largely resulted in aggregation of insoluble material, presenting as inclusion bodies (**Figure 3.5**). This came as no

surprise, as *E. coli* is a relatively basic expression system, primarily geared towards the production of simple, primarily prokaryotic proteins. No periplasmic signal sequence was incorporated, severely limiting the capacity of these cells to form disulphide bonds due to the reducing nature of the cell cytoplasm (Prinz et al., 1997), which was likely a major contributing factor in the products' inability to fold correctly. However, in the cells expressing sRAGE, a form of RAGE lacking the N-terminal transmembrane region, no inclusion bodies were visible in the images obtained via TEM. This was initially promising, suggesting the potential generation of a soluble product that could be purified. However, further western blot analysis of cell lysates expected to be expressing sRAGE were blank, indicating a lack of protein expression at all. While production of soluble sRAGE from a murine origin in *E. coli* has previously been reported, facilitated by the presence of an N-terminal glutathione S-transferase fusion tag (Kumar et al., 2018), there is currently no literature available on the production of human-derived sRAGE in *E. coli*. Whilst for the purposes of this project, these antigens were dropped from further study, there is still considerable value in raising polyclonal antibodies to purified inclusion bodies and unfolded material, as the host immune response may generate antibodies recognising rare epitopes not exposed in the correctly folded antigen. This opportunity provides value in generating diagnostics, as it is entirely possible that misfolded target proteins may be abundant in certain disease states.

The remainder of this chapter focused primarily on the expression, purification and characterisation of *P. aeruginosa* elastase, as this biomarker candidate proved the most promising in initial screening experiments. The clinical significance of this virulence factor in the field of cystic fibrosis lung infections also made it an attractive target to pursue for the development of an assay for the prediction of pulmonary exacerbations and early stage infection, as described in further detail in **Section 1.4**. Upon successful expression of this recombinant protein, the focus of this project transitioned towards the goal of developing an anti-elastase immunoassay through the raising of anti-elastase polyclonal antibodies via immunisation with recombinant elastase (see Chapter 4 and 5). More information on the rationale behind the focus on this particular antigen is provided in **Section 3.1**.

Trial expression of the *P. aeruginosa* proteases staphylolysin (*lasA*) and elastase (*lasB*) were performed in the same *E. coli* strain, BL21*(DE3)pLysS, and while no soluble staphylolysin was produced, expression of elastase was observed in these early experiments. The native signal sequence of the *lasB* structural gene allowed for localisation of the recombinant product in the *E. coli* periplasm (**Figure 3.8**), providing an oxidising environment for the proper formation of disulphide bonds which eliminated the requirement for complicated refolding procedures.

Under the 'optimised' expression conditions developed during this study, it was possible to purify approximately 1 mg of recombinant elastase from the combined periplasms of 3 x 400 mL cultures grown in terrific broth medium. While yields of 40 mg elastase per litre have previously been reported (Odunuga, Adekoya, & Sylte, 2015), a complex multi-stage refolding procedure was necessary, and attempts to replicate this method with the plasmid construct and *E. coli* strain used in this work were unsuccessful. Purification of soluble elastase from the cell periplasm was comparatively fast, cheap and simple, and for the purposes of characterisation and immunisation, the yields obtained were sufficient.

Elastase is initially synthesised as an inactive 54 kDa preproprotein, containing a 23 residue N-terminal signal peptide and 174 residue long propeptide domain (Kessler et al., 1992). This propeptide domain is known to be autoproteolytically processed (McIver, Kessler, & Ohman, 1991b) to generate mature elastase with a final size of 33 kDa. The full-length prepropeptide sequence was used for the expression of recombinant elastase in these studies, and autoproteolytic processing was observed via western blot analysis of *E. coli* cell lysates expressing *lasB* at different temperatures (**Figure 3.6**), as evident by the presence of both 54 kDa and 33 kDa bands in the lysate of cells expressing *lasB* at 37°C. The processed, 33 kDa mature protease was the dominant band observed in the periplasm of BL21*(DE3)pLysS cells expressing elastase, and appeared to be co-purified with the 19 kDa propeptide (**Figure 3.9**). Analysis of this 33 kDa band by MALDI-ToF-MS following in-gel tryptic digestion confirmed its identity as mature elastase, and the peptides identified via MASCOT search coincided with peptides found only in the mature enzyme, further supporting the autoprocessing of the propeptide domain (**Figure 3.12**). The propeptide was likely still associated with the mature enzyme upon purification, as it appeared to co-purify proportionally with the mature 33 kDa protein. There is some support for this observation in the literature as, when synthesised by *P. aeruginosa*, the propeptide is reported to remain non-covalently associated with mature elastase prior to secretion (Kessler & Safrin, 1988), and the same interaction appears to occur for this recombinant material.

Degradation of the propeptide was evident following buffer exchange into PBS via dialysis; however, it would appear that there was still some, presumably non-covalent, association with the mature protease, as this <15 kDa material remained present in purified elastase that had been concentrated using a spin concentrator with a 30 kDa molecular weight cut-off. Subsequent MALDI-ToF-MS analysis attempts identified this smaller band as the elastase propeptide domain, though only a single peptide was identified (**Figure 3.13**). While the data supports that the propeptide is autoproteolytically processed by the recombinant elastase, further processing or degradation was also observed, indicated by the loss of the C-terminal

histidine tag following buffer exchange dialysis (**Figure 3.10**). A slight band shift was observed in the Coomassie blue stained polyacrylamide gel, indicating the potential cleavage of the tag (**Figure 3.9**). The DNA sequence designed for elastase expression incorporated a prothrombin cleavage site immediately preceding a 6x histidine tag to facilitate easy removal of the tag following purification, however, this proved to be unnecessary. While it is unclear exactly why this processing occurred, no further degradation was evident and it did not seem to impact upon the resulting protein's stability or activity in any way.

Assessment of recombinant elastase via gelatin zymography confirmed the 33 kDa protein's gelatinase activity (**Figure 3.14**). Absence of Coomassie blue staining at a molecular weight of 33 kDa in both the purified protein and in a sample of cell periplasm from *lasB*-expressing BL21*(DE3)pLysS cells indicated degradation of gelatin in the polyacrylamide gel, demonstrating that the recombinant product was active prior to purification. Digestion of gelatin was observed not only at the specified molecular weight, but as the protease migrated through the gel, suggesting a level of gelatinase activity was retained even whilst partially unfolded.

The specific protease activity of recombinant elastase was investigated quantitatively via a highly sensitive FRET-based assay previously designed to monitor the activities of native elastase and staphylolysin (Elston et al., 2007). This assay is capable of measuring the activity of elastase at nanomolar concentrations through cleavage of an internally quenched fluorescent peptide with the sequence Dabsyl-Alanine-Alanine-Phenylalanine-Alanine-Edans. Initial rate curve experiments undertaken in the presence of 10 µM peptide substrate and varying concentrations of elastase were undertaken to measure the protease activity of recombinant elastase at concentrations as low as 1 nM, demonstrating the highly sensitive nature of this assay (**Figure 3.16**). A linear relationship was established between the initial rate of peptide hydrolysis and concentration of elastase with high confidence ($R^2 = 0.9921$) (**Figure 3.17**), though the calculated value for initial rate, *V*, in comparison to the values reported by Elston *et al.* was noticeably low ($V = 0.8818$ [elastase (nM)] – 0.2185 against $V = 4.96$ [elastase] + 0.82); approximately 5-fold lower than that of native elastase. There is, however, a potential explanation for this observed difference in activity. As noted above, the propeptide domain appears to remain non-covalently associated with the recombinant product following purification. When synthesised by *P. aeruginosa*, the cleaved propeptide acts to inhibit the protease activity of elastase prior to disruption of this non-covalent association upon secretion from the periplasm (Kessler & Safrin, 1994), and so it is possible that partial inhibition is taking place in the recombinant elastase as well. Alternatively, it may be the case that the recombinant elastase used in these experiments

is a mixture of fully processed, active elastase and propeptide-inhibited elastase, meaning the concentrations of active elastase used may have actually been lower than recorded.

Protein stability is also an important consideration in the generation of a recombinant immunogen. The conformational stability of recombinant elastase was assessed via unfolding in the presence of the denaturant guanidine hydrochloride. The resulting denaturation curve showed the properties expected for a stable, fully folded single domain (**Figure 3.19** and **Figure 3.20**), characterised by a sigmoidal shape indicating a two-state transition between the folded and unfolded protease, demonstrating the co-operative unfolding of the recombinant single domain protease. As denaturation was only performed over a 10 minute period, it is unlikely that full unfolding was achieved. As such, the denaturation curve is not as smooth as anticipated, meaning attempts to calculate ΔG^0 were inaccurate. In order to calculate a more accurate free energy change, overnight denaturation would be required.

Although the activity of recombinant elastase may have been lower than that of native elastase previously reported, this was unlikely to pose a problem for immunisation and the raising of polyclonal antibodies. For the purposes of this study, it was important to generate an antigen that was as close to its native counterpart as possible in order to elicit an authentic immune response, generating polyclonal antibodies that were more likely to recognise native epitopes. As the protease was able to recognise its target substrates in a specific manner, and exhibited the properties of a stable, single-domain globular protein, it was considered a suitable immunogen for the raising of polyclonal antibodies. There was scope for further detailed characterisation of the recombinant elastase, but for the purposes of this particular study the characterisation work described within this chapter was deemed sufficient. In the future, it may also be of interest to immunise animals with fully unfolded or partially unfolded elastase, as this could provide a broader selection of epitopes from which to screen antibody binding, and may potentially result in the generation of higher sensitivity anti-elastase antibodies.

Chapter 4

Assessment of Polyclonal Anti-Elastase Antibodies and Application of these to the Development of Lateral Flow and Sandwich ELISAs for Elastase

4.1 Introduction to the Work Described in this Chapter

This chapter describes the characterisation of polyclonal antibodies raised in rabbits and sheep immunised with the recombinant elastase generated as described in Chapter 3, as well as the utilisation of these for the development of lateral flow and enzyme linked immunosorbent assay prototype diagnostic tests. Two rabbits were initially immunised, hereafter referred to as RA528 and RA529, and prototype assays were developed incorporating the generated polyclonal antibodies prior to monoclonal antibody development. Following unsuccessful attempts to use phage display to isolate monoclonal antibodies from the rabbits, described in further detail in Chapter 5, two sheep were also immunised with recombinant elastase, hereafter referred to as SA562 and SA563. Immune responses were measured via serum ELISA and specific polyclonal antibodies were purified from antiserum via affinity purification. Purified antibodies were characterised via western blot and a synthetic peptide array prior to application in LFAs and sandwich ELISAs. The work described in this chapter also encapsulates the optimisation of these diagnostic assays and assessment of native elastase detection in laboratory and clinical strains (in collaboration with Imperial College) of *P. aeruginosa*.

Immunoassays have routinely been used as diagnostic assays at the point of care due to their often high sensitivity and specificity, as well as their low reagent cost and rapid turnaround time. In the case of ELISAs, results can be obtained in a matter of hours, whereas LFAs, though usually at the cost of impaired sensitivity compared to ELISA, can generate a result in as few as 5-10 minutes. These qualities make immunoassays ideal diagnostic assays for use in a clinical or point-of-care (e.g. in the home) setting, as patients can receive results on the day of examination and rarely is there a need for samples to be sent to an external laboratory. The associated low reagent cost and simplicity of use is a desirable factor in the distribution of these assays to less economically developed regions, particularly where laboratory infrastructure is sparse or absent.

Some notable diagnostic assays for the detection of *P. aeruginosa* in cystic fibrosis patients are described in **Section 1.3.3.1.** These include sputum culture, the current "gold standard" diagnostic approach, PCR-based assays, crossed immunoelectrophoresis and serum ELISAs

designed to examine a patient's immune response to pathogens. While all of these assays have their advantages, many are time-consuming, require costly reagents, or require specialised equipment and trained scientists in order to generate and interpret the results. Furthermore, when looking at an immune response to an antigen rather than the antigen itself, false negative results can be prevalent as specific antibodies may remain present even when the pathogen itself is absent. Thus, the use of immunoassays targeting specific virulence factors such as elastase may provide a window of opportunity with which to rapidly detect ongoing infections, with a particular focus on early infection and episodes of increased virulence.

The aim of the work in this chapter was to develop prototype lateral flow and sandwich ELISA format immunoassays to act as a proof of concept for further device and antibody development. There is an ongoing need for reliable, sensitive, low-cost diagnostic assays to identify *P. aeruginosa* in the airways of cystic fibrosis patients not only for applications in early detection, but also as a measure of virulence for the prediction of pulmonary exacerbations.

4.2 Immunisation of Animals with Recombinant Elastase

4.2.1 Immunisation of New Zealand White Rabbits with Recombinant Elastase

Two New Zealand White rabbits, hereafter referred to as RA528 and RA529, were immunised with recombinant elastase by Orygen Antibodies Ltd. (commissioned by the industrial partner, Mologic Ltd., after completion of the appropriate ethical assessments and permissions) in the presence of Freund's complete adjuvant. Following initial immunisation, 2 further antigen boosts were performed at 4 week intervals and test bleeds taken one week after each boost. Upon administration of the final antigen boost, terminal bleeds were performed and peripheral blood lymphocytes were prepared from the spleens. Prior to ELISA, serum was clarified via centrifugation at 20,000 x g followed by filtration through a 0.22 µm syringe filter. Indirect serum ELISAs were carried out to track the rabbits' immune responses to the recombinant elastase. Serum from each bleed was prepared via 1/5 serial dilutions made up in an assay buffer consisting of PBS containing 1% BSA and 0.1% Tween-20, at dilutions of 1/200, 1/5000, 1/25000, 1/125000 and 1/625000. Indirect ELISAs were performed as described in **Section 2.4.8** on 96 well Nunc-Immuno™ MaxiSorp™ plates coated with 100 ng of recombinant elastase. Specific anti-elastase titre for RA528 at the time of the final test bleed prior to the terminal bleed was estimated to be approximately 1/25000 (**Figure 4.1**), here defined as the dilution of the serum at which the ELISA test produces an absorbance value of 1.0. This observed titre was a 5-fold improvement over the initial test bleed taken 4 weeks after immunisation. Using this titre definition, specific anti-elastase titre from RA529 following the final test bleed was estimated to

be closer to 1/10000, approximately a 5-fold improvement over the initial test bleed (**Figure 4.2**).

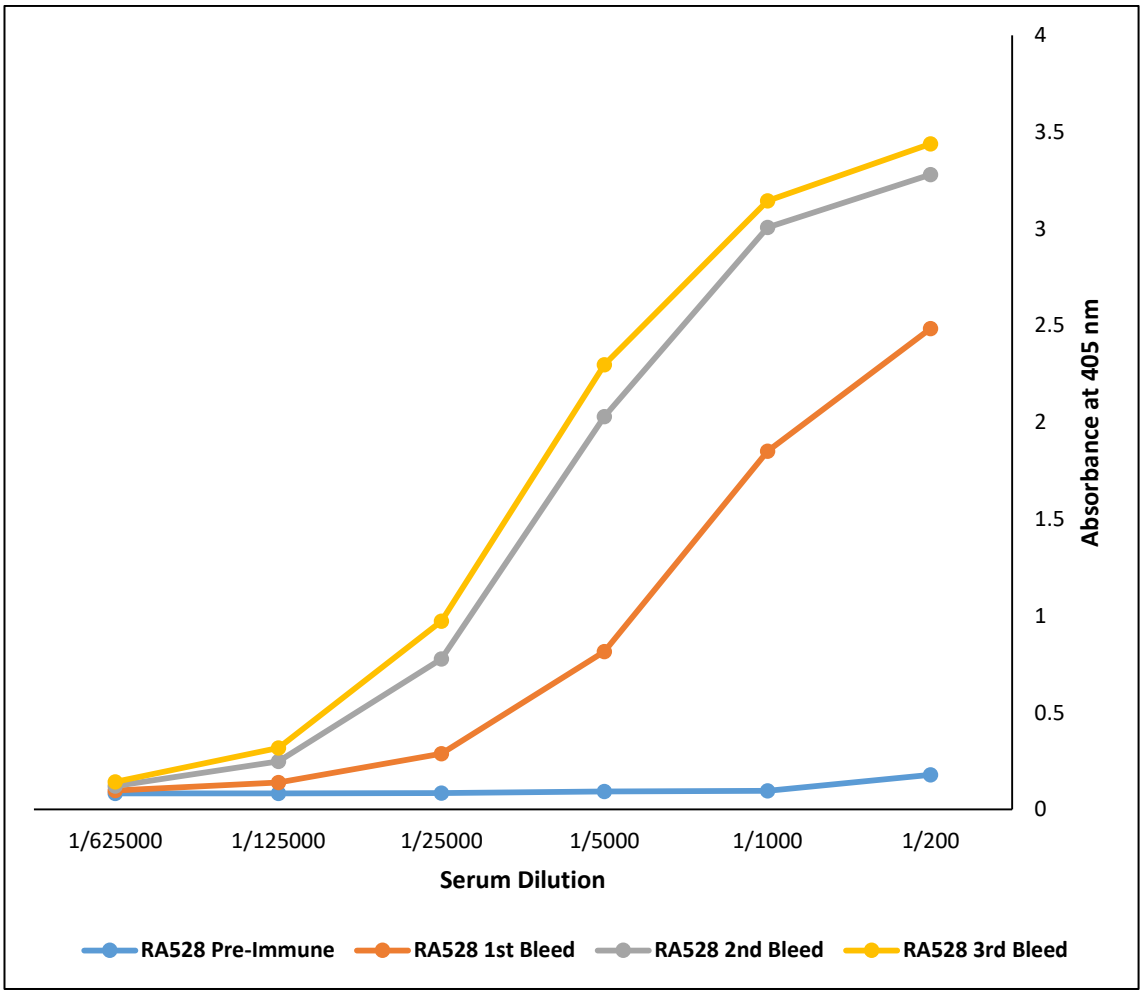

Figure 4.1 | Specific anti-elastase IgG serum dilution curves from test bleeds of rabbit RA528 as measured via indirect ELISA. (n=1, where each sample was measured twice).

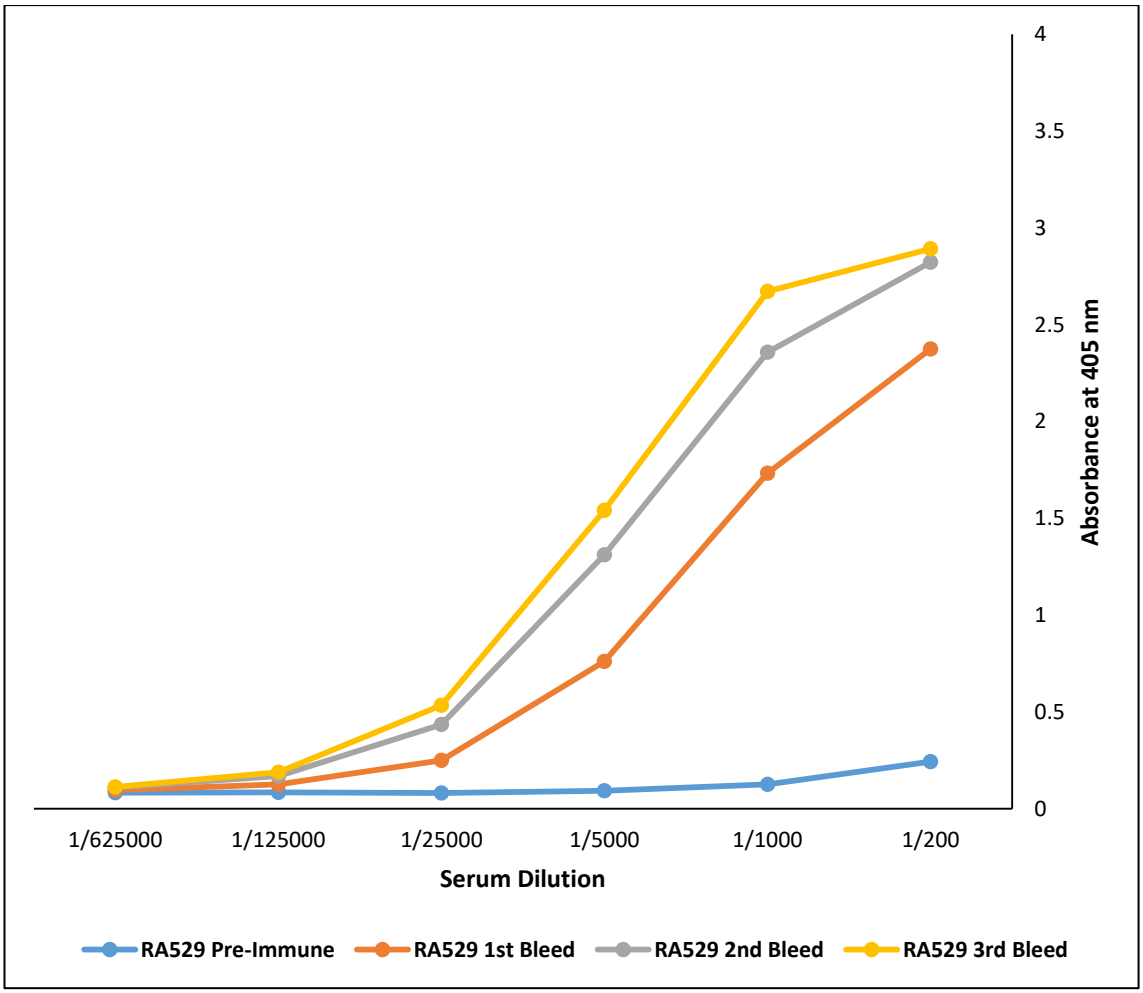

Figure 4.2 | Specific anti-elastase IgG serum dilution curves from test bleeds of rabbit RA529 as measured via indirect ELISA. (n=1, where each sample was measured twice).

4.2.2 Immunisation of Suffolk Sheep with Recombinant Elastase

Two Suffolk Sheep, hereafter referred to as SA562 and SA563, were immunised with recombinant elastase (as described for the rabbit immunisations) by Orygen Antibodies Ltd. in the presence of Freund's complete adjuvant. Scheduled antigen boosts and test bleeds were taken at regular intervals as for the rabbits (every 4 weeks after immunisation) and specific immune responses were again measured via indirect serum ELISA at serum dilutions of 1/200, 1/1000, 1/5000, 1/25000, 1/125000 and 1/625000. Prior to ELISA, serum was clarified via centrifugation at 20,000 x g followed by filtration through a 0.22 µM syringe filter. Sheep serum ELISAs were performed using an anti-sheep IgG antibody conjugated to horseradish peroxidase, and were developed using TMB as a substrate. All serum-handling work including antibody purification, ELISA and antibody labelling was performed in collaboration with Steve Eida at the site of the industrial partner, Mologic Ltd.

Specific anti-elastase titre for sheep SA562 at the time of the final test bleed was approximately 1/5000 (**Figure 4.3**), a five-fold increase from the first test bleed, whereas specific anti-elastase tire for sheep SA563 was considerably lower, closer to a dilution of 1/100 (**Figure 4.4**). Overall, serum titres achieved from immunisation of sheep were much lower than those obtained from rabbits. However, this may be due to differences in measuring apparatus and substrate compositions used to assess each, as the concentration of specific antibody obtained via purification from serum remained similar between the four animals.

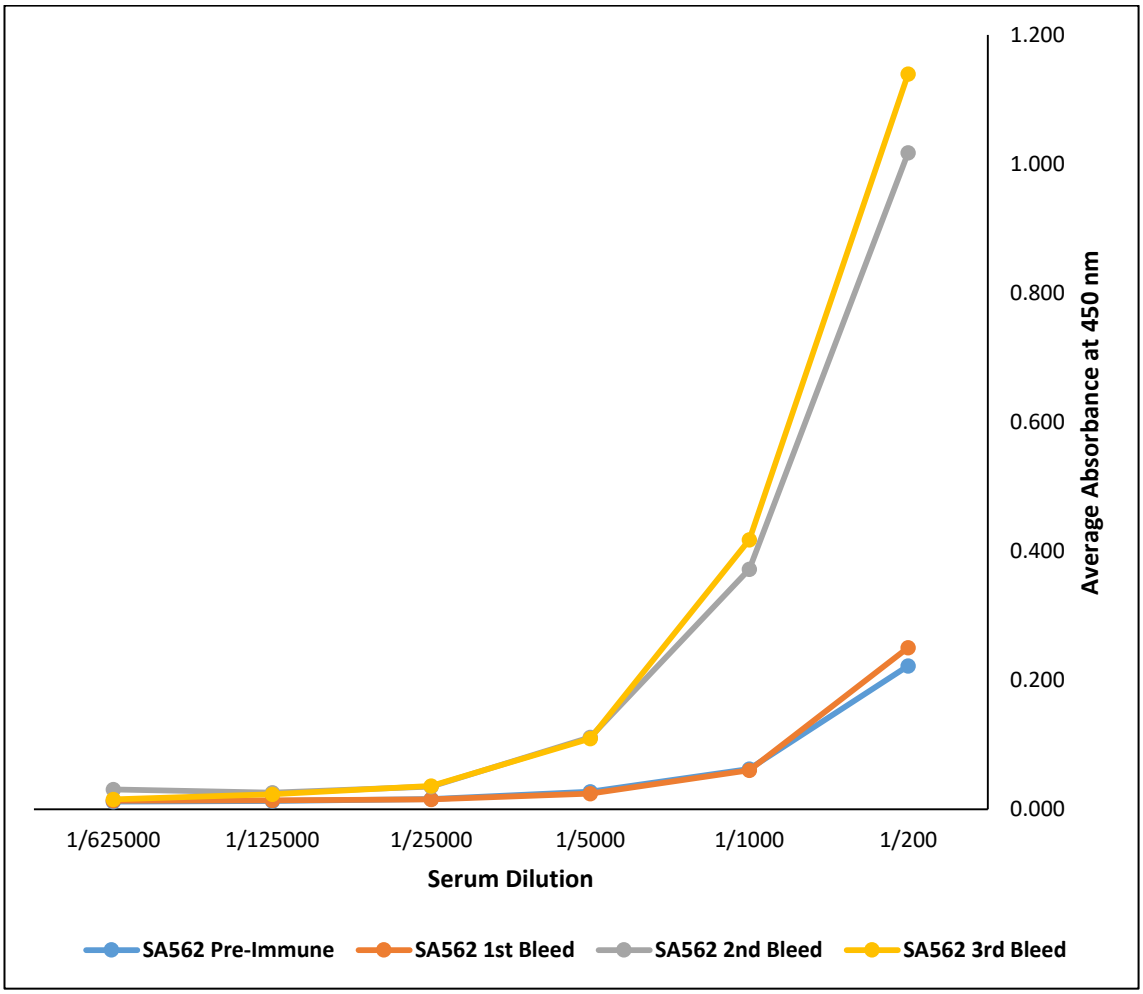

Figure 4.3 | Specific anti-elastase IgG serum dilution curves from test bleeds of sheep SA562 as measured via indirect ELISA. (n=1, where each sample was measured twice).

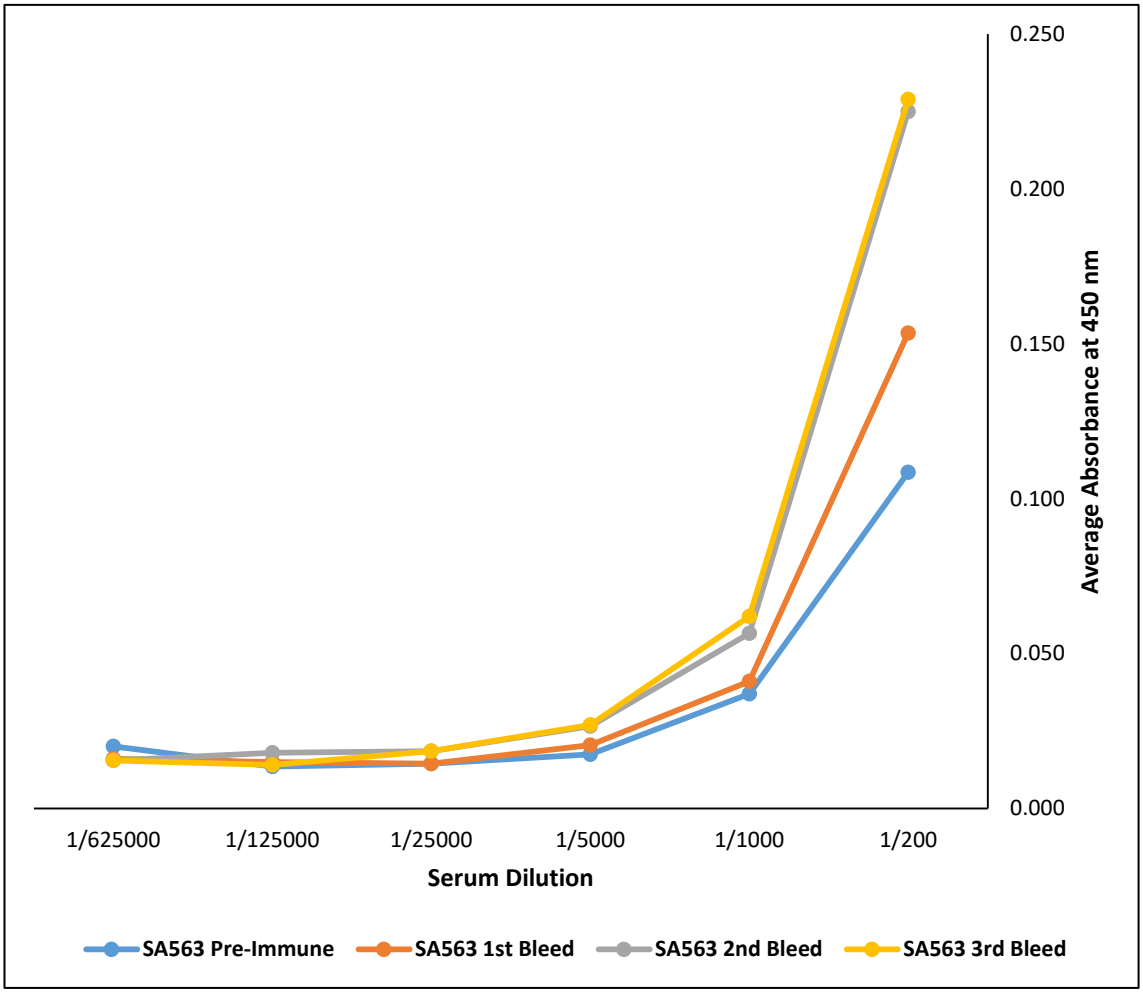

Figure 4.4 | Specific anti-elastase IgG serum dilution curves from test bleeds of sheep SA563 as measured via indirect ELISA. (n=1, where each sample was measured twice).

4.3 Affinity Purification of Anti-Elastase Polyclonal Antibodies from Antiserum

Recombinant elastase (1 mg) was coupled to a 1 mL HiTrap™ NHS-activated HP affinity column (GE Healthcare) following the manufacturer's protocols in standard coupling buffers in order to produce an anti-elastase polyclonal antibody affinity column. Clarified serum from each animal was loaded onto the assembled affinity column and purification was performed as described in **Section 2.3.6**. Purified antibody was buffer exchanged into PBS via a PD-10 desalting column (GE Healthcare) and concentrated to an appropriate concentration via a VivaSpin 5000 30 kDa MWCO concentrator column (Sartorious). Concentration of specific anti-elastase pAb in serum samples was determined via measurement of anti-elastase pAb eluted from the column by absorbance at 280 nm. 200 µg of each affinity purified pAb was labelled with horseradish

peroxidase via the Lightning-Link HRP Antibody Labelling System (Novus Biologicals), following the manufacturer's protocols, to act as detector antibodies.

Table 4.1 | Determination of specific anti-elastase polyclonal antibody titre in the serum of immunised animals as measured via affinity purification.

Animal	Volume of serum applied to column (mL)	Amount of anti-elastase pAb eluted (µg)	[Specific antibody in serum] (µg/mL)
RA528	2	308	154
RA529	2	252	126
SA562	2	330	165
SA563	2	340	170

4.4 Mapping of Linear Elastase Epitopes Recognised by Polyclonal Antibodies via Peptide Array

A synthetic peptide array was constructed by Dr James Schouten at the site of the industrial partner, Mologic Ltd. in order to determine linear elastase binding epitopes for the purified rabbit antibodies. The array contained a series of overlapping 15 amino acid residue peptides comprising the full sequence of mature elastase, dried onto a nitrocellulose membrane. When probed with a HRP labelled antibody and developed in TMB substrate, developed spots where peptides were immobilised indicate antibody binding. Identified linear epitopes were defined as regions of high HRP intensity flanked by regions of diminishing intensity. The array was probed with 1 µg/mL of HRP labelled RA528 antibody, following the method outlined in **Section 2.4.10**. Strong binding was observed exclusively in the N-terminal region of the mature protein (**Figure 4.5**), suggesting that the major linear epitope lies within this region. As no other linear epitope areas were observed, this suggests that other major antibody populations within the polyclonal population are likely to be against, and bind, conformational epitopes. When modelled using the molecular graphics system PyMOL, the linear epitope recognised was predicted to be a beta hairpin motif, comprised primarily of surface-exposed hydrophobic amino acids (**Figure 4.6**). Due to the shelf-life of the array and the fact that the anti-elastase pAbs raised in sheep were generated at a much later date, they were not assessed via this array.

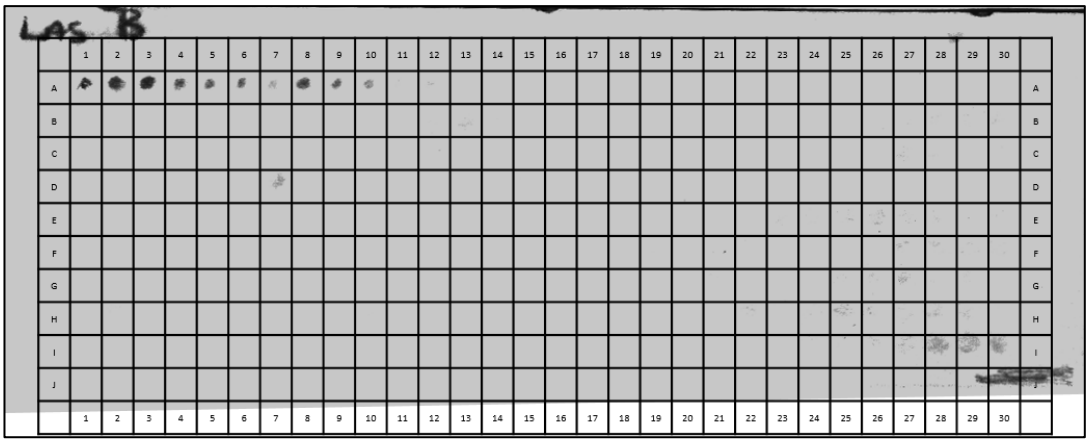

Figure 4.5 | Elastase peptide array probed with 1 μg/mL HRP-conjugated anti-elastase RA528 polyclonal antibody. Each cell on the grid overlay corresponds to a 15 residue peptide from the mature elastase sequence, with each sequential cell containing the following 15 residues in an overlapping fashion such that cell 2 contains residues 1-15, cell 3 contains residues 2-16, and so on. The amino acid sequences of the first 10 peptides are shown in **Table 4.2**. A pencil mark is made in cell 1 in order to anchor the grid.

Table 4.2 | Amino acid sequences of the first 9 peptides (A2-10) recognised by the RA528 polyclonal antibody RA528.

Grid Reference	Amino Acid Sequence
A2	AEAGGPGGNQKIGKY
A3	EAGGPGGNQKIGKYT
A4	AGGPGGNQKIGKYTY
A5	GGPGGNQKIGKYTYG
A6	GPGGNQKIGKYTYGS
A7	PGGNQKIGKYTYGSD
A8	GGNQKIGKYTYGSDY
A9	GNQKIGKYTYGSDYG
A10	NQKIGKYTYGSDYGP

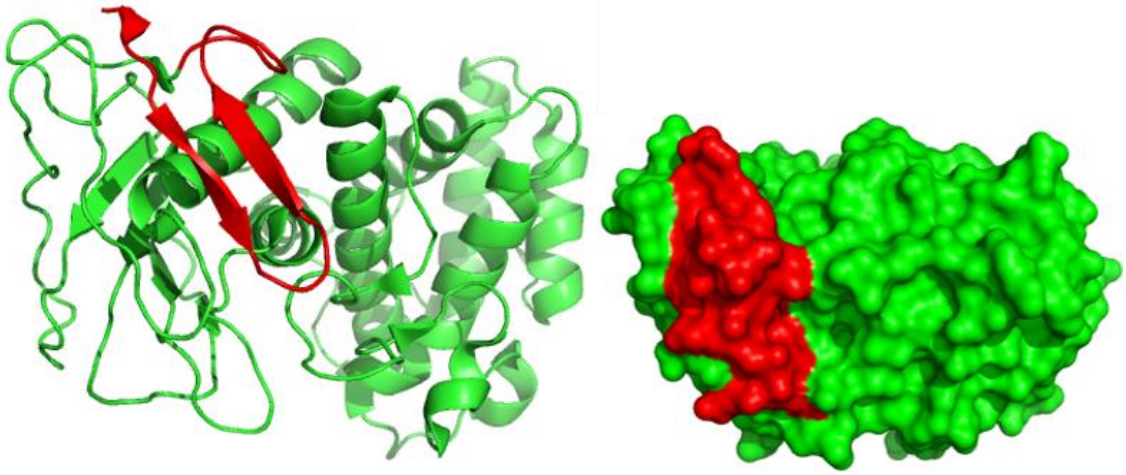

Figure 4.6 | The linear epitope of elastase mapped as recognised by the RA528 detector antibody as determined by peptide array (**Figure 4.5**), modelled in PyMOL. Elastase is shown as secondary structure (left) and as a space-filling model (right). The linear epitope is highlighted in red.

4.5 Development of an ELISA Sandwich Assay for Elastase Utilising Affinity Purified Antibodies

4.5.1 Reagent Optimisation during Development of a Rabbit Sandwich ELISA for Elastase

To optimise the capture and detector rabbit antibody combinations and dilutions for a sandwich ELISA to detect elastase, an initial sandwich ELISA experiment was performed in which capture antibodies were tested at concentrations of 0.1 µg/mL and 1 µg/mL, in combination with detector antibody dilutions of 1/2000, 1/4000 and 1/8000. Both rabbit-derived antibodies were tested separately as well as in combination in order to determine the optimal conditions for measuring elastase with minimal background and high sensitivity. A 96 well Nunc-Immuno™ MaxiSorp™ plate was coated with dilutions of capture antibody and 100 ng/mL elastase was used as a standard antigen concentration for these initial experiments. The combinations with the highest signal to noise ratios were selected as a basis for further ELISA-based assays. In regards to the rabbit polyclonal antibodies, the four best performing antibody combinations were 1 µg/mL RA528 with 1/2000 HRP-RA528, 1 µg/mL RA528 with 1/4000 HRP-RA528, 1 µg/mL RA528 with 1/2000 HRP-RA529 and 1 µg/mL RA529 with 1/4000 HRP-RA529 (**Figure 4.7**).

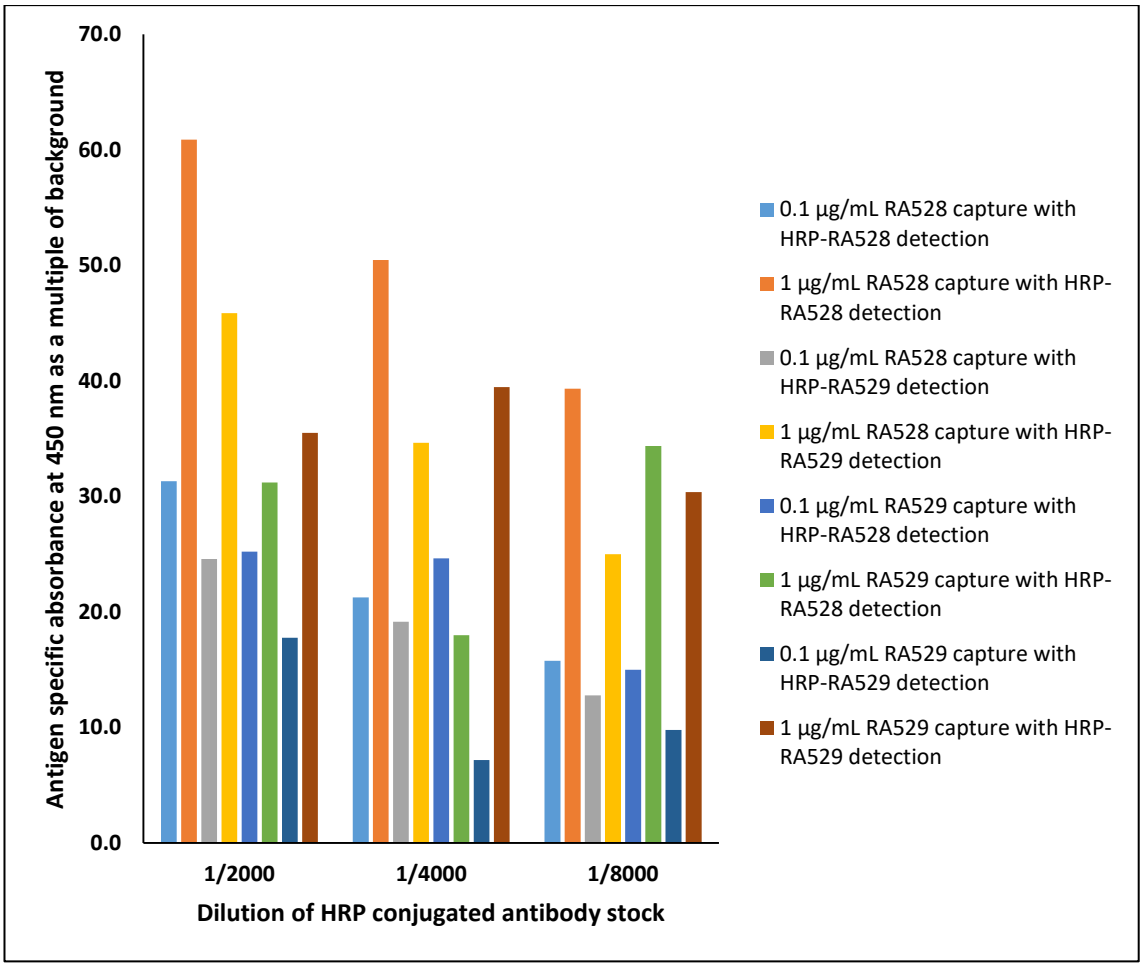

Figure 4.7 | Reagent optimisation for a sandwich ELISA to detect elastase using affinity purified rabbit polyclonal antibodies. Absorbance was read at 450 nm and signal to noise ratio is plotted.

4.5.2 Assessment of Rabbit Polyclonal Antibody Sensitivity via Sandwich ELISA

The four best antibody combinations determined in **Section 4.4.1** were carried forward for further sensitivity testing via an elastase sandwich ELISA. In this assay, A 96 well Nunc-Immuno™ MaxiSorp™ plate was coated with dilutions of capture antibody and the concentration of elastase added was varied. Serial dilutions of recombinant elastase were prepared at concentrations of 100, 50, 25, 12.5, 6.25, 3.13 and 1.56 ng/mL and sandwich ELISAs were performed as described in **Section 2.4.9** (**Figure 4.8**).

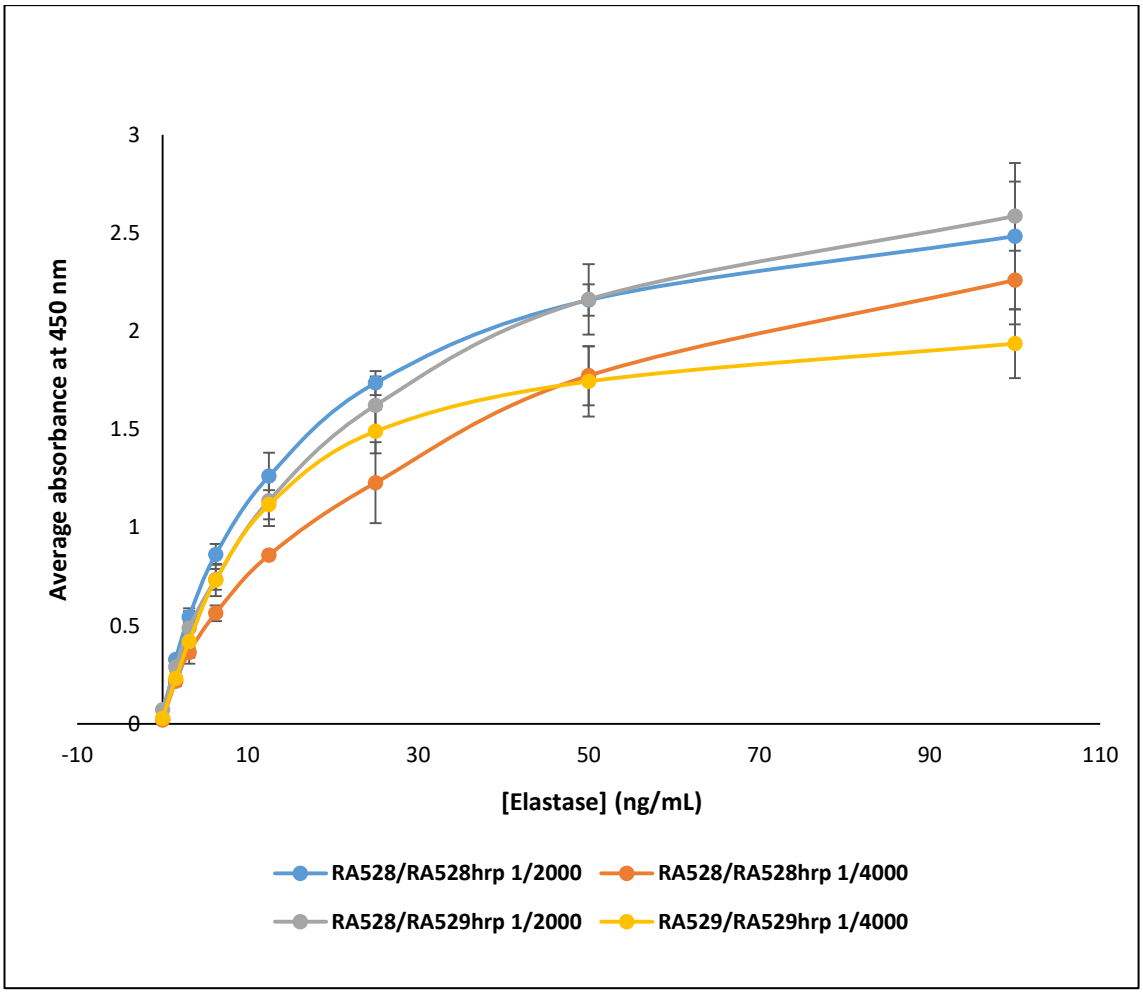

Figure 4.8 | Initial sensitivity tests for a sandwich ELISA incorporating the 4 rabbit anti-elastase polyclonal antibody combinations with the greatest signal to noise ratio, as established in the work presented in **Figure 4.7**. (n=1, where each sample was measured 3 times)

Four parameter logistic fit curves were generated from the standard curves using the Four Parameter Logistic Curve Calculator from AAT Bioquest®. Using these curves, lower limits of detection (LLODs) were calculated for each antibody combination. The RA528 detector antibody, in combination with the RA528 capture antibody, had LLODs of 79 and 27 pg/mL when diluted 1/2000 and 1/4000 respectively (**Figure 4.9**), whilst the RA529 detector antibody had similar LLODs of 89 pg/mL with the RA528 capture antibody and 29 pg/mL with the RA529 capture antibody, at a detector dilution of 1/4000 (**Figure 4.10**).

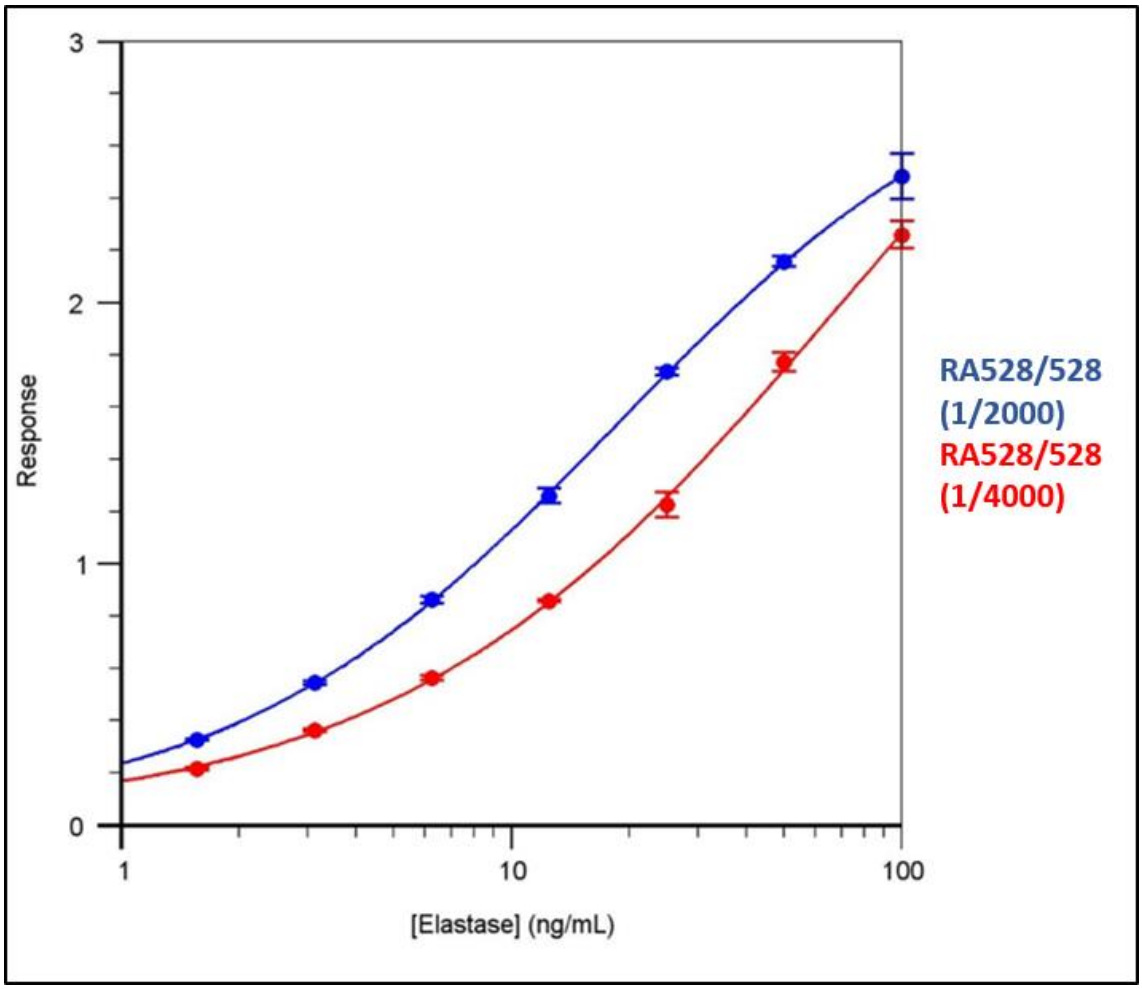

Figure 4.9 | Four parameter logistic fit curve to determine the lower limit of detection of elastase for the RA528 capture antibody in combination with the RA528 detector antibody at a 1/2000 dilution (blue) and a 1/4000 dilution (red) in a sandwich ELISA format. (n=1, where each sample was measured 3 times).

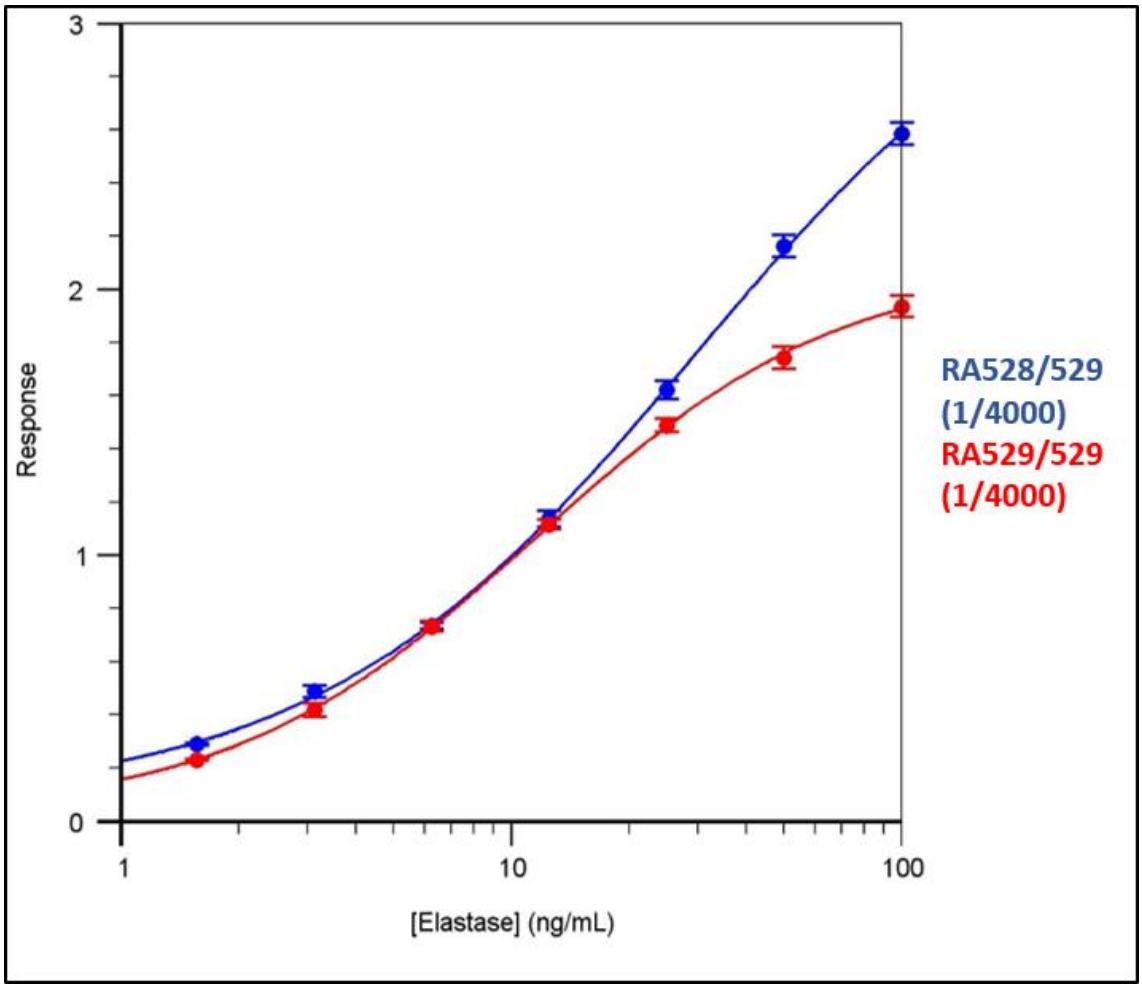

Figure 4.10 | Four parameter logistic fit curve to determine the lower limit of detection of elastase for the RA529 detector antibody at a dilution of 1/4000 in combination with the RA528 and RA529 capture antibodies in a sandwich ELISA format. (n=1, where each sample was measured 3 times).

Following on from these initial sensitivity tests, the antibody combination RA528/528hrp 1/4000 was selected for further assessment. Once again, a sandwich ELISA was performed using this combination of capture and detection antibodies, and elastase concentrations were measured from a concentration of 1 ng/mL through to 16.125 pg/mL. The calculated estimated LLOD from this curve was 76.9 pg/mL, slightly higher than the LLOD established from the previous 4 parameter fit logistic curve (**Figure 4.11**).

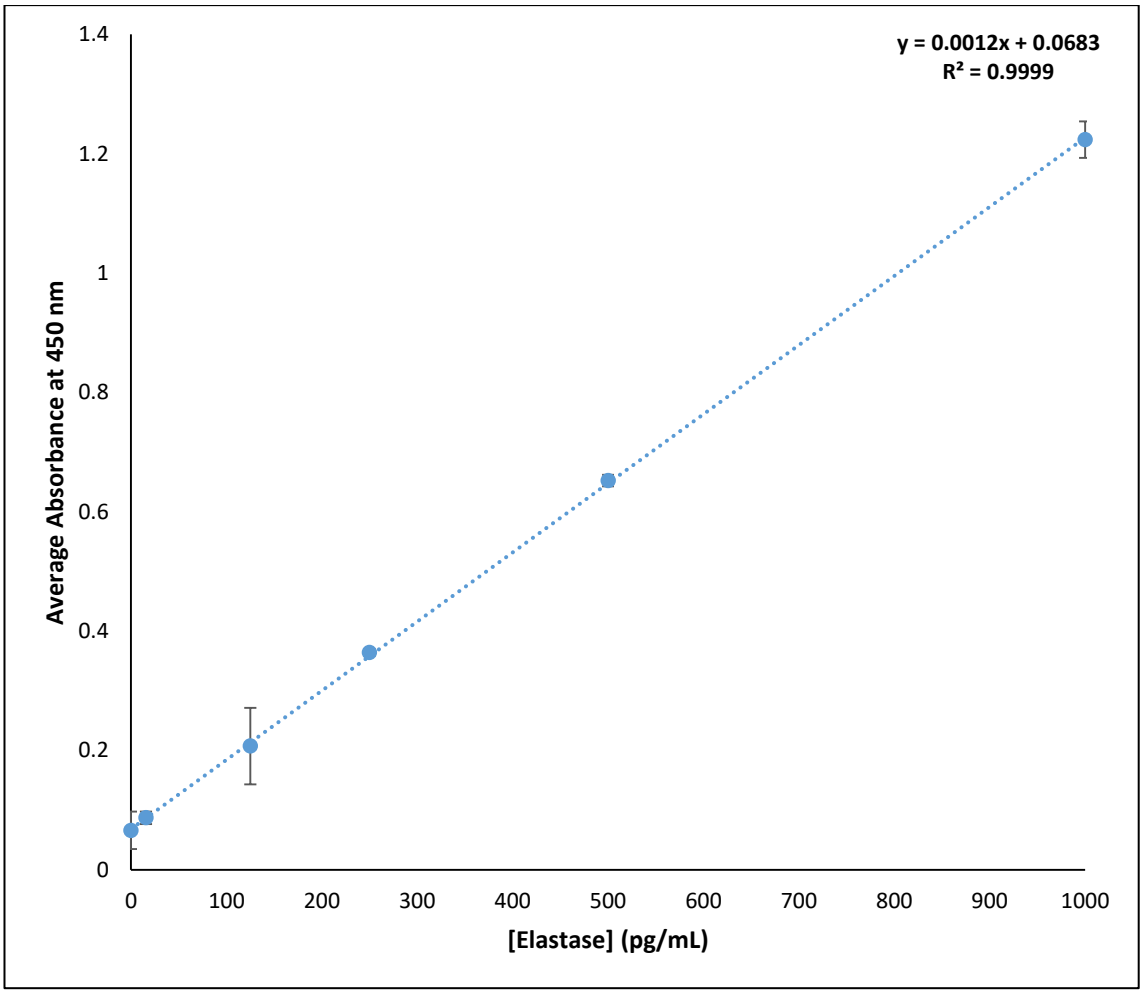

Figure 4.11 | Standard curve for detection of pg/mL concentrations of elastase via sandwich ELISA, at a capture antibody concentration of 1 µg/mL and a detector antibody dilution of 1/4000. (n=1, where each sample was measured 4 times).

4.5.3 Reagent Optimisation for Development of a Sheep Sandwich ELISA for Elastase

As in **Section 4.4.1**, the affinity purified anti-elastase polyclonal antibodies raised in sheep were assessed via sandwich ELISA in order to optimise reagent combinations for an anti-elastase sandwich ELISA. As described previously for the rabbit antibodies, capture antibodies from both animals were tested at concentrations of 0.1 µg/mL and 1 µg/mL and detection antibodies were tested at dilutions of 1/2000, 1/4000 and 1/8000, using 100 ng/mL elastase as a standard antigen concentration. The 4 antibody combinations yielding the greatest signal to noise ratios were selected for further experimental work. For polyclonal antibodies purified from sheep serum, the four antibody combinations yielding the highest signal to noise ratio were SA562 with 1/8000 HRP-SA562, SA562 with 1/4000 HRP-SA562, SA563 with 1/4000 HRP-SA562 and SA563 with 1/2000 HRP-562 (**Figure 4.12**).

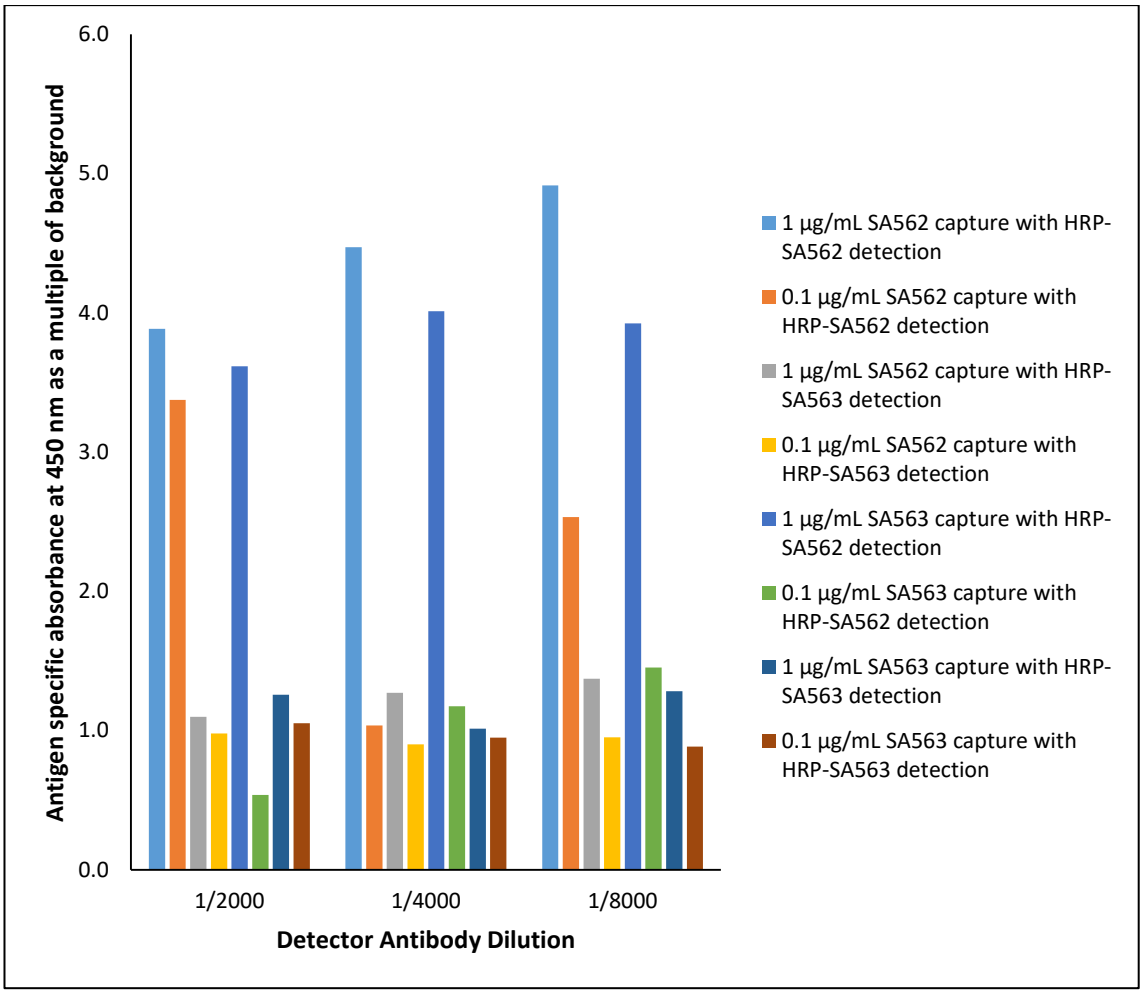

Figure 4.12 | Reagent optimisation for a sandwich ELISA to detect elastase using affinity purified sheep polyclonal antibodies. Absorbance was read at 450 nm and signal to noise ratio is plotted.

4.5.4 Assessment of Sheep Polyclonal Antibody Sensitivity via Sandwich ELISA

The four best antibody combinations determined in **Section 4.5.3** were carried forward for further sensitivity testing via an elastase sandwich ELISA. ELISAs were performed as described in **Section 4.5.2** using the described ng/mL concentrations of recombinant elastase to establish standard curves (**Figure 4.13**).

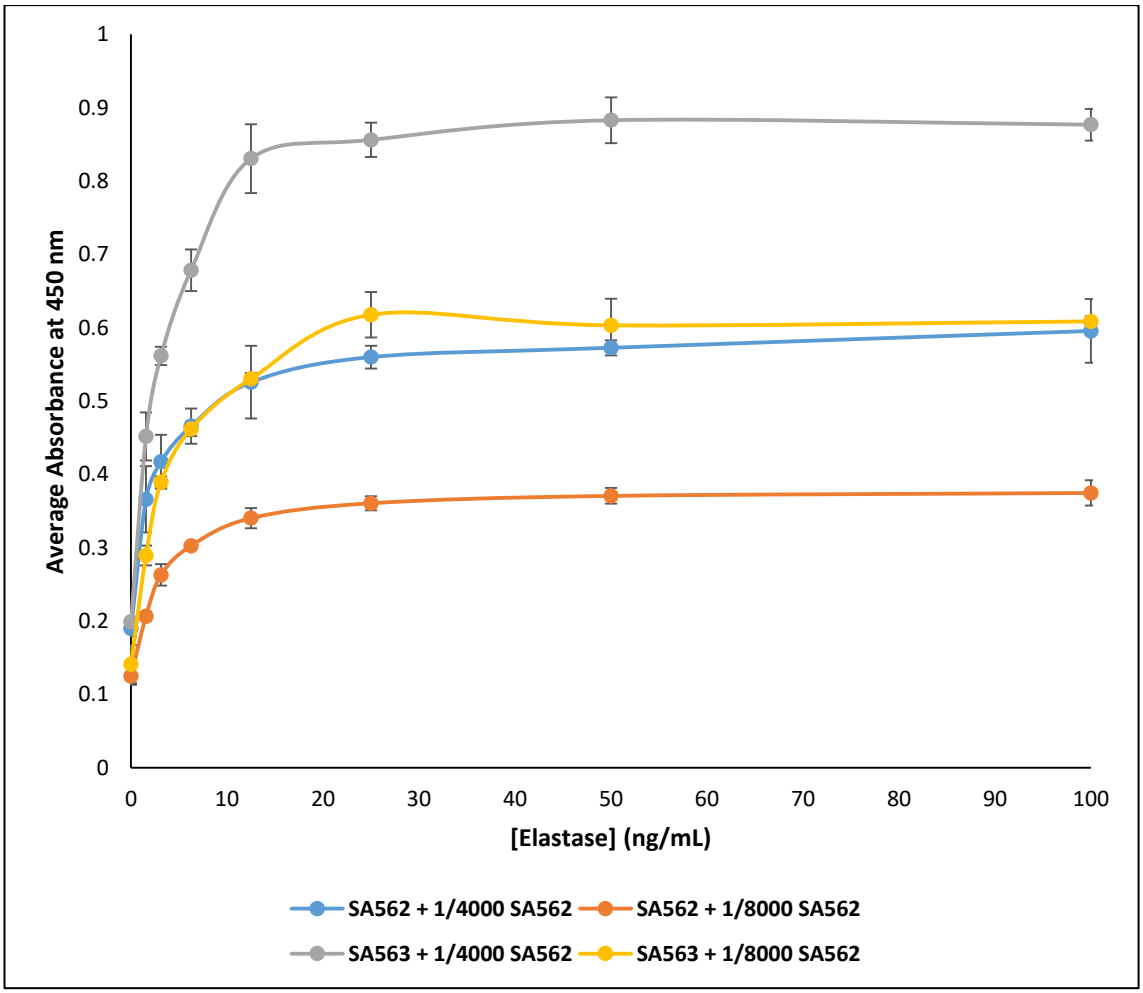

Figure 4.13 | Initial sensitivity tests for a sandwich ELISA incorporating the 4 sheep anti-elastase polyclonal antibody combinations with the greatest signal to noise ratio, as established in **Figure 4.12**. (n=1, where each sample was measured 3 times).

When compared to the initial sensitivity tests for affinity purified rabbit anti-elastase pAbs, the sheep antibody ELISA appeared to be more limited due to a moderate level of background signal generated in the absence of antigen. In order to investigate this and try and minimise the background, an additional optimisation ELISA was performed in which multiple variables were examined. The addition of an initial blocking step in 5% MPBS prior to addition of antigen, preparation of the detector antibody in 5% MPBS rather than 1% BSA, and a further detector antibody dilution of 1/16000 were all investigated in an attempt to minimise background signal. Each variable was tested in the presence of 100 ng/mL recombinant elastase and in 1% PBSTB assay buffer with no antigen, and the signal to noise ratio was calculated for each condition. From these ELISAs, it was determined that by preparing the HRP-labelled detector antibody in 5% MPBS, or blocking the plate prior to addition of antigen, background signal could be reduced (**Figure 4.14**). However, it was not possible to entirely eliminate this background noise. As the

signal to noise ratios for the "Blocked plate, detector in 1% BSA" and "Unblocked plate, detector in 5% MPBS" conditions were comparable at the 1/4000 and 1/8000 dilutions, it was decided that the protocol going forward would incorporate the detector in 5% MPBS approach, as addition of a full blocking step did not substantially impact the signal to noise ratio and resulted in an additional hour of assay time.

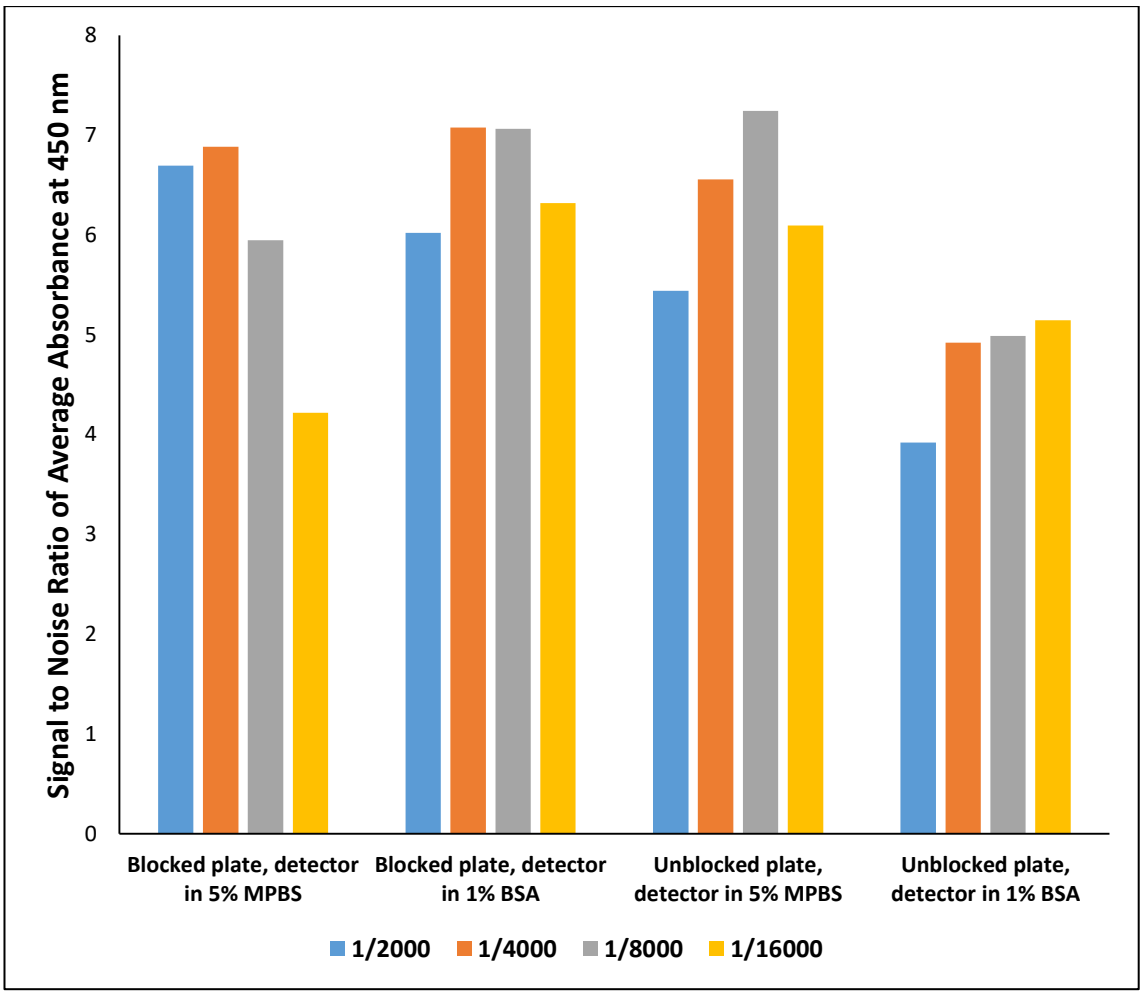

Figure 4.14 | Protocol optimisation for a sandwich ELISA to detect recombinant elastase using affinity purified sheep polyclonal antibodies. Absorbance was read at 450 nm and the signal to noise ratio was plotted. (n=1, where each sample was measured 3 times).

Standard curves were again established using the optimised protocol. Both capture antibodies were tested at a concentration of 1 µg/mL in combination with the SA562 HRP-labelled detector antibody at a dilution of 1/4000 and elastase concentrations ranging from 100 ng/mL to 1.56 ng/mL used (**Figure 4.15**).

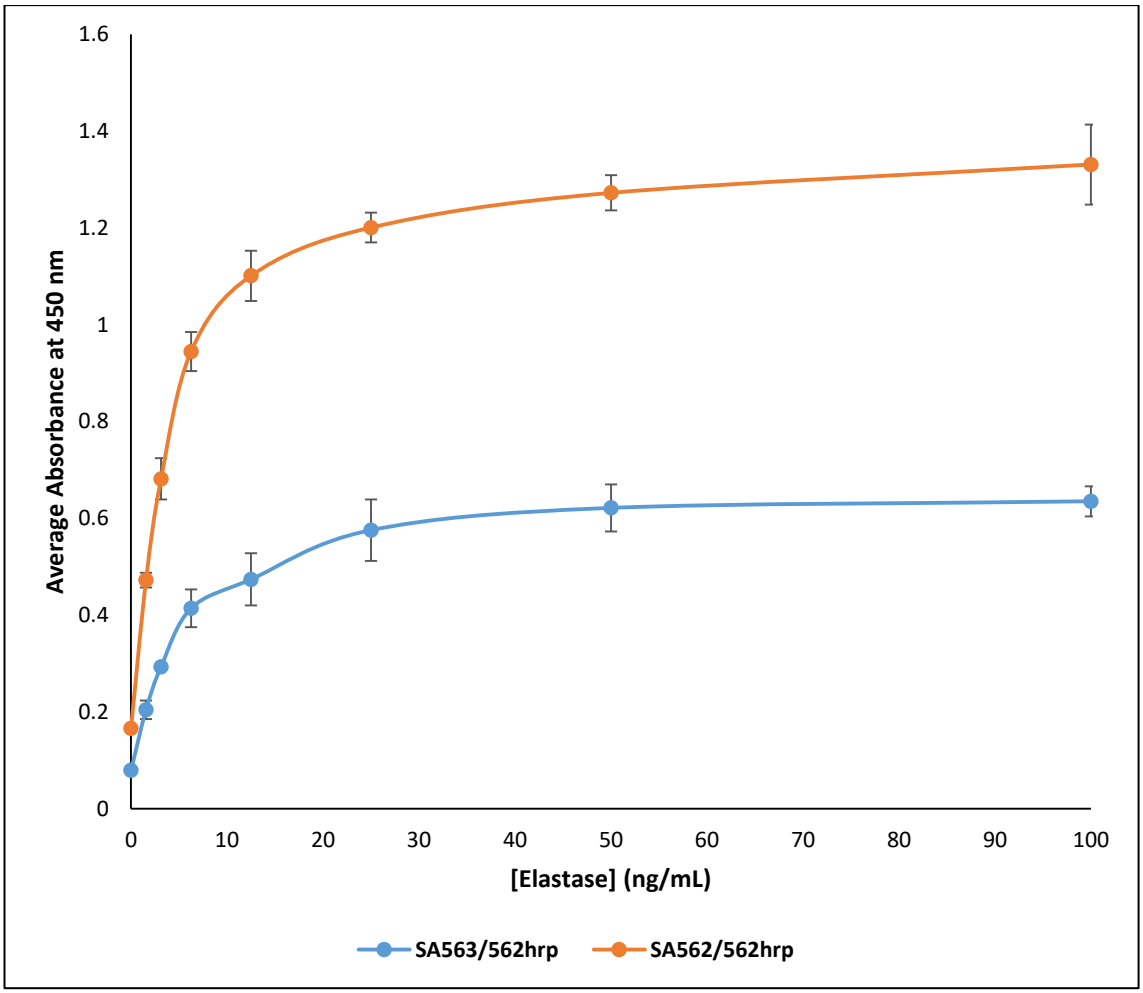

Figure 4.15 | Sensitivity tests for an anti-elastase sandwich ELISA incorporating the two different affinity purified sheep polyclonal antibodies. (n=1, where each sample was measured 3 times).

In order to establish LLODs for each antibody combination, a 4 parameter logistic fit curve was produced using the Four Parameter Logistic Curve Calculator from AAT Bioquest®. For the SA563 capture antibody, the LLOD was calculated as 169 pg/mL, whereas for the SA562 capture antibody, this value was higher at 266 pg/mL (**Figure 4.16**). Despite the higher limit of detection, the SA562 capture antibody was determined to perform better due to its lower level of variance between repeats and greater range of signal.

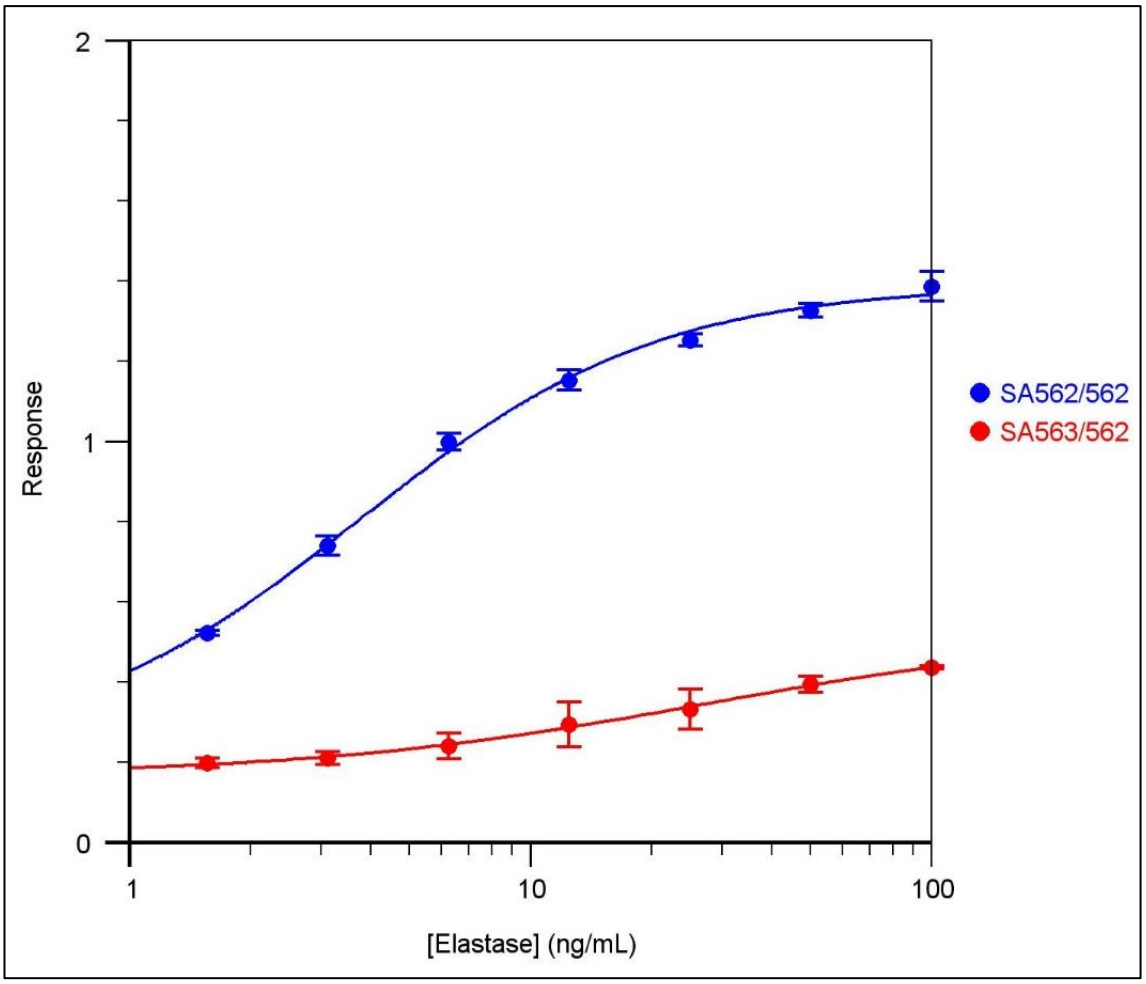

Figure 4.16 | Four parameter logistic fit curve to determine the lower limit of detection of elastase for each capture antibody combination using the described sheep antibodies under the optimised sandwich ELISA protocol. (n=1, where each sample was measured 3 times).

4.5.5 Assessment of Clinically Relevant *P. aeruginosa* Strain Supernatants via ELISA for Elastase

Clinically relevant *P. aeruginosa* isolates were provided by the National Heart and Lung Institute, Imperial College London, by Prof. Jane Davies, that were subsequently tested via sandwich ELISA for elastase expression to validate the ability of the ELISA to detect relevant amounts of elastase in such samples. Isolates were plated on LB agar plates and allowed to grow overnight at 37°C. The following day, 3 mL liquid cultures were set up from a single colony, grown overnight in LB medium at 37°C with shaking. After overnight growth, culture supernatants were harvested via centrifugation at 2,500 x g for 10 minutes and diluted 1:1 with 2% PBSTB assay buffer for ELISA analysis. Sandwich ELISAs were performed with the SA562 capture and detection antibodies using the protocol established in **Section 4.5.4**. 31 "first isolates" were tested; isolates obtained at first confirmation of *P. aeruginosa* infection in cystic fibrosis patients, and 20 "chronic

isolates" were obtained from chronically infected cystic fibrosis patients. Of these 20 chronic isolates, 3 did not grow (CH5, CH15 and CH18) and as such were not included in the ELISA tests performed. A range of negative controls were also assessed to ensure no cross-reactivity with other bacteria commonly associated with cystic fibrosis (**Figure 4.20**). These negative controls included supernatants from the culture of *Escherichia coli, Staphylococcus aureus, Klebsiella pneumoniae, Achromobacter xylosidans, Serracia marcescens, Stenotrophomonas maltophilia* and *Burkholderia cepacia* complex.

20 samples were assessed per ELISA plate, including 3 confirmed negative controls for the first isolate and chronic isolate plates, and a recombinant elastase standard curve ranging from 0-100 ng/mL elastase in order to establish lower limits of detection. For these assays, LLOD was defined as the minimum absorbance value for a positive test, and was calculated as the mean absorbance on the standard curve at 0 ng/mL elastase plus three standard deviations. Three technical replicates were performed for each sample on the same ELISA plate.

From these ELISAs, 29/31 first isolate supernatants tested returned a positive result which, following one-way ANOVA and grouping via the Tukey method with a 95% confidence interval (**Figure 4.17b** and **Figure 4.18b**), were determined to be significantly different from the negative control groups, which comprised supernatants from *S. aureus*, *E. coli* and *S. marcescens*. Of the 17 chronic isolate supernatants tested, 14 returned a positive result based on the established LLOD from the plate's standard curve (**Figure 4.19a**). However, following one-way ANOVA and Tukey grouping, only 12 chronic isolates were found to differ significantly from the negative control supernatants (**Figure 4.19b**).

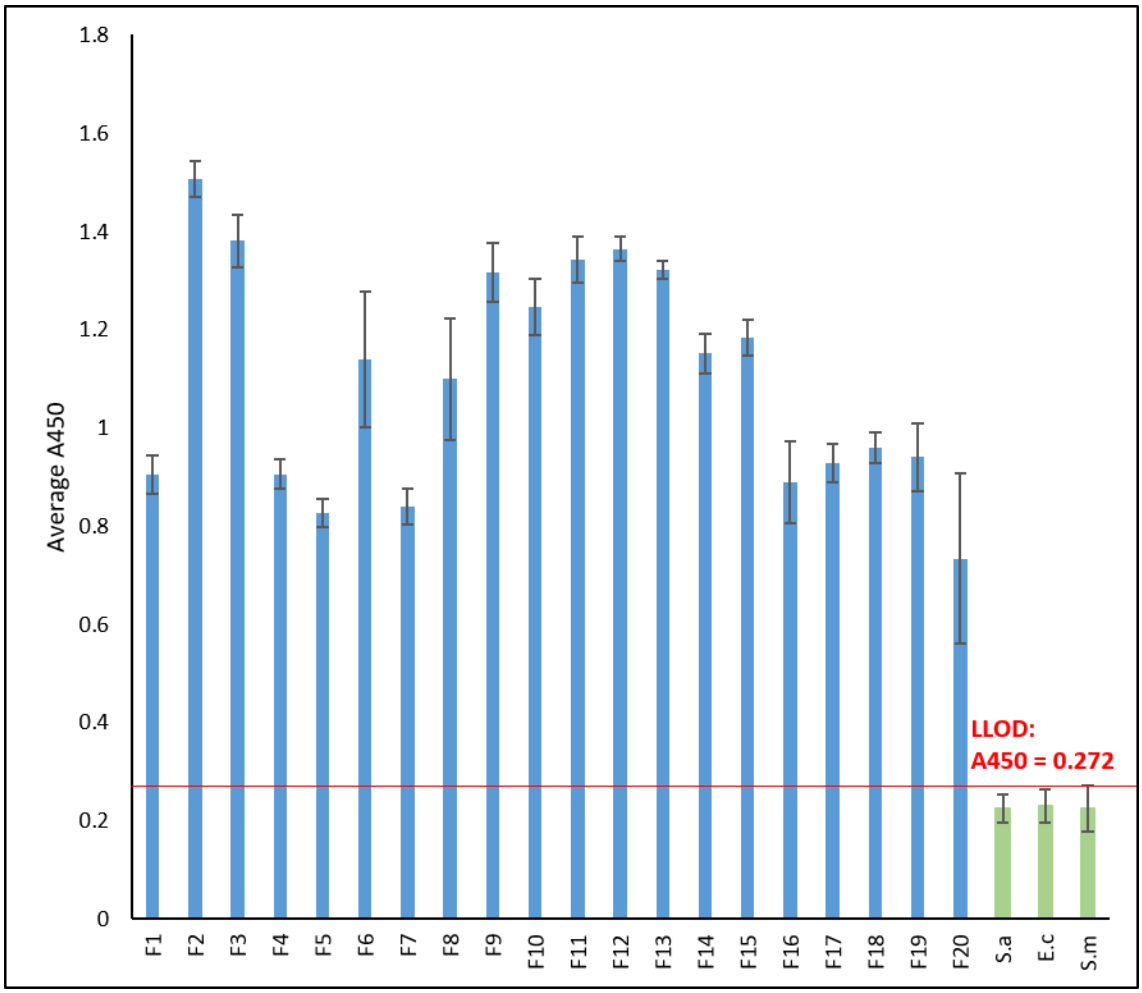

Figure 4.17a | Assessment of *P. aeruginosa* First Isolates, cultured from cystic fibrosis patient sputum samples, via anti-elastase sandwich ELISA. (n=1, where each sample was measured 3 times). The red line indicates the LLOD, calculated as the mean value of absorbance at 0 ng/mL recombinant elastase + 3 standard deviations.

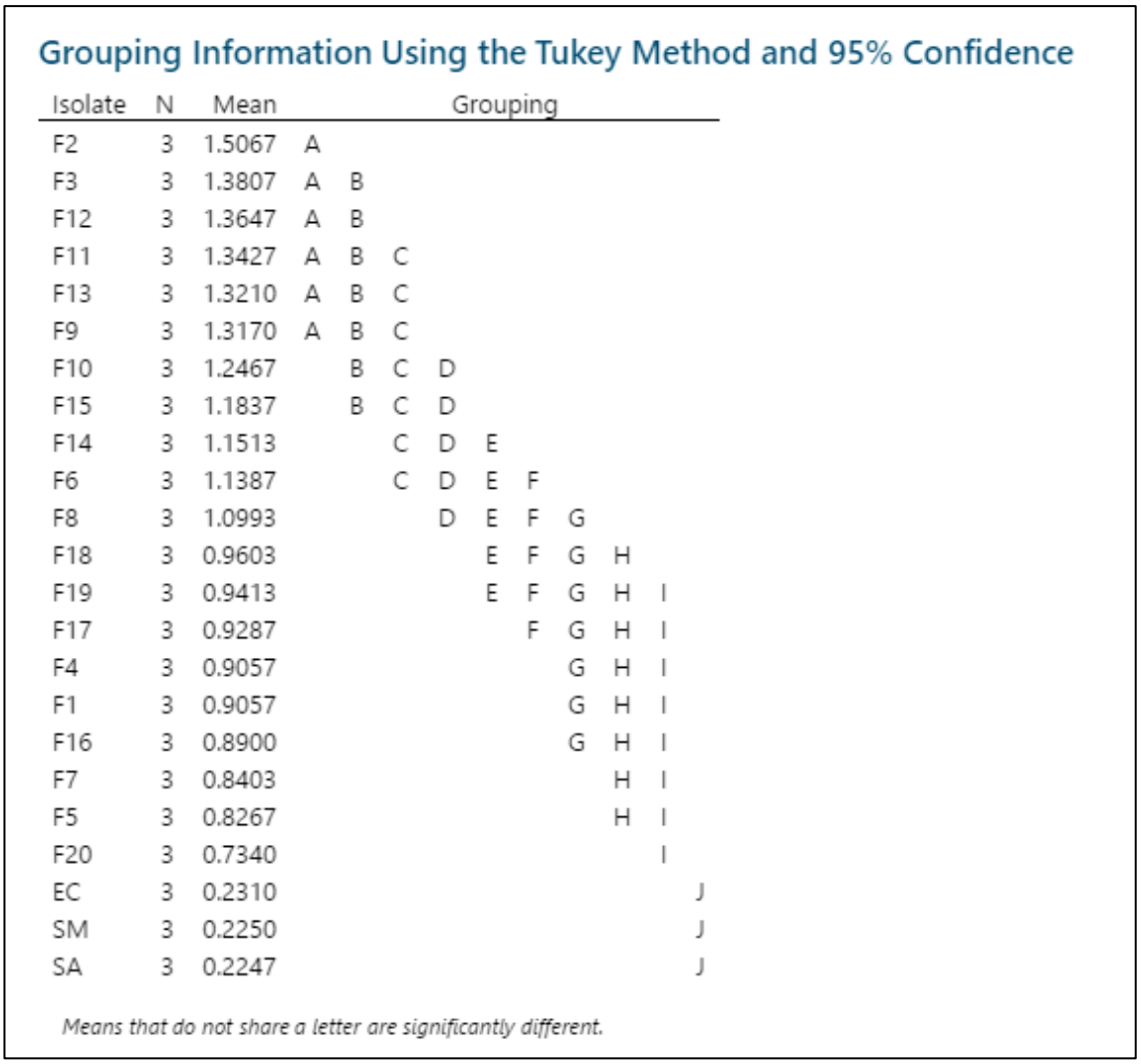

Grouping Information Using the Tukey Method and 95% Confidence

Isolate	N	Mean	Grouping								
F2	3	1.5067	A								
F3	3	1.3807	A	B							
F12	3	1.3647	A	B							
F11	3	1.3427	A	B	C						
F13	3	1.3210	A	B	C						
F9	3	1.3170	A	B	C						
F10	3	1.2467		B	C	D					
F15	3	1.1837		B	C	D					
F14	3	1.1513			C	D	E				
F6	3	1.1387			C	D	E	F			
F8	3	1.0993				D	E	F	G		
F18	3	0.9603					E	F	G	H	
F19	3	0.9413					E	F	G	H	I
F17	3	0.9287						F	G	H	I
F4	3	0.9057							G	H	I
F1	3	0.9057							G	H	I
F16	3	0.8900							G	H	I
F7	3	0.8403								H	I
F5	3	0.8267								H	I
F20	3	0.7340									I
EC	3	0.2310									J
SM	3	0.2250									J
SA	3	0.2247									J

Means that do not share a letter are significantly different.

Figure 4.17b | Grouping of First Isolates and negative controls via the Tukey Method following one way ANOVA. The three control strains "EC, SM and SA" correspond to *E. coli*, *S. marcescens* and *S. aureus*, and were found to be significantly different from the First Isolate test group (Groups A – I).

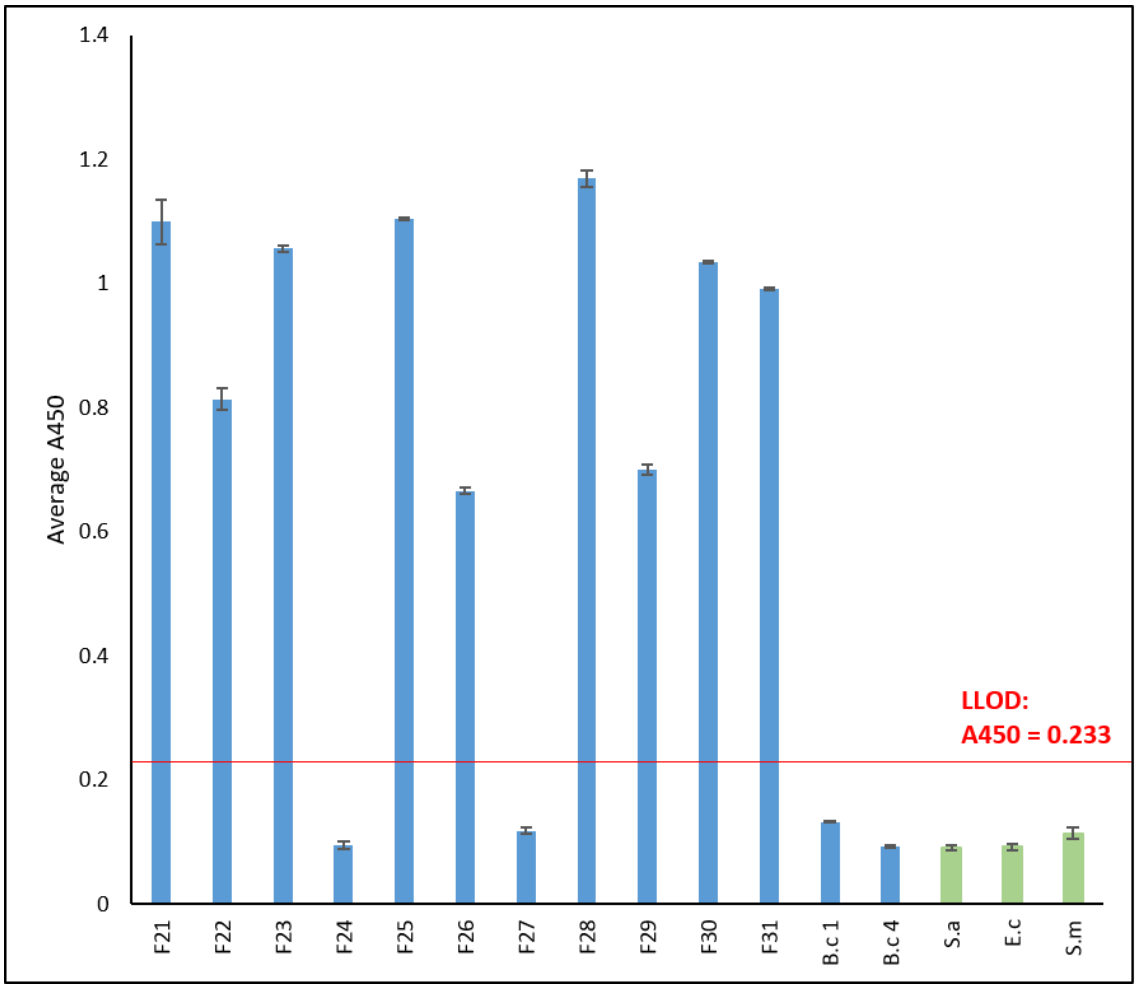

Figure 4.18a | Assessment of *P. aeruginosa* First Isolates, cultured from cystic fibrosis patient sputum samples, via anti-elastase sandwich ELISA. Two *B. cepacia* complex isolates have been included as additional negative control samples. (n=1, where each sample was measured 3 times). The red line indicates the LLOD, calculated as the mean value of absorbance at 0 ng/mL recombinant elastase + 3 standard deviations.

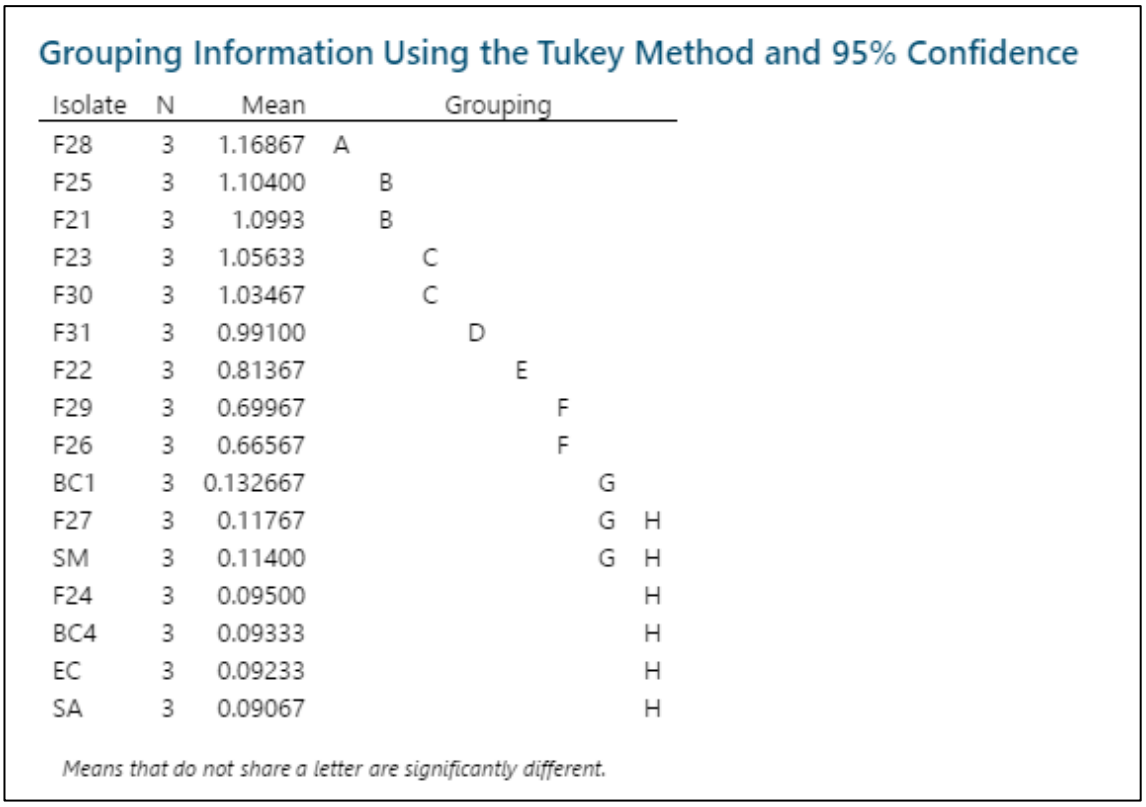

Grouping Information Using the Tukey Method and 95% Confidence

Isolate	N	Mean	Grouping							
F28	3	1.16867	A							
F25	3	1.10400		B						
F21	3	1.0993		B						
F23	3	1.05633			C					
F30	3	1.03467			C					
F31	3	0.99100				D				
F22	3	0.81367					E			
F29	3	0.69967						F		
F26	3	0.66567						F		
BC1	3	0.132667							G	
F27	3	0.11767							G	H
SM	3	0.11400							G	H
F24	3	0.09500								H
BC4	3	0.09333								H
EC	3	0.09233								H
SA	3	0.09067								H

Means that do not share a letter are significantly different.

Figure 4.18b | Grouping of First Isolates and negative controls via the Tukey Method following one way ANOVA. The control strains “EC, SM and SA” were found to be significantly different from the First Isolate test group. Isolates F24 and F27, which returned negative results, also grouped with the negative groups (groups G & H), as well as the additional control strains BC1 and BC4.

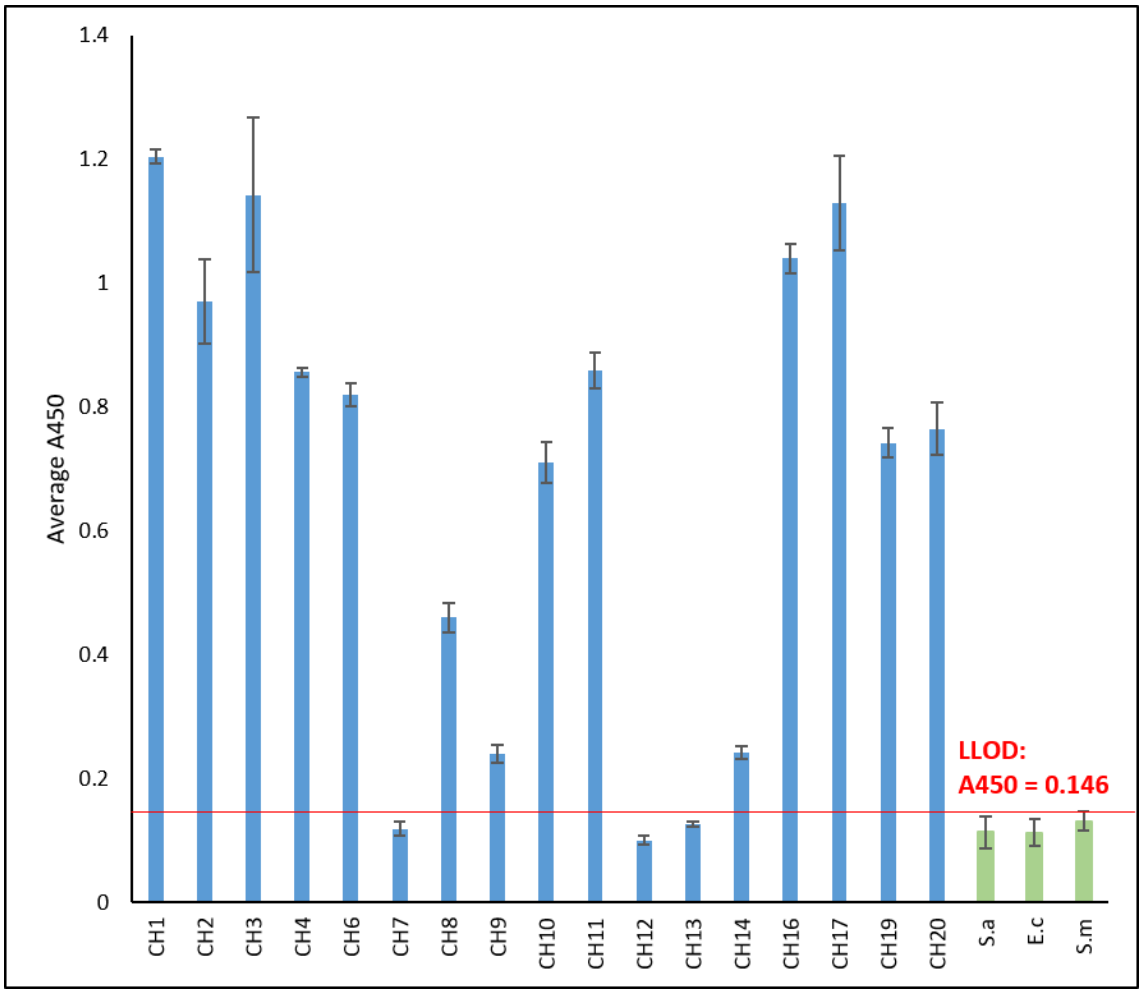

Figure 4.19a | Assessment of *P. aeruginosa* Chronic Isolates, cultured from cystic fibrosis patient sputum samples, via anti-elastase sandwich ELISA. (n=1, where each sample was measured 3 times). The red line indicates the LLOD, calculated as the mean value of absorbance at 0 ng/mL recombinant elastase + 3 standard deviations.

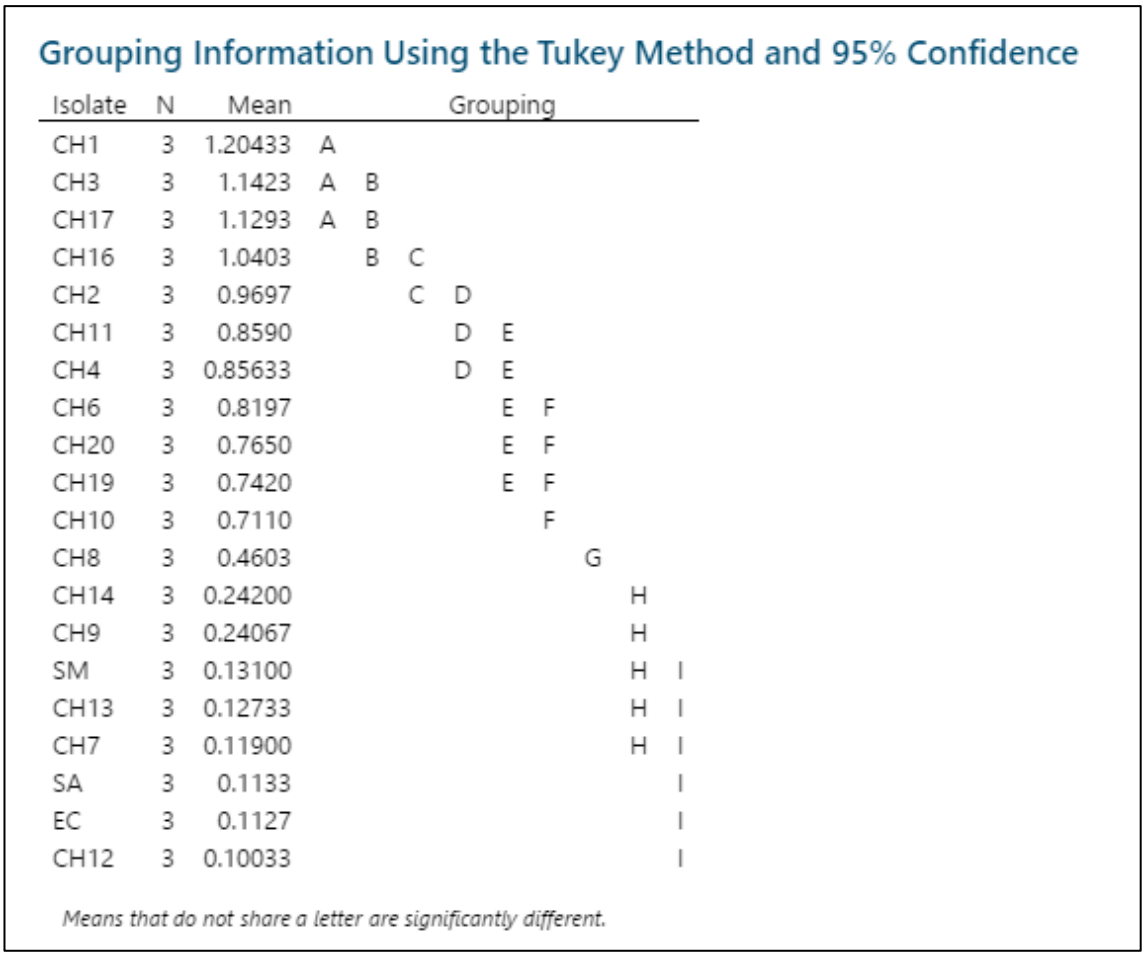

Grouping Information Using the Tukey Method and 95% Confidence

Isolate	N	Mean	Grouping							
CH1	3	1.20433	A							
CH3	3	1.1423	A	B						
CH17	3	1.1293	A	B						
CH16	3	1.0403		B	C					
CH2	3	0.9697			C	D				
CH11	3	0.8590				D	E			
CH4	3	0.85633				D	E			
CH6	3	0.8197					E	F		
CH20	3	0.7650					E	F		
CH19	3	0.7420					E	F		
CH10	3	0.7110						F		
CH8	3	0.4603							G	
CH14	3	0.24200								H
CH9	3	0.24067								H
SM	3	0.13100								H I
CH13	3	0.12733								H I
CH7	3	0.11900								H I
SA	3	0.1133								I
EC	3	0.1127								I
CH12	3	0.10033								I

Means that do not share a letter are significantly different.

Figure 4.19b | Grouping of chronic isolates and negative controls via the Tukey Method following one way ANOVA. The three control strains "EC, SM and SA" correspond to *E. coli*, *S. marcescens* and *S. aureus*, and were found to be significantly different from the chronic isolates which returned absorbances higher than the determined LLOD. Though isolates CH9 and CH14 returned positive results following the LLOD criteria, they were not shown to be significantly different from the negative control group (group I).

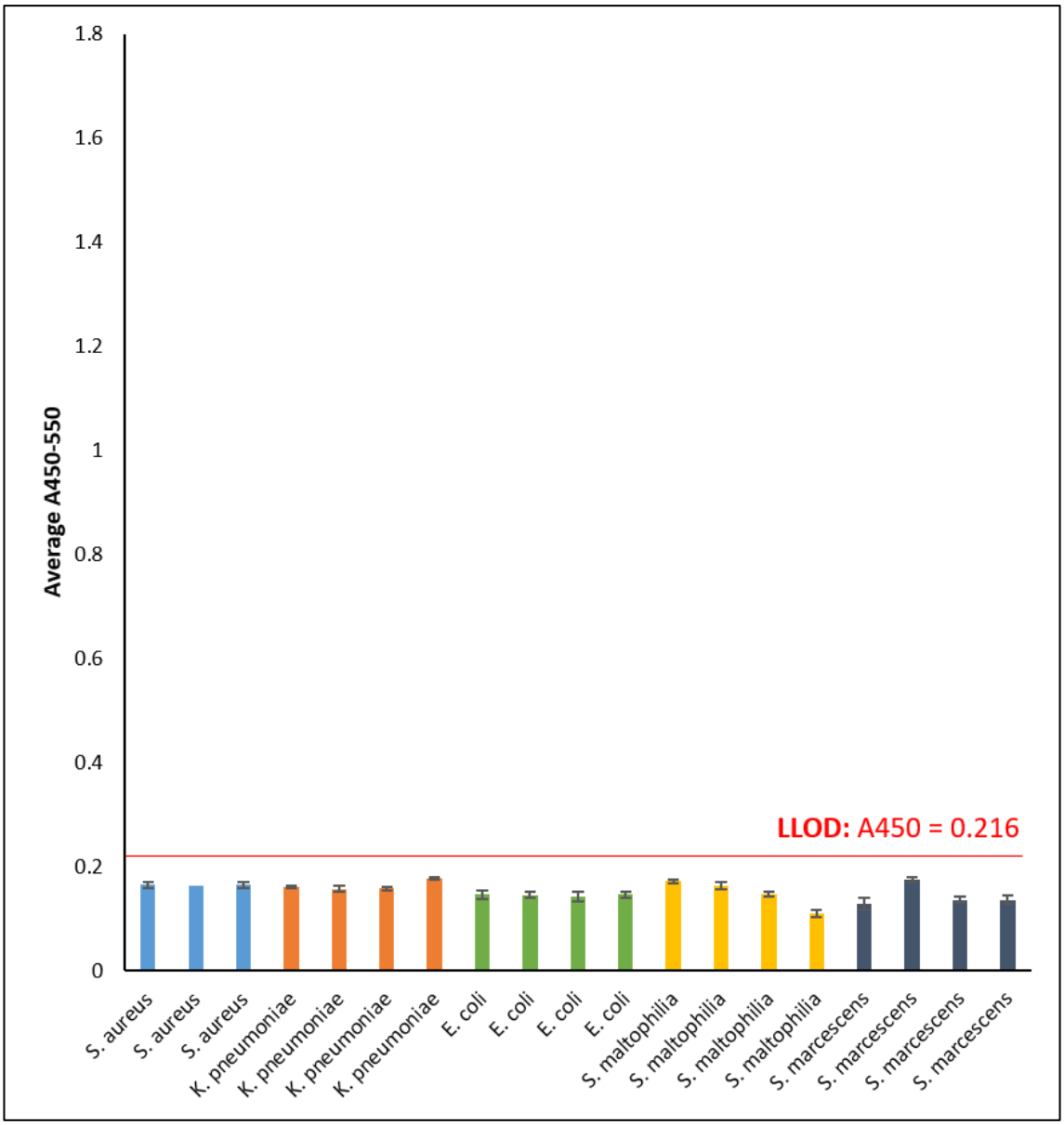

Figure 4.20 | Assessment of culture supernatants from a range of Gram negative and Gram positive bacterial strains, diluted 1/2, via anti-elastase sandwich ELISA for presence of elastase. (n=1, where each sample was measured 3 times). The red line indicates the LLOD, calculated as the mean value of absorbance at 0 ng/mL recombinant elastase + 3 standard deviations.

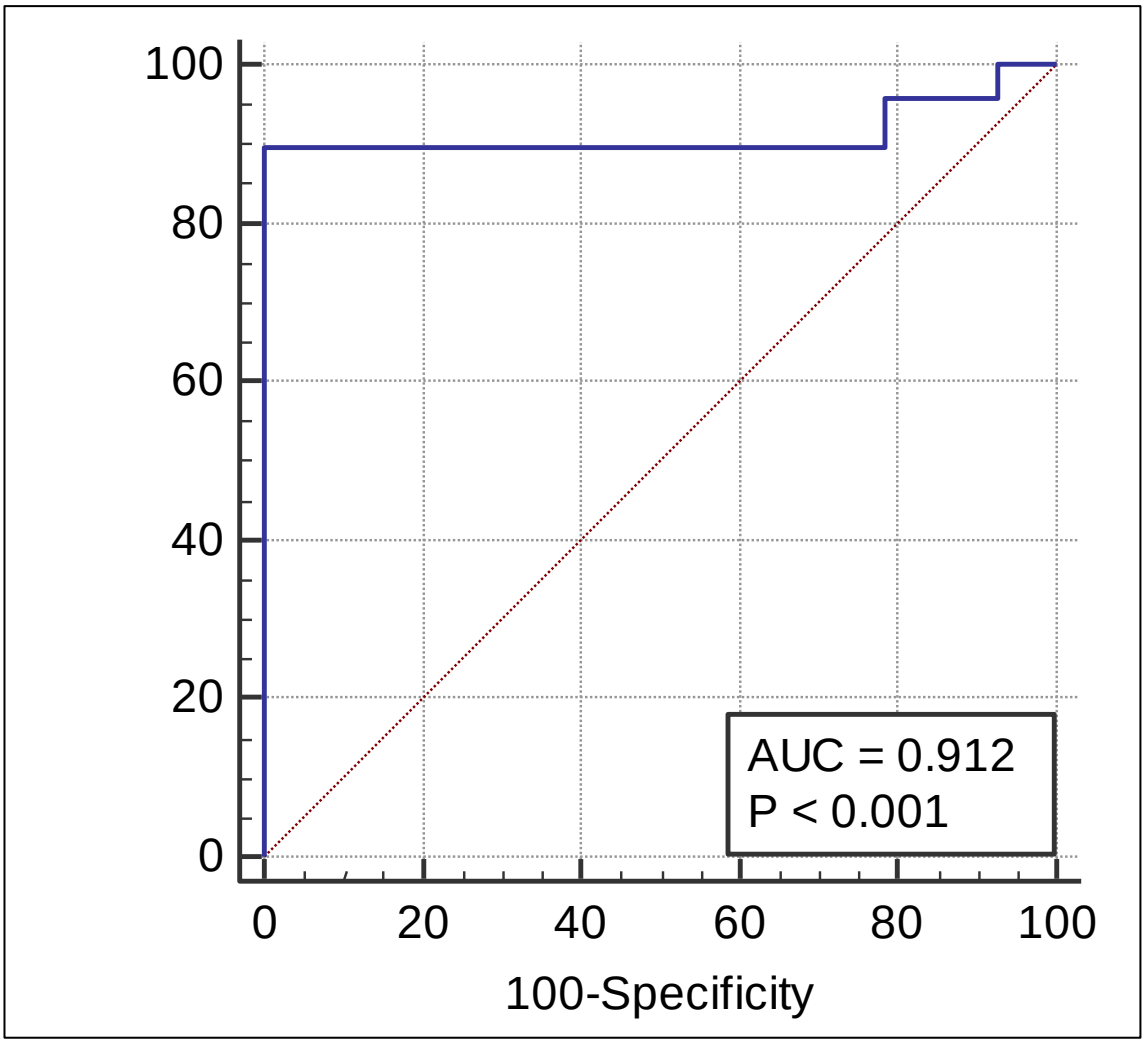

Figure 4.21 | Receiver operator curve (ROC) curve constructed from the ELISA results obtained from testing culture supernatants from 31 *P. aeruginosa* First Isolates, 17 Chronic Isolates and 19 non-*P. aeruginosa* controls for elastase expression.

Table 4.3 | Area under the curve (AUC) and 95% confidence intervals (CI), Youden index, percent sensitivity, percent specificity and their respective 95% confidence intervals determined from the ROC analysis in Figure 4.21.

AUC	AUC 95% CI	Youden Index	Sensitivity (%)	Sensitivity 95% CI	Specificity (%)	Specificity 95% CI
0.912	0.825–0.965	0.8958	89.58	77.3-96.5	100	87.7-100

4.6 Development of a Lateral Flow Assay for the Detection of Elastase Using Affinity Purified Rabbit Polyclonal Antibodies

4.6.1 Conjugation of Colloidal Gold to Affinity Purified Antibodies

Conjugation of colloidal gold nanoparticles to the rabbit RA528 affinity purified anti-elastase pAbs was carried out as described in **Section 2.6.1**. A variety of conjugation buffers were tested across a broad pH range from pH 5.0 to pH 9.3 and the most stable conjugate was determined via visual inspection. A colour change from red to dark purple indicates the precipitation of gold nanoparticles, meaning the conjugate was considered to be unstable. Through this assay, it was determined that any buffer above pH 6.0 would be appropriate, and so borate pH 8.5, a buffer commonly used for gold nanoparticle conjugation, was selected as the final conjugation buffer (**Figure 4.22**). Following buffer selection, the concentration of antibody to be conjugated was also determined by conjugating at concentrations of 5, 10 and 15 μg/mL. At antibody concentrations below 15 μg/mL, colloidal gold nanoparticles precipitated out of solution, so this concentration was established as the minimum for conjugation (**Figure 4.23**). Once optimised, a large-scale antibody conjugation reaction was performed in which 225 μg total antibody was labelled with colloidal gold.

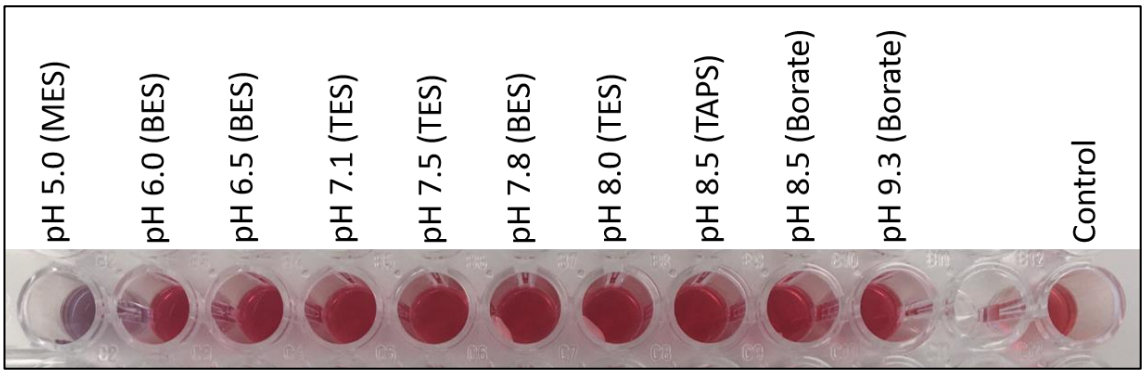

Figure 4.22 | Conjugation of 1.5 μg of anti-elastase rabbit RA528 polyclonal antibody to colloidal gold nanoparticles in a variety of buffers across a broad pH range. Dark purple (e.g. as observed at pH 5.0) is indicative of precipitation and is undesirable whilst a red colour indicates formation of a stable conjugate solution.

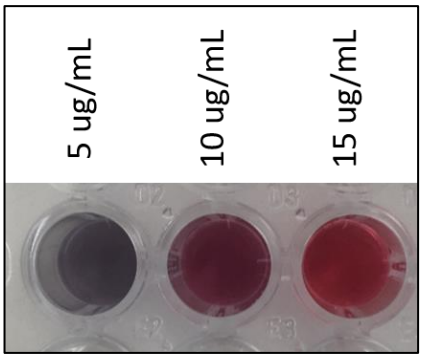

Figure 4.23 | Conjugation of a range of anti-elastase rabbit RA528 polyclonal antibody concentrations in borate pH 8.5 with colloidal gold nanoparticles.

4.6.2 Assembly and Initial Testing of an Anti-Elastase Lateral Flow Assay

All lateral flow work was performed at the site of the industrial partner, Mologic Ltd., in collaboration with Dr. Mike Johnson. Lateral flow "wet strips" were produced as described in **Section 2.6.2** via plotting of affinity purified RA528 antibody at a concentration of 1 mg/mL on a UniSart® CN140 membrane. The strips were immersed for 10 minutes in a solution containing 4 µL gold-conjugated detector antibody and 36 µL recombinant elastase at a concentration range of 0.01-1000 ng/mL before reading the test line intensity using a cube reader device, a small handheld lateral flow reader device provided by the industrial partner Mologic Ltd. With this device, a reported cube absorbance unit reading of 10 or higher was considered to be a positive result, confirming the presence of the antigen of interest in the applied sample. Initial "wet testing" of lateral flow strips resulted in an estimated limit of detection between 0.1 and 1 ng/mL elastase, with an average cube absorbance reading of 11.75 (n=2) at 1 ng/mL (**Figure 4.25**).

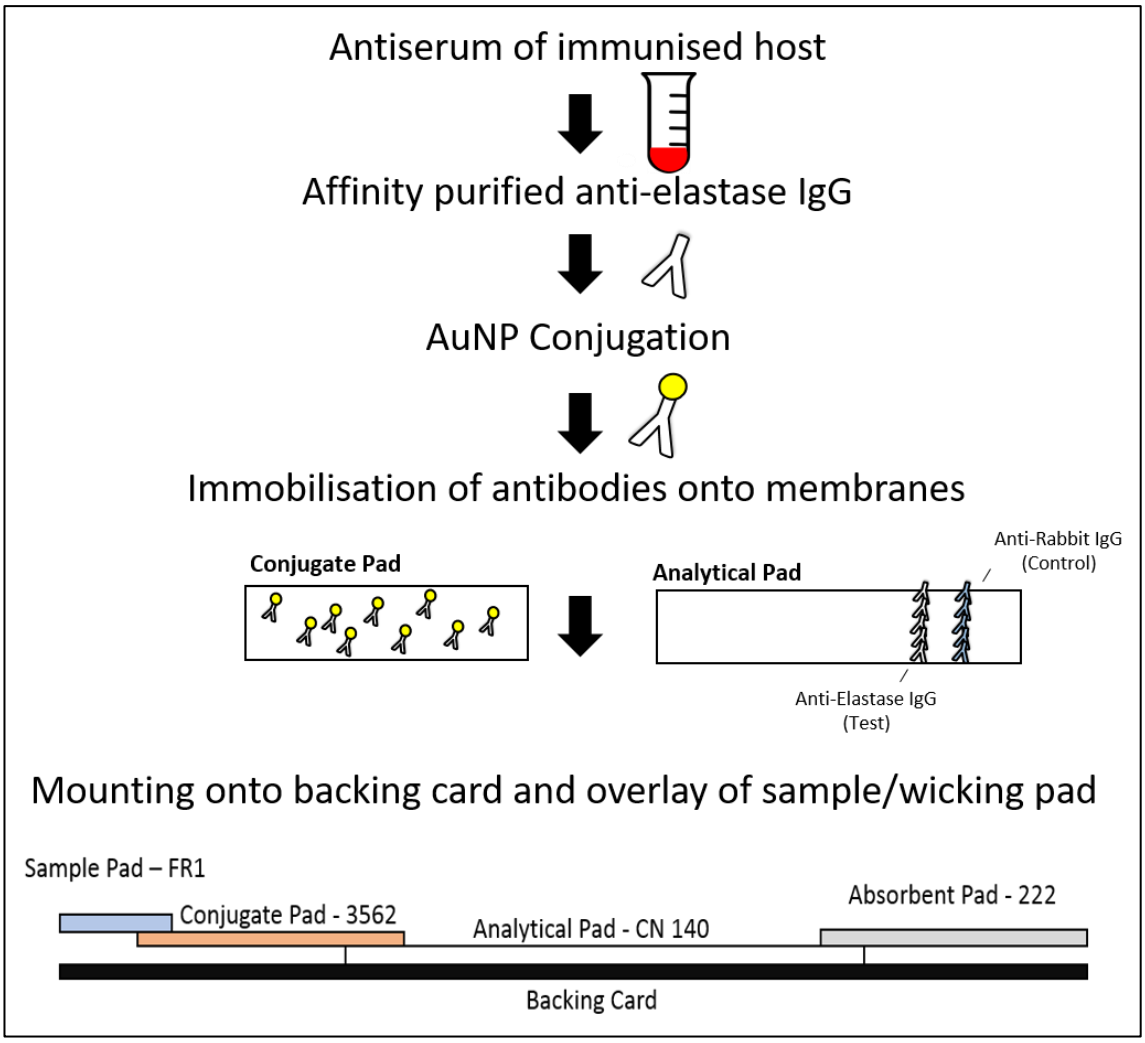

Figure 4.24 | Schematic outlining the workflow of assembly for a typical lateral flow assay. Specific polyclonal antibody is affinity purified from the antiserum of an immunised host animal and a proportion of this is labelled with gold nanoparticles (AuNP). The unlabelled antibody is immobilised on an analytical membrane along with an anti-species IgG control antibody, and the gold-labelled antibody is dried onto a conjugate pad. The separate pads are mounted, overlapping, onto a backing card along with a sample membrane pad and absorbent or wicking pad.

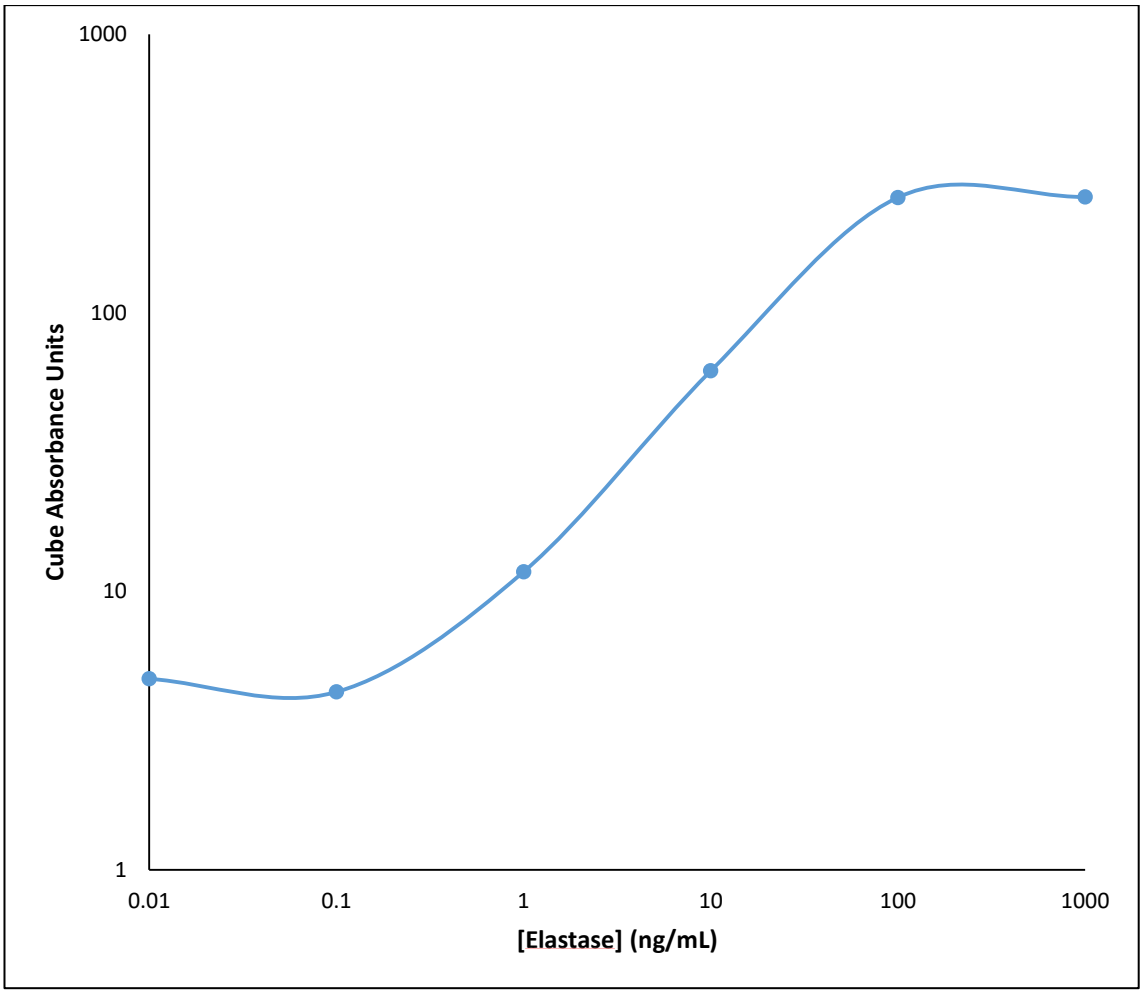

Figure 4.25 | Standard curve for detection of purified recombinant elastase derived from initial "wet tests" of an anti-elastase lateral flow assay. Absorbance readings above 10 units were regarded as a positive result.

Following preliminary "wet testing", prototype lateral flow assay devices were assembled as outlined in **Section 2.6.5**. As these devices were prototypes, a control line containing gold-conjugated anti-species IgG was not included. In place of this, a red line was drawn in pen along the backing card, which would only become visible once a sample had reached the end of the device, once the overlapping CN140 membrane became wet and transparent. A schematic outlining the assembly of a typical lateral flow device is depicted in **Figure 4.24.**

Standard curves for prototype lateral flow devices were constructed via the addition of 80 µL dilutions of recombinant elastase of known concentrations followed by a 10 minute incubation and the test line intensity read using a cube reader device. As in the "wet testing" phase, device sensitivity was assessed as being between 0.1 and 1 ng/mL, with a cube absorbance reading of 22.05 at 1 ng/mL elastase (**Figure 4.26**).

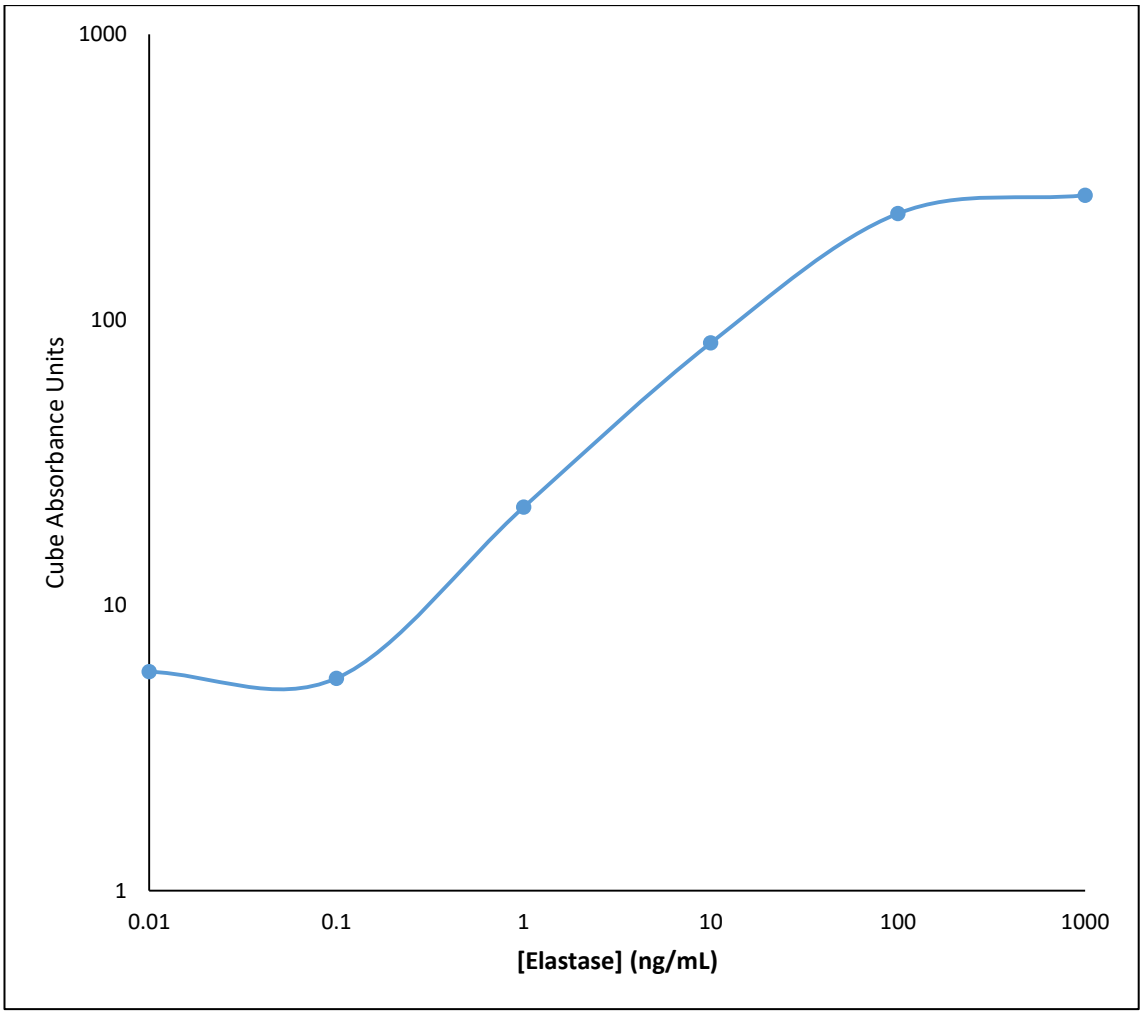

Figure 4.26 | Standard curve for detection of purified recombinant elastase derived from initial "dry tests" of an anti-elastase lateral flow assay device. Absorbance readings above 10 units were regarded as a positive result.

4.6.3 Lateral Flow Signal Amplification via Enzyme Conjugation

In an attempt to improve the sensitivity of the anti-elastase lateral flow assay, wet tests were performed using the HRP labelled RA528 polyclonal antibody in place of a gold nanoparticle detection system. It has previously been reported that the use of such an enzyme labelling approach can improve sensitivity of a lateral flow assay as much as 10-fold (Parolo et al., 2013). Initially, wet tests were performed at a range of detector antibody dilutions in order to determine the ideal parameters for signal enhancement with minimal background signal. The procedure for this assay is described in **Section 2.6.4**. From this data, a detector antibody dilution of 1/8000 was selected, due to its relatively high signal to noise ratio in comparison with other dilutions. Whilst the signal to noise ratio was slightly higher for the 1/4000 antibody dilution (**Figure 4.27**), upon visual inspection there was a clearer differentiation between

positive and negative tests in the 1/8000 samples. However, both conditions resulted in a degree of background signal which could be mistaken for a positive result. An 8-point standard curve was then constructed using recombinant elastase at doubling dilutions from 100 ng/mL to 0 ng/mL. Enhancement with HRP-labelled RA529 polyclonal antibody did not improve the sensitivity of the anti-elastase lateral flow assay, as the standard curve suggested a sensitivity of between 3.13 - 6.25 ng/mL (**Figure 4.28**), whereas a sensitivity of below 1 ng/mL had been previously established (**Figure 4.25**).

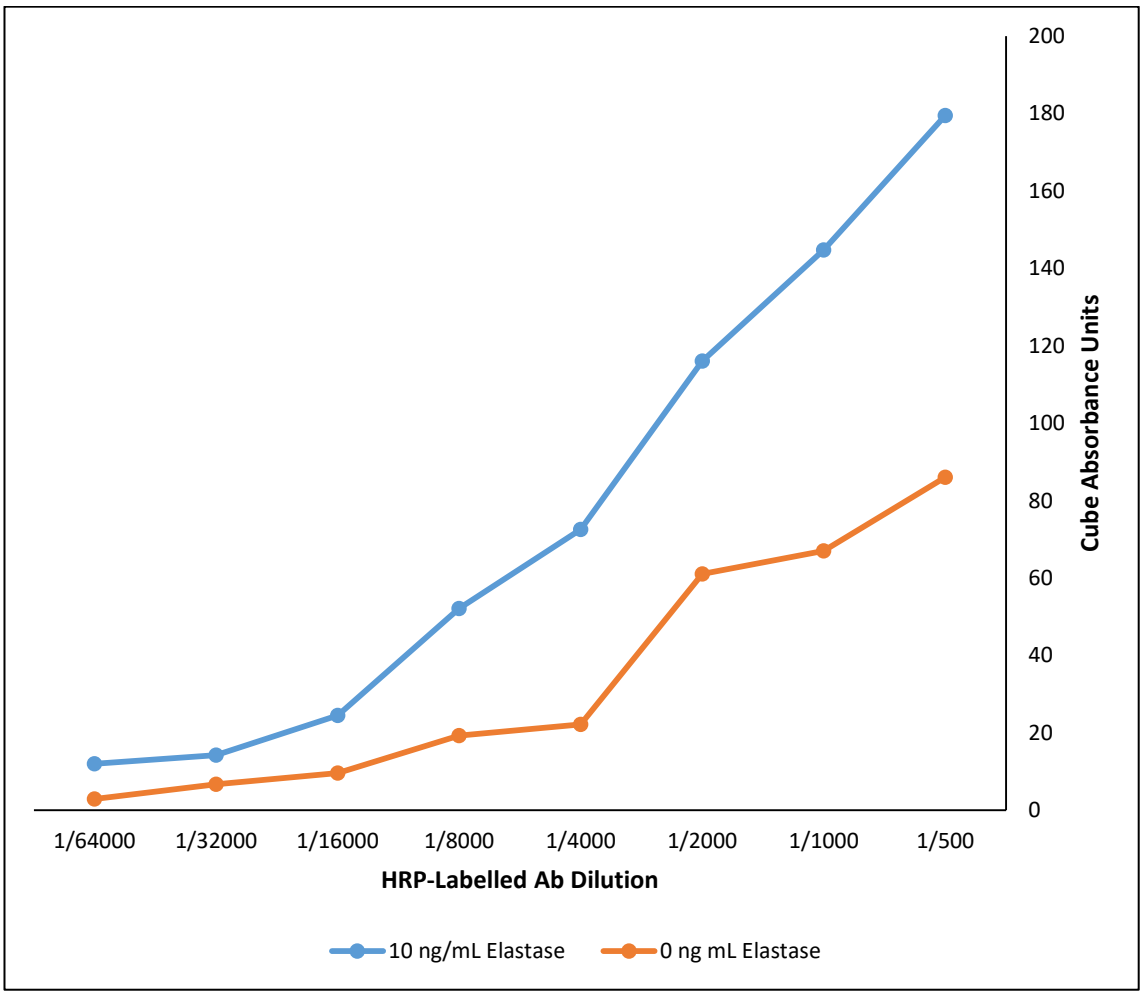

Figure 4.27 | Detector antibody titration for an enzyme-enhanced anti-elastase lateral flow assay in the presence and absence of recombinant elastase.

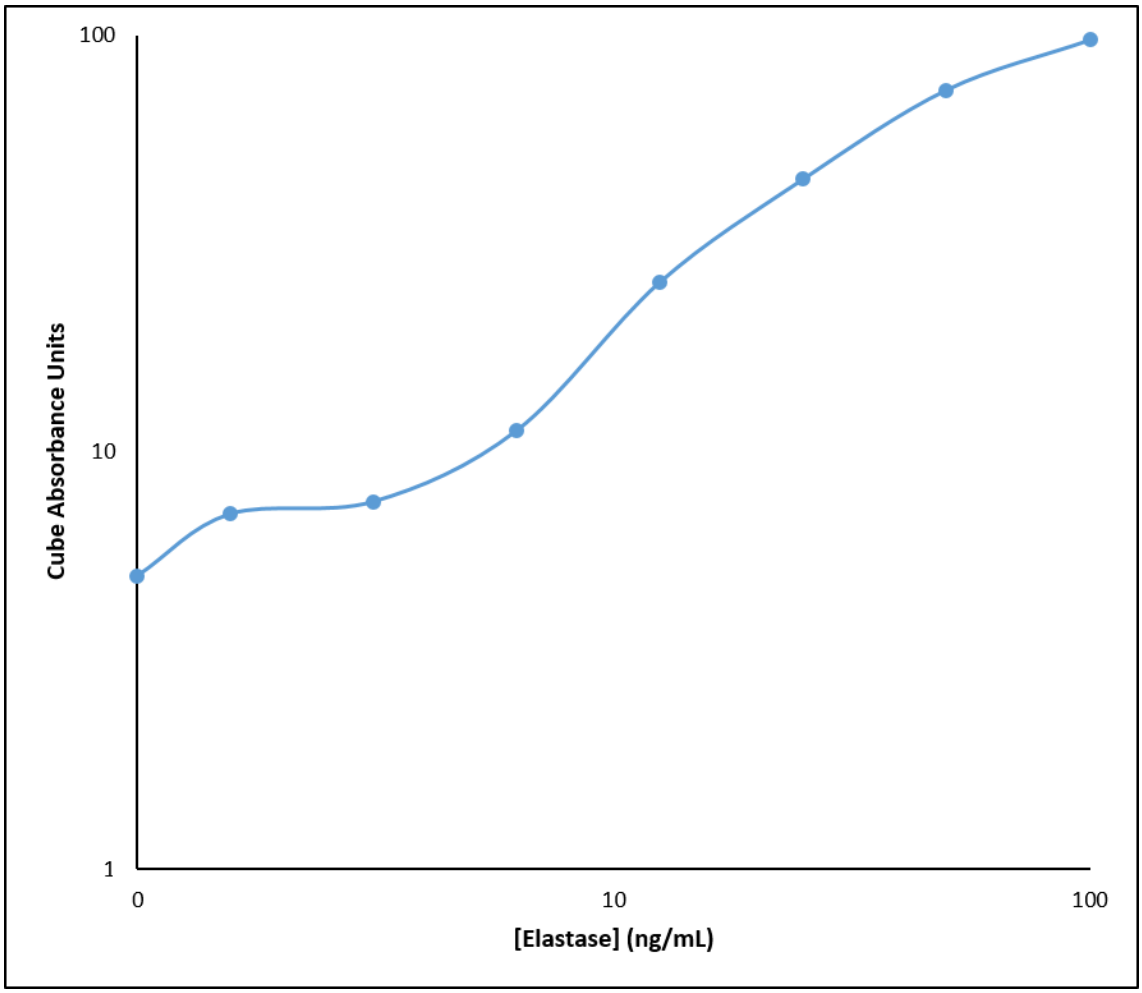

Figure 4.28 | Standard curve derived from HRP-enhanced "wet tests" of an anti-elastase lateral flow assay device for detection of purified recombinant elastase. Absorbance readings above 10 units were regarded as a positive result.

4.6.4 Assessment of the Lateral Flow Assay using *P. aeruginosa* Laboratory Strain Supernatants

To test the ability of the lateral flow device prototypes to detect native elastase, overnight cultures of the commonly studied *P. aeruginosa* laboratory strains PA14 and PAO1 were set up. An additional culture of PAO1 with a deletion in the *lasR* quorum sensing regulatory gene was set up, which was expected to have considerably lower levels of *lasB* expression. Cells were grown at 37°C in 5 mL LB medium and, following centrifugation, supernatant was applied to the devices at a dilution of 1/50. Test line intensity was read after a 10 minute incubation period using a cube absorbance reader device. As predicted, supernatant from the PA14 and PAO1 strains returned a positive result, generating cube absorbance values of over 200, whilst the Δ*lasR* mutant supernatant returned a mean value of 13 units (**Figure 4.29**).

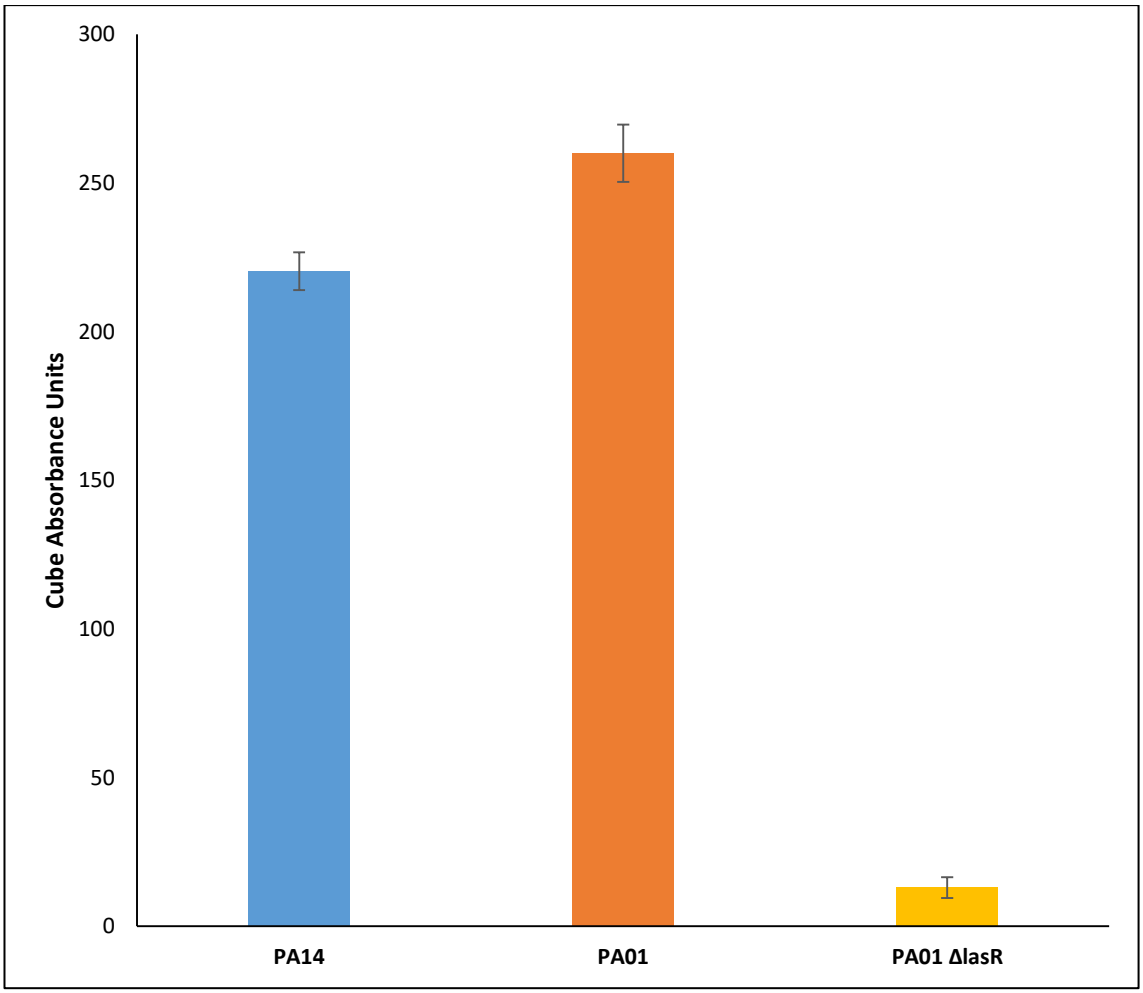

Figure 4.29 | Assessment for elastase presence in *P. aeruginosa* laboratory strain supernatants from a 5 mL overnight culture using the lateral flow assay developed and described in previously sections. The *lasR* deletion mutant PA01ΔlasR strain shows much reduced elastase expression as expected compared to the two native laboratory strains (PA01 and PA14).

4.7 Discussion

Rabbits are one of the most commonly used animals for the production of polyclonal antibodies against a target antigen, both in diagnostic and biotherapeutic applications. This is in part due to the relatively low cost of housing rabbits compared to larger animals, combined with their ability to generate sufficient volumes (10s of mLs) of high-titre antisera, typically having high affinity. Blood sampling can be performed easily at the marginal ear vein and, compared to larger animals, small amounts of antigen are typically required for immunisation (Hanly, Artwohl, & Bennett, 1995). Sheep, on the other hand, are primarily used for the production of antibodies for commercial purposes, as much larger volumes of antisera can be produced. However, sheep are much more expensive to maintain than rabbits, requiring special housing facilities, and often a larger amount of antigen is required per immunisation, which may be a limiting factor in the instance of expensive or difficult to produce recombinant antigens (Delahaut, 2017).

When comparing the immune responses of the four animals immunised with recombinant elastase via serum ELISA, there initially appeared to be a wide degree of variability. When comparing the differences between animals of the same species, the immune response from rabbit RA528 appeared far greater than that of RA529 (**Figure 4.1** and **Figure 4.2**), providing a positive ELISA result at a serum dilution of 1/25000 as opposed to an estimated dilution of 1/10000 for RA529 material. However, after affinity purification of the antibodies from the sera, a similar concentration of specific antibody was found in the serum of each rabbit (**Table 4.1**). As such, this difference in immune response as observed from the serum ELISA is more likely due to differences in the epitopes recognised by each population of pAb, rather than the actual concentration or titre of pAb. In further support of this, the probing of a synthetic anti-elastase peptide array with a HRP-labelled anti-elastase antibody purified from the serum of RA528 identified a strong linear epitope at the N-terminal region of mature elastase (**Figure 4.5** and **Figure 4.6**), whereas probing of the same array with the antibody from rabbit RA529 yielded no detectable signal whatsoever. While such an array is only capable of mapping linear epitopes, there are likely to be differences in recognised conformational epitopes between the two polyclonal populations as well, further impacting on the sensitivity of the antibodies and, as such, the intensity of the signal achieved via ELISA.

Serum ELISA data generated for the recombinant elastase immunised sheep was somewhat more difficult to compare. The overall signal for each animal was far lower than that of the immunised rabbits, likely due to differences in equipment and reagents, complicating

comparison between the two species using this data. Serum ELISAs on rabbit antiserum were performed at Mologic Ltd., using an alkaline phosphatase-conjugated anti-IgG antibody with a commercial substrate solution, whereas serum ELISAs on sheep serum were performed at the University of Kent, using a horseradish peroxidase-conjugated anti-IgG antibody with a non-commercial TMB substrate solution. While the protocols used remained the same, different plate reader devices were used to read the ELISA plates, resulting in differences between the average absorbance scales seen between the serum ELISA curves. For instance, while the rabbit serum ELISA cut-off for a positive result was considered to be 1 absorbance unit, the sheep serum ELISA cut-off was 0.1 absorbance units, as there was a clear difference between this value and a negative result when compared by eye. The concentration of specific anti-elastase polyclonal antibody in the serum of immunised sheep remained comparable with that of the rabbits (**Table 4.1**), indicating similar immune responses to recombinant elastase across all four animals immunised.

Across all 4 immunised animals, there was a clear improvement in antibody titre following successive "booster" immunisations as a result of the adaptive immune system. The initial "innate" immune response responds rapidly, but lacks specificity and largely consists of IgM class antibodies (Boes, 2001). This response is also short-lived, declining shortly after the antigen is cleared, and it is this response that is observed in the "1st bleed" data, as made evident by considerably lower titre measurements. Subsequent bleeds demonstrate the adaptive immune response, reflecting the immunologic memory of the animals, and resulting in a higher titre, consisting primarily of IgG class antibodies. In order to improve serum titre of anti-elastase antibodies in the future should this be desired, it may be preferable to cross-link the antigen molecules to each other, or to an immunogenic carrier protein, as larger proteins typically increase the likelihood of generating good T-cell epitopes and generally improve immunogenicity, which may result in a higher titre and specific concentration of antibody in the serum.

Prototype sandwich ELISA diagnostic assays incorporating the affinity purified anti-elastase polyclonal antibodies were developed after investigating the 'best' reagent combinations and protocol modifications from those investigated. In order to reduce background signal to a minimum whilst maximising absorbance, antibodies from each rabbit were tested in combination with each other at two capture antibody concentrations, 0.1 µg/mL and 1 µg/mL, and three detector antibody dilutions, 1/2000, 1/4000 and 1/8000. Recombinant elastase standard curves were produced for the four best performing antibody pairs in order to establish

lower limits of detection. This optimisation was also performed for affinity purified polyclonal antibodies derived from immunised sheep.

From the antibodies derived from immunised rabbits, the RA528 capture antibody consistently provided the highest signal to noise ratio, and was shown to be most effective when paired with a detector antibody derived from the same animal (**Figure 4.7**). When used in combination at a capture concentration of 1 μg/mL and detector dilution of 1/4000, a lower limit of detection for recombinant elastase of 27 pg/mL was established (**Figure 4.9**), tenfold more sensitive than the previous anti-elastase sandwich-ELISA described by Jaffar-Bandjee *et al.* (Jaffar-Bandjee et al., 1993), and requiring substantially lower amounts of antibody per assay.

When comparing polyclonal antibodies derived from sheep, the SA562 capture and detection antibodies, at 0.1 μg/mL and 1/4000 dilution respectively, were determined to perform the best. A lower limit of detection of 266 pg/mL was established (**Figure 4.16**), approximately 10-fold less sensitive than that of the rabbit-derived antibodies, as a higher degree of background signal was observed in assays incorporating these antibodies. In order to counteract this, sheep detector antibody dilutions were made up in 5% skimmed milk to act as a stronger blocking buffer, which marginally improved the signal:noise ratio (**Figure 4.14**). From comparison of the immune responses between animals, as noted above, it seems likely that the rabbit pAbs were, in general, of higher affinity and thus produced a more sensitive assay. Despite the lower sensitivity, a considerably larger volume of serum was able to be harvested from the immunised sheep, resulting in far greater amounts of anti-elastase pAb purified. As a result, the RA528 capture antibody was incorporated into a prototype lateral flow assay format, as described in **Section 4.6**, whereas the SA562 capture and detection antibodies were retained for further ELISA format experiments, as described in **Section 4.5**.

The supernatants of clinically relevant strains of *P. aeruginosa* were assessed via a sandwich ELISA incorporating the SA562 capture and detection antibodies for the presence of elastase. These strains were provided by the laboratory of Professor Jane Davies of the National Heart and Lung Institute, Imperial College London. *Pseudomonas* strains were cultured from samples obtained from 31 cystic fibrosis patients at first isolation of *P. aeruginosa*, as well as from 17 chronically infected patients in order to assess the utility of the assay in detecting early infections as opposed to more established infections. The purpose of this set of experiments was to provide a proof of concept, and validation, of the anti-elastase ELISA as a tool for detection of clinically relevant *P. aeruginosa* strains in order to justify further development of the assay. It is important to note that detection of elastase in culture supernatants does not

necessarily indicate the assay will be able to detect elastase in direct patient samples, such as sputum or bronchoalveolar lavage fluid, as the levels of elastase present in culture supernatant is expected to be much higher. However, it does provide insight into the assays capability to identify *P. aeruginosa* strains present at both early and late stage infections.

From 31 first isolates tested, 29 strains returned a positive result, in this case defined as reaching an absorbance value above the established LLOD (**Figure 4.17a** and **Figure 4.18a**), and supported via one-way ANOVA and Tukey grouping in which positive results were shown to differ significantly from the negative control strains run alongside the isolates (**Figure 4.17b** and **Figure 4.18b**). Elastase is known to be a key player in the early stages of *P. aeruginosa* infection, assisting in the colonisation of the bacterium via solubilisation of elastin in human tissues (Wretlind & Pavlovskis, 1983). As such, it was predicted that this assay would be more appropriate for detecting early infections, as demonstrated by its ability to correctly diagnose 93.5% of first isolates tested.

Assessment of chronic isolates returned less consistent results. Of the 20 isolates provided, only 17 recovered successfully and of those 17, only 12 returned a significant positive result for elastase using the ELISA developed in this study (**Figure 4.19a** and **Figure 4.19b**). Due to the nature of the las quorum sensing pathway in *P. aeruginosa*, discussed in detail in **Section 1.2.2**, it is predicted that these negative results are due to a switching off of the *lasB* structural gene which encodes elastase, resulting in the isolation of non-elastase producing strains. Analysis via qPCR may further elucidate this mechanism. Mutations in the *lasR* regulatory gene resulting in a loss of virulence are commonly associated with chronic *P. aeruginosa* infections (D'Argenio et al., 2007), and so it was anticipated that elastase detection would be less consistent among these samples. As such, the assay in its current form appears to be better suited to the early detection of *P. aeruginosa*, when virulence is consistently high and the bacterium is primarily non-mucoid. It is at this stage that *P. aeruginosa* is most susceptible to antibiotic treatment, and so there is an urgent need for a rapid diagnostic assay for early infections. Additionally, the assay may also have potential as a predictor of pulmonary exacerbations, periods of acute worsening of symptoms, though more work is required, particularly with clinical samples, as although detection of elastase appears to vary among the chronic isolates tested, it is unclear whether this directly correlates with virulence.

To assess the specificity of the ELISA, 20 "control isolates" were also provided. These isolates included a range of Gram negative and Gram positive bacteria commonly associated with cystic fibrosis infections, and were assessed to ensure that the assay would not mis-identify *P.*

aeruginosa (i.e. that it would not give a positive result due to cross-reactivity with protein(s) from other bacterial species). Of the 19 non-*Pseudomonas* strains that were successfully revived, all supernatant samples gave negative results (**Figure 4.20**), demonstrating the highly specific nature of the anti-elastase pAbs generated in this study. In addition to these control strains, 2 *Burkholdera cepacia* complex strains were provided, which also returned negative results (**Figure 4.18a**).

The next logical step in the development of this assay towards clinical application is to begin assessing patient samples directly. Ideally the assay would be implemented at the point of care, requiring a rapid turnover as opposed to the 16-hour culture time required to obtain a supernatant sample. Sputum samples, bronchoalveolar lavage fluid and exhaled breath condensate are of particular interest, although the sensitivity of the assay in its current form may pose a limitation. Additionally, in regards to sputum samples in particular, sample preparation protocols must be carefully considered so as not to impact the assay or denature any native elastase which may be present in the sample, as this may result in false negative results.

Lateral flow assays are ideal diagnostic assays for use in the clinic or at the point of care, due to their simplicity of use, low cost and rapid turnaround time, as described in detail in **Section 1.5.2**. In the context of cystic fibrosis, rapid diagnosis of *P. aeruginosa* infections is crucial in establishing early treatment and, as such, there is an urgent need for a diagnostic test from which results can be quickly attained. Anti-elastase pAbs purified from rabbit RA528 were incorporated into a prototype lateral flow assay device, selected based on their observed high sensitivity within an ELISA format. An estimated sensitivity of approximately 1 ng/mL elastase was observed in both a wet and dry assay format, tested with pure recombinant elastase (**Figure 4.25** and **Figure 4.26**). As anticipated, the sensitivity of the lateral flow assay was considerably lower than that of the ELISA; approximately 40-fold so. However, lateral flow assays compensate for a typically lower detection range through their rapid turnaround time. While this assay is not as sensitive, results were obtained 10 minutes following sample application, as opposed to 3 hours for an ELISA and, in the case of dry testing, no further steps were required. Attempts to enhance the assay sensitivity via use of a HRP-conjugated detector antibody as opposed to a gold nanoparticle (AuNP) conjugated detector antibody were unsuccessful, resulting in moderate background signal and no observable increase in sensitivity (**Figure 4.28**). Despite this, there are various other approaches that could be taken to try and enhance the sensitivity of a lateral flow assay, as reported in the literature. For instance, loading of AuNPs with the HRP enzyme rather than directly labelling the antibody, followed by development in either TMB or

AEC substrate has been shown to improve LFA sensitivity by up to one order of magnitude in an anti-IgG diagnostic (Parolo et al., 2013). Further enhancement has been achieved through the coating of AuNPs with sub-10 atomic layers of platinum (Gao et al., 2017). This method has been shown to improve sensitivity by two orders of magnitude which would, in theory, bring the anti-elastase LFA more in line with the sandwich ELISA in terms of sensitivity. Ultimately, development of high-affinity monoclonal anti-elastase antibodies is necessary in order to reliably improve the sensitivity of this assay, both in a lateral flow and ELISA format.

Preliminary tests of prototype LFAs with non-recombinant elastase were carried out via application of culture supernatant from the *P. aeruginosa* laboratory strains PA14, PAO1 and PAO1ΔlasR, a mutant strain of PAO1 with a deletion in the *lasR* regulatory gene responsible for activation of the las quorum sensing pathway, resulting in a downregulation of *lasB* expression (D'Argenio et al., 2007). As predicted, cube absorbance readings for the *lasR* deficient mutant strain supernatant were much lower than those of the PA14 and PAO1 wild-type supernatants (**Figure 4.28**), demonstrating the assays ability to recognise wild-type elastase, as well as its specificity of this assay for elastase over other *Pseudomonas* proteins.

The anti-elastase lateral flow assay described in this chapter in its current form is able to differentiate between elastase producing and non-producing strains of *P. aeruginosa*, and can detect recombinant elastase at concentrations as low as 1 ng/mL, requiring only 10 minutes of assay time from sample application to results. Monoclonal antibody development could enhance this limit of detection further, and if combined with the signal-enhancing techniques described above, such as incorporation of platinum-coated AuNPs, there is potential for this assay to become clinically viable. Testing with clinical isolates was not performed due to the limited availability of prototype devices, but it is predicted that similar patterns of detection would be observed between the sheep antibody sandwich ELISA and rabbit antibody LFA.

Chapter 5

Application of Phage Display Technology to Generate Anti-Elastase Monoclonal Antibody Fragments

5.1 Introduction to the Work Described in this Chapter

This chapter describes attempts to generate monoclonal antibody fragments to elastase via antibody phage display. Large, diverse immune libraries were prepared from RNA derived from peripheral blood lymphocytes, extracted from the spleens of three immunised animals: rabbit RA528, sheep SA562 and sheep SA563. These libraries were subsequently panned against recombinant elastase through phage display biopanning, utilising the M13KO7 helper phage and phage-competent *Escherichia coli* strain TG-1.

The generation of monoclonal antibody fragments is desirable for immunoassay development for a multitude of reasons. Soluble Fabs and scFvs can be easily expressed in the periplasm of *E. coli* cells, providing a fast, low-cost platform for the production of recombinant antibody fragments. On-the-other-hand, production of polyclonal antibodies requires frequent immunisation of animals with antigens, which must also be produced or sourced elsewhere. Producing monoclonal antibody fragments also guarantees that the same epitopes will always be recognised, whilst binding modes of polyclonal antibodies can vary wildly, resulting in variation in both specificity and sensitivity of the assay. In order to produce a reproducible immunoassay at a low cost, it is crucial to establish a platform for monoclonal antibody production. Furthermore, removal of the Fc domain is known to reduce nonspecific binding as a result of Fc interactions, and higher sensitivities can often be achieved due to a reduction in steric hindrance.

The process of antibody phage display was first described by Clackson *et al.* in 1991 in which recombinant scFv fragments specific to the hapten 2-phenyloxazol-5-one were generated via construction of immune libraries from the spleens of immunised mice (Clackson et al., 1991). Since its inception, antibody phage display has routinely been used as a tool to generate recombinant monoclonal antibody fragments such as Fabs and scFvs. As described in further detail in **Section 1.6**, there are many advantages of using phage display to generate monoclonal antibodies over traditional methods such as hybridoma technology. The unique ability to physically link antibody phenotype with genotype is desirable, allowing easy sequencing and cloning of antibody DNA following selection of a preferred clone.

The aim of the work described in this chapter was to try and generate a minimum of two high affinity monoclonal Fab or scFv fragments, specific to elastase and recognising different epitopes, in order to be incorporated into a lateral flow diagnostic device. All phage display work was performed at Mologic Ltd.'s satellite facility in York in collaboration with Dr. Matthew Tyreman.

5.2 Generation of a Recombinant Fab Fragment Library from Peripheral Blood Lymphocytes of Immunised Rabbits

5.2.1 Amplification of Heavy and Light Chain Antibody DNA Repertoires

In order to generate an immune library of Fab fragments, total RNA was extracted from peripheral blood lymphocytes prepared from the spleens of immunised rabbits, as described in **Section 2.5.1**. From this RNA, cDNA was generated using the techniques outlined in **Section 2.5.2**, and used as a template for the amplification of heavy chain and kappa light chain gene variants via polymerase chain reaction. In order to minimise amplification bias, primers were organised into sets of 3-5 reverse primers paired with a single forward primer for the heavy chain and a single forward primer for the kappa light chain, resulting in 8 separate PCR reactions. Following amplification, the desired products were isolated by 1% agarose gel electrophoresis (**Figure 5.1** and **Figure 5.2**) and purified as described in **Section 2.5.3**. The dominant bands observed migrated to a size of approximately 600 base pairs, with some smaller mis-primed PCR products generated as well.

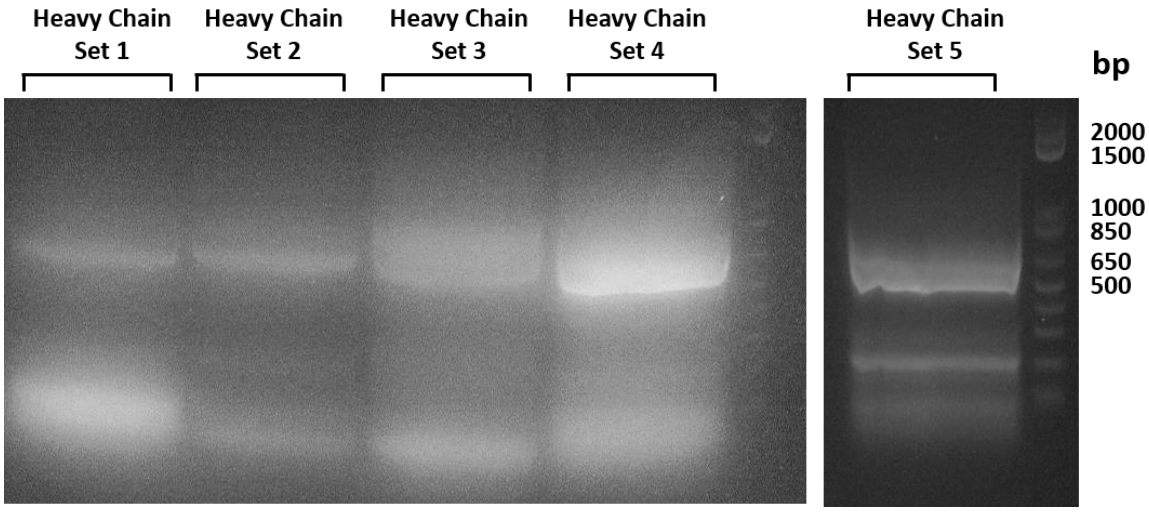

Figure 5.1 | Agarose gel electrophoresis analysis of the amplified heavy chain variants (approx. 600 bp) from a generated cDNA template. Each lane comprises a different set of reverse primers coupled with a single forward primer. Primers were designed to incorporate a NotI restriction site on the 5' end of the heavy chain gene fragment and an NcoI restriction site on the 3' end to facilitate cloning into the phagemid vector.

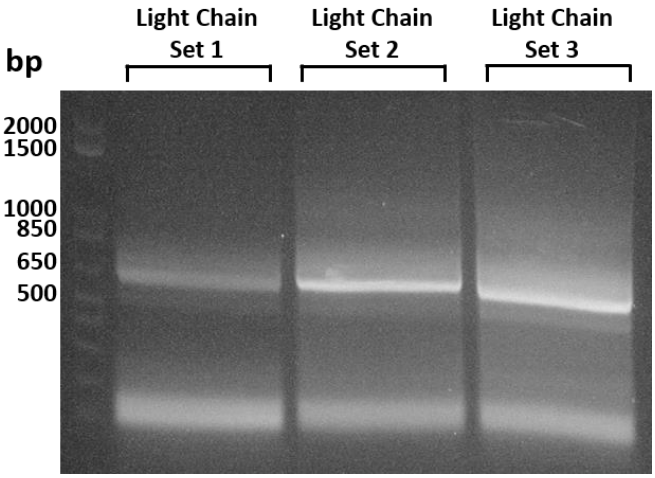

Figure 5.2 | Agarose gel electrophoresis analysis of the amplified kappa light chain variants (approx. 600 bp) from a generated cDNA template. Each lane comprises a different set of reverse primers coupled with a single forward primer. Primers were designed to incorporate an XbaI restriction site on the 5' end of the heavy chain gene fragment and an SfiI restriction site on the 3' end to facilitate cloning into the phagemid vector.

5.2.2 Construction of a Light Chain Fab Library

Assembly of the light chain library was carried out via restriction digest, ligation into the pSFD phagemid, and subsequent electroporation into the *E. coli* strain TG-1 as described in **Sections 2.5.5 - 2.5.7**. The pSFD phagemid is an in-house phagemid used by the industrial partner, Mologic Ltd., and as such access to the plasmid sequence and components is protected by a confidentiality agreement. The library was serially diluted and grown overnight at 37°C on TYE agar plates containing 1% glucose and 100 µg/mL ampicillin and the library size estimated by counting the number of colonies on plates containing <250 colonies (**Table 5.1**). From these plates, a colony PCR screen was performed using *Taq* polymerase from NEB as outlined in **Section 2.5.8** with the light chain forward primer "Rb CK1/2 3' Xba-For" and M13 reverse universal sequencing primer. From 18 individual colonies selected for screening, 9 clones appeared positive for κ-light chain DNA, suggesting approximately half of the library contained a κ-light chain variant (**Figure 5.3**).

Table 5.1 | Estimation of the anti-elastase light chain library size from agar plates streaked with serial dilutions of the transformed light chain library.

Dilution	Number of Colonies	Colonies / mL	Estimated No. of Clones (CFU)
1×10^{-7}	49	4.90×10^{9}	4.90×10^{10}
1×10^{-6}	155	1.55×10^{9}	1.55×10^{10}
1×10^{-5}	101	1.01×10^{8}	1.01×10^{9}
1×10^{-4}	306	3.06×10^{7}	3.06×10^{8}

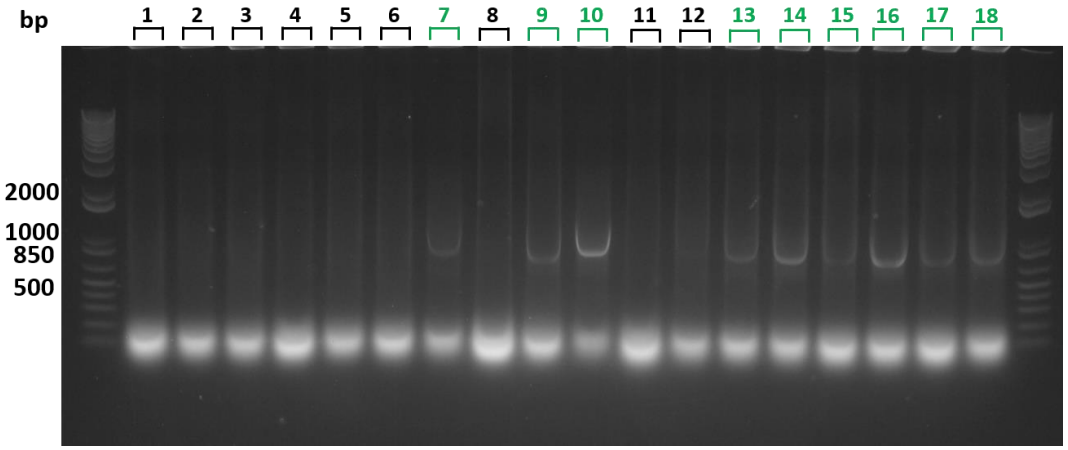

Figure 5.3 | Agarose gel electrophoresis analysis of colony PCR products obtained from the screening of the light chain Fab library. 18 individual clones were screened from single colonies of combined transformation reactions. Positive clones are denoted in green and display a single band at approximately 700 bp.

5.2.3 Assembly and Assessment of the Full Length Anti-Elastase Fab Library

In order to facilitate assembly of the full length Fab library, light chain library DNA was purified using the Zyppy Midiprep purification kit (ZymoResearch) and digested with the NotI and NcoI restriction enzymes as described in **Section 2.5.5**. Heavy chain PCR product was digested in parallel with the same restriction enzymes and then subjected to ligation and electroporation as described above for the light chain. The final library size was estimated by counting colonies as described in **Section 5.2.2** (**Table 5.2**) and colony PCR was performed using the heavy chain forward primer "Rb-Hinge-Not-For" and the M13 reverse universal sequencing primer. From 18 colonies selected for screening, 9 clones returned positive for both antibody chains, 5 returned positive for a single antibody chain, and 4 returned negative for both chains, resulting in a final library which, while containing a large number of total clones overall, consisted of approximately 50% background *E. coli* containing empty phagemid vector (**Figure 5.4**).

Table 5.2 | Estimation of the completed anti-elastase Fab library size from agar plates streaked with serial dilutions of the transformed library.

Dilution	Number of Colonies	Colonies / mL	Estimated No. of Clones (CFU)
1×10^{-7}	425	4.25×10^{10}	4.25×10^{11}
1×10^{-6}	355	3.55×10^{9}	3.55×10^{10}
1×10^{-5}	425	5.68×10^{8}	5.68×10^{9}

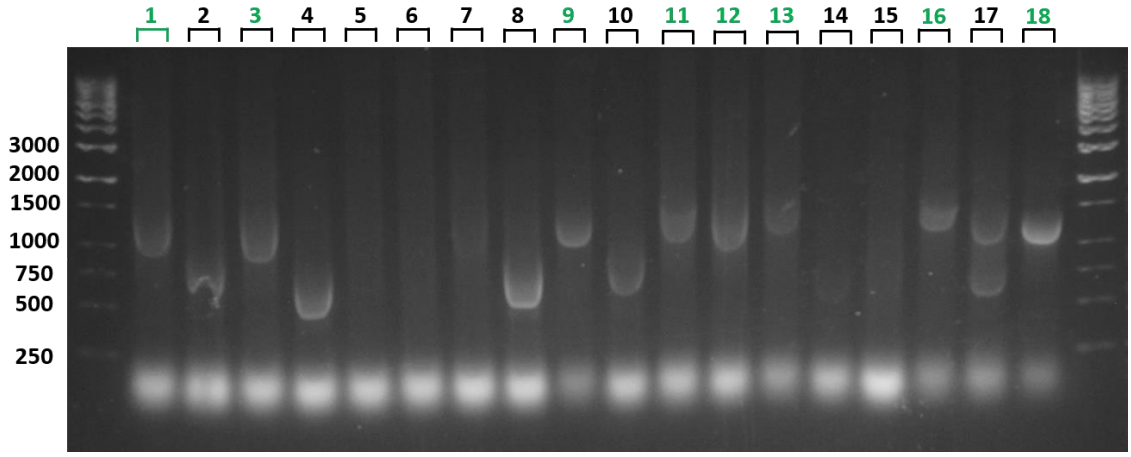

Figure 5.4 | Agarose gel electrophoresis analysis of colony PCR products obtained from the screening of the fully assembled anti-elastase Fab library. 18 individual clones were screened from single colonies of combined transformation reactions. Positive clones are denoted in green and display a single band at approximately 1300 bp, indicating presence of both heavy and light chain gene fragments. Lanes containing a single band at approximately 700 bp contain a single antibody chain whereas lanes with no clear band indicate background phagemid with no antibody chains present.

Following colony PCR, the remaining PCR products for successful clones were purified using the Invitrogen PureLink Quick PCR Purification Kit and subjected to restriction digests. Half of the purified DNA was digested with the restriction enzyme HaeIII, known to cut more frequently within the light chain, and the remaining half was digested with the restriction enzyme BstNI, known to cut more frequently in the heavy chain, under the conditions described in **Section 2.5.8**. Diversity of the library was determined by the presence of a variety of restriction patterns when electrophoretically separated on a 3% agarose gel (**Figure 5.5**). From these digests, the library was confirmed to be sufficiently diverse for subsequent enrichment via phage display biopanning.

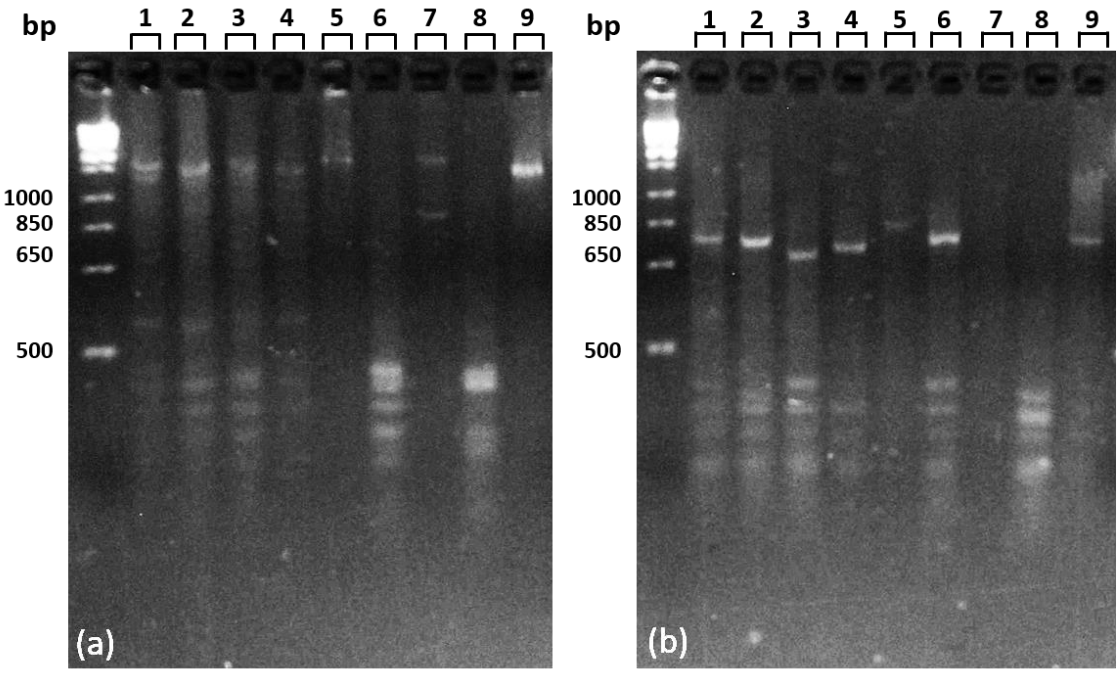

Figure 5.5 | DNA fingerprinting of purified PCR products from successful colony PCRs. Samples were digested with **(a)** BstNI to determine heavy chain diversity, and **(b)** HaeIII to determine light chain diversity, and analysed on a 3% agarose gel.

5.3 Enrichment of an Immune Rabbit Fab Library via Phage Display Biopanning

TG-1 *E. coli* cultures transformed with the assembled Fab library were grown to an OD600 of 0.5 and infected with the M13KO7 helper phage as described in **Section 2.5.9**. The assembled rabbit anti-elastase Fab library was grown and infected with the M13KO7 helper bacteriophage, an industry-standard helper phage for antibody phage display, overnight, and the resulting recombinant phage was harvested via PEG precipitation as outlined in **Sections 2.5.9 - 2.5.10**. Purified phage was subjected to biopanning using immunotubes coated with 10 µg/mL recombinant elastase, performed as described in **Section 2.5.11**. Following each round of panning, TG-1 cells were re-infected with the eluted phage, grown overnight on a selective TYE bioassay plate and recovered. Enriched libraries were once again grown and reinfected with the M13KO7 helper phage for subsequent biopanning. Two rounds of phage display biopanning were performed at an elastase concentration of 10 µg/mL followed by a final round at the reduced concentration of 1 µg/mL in order to select for high affinity binding antibodies. At the end of the phage biopanning stage, harvested phage from each round was analysed via polyclonal phage ELISA (**Figure 5.6**). No enrichment was observed across the three rounds of biopanning, as shown by a lack of any substantial increase in average absorbance at 450 nm

between the pre-pan and pan 3 harvested bacteriophage. As such, the final library was deemed unfit for monoclonal Fab selection via monoclonal ELISA.

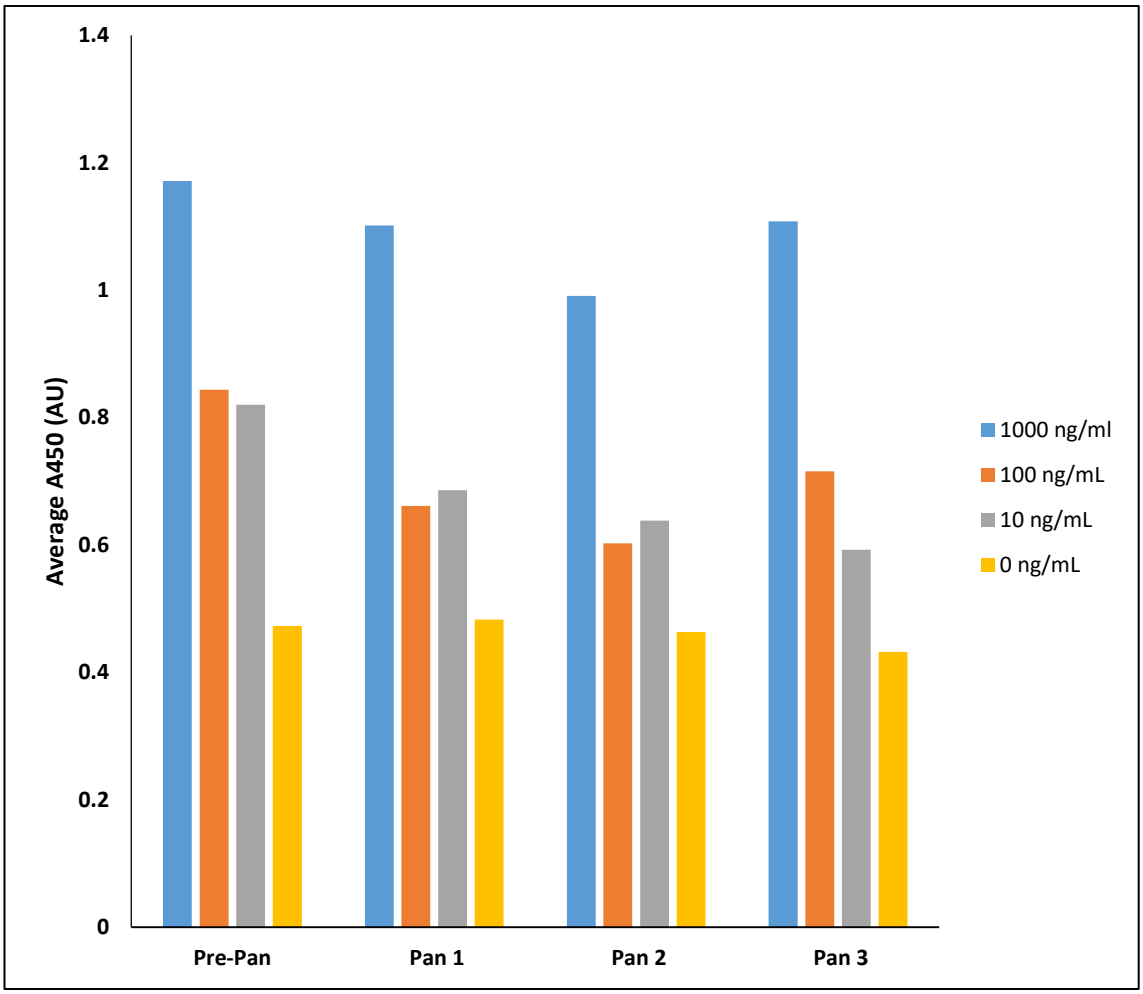

Figure 5.6 | Polyclonal phage ELISA readings for a recombinant elastase immune rabbit Fab library enriched via three rounds of phage display biopanning.

5.4 Generation of Recombinant scFv Fragment Libraries

Following a failure to produce anti-elastase monoclonal rabbit Fab fragments, scFv immune libraries were constructed as an alternate means of producing monoclonal anti-elastase antibody fragments, as previous studies have reported successful phage display and expression of rabbit scFv fragments in *E. coli* (Vu et al., 2017; Xu et al., 2017).

5.4.1 Generation of a Recombinant scFv Library Derived from the Existing Fab Library

Due to the limited amount of available peripheral blood lymphocytes from the immunised rabbits, an initial scFv library was generated using the previously constructed Fab library as a DNA template, to first ensure that amplification would be possible with the synthesised primers.

scFv DNA was ligated into a modified phagemid vector as a single fragment, following a similar process to that used to build rabbit Fab libraries.

5.4.1.1 Amplification of Variable Heavy and Light Chain Antibody DNA Repertoires

Using the rabbit Fab library built in **Section 5.2** as a template, variable region heavy and kappa light chain gene variants were amplified via polymerase chain reaction, using 25 combinations of primers adapted from Vu *et al*. (Vu et al., 2017). These primers were altered in order to incorporate an alternate linker region to facilitate a library build in the industrial partner's in-house modified phagemid system. A list of primers used for this amplification can be found in **Table 2.9**. Following amplification, the desired products were separated on a 1% agarose gel (**Figure 5.7, Figure 5.8** and **Figure 5.9**) and purified as described in **Section 2.5.3**. The purified DNA was then used as a template for an additional pull-through PCR step in which the heavy and light chain genes were joined via a flexible linker using a set of pull-through primers. This PCR product was also separated on a 1% agarose gel (**Figure 5.10**) and purified before being cloned into the phagemid vector. Amplification of scFv DNA yielded similar levels of PCR product for each primer combination, the exception being the light chain reverse primer R5, which failed to amplify successfully.

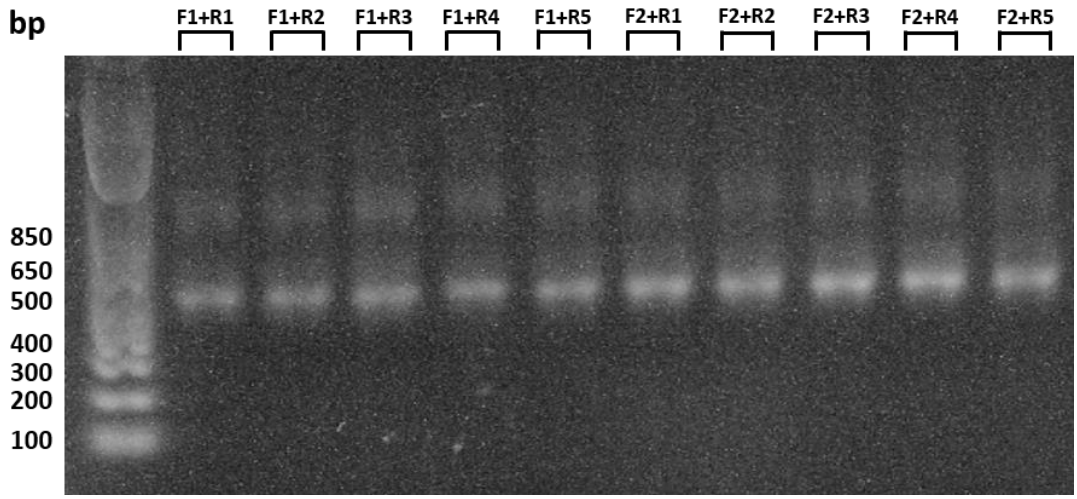

Figure 5.7 | Amplification of rabbit variable heavy chain DNA (approx. 500 bp) from a previously constructed anti-elastase Fab library template. Primers were designed to incorporate an SfiI restriction site to facilitate cloning into the phagemid vector.

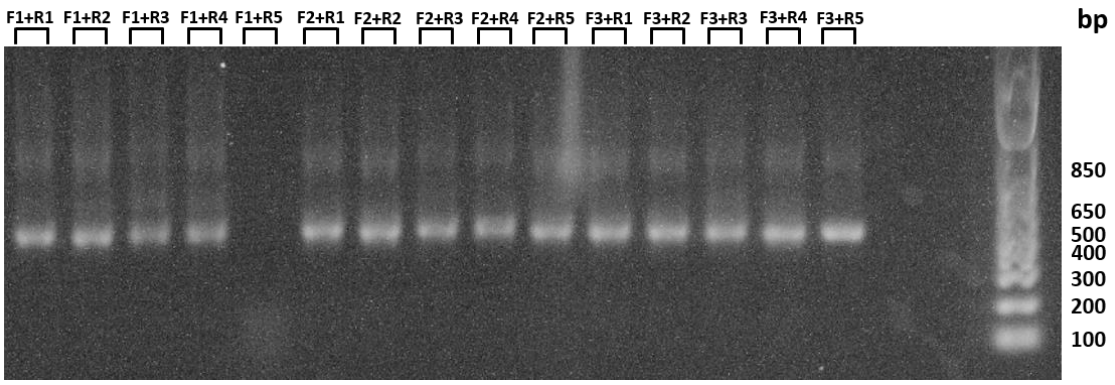

Figure 5.8 | Amplification of rabbit variable kappa light chain DNA (approx. 500 bp) from a previously constructed anti-elastase Fab library template. Primers were designed to incorporate a short, flexible linker and NotI restriction site to facilitate cloning into the phagemid vector.

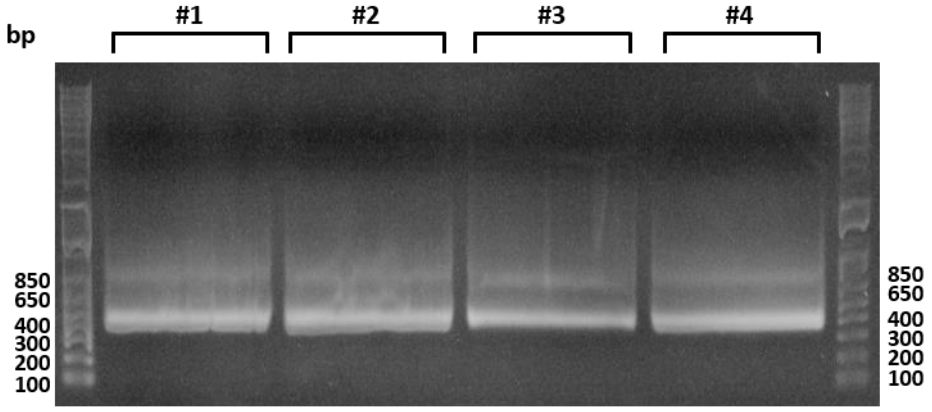

Figure 5.9 | Agarose gel electrophoresis analysis of the pooled scFv PCR products for gel extraction and purification. Each lane contains approximately 250 µL of PCR product.

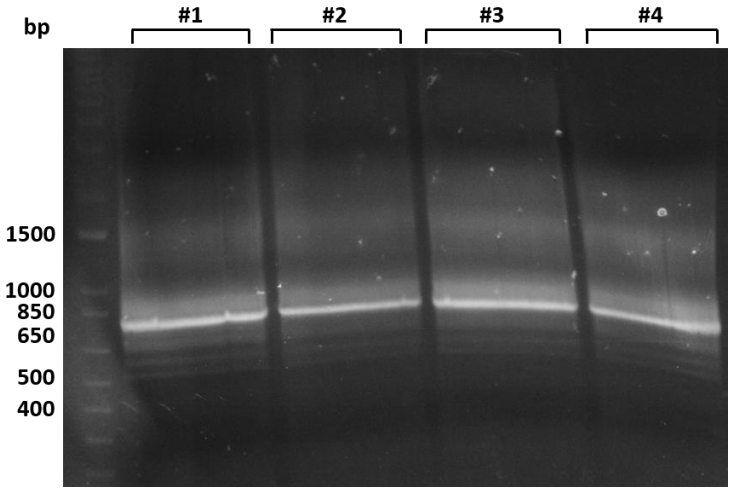

Figure 5.10 | Agarose gel electrophoresis analysis of the final pooled scFv fragments, assembled via pull-through PCR (approx. 700 bp).

5.4.1.2 Modification of the Phagemid Vector to Allow Cloning of scFv Fragments

The phagemid vector was modified via removal of stuffer DNA and ligation of a short oligonucleotide string, synthesised by GeneArt Gene Synthesis (ThermoFisher Scientific™). This removed problematic restriction sites, introduced compatible restriction sites and a *pelB* signal peptide in order to direct the expressed scFv into the *E. coli* periplasm following phage display biopanning. The vector and oligonucleotide insert were digested with HindIII and MfeI restriction endonucleases and re-ligated together. Confirmation of successful ligation was performed via colony PCR (**Figure 5.11**).

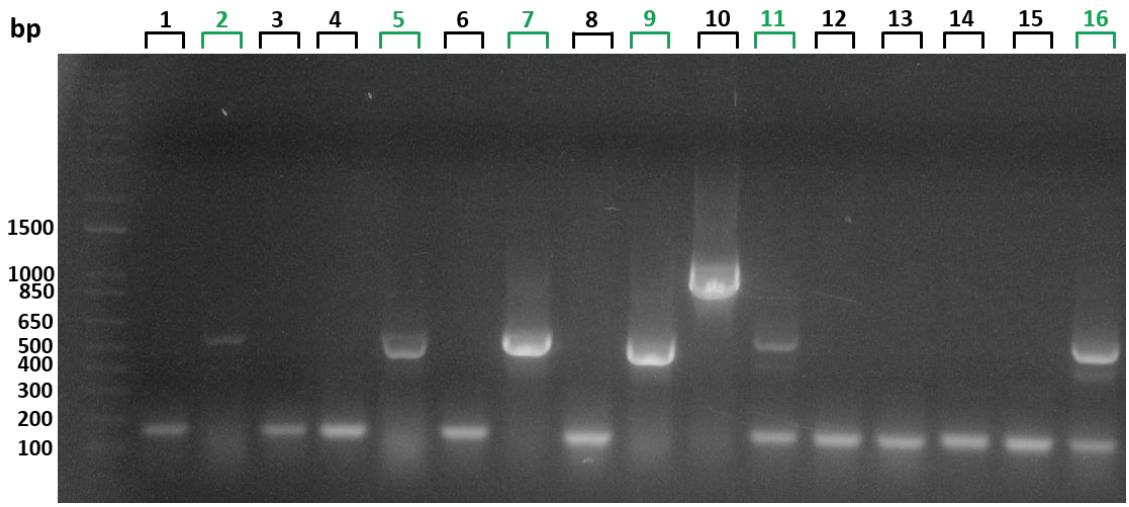

Figure 5.11 | Agarose gel electrophoresis analysis of the modified PSFD vector, confirmed via colony PCR. Positive clones are denoted in green and display a single band at approximately 500 bp. Of these positive clones, clone 5 was selected to be re-transformed and purified.

5.4.1.3 Assembly and Assessment of an Anti-Elastase scFv Library

Following pull-through PCR, the scFv DNA and modified phagemid were purified as described in **Section 2.5.4** and digested with the restriction endonucleases SfiI-HF and XbaI using the conditions described in **Section 2.5.5**. Digested DNA was ligated and transformed as described in **Section 2.5.6** and **2.5.7** and the library screened via colony PCR (**Figure 5.12**). The final library size was estimated by counting of colonies on transformation plates, yielding a library size of approximately 1.5 x 10^8 clones (**Table 5.3**). From 30 colonies selected for colony PCR, 25 were positive for scFv DNA as determined via agarose gel electrophoresis, suggesting a low level of background in the final scFv library.

Table 5.3 | Estimation of the anti-elastase scFv library size from agar plates streaked with serial dilutions of the transformed library.

Dilution	Number of Colonies	Colonies / mL	Estimated No. of Clones (CFU)
1×10^{-4}	160	1.6×10^{7}	1.6×10^{8}
1×10^{-5}	15	1.5×10^{7}	1.5×10^{8}
1×10^{-6}	2	2×10^{8}	2×10^{8}

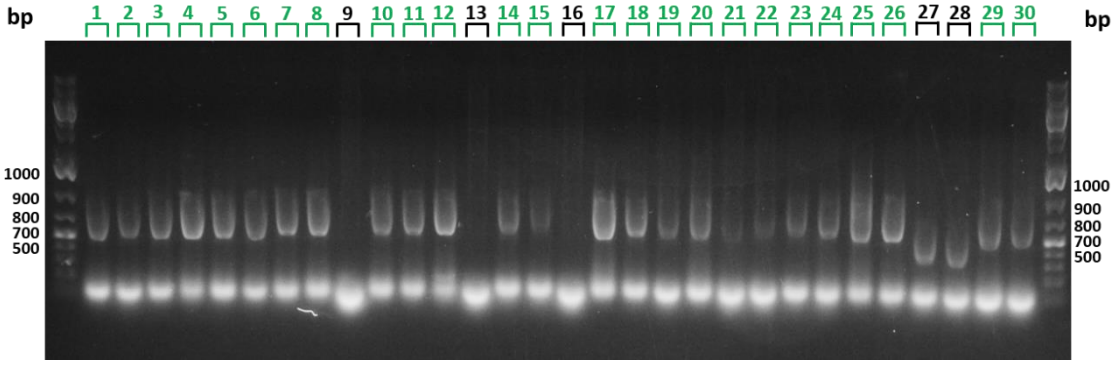

Figure 5.12 | Agarose gel electrophoresis analysis of the colony PCR products obtained from the screening of the scFv library. 30 individual clones were screened from single colonies of the combined transformation reactions. Positive clones are denoted in green, having a band at approximately 750 bp.

20 positive clones were selected for diversity analysis via restriction digest. Purification and digestion was performed as outlined in **Section 2.5.8**, followed by separation on 3% agarose gels (**Figure 5.13** and **Figure 5.14**). A large degree of diversity was observed within the selected clones, as evident by a wide variety of restriction patterns in each chain following digestion.

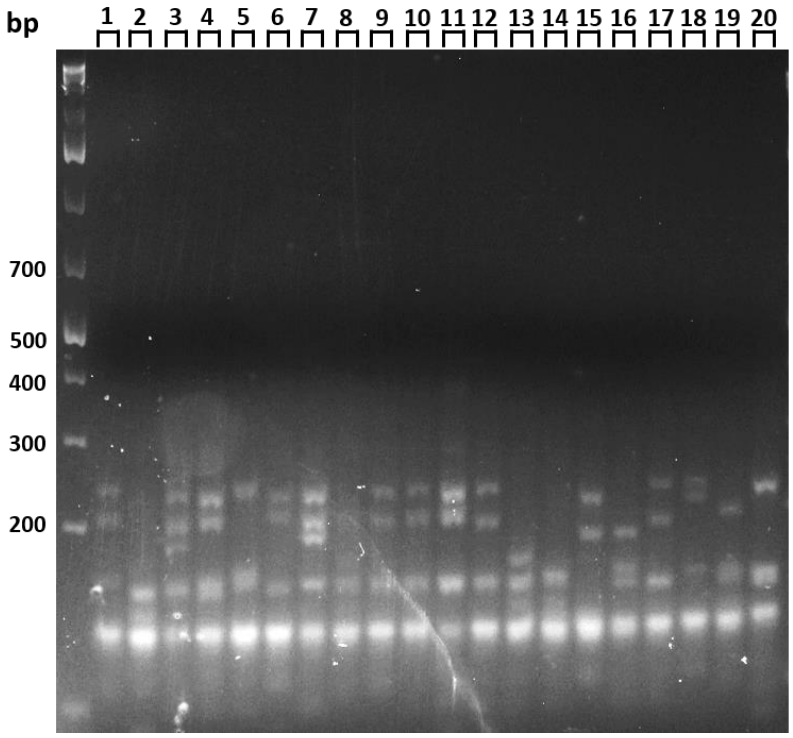

Figure 5.13 | DNA fingerprinting of 20 purified PCR products from successful colony PCRs. Samples were digested with BstNI and analysed on a 3% agarose gel in order to assess heavy chain diversity.

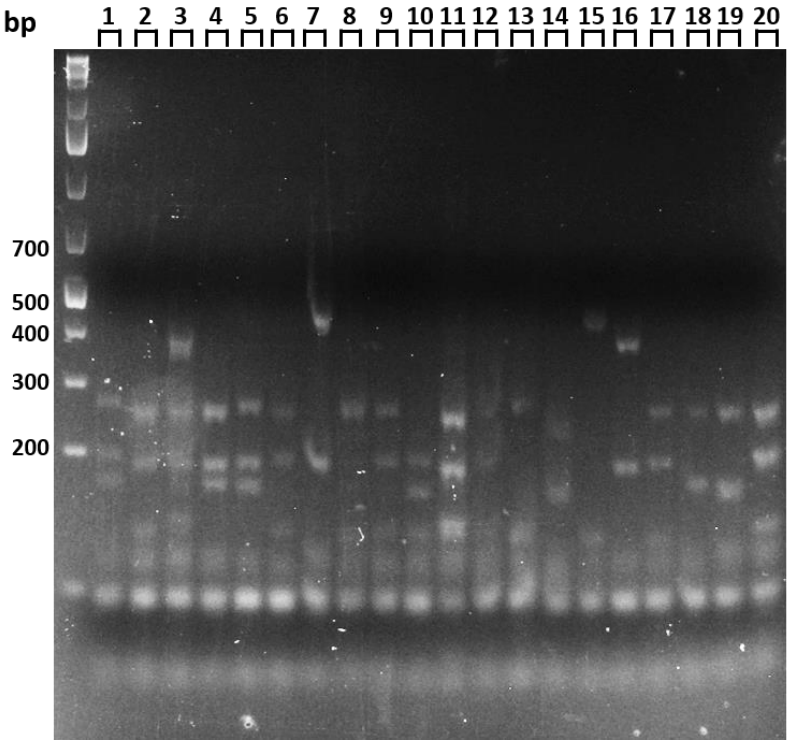

Figure 5.14 | DNA fingerprinting of 20 purified PCR products from successful colony PCRs. Samples were digested with HaeIII and analysed on a 3% agarose gel in order to assess light chain diversity.

5.4.2 Generation of a Recombinant scFv Library Derived from Peripheral Blood Lymphocytes of Immunised Rabbits

Following the construction and biopanning of an anti-elastase scFv library derived from a pre-existing Fab library, a second anti-elastase scFv library was generated using RNA derived from the peripheral blood lymphocytes of rabbits immunised with recombinant elastase. From this RNA, cDNA was generated as described in **Section 2.4.1.2** to be used as a template.

5.4.2.1 Amplification of the Variable Heavy and Light Chain Antibody cDNA Repertoire

Amplification and purification of rabbit heavy and light chain gene variants was performed as described in **Section 5.4.1.1** (**Figure 5.15** and **Figure 5.16**). Purified DNA was subjected to pull-through PCR to assemble full-length scFv fragments using the same set of pull-through primers as before (**Figure 5.17**).

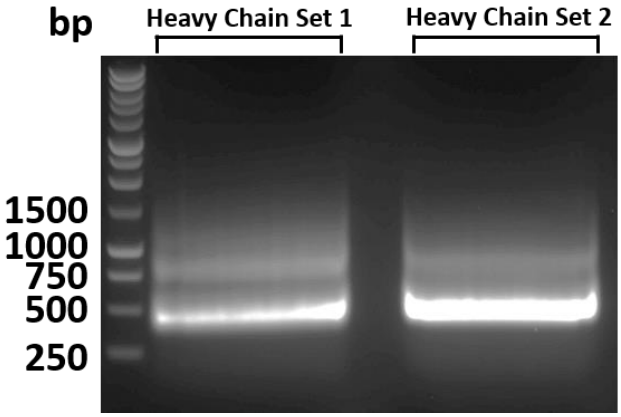

Figure 5.15 | Amplification of rabbit anti-elastase variable heavy chain DNA (approx. 500 bp) from a cDNA template prepared from extracted RNA of recombinant elastase immunised rabbits.

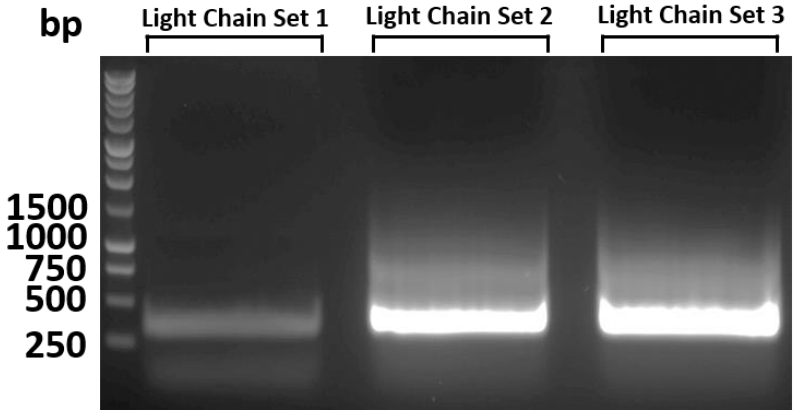

Figure 5.16 | Amplification of rabbit anti-elastase variable kappa light chain DNA (approx. 500 bp) from a cDNA template prepared from extracted RNA of recombinant elastase immunised rabbits.

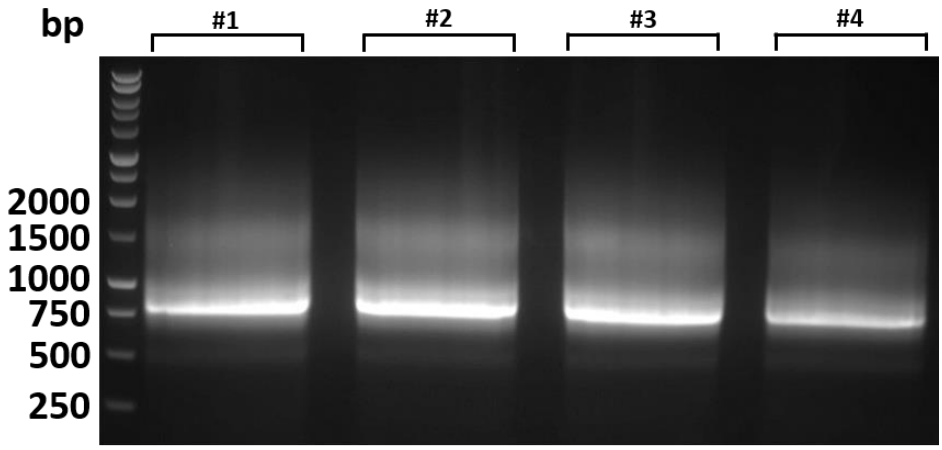

Figure 5.17 | Agarose gel electrophoresis analysis of the full-length anti-elastase scFv gene repertoire, assembled via pull-through PCR. The presence of a band at approximately 750 bp confirms successful amplification.

5.4.2.2 Assembly and Assessment of a Recombinant anti-Elastase scFv Library

scFv DNA was digested and ligated into the modPSFD vector using the same conditions described in **Sections 2.5.4-2.5.7**, and the assembled library was screened via colony PCR, using a heavy chain forward primer and M13 reverse primer (**Figure 5.18**). Colonies were again counted in order to estimate library size (**Table 5.4**).

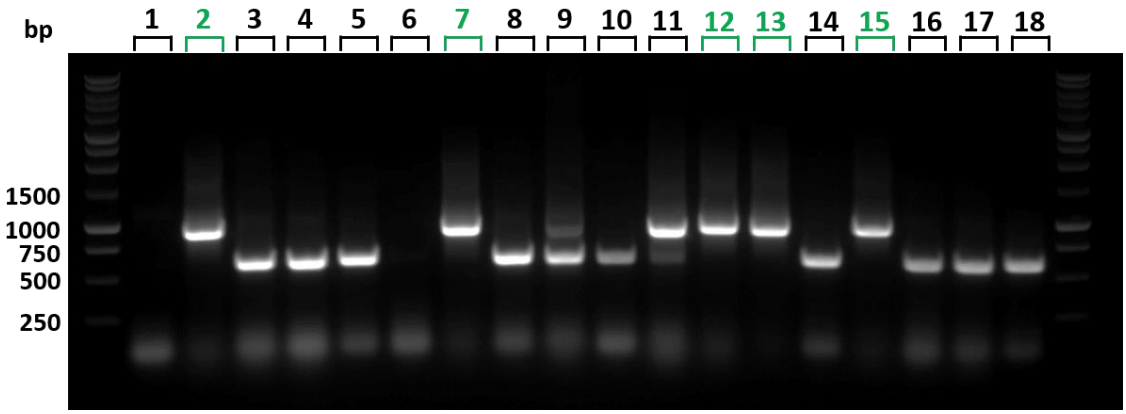

Figure 5.18 | Agarose gel electrophoresis analysis of the colony PCR products obtained from the screening of the anti-elastase scFv library. 18 individual clones were screened from single colonies of the combined transformation reactions. Positive clones are denoted in green and display a band at approximately 750 bp.

Table 5.4 | Estimation of the scFv library size from agar plates streaked with serial dilutions of the transformed library.

Dilution	Number of Colonies	Colonies / mL	Estimated No. of Clones (CFU)
1×10^{-2}	110	1.10×10^{5}	1.10×10^{6}
1×10^{-3}	17	1.70×10^{5}	1.70×10^{6}

Five positive clones were purified from a 1% agarose gel and subjected to diversity screening via restriction digestion as described in **Section 5.4.1.3** (**Figure 5.19**). Despite the smaller library size, diversity was still observed between the selected clones, allowing the library to advance to the phage display biopanning stage.

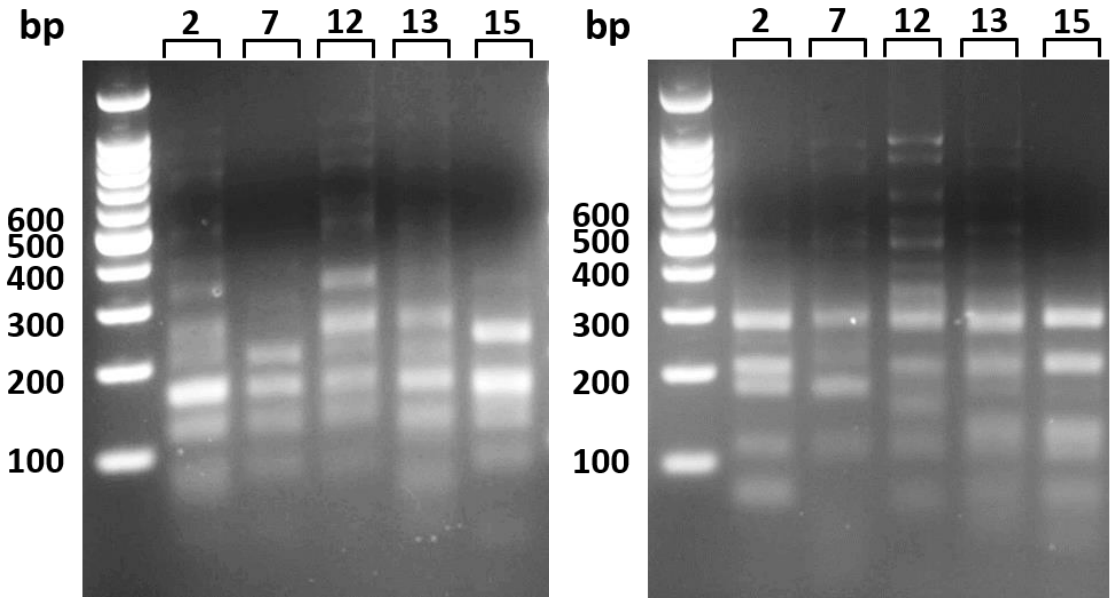

Figure 5.19 | Diversity screening of the scFv anti-elastase library. DNA fingerprinting of 5 purified PCR products from successful colony PCRs. Samples were digested with BstNI (left) or HaeIII (right) and analysed on 3% agarose in order to assess heavy chain and light chain diversity respectively.

5.5 Enrichment of Immune Rabbit anti-Elastase scFv Libraries via Phage Display Biopanning

Enrichment of the assembled scFv libraries was carried out generally following the same methods as in described in **Section 5.3**. However, an additional round of panning was included at a concentration of 10 µg/mL elastase before reducing to 1 µg/mL for the final round. Following polyclonal phage ELISA, once again no enrichment was observed after four rounds of phage

display biopanning across either scFv library (**Figure 5.20**). As before, the libraries were deemed unfit for monoclonal antibody fragment selection.

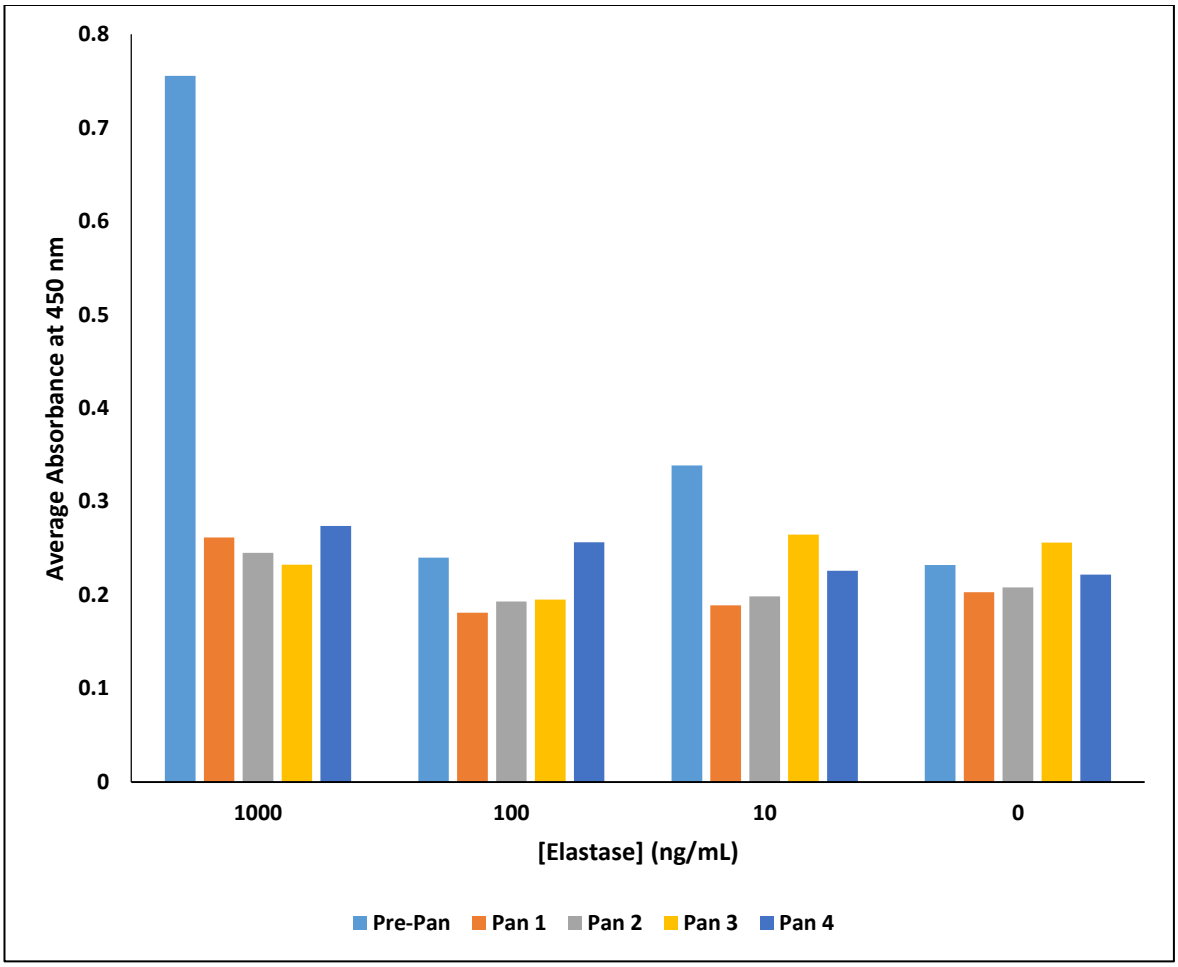

Figure 5.20 | Polyclonal phage ELISA readings for an anti-recombinant elastase immune rabbit scFv library derived from peripheral blood lymphocytes of an immunised rabbit enriched via four rounds of phage display biopanning.

5.6 Generation of a Recombinant Fab Fragment Library from Peripheral Blood Lymphocytes of Immunised Sheep

As successful isolation of monoclonal clones from the rabbit material was unsuccessful, a recombinant Fab library was generated from peripheral blood lymphocytes extracted from the spleens of 2 sheep immunised with recombinant elastase. This library was intended to act as a positive control library, as the protocol performed by the industrial partner routinely uses sheep material to produce recombinant antibody fragments via phage display. Following immunisation with recombinant elastase, PBLs were extracted from the spleens of two sheep. As before, RNA

was extracted from the prepared PBLs and a cDNA template was generated using species specific primers.

5.6.1 Amplification of Variable Heavy and Light Chain Antibody DNA Repertoires

Variable heavy and light chain antibody DNA repertoires were amplified via PCR, as outlined in **Section 2.5.3.1**. Sheep-specific primers were organised into 3 sets of heavy chain primers and 4 sets of light chain primers, in order to minimise amplification bias. Following PCR, amplified DNA fragments were separated on a 1% agarose gel (**Figure 5.21** and **Figure 5.22**) and purified via the Wizard® SV Gel and PCR Clean-Up system (Promega).

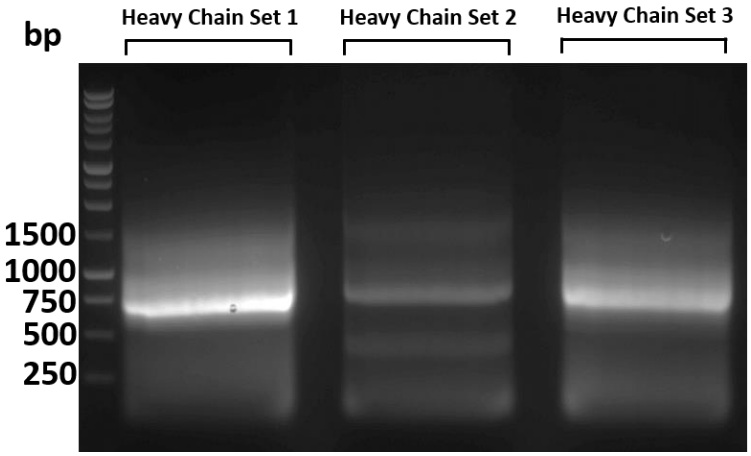

Figure 5.21 | Agarose gel electrophoresis analysis of the amplified sheep heavy chain variants (approx. 700 bp) from a generated cDNA template. Each lane comprises a different set of reverse primers coupled with a single forward primer. Primers were designed to incorporate a NotI restriction site on the 5' end of the heavy chain gene fragment and an NcoI restriction site on the 3' end to facilitate cloning into the phagemid vector.

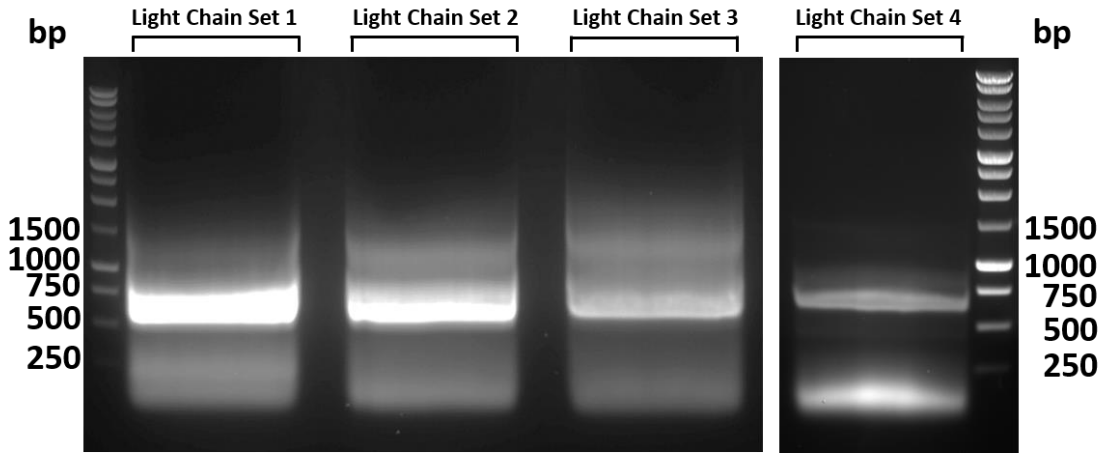

Figure 5.22 | Agarose gel electrophoresis analysis of the amplified sheep light chain variants (approx. 700 bp) from a generated cDNA template. Each lane comprises a different set of reverse primers coupled with a single forward primer. Primers were designed to incorporate a XbaI restriction site on the 5' end of the heavy chain gene fragment and an SfiI restriction site on the 3' end to facilitate cloning into the phagemid vector.

5.6.2 Construction of an anti-Elastase Light Chain Fab Library

Assembly of the sheep Fab light chain library was performed via restriction digest, ligation and electroporation into TG-1 *E. coli* following the same protocols as described in **Section 5.2.2**. Following transformation of the pooled electroporation reactions, colonies were counted in order to estimate the library size (**Table 5.5**), and a colony PCR screen was performed as outlined in **Section 2.5.8**, using a forward primer specific for the sheep light chain and an M13 reverse universal sequencing primer (**Figure 5.23**). From 18 colonies picked, 14 clones returned positive for light chain DNA, suggesting an insertion rate of 78% for a library of approximately 1.3 x 10^5 clones.

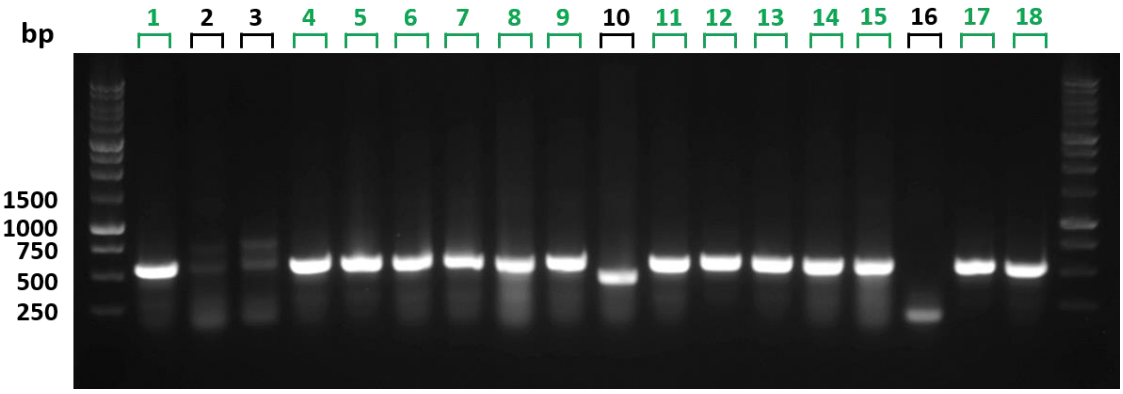

Figure 5.23 | Agarose gel electrophoresis analysis of colony PCR products obtained from the screening of the light chain Fab library. 18 individual clones were screened from single colonies of combined transformation reactions. Positive clones are denoted in green and display a single band at approximately 700 bp.

Table 5.5 | Estimation of the light chain anti-elastase Fab library size from agar plates streaked with serial dilutions of the transformed library.

Dilution	Number of Colonies	Colonies / mL	Estimated No. of Clones (CFU)
1×10^{-5}	5	5.00×10^{5}	5.00×10^{6}
1×10^{-4}	13	1.30×10^{5}	1.30×10^{6}
1×10^{-3}	29	2.90×10^{4}	2.90×10^{5}
1×10^{-2}	135	1.35×10^{4}	1.35×10^{5}

5.6.3 Assembly and Assessment of the Full Length Anti-Elastase Fab Library

As in **Section 5.2.3**, 16 µg of light chain library DNA was digested with the NotI and NcoI restriction enzymes. Gel purified heavy chain DNA was pooled in equal quantities and digested with the same enzymes, followed by a 16 hour ligation at 16°C and subsequent transformation into TG-1 *E. coli* as before. The final library size was again calculated (**Table 5.6**), and colony PCR was performed on 18 colonies selected at random from TYE agar plates containing the transformed library, using the sheep heavy chain forward primer and M13 reverse universal sequencing primer (**Figure 5.24**). The assembled sheep Fab library was estimated to contain approximately 1×10^{6} clones, with a 50% insertion rate for both antibody chains.

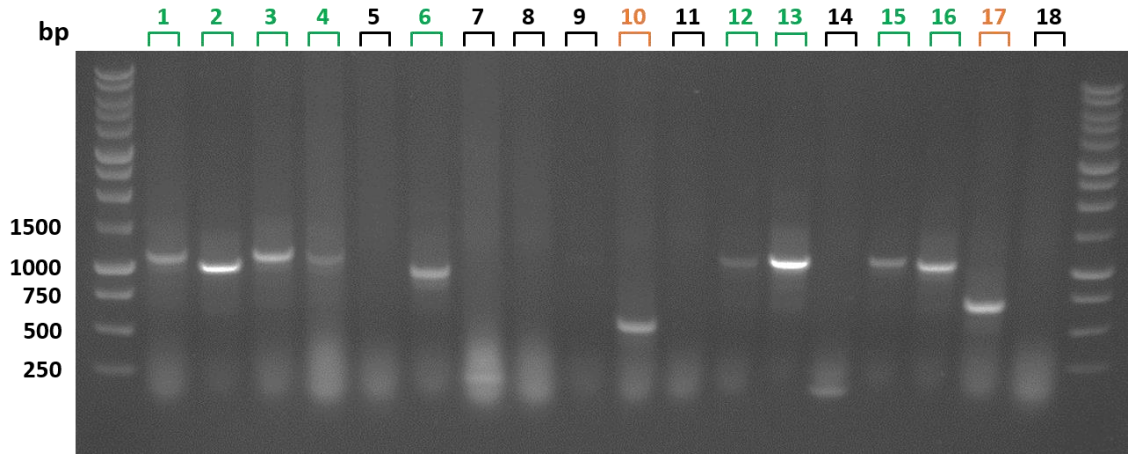

Figure 5.24 | Agarose gel electrophoresis analysis of colony PCR products obtained from the screening of the fully assembled sheep derived anti-elastase Fab library. 18 individual clones were screened from single colonies of combined transformation reactions. Presumed positive clones are denoted in green and display a single band at approximately 1200 bp. Lanes labelled in orange show clones containing only DNA from a single antibody chain.

Table 5.6 | Estimation of the fully assembled Fab library size from agar plates streaked with serial dilutions of the transformed library.

Dilution	Number of Colonies	Colonies / mL	Estimated No. of Clones (CFU)
1×10^{-5}	20	2.00×10^{6}	2.00×10^{7}
1×10^{-4}	58	5.80×10^{5}	5.80×10^{6}
1×10^{-3}	46	4.60×10^{4}	4.60×10^{5}
1×10^{-2}	216	2.16×10^{4}	2.16×10^{5}

Remaining PCR product for the clones shown to contain both heavy and light antibody chains was purified via the Wizard® SV Gel and PCR Clean-Up system (Promega) and subjected to restriction digestion with the FastDigest™ restriction enzymes MvaI and BsuRI (ThermoFisher Scientific™) in order to assess the diversity of heavy chain and light chain DNA respectively. Digested material was separated on a 3% agarose gel (**Figure 5.25**). A very low level of diversity was observed for both antibody chains in the completed sheep Fab library. Digestion of 8 clones with BsuRI resulted in only a single unique DNA fingerprint for the light chain, whereas more diversity, albeit limited, was observed in the heavy chain, displaying 4 unique fingerprints.

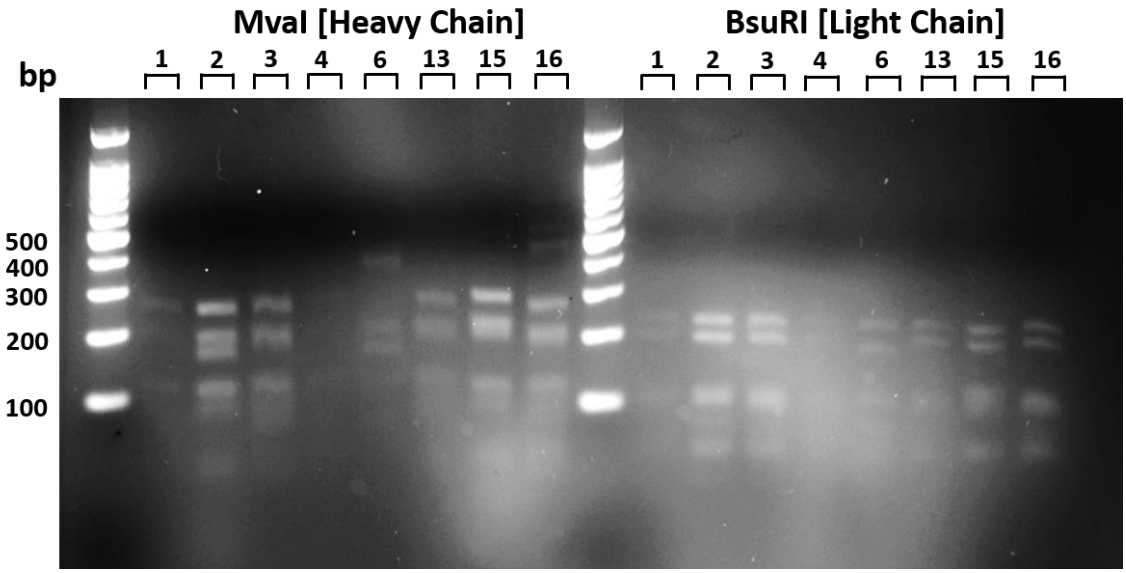

Figure 5.25 | DNA fingerprinting of 8 purified PCR products from successful colony PCRs. Samples were digested with MvaI (left) or BsuRI (right) and analysed on 3% agarose gel in order to assess heavy chain and light chain diversity respectively.

5.7 Enrichment of an Immune Sheep Anti-Elastase Fab Library via Phage Display Biopanning

Enrichment of the fully assembled sheep anti-elastase Fab library was performed via phage display biopanning in immunotubes, following the methods described for the previous two libraries. Three rounds of panning were performed at an elastase concentration of 10 µg/mL, followed by a final round of panning at 1 µg/mL, for a total of four rounds of panning. Polyclonal phage ELISA was performed using purified phage obtained following infection of libraries after each round of panning, but no clear enrichment was observed (**Figure 5.26**). As a result, no monoclonal selection steps were subsequently performed.

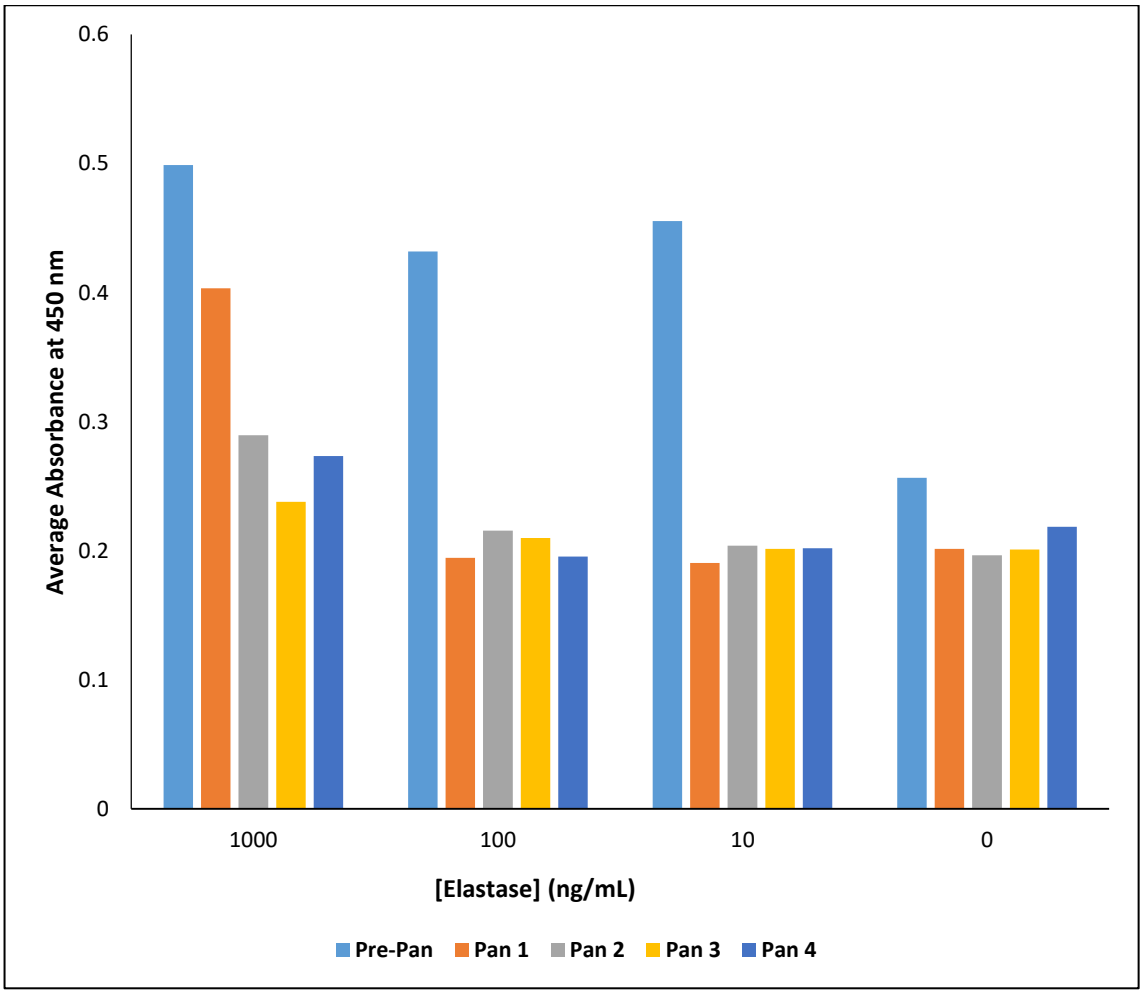

Figure 5.26 | Polyclonal phage ELISA readings for a recombinant anti-elastase immune sheep Fab library enriched via four rounds of phage display biopanning.

5.8 Discussion

Amplification of antibody chain variants from the PBLs of immunised rabbits initially appeared promising in generating what appeared to be the appropriate fragments (**Figure 5.1** and **Figure 5.2**). However, enrichment for anti-elastase antibody fragments via phage display biopanning proved unsuccessful, amplifying only background phage (or "bald phage"; non-specifically bound phage without a displayed p3-antibody fusion protein) as determined via polyclonal phage ELISA (**Figure 5.6**). The final library size for the Fab library derived from rabbit RA529 contained approximately 1 x 10^{10} clones (**Table 5.2**), as determined by counting the colonies on plates containing the serially diluted library, and DNA fingerprinting of 9 colonies showed the presence of diversity (**Figure 5.5**). However, this is a small sample size and may not necessarily have been representative of the larger library, and it is therefore possible that the diversity of the Fab library was skewed, reducing the likelihood of successful enrichment of elastase-specific antibody fragments. Colony PCR of 18 clones from the established library returned 9 clones containing both antibody chains (**Figure 5.4**), suggesting the library contained 50% empty or single antibody chain phagemid. This high degree of background may have also had a negative impact on the subsequent library enrichment process, and may have been a result of inefficient ligation of digested vector and antibody DNA insert, or poor transformation efficiency of the TG-1 competent cells. It is noted that the initial cloning of light chain DNA into the phagemid vector resulted in similar levels of background, with approximately 50% of transformed cells containing a light chain sequence as determined via colony PCR (**Figure 5.3**). It is difficult to pin-point exactly which stage in the process was the limiting factor in the generation of a large, diverse immune library, as there are many potentially limiting steps throughout the library build process which can have an impact at a later stage. A more reliable method of assessing library diversity which could be implemented in the future would be to deep-sequence a library sub-sample via next generation sequencing (NGS) using a sequencer such as the Illumina MiSeq®. This would provide detailed insight into the variety of different clones found within the built variant library. Alternatively, if no such device is available, Sanger sequencing of purified library DNA would provide a rough estimate of library diversity, as the least conserved positions within the highly diverse CDR loops (in particular, within CDR3) would be expected to provide a "noisy" trace at positions of diversity.

A further factor in the library construction process which may have had a negative impact on the quality of the final Fab library is the preparation of high quality RNA from the extracted PBLs. Typical yields for RNA extraction from PBLs are in the region of 5 µg per PBL processed, as suggested by the industrial partner's standard operating procedures. However, observed yields

were closer to 1 µg RNA per PBL following the same protocols. A reduced RNA yield will severely impact subsequent cloning steps in a library build, as the resulting cDNA template used for PCR amplification of antibody chain DNA variants will not necessarily be representative of the full immune repertoire of the immunised animal source. This leads to an over-representation of certain clones via multiple rounds of PCR amplification and an overall bias in the final library, further reducing the likelihood that antibody fragments specific to the antigen of interest will be amplified or enriched via phage biopanning.

The phagemid vector selected for this work, the pSFD phagemid, is an in-house vector used by the industrial partner Mologic Ltd., which has been successfully utilised by them in the past to produce recombinant sheep Fabs. Access to the exact sequence and details of the phagemid components is protected by a confidentiality agreement, and such information has not been made available at the time of writing. As a result, it is difficult to pin-point any potential issues in relation to the cloning and overall build of the libraries described in this chapter. As no sequencing was performed, it is impossible to know whether a point mutation or frameshift occurred which may have impacted on the subsequent expression of recombinant antibody fragments. Ideally, in order to counter this in future, a commercial phagemid system could be implemented such as the pADL line of phage display vectors (Antibody Design Labs).

It is also possible that the generation of rabbit anti-elastase Fab fragments via phage display was unsuccessful due to the presence of an additional disulphide bridge, which is unique to rabbits (McCartney-Francis et al., 1984). Rabbit kappa light chain isotypes are divided into two categories: κ1 and κ2. Typically, κ1 isotypes account for up to 90% of serum antibodies, with the remainder consisting of lambda light chains and κ2 light chains (Mage, 1998). Of these κ1 isotypes, the majority contain a disulphide bridge that links framework region 3 of the light chain variable domain to the constant domain at Cys80 and Cys171 (McCartney-Francis et al., 1984), which likely causes complications for the expression of rabbit Fabs in *E. coli*. It is therefore suggested that the majority of clones present in the Fab library were likely toxic to the cell or expressed in quantities too low (or may have been incorrectly folded and hence aggregated and not displayed on the surface) for efficient enrichment to take place, substantially reducing the number of viable clones in the library and increasing the level of background. This would potentially lead to amplification of background phage over specific phage during the biopanning stage. To overcome this potential problem, a different host organism for expression and display could be utilised, such as *Pichia pastoris*. However, this would require a complete re-design of the approach described above, and as such was not considered as a viable alternative during the work described here.

A potential workaround for the issue of disulphide bond complexity within rabbit light chain allotypes would be to generate chimeric Fab fragments by fusing the rabbit variable regions to constant regions from another species, such as humans, eliminating the potentially problematic disulfide bridge. Generation of chimeric human-rabbit Fab libraries has been reported in the literature (Weber, Peng, & Rader, 2017). Particularly of note is the generation of a chimeric immune library to the HIV-1 regulatory protein Rev, in which a library of approximately 2 x 10^8 clones was produced, which was then successfully enriched via phage biopanning using this approach (Stahl et al., 2010). Successful expression of soluble monoclonal chimeric Fabs was achieved in *E. coli* by directing the V_H-C_H and V_κ-C_κ chains into the periplasmic space via OmpA and PelB signal sequences and, upon assessment, a high binding affinity was observed. A similar approach was used more recently to generate monoclonal chimeric Fabs to the Hepatitis B e-antigen with high affinity and specificity (Zhuang et al., 2017). Humanisation of rabbit antibody fragments has been frequently documented in the literature, and does not appear to have substantial impact on either the specificity or affinity to the target antigen (Popkov et al., 2003).

Generation of recombinant rabbit scFv fragments was considered a favourable alternative to the production of chimeric human-rabbit Fab fragments, as it was achievable via a small phagemid modification and use of a readily available published primer set (Vu et al., 2017). This approach eliminated the constant region entirely, potentially providing a molecule that the expression system (TG-1 *E. coli*) should be capable of expressing, and the generation of recombinant scFv libraries from immunised rabbits is well documented in the literature (Rüdiger Ridder, Rita Schmitz, 1989; Vu et al., 2017; Xu et al., 2017).

Due to the minimal amount of peripheral blood lymphocytes remaining from rabbit RA528 following construction of the Fab library, scFv DNA was initially amplified using this Fab library DNA as a template (**Figure 5.7** and **Figure 5.8**). Following assembly into the same phagemid vector, modified to allow periplasmic expression of scFv fragments, this library appeared to show a good degree of diversity in both the heavy and light chain. However, as with the previously rabbit Fab library, phage display biopanning resulted in no clear enrichment of anti-elastase antibody fragments. As previously explained, there are many factors which may contribute to the failure of producing monoclonal antibodies via phage display. With regards to this particular library, it is plausible that if the diversity of the Fab library was already skewed away from antibody fragments specific to elastase, then by amplifying scFv DNA from this template, the chances of amplifying elastase specific antibody DNA was further reduced, effectively biasing the library even further away from this target.

With this possibility in mind, a second scFv library was generated using the remaining PBLs from rabbit RA528, as this would provide an unbiased cDNA template from which to amplify scFv DNA. Amplification of scFv DNA and subsequent pull-through assembly appeared to be successful (**Figure 5.15, Figure 5.16** and **Figure 5.17**), and a recombinant scFv library containing approximately 1 x 10^6 clones was constructed. However, the insertion rate for this library was considerably lower than that of the previously generated scFv library (**Figure 5.18**), resulting in a high degree of background phagemid. This may have contributed to the subsequent failure of this library to enrich for anti-elastase scFvs (**Figure 5.20**), as each round of panning likely amplified background phage, outcompeting any potential anti-elastase presenting phage. Additionally, the overall size of this library was considerably smaller than libraries built previously. Without taking the low insertion rate into consideration, 1 x 10^6 clones is considered at least 10-fold too small to reliably amplify a single antigen-specific clone, by the standards of the industrial partner Mologic Ltd., and so it is likely that this library simply wasn't large enough to represent the full immune repertoire of the immunised rabbit. There are, again, a number of factors which may have influenced this. Most notably, there was a limited amount of extracted rabbit material available at the beginning of this build, resulting in a far lower RNA yield than observed when generating the Fab library. This has the knock-on effect of producing a cDNA template which may only cover a limited portion of the rabbit's immune repertoire, biasing subsequent PCR amplification of scFv DNA rather than providing accurate representation of all heavy and light chain variants. This bias may have been further amplified following pull-through assembly of full length scFv genes, resulting in low genetic diversity and further reducing the chances of successful enrichment of antigen-specific clones.

There may have been some impact on both ligation and transformation efficiency brought about by differences in equipment and reagents used in this library build. Whilst the initial rabbit Fab and scFv library builds were carried out at the industrial partner's phage display facility, the second scFv library build and subsequent sheep Fab library builds were performed at the University of Kent, using different electroporation equipment, incubators, and enzymes from different suppliers. It is difficult determine if these changes had an impact on the resulting library sizes and diversity and the standard operating procedures otherwise remained identical between both library builds.

A recombinant sheep Fab immune library was constructed in parallel with the second rabbit scFv library. Whilst rabbit antibody fragment libraries have not previously been produced by the industrial partner, sheep Fab libraries are routinely constructed and panned successfully. PCR amplification generated the expected products (**Figure 5.21** and **Figure 5.22**), and a high light

chain insertion rate implied a good degree of variation (**Figure 5.23**). However, heavy chain insertion was considerably lower, resulting in a library of approximately 1 x 10^6 clones, 50% of which contained both antibody chains (**Figure 5.24**). DNA fingerprinting showed a low degree of diversity in the heavy chain and only a single unique variant in the light chain (**Figure 5.25**) and upon phage display biopanning, as expected, no enrichment of anti-elastase Fab fragments was observed (**Figure 5.26**). It is possible that this library generation was impacted by the same reagent or equipment based issues experienced by the second rabbit scFv library. Although the overall immune response observed by the immunised sheep appeared slightly lower than the response seen in the rabbits, similar levels of anti-elastase polyclonal antibody were found in the serum, and so it is unlikely that this was a contributing factor. It may also be possible that the quality of PBLs prepared was low, leading to poor quality RNA extraction and an overall bias of the library towards specific antibody chain variants, potentially explaining the presence of a single light chain variant in the established library. This sheep Fab library build procedure was repeated by researchers based at the industrial partner, who found the same challenges in achieving a high rate of insertion for heavy chain DNA.

In terms of future assay development, generation of high affinity monoclonal antibodies remains the most desirable route. As stated previously, in order for an immunoassay to be reproducible and able to be manufactured at a large scale, incorporation of monoclonal antibodies is necessary. Thus, further attempts at phage display are required in order to continue this work, which will require new immunisations and modifications to the protocols used in the work described above. It may also be beneficial to utilise different phagemid vectors, or to modify the primer sets used for immune repertoire amplification, as generating a diverse antibody library containing a large number of clones is crucial for successful enrichment and monoclonal antibody selection. These aspects are further explored in Chapter 6.

Chapter 6

Overall Discussion

The work detailed in this thesis explores the development of ELISA and lateral flow format immunodiagnostic assays in order to detect elastase as a biomarker of *P. aeruginosa* presence in Cystic Fibrosis patients. The ultimate goal of the work is to produce a rapid, sensitive and specific diagnostic assay which is able to detect the presence of elastase, and hence the *P. aeruginosa* bacterium, during the early stages of infection. The assay development process began with the cloning, expression, purification and characterisation of the recombinant antigen, elastase, which was then used to immunise two sheep and two rabbits in order to generate elastase-specific polyclonal antibodies. Anti-elastase pAbs were then incorporated into immunodiagnostic assays which were optimised, assessed and validated initially using recombinant elastase and subsequently laboratory strains and clinical isolates of *P. aeruginosa*. Attempts were made to generate high-affinity monoclonal antibody fragments via antibody phage display, though this approach was not successful during the studies described here.

The work described in the results chapters outlines the establishment of a highly sensitive sandwich ELISA format immunodiagnostic assay, which was demonstrated when using sheep polyclonal anti-elastase antibodies to detect native *P. aeruginosa* elastase cultured from clinically relevant isolates with a lower limit of detection of 266 pg/mL. Antibodies derived from rabbits demonstrated an even high sensitivity, with a lower limit of detection of 27 pg/mL, although these were not used to assess clinically relevant isolates. These prototype assays were also highly specific, showing no cross-reactivity across a variety of bacterial species. The assay developed thus shows great potential as an early predictor of *P. aeruginosa* infections in Cystic Fibrosis patients, which would allow antimicrobial treatment to begin earlier, potentially reducing the risk of developing a chronic infection. Further development is required in order to achieve the required sensitivity for use with direct patient samples, but in its current form the assay provides a good proof of concept for future work.

The first results chapter (Chapter 3) describes the expression and purification of recombinant elastase, a secreted protease of *P. aeruginosa* under the control of the las quorum sensing pathway, in the *E. coli* protein expression strain BL21*(DE3)pLysS, and its subsequent characterisation prior to immunisation. The protease was successfully purified via nickel affinity chromatography without the need for refolding by utilising the native signal sequence of the *lasB* structural gene to localise the recombinant product to the *E. coli* periplasm, an oxidising environment more conducive to disulphide bond formation (Georgiou & Segatori, 2005).

Although only mg amounts of recombinant elastase were produced, this method proved to be low cost, and substantially less complex and time-consuming than previously reported methods of producing recombinant elastase (Odunuga et al., 2015), and provided sufficient protease for characterisation, immunisation and assay development. However, for large-scale production of elastase (i.e. for inclusion in a commercial ELISA), further optimisation of this expression protocol may be necessary, or use of scale-up procedures. For the purposes of generating recombinant elastase material for use in this study, cells were grown in 2 L shake flasks. Higher yields would be achievable via controlled larger scale fermentation where much higher ODs are obtained and higher expression yields result. Further variation of induction time and the concentration of IPTG for induction may also improve soluble protein yields, as this was not explored thoroughly in this work. Use of an *E. coli* strain more suitable for expressing disulphide-bonded proteins, such as SHuffle (Ren, Ke, & Berkmen, 2016), may further enhance recombinant elastase yields, as fractionation of *lasB*-expressing BL21*(DE3)pLysS cells demonstrated that a moderate amount of insoluble material was also produced (**Section 3.3.3**).

Recombinant elastase was recovered at high purity via nickel affinity chromatography (estimated at >90% from SDS-PAGE analysis), with no requirement for further purification steps for immunisation of animals. Upon purification it was discovered that the recombinant elastase was autoprocessed into its 33 kDa active form prior to cell lysis and the cleaved propeptide remained non-covalently associated with the mature protease, in keeping with the protease's behaviour in *P. aeruginosa* (Kessler & Safrin, 1988; Kessler et al., 1998). Degradation of the propeptide was evident following buffer exchange and concentration, and its presence did not appear to have an impact on the activity of the recombinant product to digest gelatin (**Figure 3.14**) or hydrolyse an elastase-specific fluorogenic peptide (**Figure 3.15**), despite previous studies demonstrating the inhibitory effect of the propeptide on mature elastase in *P. aeruginosa* (Kessler & Safrin, 1994). While recovery was achieved with a high degree of purity, it is clear from SDS-PAGE analysis that much of the recombinant product was not recovered. Recombinant elastase did not appear to bind strongly to the column, as much of this was washed from the column at low concentrations of imidazole. Further optimisation of the IMAC purification protocol may be necessary in order to ensure the most efficient recovery of protein from the periplasm, which may be achieved via a larger bed volume of nickel-chelating sepharose resin, or alterations to the purification buffers used in order to improve binding of the protease to the resin. It is noted that some C-terminal degradation was observed following buffer exchange and concentration, as evident by a loss of signal when western blotting with an anti-his tag antibody. Although this degradation does not appear to impact on the activity of the

mature protease, it is possible that the antibodies raised against it may differ in their epitope recognition.

Assessment of the recombinant elastase product for activity via gelatin zymography and a FRET-based peptide assay adapted from a previous study (Elston et al., 2007) demonstrated the specific protease activity of the purified recombinant elastase. From these studies, generally lower activity was observed than has been reported in the past, but the mature protease was shown to be active following autoprocessing at concentrations as low as 1 nM. The recombinant elastase was also shown to have high conformational stability, demonstrated via refolding assays in the presence of guanidine hydrochloride, and as such was considered a suitable candidate for immunisation of animals against which to raise polyclonal antibodies.

Assessment of polyclonal antibodies and the development of prototype immunodiagnostic assays is described in the second results chapter (Chapter 4). Immunisation with recombinant elastase was performed in 2 rabbits and, at a later date, 2 sheep. Serum dilution ELISAs were subsequently performed in order to track the immune response and estimate antibody titre. Initial immunisations performed in rabbits showed a typical immune response, with a considerable rise in titre following the first booster immunisation, resulting from the adaptive immune response (Ren et al., 2016). Although the serum ELISAs initially suggested that the immunised rabbits had responded more strongly to the recombinant elastase compared with the immunised sheep, quantification of specific antibody in the serum via affinity purification suggested that similar levels of anti-elastase antibody were present in each animal (**Table 4.1**).

The optimisation of prototype ELISAs based on the 4 polyclonal antibodies purified across the 4 immunised animals is discussed in detail in **Section 4.7**. Once appropriate capture antibody concentrations, detector antibody dilutions and an optimised protocol were established, assay sensitivity was assessed via the construction of standard curves using recombinant elastase. In its current form, the anti-elastase sandwich ELISA incorporating rabbit pAb RA528 has a lower limit of detection of 27 pg/mL and is 10-fold more sensitive than previously reported anti-elastase ELISAs (Jaffar-Bandjee et al., 1993). On-the-other-hand, the ELISA incorporating sheep pAb SA562 has a lower limit of detection of 226 pg/mL, but a considerably higher amount of antibody was produced due to the larger bleed volume that can be obtained from sheep. It is for this reason that the sheep SA562 pAbs were used for subsequent ELISA studies, whereas experiments on monoclonal antibody development via antibody phage display were performed using material derived from immunised rabbit RA528.

A key experiment in the validation of this assay as a potentially viable immunodiagnostic in the clinic was the assessment of *P. aeruginosa* clinical isolates, derived from cystic fibrosis patient samples provided by Prof. Jane Davies and the National Heart and Lung Institute at Imperial College London. The prototype ELISA was capable of detecting elastase in the culture supernatant of 29/31 "first isolates", isolates obtained at first identification of *P. aeruginosa*, generally considered to be acute, early-stage infections. These isolates are typically considered to be highly virulent strains, and so it was predicted that elastase production would be higher in these samples. Detection of *P. aeruginosa* elastase in these first isolates shows promise for the assay's potential as a diagnostic for early-stage infections.

The assay was less consistent with its ability to detect elastase in chronic *P. aeruginosa* isolates. Of 17 total chronic isolates, the assay was only able to recognise 12 confidently. This is likely due to the nature of elastase as a virulence factor under the control of the hierarchical las quorum sensing pathway (Nadal Jimenez et al., 2012). In chronic infections, *P. aeruginosa* is typically mucoid, as described in **Section 1.3.2.2**, and the quorum sensing pathways are thought to be suppressed in some instances due to a mutation in the *lasR* regulatory gene (D'Argenio et al., 2007), resulting in a loss of virulence and, as a result, a reduction in *lasB* expression, the structural gene encoding elastase. Thus, it might be expected that there would not be elastase present in all such isolates and hence a differential expression across such isolates would be expected and is consistent with the results reported here.

Due to this distinction between acute infections harbouring primarily planktonic, virulence factor-expressing isolates and chronic infections consisting predominantly of mucoid, biofilm-residing isolates (Z. Li, 2005), it is posited that this assay is more appropriate for the detection of early stage infections. Elastase is often implicated in the initial stages of infection (Wretlind & Pavlovskis, 1983), and planktonic isolates are often implicated in instances of pulmonary exacerbation (Fothergill et al., 2010). As such, elastase remains an important potential biomarker for acute infection and prediction of pulmonary exacerbation. Although somewhat restrictive in that the assay is unable to reliably detect late-stage infections, a specificity for acute infections is beneficial as it allows for early detection of *P. aeruginosa* in a state more receptive to antibiotic treatment (Talwalkar & Murray, 2016).

Specificity of the elastase assay was assessed via a range of gram negative and gram positive bacterial isolates provided together with the *P. aeruginosa* clinical isolates. Multiple strains of *E. coli*, *S. aureus*, *S. marcescens*, *S. maltophilia*, *K. pneumoniae* and *B. cepacia* complex were tested and all returned absorbance values below the lower limit of detection, demonstrating no cross-

reactivity of the anti-elastase pAbs with other bacterial species frequently associated with cystic fibrosis disease states (Frayman et al., 2017). From the work carried out thus far, false negatives appear to be more likely to occur than false positives, likely due to the nature of elastase expression in the *P. aeruginosa* life cycle as discussed above. Primarily, this relates to the assay's inability to reliably detect chronic isolates of *P. aeruginosa* as a result of the mucoid switch, associated with the downregulation of virulence factors including elastase (Smith et al., 2006).

A useful form for such a diagnostic as that described here is as a paper-based lateral flow assay device. This approach makes use applicable at the point of care and requires low technology levels. As previously noted, the rabbit RA528 pAbs, although in shorter supply, appeared to be more sensitive and as such were incorporated into prototype lateral flow diagnostic devices, capable of detecting recombinant elastase at a concentration of 1 ng/mL. There is often a trade-off in sensitivity associated with lateral flow immunoassays, compensated by their considerably faster turnaround time and ease of use (Sajid et al., 2015). The current "gold standard" diagnostic assay for detection of *P. aeruginosa* infection in CF patients is sputum culture or culture of bronchoalveolar lavage fluid (BAL), which can take upwards of 72 hours to return a result (Seidler et al., 2016). Lateral flow immunoassays, on the other hand, are able to return a result within 10 minutes of sample application, and as such are desirable diagnostic tools for use in a clinical or home setting. The greatest challenge to this approach is in developing an assay with a sensitivity sufficient to detect the bacterium in a patient sample without compromising assay time or accessibility.

Further development of the assays described in this thesis could improve the sensitivity to a range in which direct patient samples could be directly assessed. It is difficult to accurately estimate the concentration range at which elastase may be found in the sputum of infected patients, but the current target sensitivity is predicted to be in the low pg/mL region. For use in a point of care diagnostic assay, it is expected that sputum samples will require additional processing steps which may further dilute elastase in the sample. As previously discussed, testing culture supernatants of first isolates isolated from CF patients has demonstrated the prototype ELISA's ability to detect elastase in clinically relevant *P. aeruginosa* strains and differentiate between other bacteria commonly associated with CF. However, the levels of elastase present in supernatant samples are expected to be far higher (previous ELISA assessment of clinical isolate supernatants reported concentrations higher than 100 ng/mL when compared to a recombinant elastase standard curve (**Section 4.5.5**)) than those found in a direct sample, such as sputum, bronchoalveolar lavage, or exhaled breath condensate, and the overnight culture time is not ideal for a rapid diagnostic test. Ideally, an assay would be

consolidated into a lateral flow format device to be used at the point of care, providing rapid turnover of results in the clinic, without the need for an external laboratory or specialised equipment. An ideal point of care diagnostic assay should meet the ASSURED criteria outlined in **Section 1.5.1** (Peeling et al., 2006), and for this assay to achieve these requirements further antibody development and signal enhancing techniques are likely to need to be employed. As described in **Section 4.7**, various signal enhancing methodologies can be utilised to improve lateral flow assay signals, such as loading gold nanoparticles with an enzyme such as horseradish peroxidase (Parolo et al., 2013) or coating of gold nanoparticles with platinum nanolayers (Gao et al., 2017), which has been reported to improve sensitivity by up to two orders of magnitude. This signal enhancement, coupled with the generation of a pair of high-affinity monoclonal antibodies via antibody phage display, may be sufficient for elastase detection in a direct patient sample, as a 100-fold enhancement may increase the LLOD of the rabbit-derived pAb ELISA from 27 pg/mL to 0.27 pg/mL.

The final results chapter (chapter 5) describes attempts to generate diverse Fab and scFv libraries from both rabbit and sheep derived peripheral blood lymphocytes (PBLs). The goal of this section of work was to generate a minimum of two high-affinity monoclonal antibody fragments, Fab or scFv, which could be produced at large scale in *E. coli*. A total of 4 libraries were generated: 1 RA528 Fab library, 2 RA528 scFv libraries, and 1 combined sheep Fab library incorporating PBLs from both immunised sheep. The initial library build (RA528 Fab) at first appeared promising, showing a high degree of diversity and a large number of clones. However, upon biopanning no enrichment was observed, likely due to the added disulphide complexity typical of rabbit light chain κ1 isotypes (McCartney-Francis et al., 1984) previously described in **Section 5.8**. The presence of this additional disulphide is likely to lead to difficulties in Fab expression in *E. coli* and, as a result, its display on the phage surface. Attempts to circumvent this via construction of scFv libraries, both from the existing Fab library and from the starting PBLs were similarly unsuccessful in their ability to be panned, likely due to their smaller library size and resulting lack of diversity. Similar problems were encountered in the construction and subsequent panning of a sheep Fab library, possibly due to low quality RNA extracted from the prepared PBLs. It is difficult to pin-point the root cause of the reduced library sizes, particularly in regards to the sheep Fab library, as sheep are routinely used as candidates for antibody phage display (Y. Li, Kilpatrick, & Whitelam, 2000). Any one stage within the library construction process can have knock-on effects on subsequent stages. For instance, poor quality RNA will generate poor quality cDNA, which will negatively impact PCR amplification of antibody chain variants. If too small an amount of antibody DNA is digested for ligation into the phagemid

vector, or is not digested fully, then the resulting transformants are likely to be skewed or limited in diversity. Ligation and transformation efficiency can similarly limit the size and diversity of antibody phage display libraries, meaning reagent quality and protocol optimisation are particularly crucial factors in antibody phage display.

There is much advantage in using monoclonal antibodies over polyclonal antibodies in immunodiagnostic assays. While pAbs can provide a good proof of concept, they are limited in supply, as well as being expensive and time-consuming to produce. Mass production of pAbs requires frequent immunisation, which in turn requires a constant supply of antigen as well as the ongoing costs of animal housing and maintenance. Further, as each animal will generate a unique antibody response to immunisation, every time a new polyclonal antibody is generated any assay using this requires re-optimisation over previous assays developed with other polyclonal antibodies. There are also ethical considerations resulting from the mass production of antibodies in animals. Due to the unique response of different animals, pAbs can vary considerably in their sensitivity and binding modes, as observed in comparisons between RA528 and RA528 anti-elastase pAbs and described in the second results chapter, which can be problematic for a commercial assay. In order to be a reliable and consistent immunodiagnostic, the antibodies incorporated must behave the same each time, and variations in antibody sensitivity as a result of differences between pAbs will compromise the robustness of the assay. As such, generation of mAbs has several distinct advantages. A higher sensitivity can be achieved by the selection of only high affinity clones via antibody phage display (H. Yang et al., 2018). Additionally, as these antibodies are being used for diagnostic purposes, they do not require an effector region and can be produced as Fab or scFv fragments, allowing their production in a low-cost, high-yield expression system such as *E. coli*. Furthermore, as the antibodies are clones, the resultant assay can be relied on to perform consistently with minimal variability. It would therefore be an important step in further development of the assay described here that mAbs are developed. As such, further work is required in order to understand and overcome the limitations of antibody phage display in producing anti-elastase mAb fragments.

The anti-elastase sandwich ELISA described in this thesis offers several advantages over many of the diagnostic assays currently available for the detection of *P. aeruginosa* in CF patients. Previously described ELISAs focus mainly on detection of antibodies against *Pseudomonas* in the serum (Pedersen et al., 1987; Tramper-Stranders et al., 2006), requiring invasive blood-sampling techniques. Additionally, host responses have been shown to vary considerably between CF patients, with culture data often conflicting with serum ELISA results (Anstead et al., 2013). The immune system cannot be considered a reliable source for such diagnoses, as anti-*Pseudomonas*

antibodies may remain in the body long after an infection has cleared, whereas detection of a virulence factor, such as elastase, is more likely to be indicative of an ongoing infection. The ELISA format also offers advantages in assay time over a method such as sputum culture, which often requires a minimum of overnight incubation before detection is possible as opposed to a 4 hour assay. The LFA prototype also shows promise for a rapid diagnostic, and offers further advantages in its simplicity, low cost and turnaround time.

Currently, the assay described in this thesis is primarily limited by its sensitivity. In order to ascertain whether it is sufficient, direct assessment with patient samples must first be performed. There is a pressing need for a diagnostic which can detect acute, early-stage *P. aeruginosa* infections in CF patients, as this will allow for antimicrobial treatment before biofilm formation and the development of a chronic infection, and so high sensitivity is a key factor. Maintaining a low cost is also important, as CF patients must be routinely tested for such infections. *P. aeruginosa* is one of the most common sources of nosocomial infections, putting CF patients at a particularly high risk (Moradali, Ghods, & Rehm, 2017).

Further development of the assay should focus on the generation of high-affinity monoclonal antibody fragments, as well as investigations into signal enhancement techniques such as those described above. As noted previously, development of monoclonal antibody fragments would be an important step forward in order to create a sensitive, reproducible assay, and further development using antibody phage display could facilitate this.

In order to ensure a greater degree of success in monoclonal antibody development than was achieved in Chapter 5, it would be important to construct a much larger, high quality and diverse variant library. In order to minimise amplification bias when generating heavy and light chain gene variants, PCRs should be performed at the lowest annealing temperature which generates a product, and cycle number should be kept to a minimum. Ideally, a well-characterised commercial phagemid vector such as Antibody Design Labs' pADL series should be used as the basis for these libraries, and library diversity should be determined on a larger scale than previously. This is able to be achieved via Next Generating Sequencing (NGS) or Sanger Sequencing of a library subsample, as opposed to the small-scale DNA fingerprinting previously performed. As DNA fingerprinting relies on a relatively small sample size, it is difficult to reliably extrapolate these data to the entire library. Whilst sequencing a library subsample still does not provide insights into the total diversity of the library, it provides a larger sampling of sequence space coverage and as such provides greater confidence towards the final quality of the built library.

Following library assembly and transformation, there are several improvements to the biopanning process that could be implemented in order to minimise risk of non-specific phage amplification and increase the likelihood of enriching for specific binders. In order to first enrich the library for antibody-presenting phage, a "clearing round" is highly recommended. In this round of selection, a very low binding pressure would be applied (an excess of target antigen, or an antibody-binding target such as protein A) in order to "clear" the library of unfolded or non-displaying variants. Following this, binding pressure could be increased via reduction of the target antigen concentration in order to more efficiently enrich for target-specific binders. In order to minimise non-specific binders, such as variants which recognise epitopes found on the selection medium (such as the streptavidin-binding motif HPQ) or blocking agent (for example, binders which recognise BSA or milk protein epitopes), it is highly recommended to alternate both selection surface and blocking solution. By using streptavidin-coated magnetic bead-antigen conjugates for one round and antigen-coated immunotubes the following round, it is possible to deplete libraries of nonspecific binders. This also has the added benefit of enriching the library for variants which recognise the antigen in multiple states, as it is likely that an antigen immobilised on a Maxisorp surface maintains a slightly altered conformation to that of a biotinylated antigen conjugated to streptavidin.

If, following multiple rounds of biopanning, the subsequently selected monoclonal antibody fragments are still not of the desired sensitivity, it may be worth considering the generation of synthetic affinity maturation libraries. These libraries may be semi-rationally designed, based on the DNA sequences of the isolated anti-elastase antibody fragments. By introducing mutations into the antigen-binding CDR loop regions via degenerate primers or trinucleotides, new libraries can be constructed with potential for the selection of higher affinity antibody fragments. These libraries may be generated via a variety of methods, including but not limited to error prone PCR to introduce diversity into CDR loops, or the use of inverse PCR and blunt ligation in order to introduce additional residues. Affinity maturation libraries can be screened as described in the previous paragraph in order to achieve significantly higher affinities for the target antigen.

Once a higher assay sensitivity has been achieved, assessment of both ELISAs and LFAs with direct patient samples should be performed. Ideally a large number of samples from a variety of clinics should be assessed (n >100), originating from a diverse group of patients of different ages and CF severity to ensure the assay's reliability and robustness. It may be useful to assess a range of different sample types as well. Typically CF samples are provided as sputum as this is easy to obtain. However, younger patients may have difficulty expectorating, and so there is an ongoing interest in *P. aeruginosa* detection from exhaled breath condensate as an alternative sample

type. This would be the least invasive method of sample acquisition, but it is currently unknown whether elastase is present in such samples at detectable levels, if at all. Urine samples are also of similar interest, but may also impart the same challenges in detection.

Whilst this thesis primarily describes the development of an assay for the early detection of *P. aeruginosa* in cystic fibrosis patients, there is scope for wider application of this assay. *P. aeruginosa* is a pathogen frequently associated with a variety of disease states including, but not limited to, chronic wounds (Serra et al., 2015), corneal infections (Sy et al., 2012) and urinary tract infections (Newman, Floyd, & Fothergill, 2017). Furthermore, *P. aeruginosa* is frequently implicated in nosocomial infections, with a cohort study reporting it to have the highest burden of all healthcare-acquired infections (Lambert et al., 2011). As such, development of a rapid diagnostic assay for *P. aeruginosa* may benefit not only cystic fibrosis patients, but could potentially also allow for earlier treatment in the context of many other disease states, potentially reducing the burden on healthcare institutes via assessment of patient samples such as urine, blood, and wound-swab extracts.

In summary, the work described in this thesis outlines the early development of a highly specific, sensitive immunodiagnostic assay which has been shown to readily detect elastase at levels as low as 26 pg/mL and can be used to recognise clinically relevant *P. aeruginosa* strains without cross-reacting with other bacterial species commonly associated with cystic fibrosis. Early stage lateral flow assays show good sensitivity and are able to differentiate between elastase producing and non-producing *P. aeruginosa* strains, though their utility with clinically relevant strains has yet to be assessed. A platform has also been established for the generation of recombinant elastase at a low cost, which may be of use for further enzyme characterisation and antibody binding studies. Whilst there is still much work required, particularly regarding the sensitivity of the assay and assessment of clinical samples, the work performed up to this point provides a good proof of concept for the further development of a rapid immunoassay diagnostic test for *P. aeruginosa* to be used in the clinic.

Bibliography

ANSTEAD, M., HELTSHE, S. L., KHAN, U., BARBIERI, J. T., LANGKAMP, M., DÖRING, G., … RAMSEY, B. (2013). Pseudomonas aeruginosa serology and risk for re-isolation in the EPIC trial ☆. *Journal of Cystic Fibrosis*, **12**(2), 147–153.

BARBAS, C. F. (2001). *Phage display : a laboratory manual*. Cold Spring Harbor Laboratory Press.

BHAGIRATH, A. Y., LI, Y., SOMAYAJULA, D., DADASHI, M., BADR, S., & DUAN, K. (2016). Cystic fibrosis lung environment and Pseudomonas aeruginosa infection. *BMC Pulmonary Medicine*, **16**(1), 1–22.

BOES, M. (2001). Role of natural and immune IgM antibodies in immune responses. *Molecular Immunology*, **37**(18), 1141–1149.

BOYD, A., & CHAKRABARTY, A. M. (1995). Pseudomonas aeruginosa biofilms: role of the alginate exopolysaccharide. *Journal of Industrial Microbiology*, **15**(3), 162–168.

BOYLE, M. P., & DE BOECK, K. (2013). A new era in the treatment of cystic fibrosis: correction of the underlying CFTR defect. *The Lancet Respiratory Medicine*, **1**(2), 158–163.

BRADFORD, M. M. (1976). A rapid and sensitive method for the quantitation of microgram quantities of protein utilizing the principle of protein-dye binding. *Analytical Biochemistry*, **72**, 248–254.

BURNS, J. L., GIBSON, R. L., MCNAMARA, S., YIM, D., EMERSON, J., ROSENFELD, M., … RAMSEY, B. W. (2001). Longitudinal Assessment of *Pseudomonas aeruginosa* in Young Children with Cystic Fibrosis. *The Journal of Infectious Diseases*, **183**(3), 444–452.

BUTLER, S. A., KHANLIAN, S. A., & COLE, L. A. (2001). Detection of early pregnancy forms of human chorionic gonadotropin by home pregnancy test devices. *Clinical Chemistry*, **47**(12), 2131–2136.

CASTELLANI, C., CUPPENS, H., MACEK, M., CASSIMAN, J. J., KEREM, E., DURIE, P., … ELBORN, J. S. (2008). Consensus on the use and interpretation of cystic fibrosis mutation analysis in clinical practice. *Journal of Cystic Fibrosis*, **7**(3), 179–196.

CATHCART, G. R. A, QUINN, D., GREER, B., HARRIOTT, P., LYNAS, J. F., GILMORE, B. F., & WALKER, B. (2011). Novel inhibitors of the Pseudomonas aeruginosa virulence factor LasB: A potential therapeutic approach for the attenuation of virulence mechanisms in pseudomonal infection. *Antimicrobial Agents and Chemotherapy*, **55**(6), 2670–2678.

CHAN, C. E., ZHAO, B. Z., CAZENAVE-GASSIOT, A., PANG, S.-W., BENDT, A. K., WENK, M. R., … HANSON, B. J. (2013). Novel phage display-derived mycolic acid-specific antibodies with potential for tuberculosis diagnosis. *Journal of Lipid Research*.

CHOI, H. J., KIM, M. H., CHO, M. S., KIM, B. K., KIM, J. Y., KIM, C., & PARK, D. S. (2013). Improved PCR for identification of Pseudomonas aeruginosa. *Applied Microbiology and Biotechnology*, **97**(8), 3643–3651.

CLACKSON, T., HOOGENBOOM, H. R., GRIFFITHS, A. D., & WINTER, G. (1991). Making antibody fragments using phage display libraries. *Nature*, Vol. 352, pp. 624–628.

COHEN, T. S., & PRINCE, A. (2012). Cystic fibrosis: A mucosal immunodeficiency syndrome. *Nature Medicine*, **18**(4), 509–519.

CONNETT, G. J. (2000). Bronchoalveolar lavage. *Paediatric Respiratory Reviews*, **1**(1), 52–56.

D'ARGENIO, D. A., WU, M., HOFFMAN, L. R., KULASEKARA, H. D., DÉZIEL, E., SMITH, E. E., … MILLER, S. I. (2007). Growth phenotypes of Pseudomonas aeruginosa lasR mutants adapted to the airways of cystic fibrosis patients. *Molecular Microbiology*, **64**(2), 512–533.

DEEP, A., CHAUDHARY, U., & GUPTA, V. (2011). Quorum sensing and bacterial pathogenicity: From molecules to disease. *Journal of Laboratory Physicians*, **3**(1), 4.

DELAHAUT, P. (2017). Immunisation – Choice of host, adjuvants and boosting schedules with emphasis on polyclonal antibody production. *Methods*, **116**, 4–11.

DOUMIT, M., BELESSIS, Y., STELZER-BRAID, S., MALLITT, K.-A., RAWLINSON, W., & JAFFE, A. (2016). Diagnostic accuracy and distress associated with oropharyngeal suction in cystic fibrosis. *Journal of Cystic Fibrosis : Official Journal of the European Cystic Fibrosis Society*, **15**(4), 473–478.

ELSTON, C., WALLACH, J., & SAULNIER, J. (2007). New continuous and specific fluorometric assays for Pseudomonas aeruginosa elastase and LasA protease. *Analytical Biochemistry*, **368**(1), 87–94.

EMERSON, J., ROSENFELD, M., MCNAMARA, S., RAMSEY, B., & GIBSON, R. L. (2002). Pseudomonas aeruginosa and other predictors of mortality and morbidity in young children with cystic fibrosis. *Pediatric Pulmonology*, **34**(2), 91–100.

ENGVALL, E., & PERLMANN, P. (1971). Enzyme-linked immunosorbent assay (ELISA). Quantitative assay of immunoglobulin G. *Immunochemistry*, **8**(9), 871–874.

FELDMAN, M., BRYAN, R., RAJAN, S., SCHEFFLER, L., BRUNNERT, S., TANG, H., & PRINCE, A. (1998). Role of flagella in pathogenesis of Pseudomonas aeruginosa pulmonary infection. *Infection and Immunity*, **66**(1), 43–51.

FOTHERGILL, J. L., MOWAT, E., LEDSON, M. J., WALSHAW, M. J., & WINSTANLEY, C. (2010). Fluctuations in phenotypes and genotypes within populations of Pseudomonas aeruginosa in the cystic fibrosis lung during pulmonary exacerbations. *Journal of Medical Microbiology*, **59**(Pt 4), 472–481.

FRAYMAN, K. B., ARMSTRONG, D. S., CARZINO, R., FERKOL, T. W., GRIMWOOD, K., STORCH, G. A., … RANGANATHAN, S. C. (2017). The lower airway microbiota in early cystic fibrosis lung disease: A longitudinal analysis. *Thorax*, **72**(12), 1104–1112.

FREE, A. H., & FLEE, H. M. (1984). Self Testing, An Emerging Component of Clinical Chemistry. *CLINICAL CHEMISTRY CLIN. CHEM*, **306**(30), 829–838.

FUCHS, H. J., BOROWITZ, D. S., CHRISTIANSEN, D. H., MORRIS, E. M., NASH, M. L., RAMSEY, B. W., … WOHL, M. E. (1994). Effect of Aerosolized Recombinant Human DNase on Exacerbations of Respiratory Symptoms and on Pulmonary Function in Patients with Cystic Fibrosis. *New England Journal of Medicine*, **331**(10), 637–642.

FUENTE-NU, D., & BREIDENSTEIN, E. B. M. (2011). Pseudomonas aeruginosa : all roads lead to resistance. *Trends in Microbiology*, **19**(8), 419–426.

GALLAGHER, L. A., MCKNIGHT, S. L., KUZNETSOVA, M. S., PESCI, E. C., & MANOIL, C. (2002). Functions required for extracellular quinolone signaling by Pseudomonas aeruginosa. *Journal of Bacteriology*, **184**(23), 6472–6480.

GAMBELLO, M. J., & IGLEWSKI, B. H. (1991). Cloning and characterization of the Pseudomonas aeruginosa lasR gene, a transcriptional activator of elastase expression. *Journal of Bacteriology*, **173**(9), 3000–3009.

GAO, Z., YE, H., TANG, D., TAO, J., HABIBI, S., MINERICK, A., … XIA, X. (2017). Platinum-Decorated Gold Nanoparticles with Dual Functionalities for Ultrasensitive Colorimetric in Vitro Diagnostics. *Nano Letters*, **17**(9), 5572–5579.

GATES-HOLLINGSWORTH, M. A., & KOZEL, T. R. (2013). *Serotype Sensitivity of a Lateral Flow Immunoassay for Cryptococcal Antigen*.

GELLATLY, S. L., & HANCOCK, R. E. W. (2013). Pseudomonas aeruginosa: New insights into pathogenesis and host defenses. *Pathogens and Disease*, **67**(3), 159–173.

GEORGIOU, G., & SEGATORI, L. (2005). Preparative expression of secreted proteins in bacteria: Status report and future prospects. *Current Opinion in Biotechnology*, **16**(5), 538–545.

GOSS, C. H., & BURNS, J. L. (2007). Exacerbations in cystic fibrosis: Epidemiology and pathogenesis. *Thorax*, **62**(4), 360–367.

GOVAN, J. R., & DERETIC, V. (1996). Microbial pathogenesis in cystic fibrosis: mucoid Pseudomonas aeruginosa and Burkholderia cepacia. *Microbiological Reviews*, **60**(3), 539–574.

HALL-STOODLEY, L., & STOODLEY, P. (2009). Evolving concepts in biofilm infections. *Cellular Microbiology*, **11**(7), 1034–1043.

HANCOCK, R. E. W. (1998). Resistance Mechanisms in Pseudomonas aeruginosa and Other Nonfermentative Gram-Negative Bacteria. *Clinical Infectious Diseases*, **27**(1), 93–99.

HANLY, W. C., ARTWOHL, J. E., & BENNETT, B. T. (1995). Review of Polyclonal Antibody Production Procedures in Mammals and Poultry. *ILAR Journal*, **37**(3), 93–118.

HOIBY, N. (1977). Antibodies against Pseudomonas aeruginosa in serum from normal persons and patients colonized with mucoid or non-mucoid Pseudomonas aeruginosa: Results obtained by crossed immunoelectrophoresis. *Acta Pathologica et Microbiologica Scandinavica. Section C, Immunology*, **85**(2), 142–148.

HØIBY, N., CIOFU, O., & BJARNSHOLT, T. (2010). Pseudomonas aeruginosa biofilms in cystic fibrosis. *Future Microbiology*, **5**(11), 1663–1674.

HOIBY, N., FLENSBORG, E. W., BECK, B., FRIIS, B., JACOBSEN, S. V, & JACOBSEN, L. (1977). Pseudomonas aeruginosa infection in cystic fibrosis. Diagnostic and prognostic significance of Pseudomonas aeruginosa precipitins determined by means of crossed immunoelectrophoresis. *Scandinavian Journal of Respiratory Diseases*, **58**(2), 65–79.

JAFFAR-BANDJEE, M. C., CARRERE, J., LAZDUNSKI, A., GUY-CROTTE, O., & GALABERT, C. (1993). Direct double antibody sandwich immunoassay for Pseudomonas aeruginosa elastase. *Journal of Immunological Methods*, **164**(1), 27–32.

KAMATH, S., KAPATRAL, V., & CHAKRABARTY, A. M. (1998). Cellular function of elastase in Pseudomonas aeruginosa: Role in the cleavage of nucleoside diphosphate kinase and in alginate synthesis. *Molecular Microbiology*, **30**(5), 933–941.

KAY, B. K., WINTER, J., & MCCAFFERTY, J. (1996). *Phage display of peptides and proteins : a laboratory manual*. Academic Press.

KAZMIERCZAK, B. I., & MURRAY, T. S. (2013). Chronic versus Acute Pseudomonas aeruginosa Infection States. In *Regulation of Bacterial Virulence* (pp. 21–39).

KEISER, N. W., BIRKET, S. E., EVANS, I. A., TYLER, S. R., CROOKE, A. K., SUN, X., … ENGELHARDT, J. F. (2015). *Defective Innate Immunity and Hyperinflammation in Newborn Cystic Fibrosis*

Transmembrane Conductance Regulator-Knockout Ferret Lungs.

KESSLER, E., & SAFRIN, M. (1988). Synthesis, processing and transport of Pseudomonas aeruginosa elastase. *Journal of Bacteriology*, **170**(11), 5241–5247.

KESSLER, EFRAT, & SAFRIN, M. (1994). The propeptide of Pseudomonas aeruginosa elastase acts as an elastase inhibitor. *Journal of Biological Chemistry*, **269**(36), 22726–22731.

KESSLER, EFRAT, SAFRIN, M., GUSTIN, J. K., & OHMAN, D. E. (1998). Elastase and the LasA protease of Pseudomonas aeruginosa are secreted with their propeptides. *Journal of Biological Chemistry*, **273**(46), 30225–30231.

KESSLER, EFRAT, SAFRIN, M., PERETZ, M., & BURSTEIN, Y. (1992). Identification of cleavage sites involved in proteolytic processing of Pseudomonas aeruginosa preproelastase. *FEBS Letters*, **299**(3), 291–293.

KIM, J. Y., KIM, Y. G., & LEE, G. M. (2012). CHO cells in biotechnology for production of recombinant proteins: Current state and further potential. *Applied Microbiology and Biotechnology*, **93**(3), 917–930.

KIPNIS, E., SAWA, T., & WIENER-KRONISH, J. (2006a). Targeting mechanisms of Pseudomonas aeruginosa pathogenesis. *Médecine et Maladies Infectieuses*, **36**(2), 78–91.

KIPNIS, E., SAWA, T., & WIENER-KRONISH, J. (2006b). Targeting mechanisms of Pseudomonas aeruginosa pathogenesis. *Médecine et Maladies Infectieuses*, **36**(2), 78–91.

KIRATISIN, P., TUCKER, K. D., & PASSADOR, L. (2002). LasR, a Transcriptional Activator of Pseudomonas aeruginosa Virulence Genes, Functions as a Multimer. *Journal of Bacteriology*, **184**(17), 4912–4919.

KNOWLES, M. R., & BOUCHER, R. C. (2002). Mucus clearance as a primary innate defense mechanism for mammalian airways. *The Journal of Clinical Investigation*, **109**(5), 571–577.

KUANG, Z., HAO, Y., WALLING, B. E., JEFFRIES, J. L., OHMAN, D. E., & LAU, G. W. (2011). Pseudomonas aeruginosa Elastase provides an Escape from phagocytosis by degrading the pulmonary surfactant protein-A. *PLoS ONE*, **6**(11).

KUMAR, V., SULAJ, A., FLEMING, T., & NAWROTH, P. P. (2018). Purification and Characterization of the Soluble form of the Receptor for Advanced Glycation End-Products (sRAGE): A Novel Fast, Economical and Convenient Method. *Experimental and Clinical Endocrinology and Diabetes*, **126**(3), 141–147.

LAARMAN, A. J., BARDOEL, B. W., RUYKEN, M., FERNIE, J., MILDER, F. J., VAN STRIJP, J. A. G., & ROOIJAKKERS, S. H. M. (2012). Pseudomonas aeruginosa Alkaline Protease Blocks Complement Activation via the Classical and Lectin Pathways. *The Journal of Immunology*, **188**(1), 386–393.

LAMBERT, M. L., SUETENS, C., SAVEY, A., PALOMAR, M., HIESMAYR, M., MORALES, I., … WOLKEWITZ, M. (2011). Clinical outcomes of health-care-associated infections and antimicrobial resistance in patients admitted to European intensive-care units: A cohort study. *The Lancet Infectious Diseases*, **11**(1), 30–38.

LI, Y., KILPATRICK, J., & WHITELAM, G. C. (2000). Sheep monoclonal antibody fragments generated using a phage display system. *Journal of Immunological Methods*, **236**(1–2), 133–146.

LI, Z. (2005). Longitudinal Development of Mucoid Pseudomonas aeruginosa Infection and Lung Disease Progression in Children With Cystic Fibrosis. *JAMA*, **293**(5), 581.

LU, D., SHEN, J., VIL, M. D., ZHANG, H., JIMENEZ, X., BOHLEN, P., … ZHU, Z. (2003). Tailoring *in Vitro* Selection for a Picomolar Affinity Human Antibody Directed against Vascular Endothelial Growth Factor Receptor 2 for Enhanced Neutralizing Activity. *Journal of Biological Chemistry*, **278**(44), 43496–43507.

LYCZAK, J. B., CANNON, C. L., & PIER, G. B. (2000). Establishment of Pseudomonas aeruginosa infection: lessons from a versatile opportunist. *Microbes and Infection*, **2**(9), 1051–1060.

MAGE, R. G. (1998). Diversification of rabbit VH genes by gene-conversion-like and hypermutation mechanisms. *Immunological Reviews*, **162**, 49–54.

MAH, T. F., & O'TOOLE, G. A. (2001). Mechanisms of biofilm resistance to antimicrobial agents. *Trends in Microbiology*, **9**(1), 34–39.

MALLOY, J. L., VELDHUIZEN, R. A. W., THIBODEAUX, B. A., O'CALLAGHAN, R. J., & WRIGHT, J. R. (2005). *Pseudomonas aeruginosa* protease IV degrades surfactant proteins and inhibits surfactant host defense and biophysical functions. *American Journal of Physiology-Lung Cellular and Molecular Physiology*, **288**(2), L409–L418.

MARSHALL, B. C., BUTLER, S. M., STODDARD, M., MORAN, A. M., LIOU, T. G., & MORGAN, W. J. (2005). Epidemiology of cystic fibrosis-related diabetes. *The Journal of Pediatrics*, **146**(5), 681–687.

MARVIG, R. L., SOMMER, L. M., MOLIN, S., & JOHANSEN, H. K. (2015). Convergent evolution and adaptation of Pseudomonas aeruginosa within patients with cystic fibrosis. *Nature Genetics*, **47**(1), 57–64.

MATHEE, K., CIOFU, O., STERNBERG, C., LINDUM, P. ., CAMPBELL, J. I. ., JENSEN, P., … KHARAZMI, A. (1999). *Mucoid conversion of Pseudomonas aeruginosa by hydrogen peroxide: a mechanism for virulence activation in the cystic fibrosis lung*. (1 999).

MATHEE, K., CIOFU, O., STERNBERG, C., LINDUM, P. W., CAMPBELL, J. I. A., JENSEN, P., … KHARAZMI, A. (1999). Mucoid conversion of Pseudomonas aeruginos by hydrogen peroxide: a mechanism for virulence activation in the cystic fibrosis lung. *Microbiology*, **145**(6), 1349–1357.

MATSUMOTO, K. (2004). Role of bacterial proteases in pseudomonal and serratial keratitis. *Biological Chemistry*, **385**(11), 1007–1016.

MAYER-HAMBLETT, N., KLOSTER, M., ROSENFELD, M., GIBSON, R. L., RETSCH-BOGART, G. Z., EMERSON, J., … RAMSEY, B. W. (2015). Impact of sustained eradication of new pseudomonas aeruginosa infection on long-term outcomes in cystic fibrosis. *Clinical Infectious Diseases*, **61**(5), 707–715.

MCCARTNEY-FRANCIS, N., SKURLA, R. M., MAGE, R. G., BERNSTEIN, K. E., & BERNSTEIN, K. E. (1984). Kappa-chain allotypes and isotypes in the rabbit: cDNA sequences of clones encoding b9 suggest an evolutionary pathway and possible role of the interdomain disulfide bond in quantitative allotype expression. *Proceedings of the National Academy of Sciences of the United States of America*, **81**(6), 1794–1798.

MCIVER, K., KESSLER, E., & OHMAN, D. E. (1991a). Substitution of active-site His-223 in Pseudomonas aeruginosa elastase and expression of the mutated lasB alleles in Escherichia coli show evidence for autoproteolytic processing of proelastase. *Journal of Bacteriology*, **173**(24), 7781–7789.

McIver, K., Kessler, E., & Ohman, D. E. (1991b). Substitution of active-site His-223 in Pseudomonas aeruginosa elastase and expression of the mutated lasB alleles in Escherichia coli show evidence for autoproteolytic processing of proelastase. *Journal of Bacteriology*, **173**(24), 7781–7789.

Miao, E. A., Andersen-Nissen, E., Warren, S. E., & Aderem, A. (2007). TLR5 and Ipaf: dual sensors of bacterial flagellin in the innate immune system. *Seminars in Immunopathology*, **29**(3), 275–288.

Mitraki, A., & King, J. (1989). Protein Folding Intermediates and Inclusion Body Formation. *Nature Biotechnology*, **7**(7), 690–697.

Moradali, M. F., Ghods, S., & Rehm, B. H. a. (2017). Pseudomonas aeruginosa Lifestyle: A Paradigm for Adaptation, Survival, and Persistence. *Frontiers in Cellular and Infection Microbiology*, **7**(February).

Morihara, K. (1964). Production of Elastase and Proteinase by Pseudomonas aeruginosa. *Journal of Bacteriology*, **88**(3), 745–757.

Nadal Jimenez, P., Koch, G., Thompson, J. a., Xavier, K. B., Cool, R. H., & Quax, W. J. (2012). The Multiple Signaling Systems Regulating Virulence in Pseudomonas aeruginosa. *Microbiology and Molecular Biology Reviews*, **76**(1), 46–65.

Newman, J. W., Floyd, R. V., & Fothergill, J. L. (2017). The contribution of Pseudomonas aeruginosa virulence factors and host factors in the establishment of urinary tract infections. *FEMS Microbiology Letters*, **364**(15), 561–565.

Odunuga, O. O., Adekoya, O. a., & Sylte, I. (2015). High-level expression of pseudolysin, the extracellular elastase of Pseudomonas aeruginosa, in Escherichia coli and its purification. *Protein Expression and Purification*, **113**, 79–84.

Ostermeier, M., & Benkovic, S. J. (2000). A two-phagemid system for the creation of non-phage displayed antibody libraries approaching one trillion members. *Journal of Immunological Methods*, **237**(1–2), 175–186.

Pande, J., Szewczyk, M. M., & Grover, A. K. (2010). Phage display: Concept, innovations, applications and future. *Biotechnology Advances*, **28**(6), 849–858.

Parolo, C., de la Escosura-Muñiz, A., & Merkoçi, A. (2013). Enhanced lateral flow immunoassay using gold nanoparticles loaded with enzymes. *Biosensors and Bioelectronics*, **40**(1), 412–416.

Parsons, H. L., Earnshaw, J. C., Wilton, J., Johnson, K. S., Schueler, P. A., Mahoney, W., & McCafferty, J. (1996). Directing phage selections towards specific epitopes. *Protein Engineering*, **9**(11), 1043–1049.

Pearson, J. P., Feldman, M., Iglewski, B. H., & Prince, A. (2000). Pseudomonas aeruginosa cell-to-cell signaling is required for virulence in a model of acute pulmonary infection. *Infection and Immunity*, **68**(7), 4331–4334.

Pedersen, S. S., Espersen, F., & Høiby, N. (1987). Diagnosis of chronic Pseudomonas aeruginosa infection in cystic fibrosis by enzyme-linked immunosorbent assay. *Journal of Clinical Microbiology*, **25**(10), 1830–1836.

Peeling, R. W., Holmes, K. K., Mabey, D., & Ronald, A. (2006). Rapid tests for sexually transmitted infections (STIs): the way forward. *Sexually Transmitted Infections*, **82**(suppl_5), v1–v6.

Pesci, E. C., Milbank, J. B. J., Pearson, J. P., McKnight, S., Kende, A. S., Greenberg, E. P., & Iglewski,

B. H. (1999). Quinolone signaling in the cell-to-cell communication system of Pseudomonas aeruginosa. *Proceedings of the National Academy of Sciences*, **96**(20), 11229–11234.

PETERS, J. E., & GALLOWAY, D. R. (1990). Purification and Characterization of an Active Fragment of the LasA Protein from Pseudomonas aeruginosa: Enhancement of Elastase Activity. *JOURNAL OF BACTERIOLOGY*, **172**(5), 2236–2240.

PÖHLMANN, C., DIESER, I., & SPRINZL, M. (2014). A lateral flow assay for identification of Escherichia coli by ribosomal RNA hybridisation. *The Analyst*, **139**(5), 1063.

POPE, R. M., APPS, J. M., PAGE, M. D., ALLEN, K., & BODANSKY, H. J. (1993). A novel device for the rapid in-clinic measurement of haemoglobin A1c. *Diabetic Medicine : A Journal of the British Diabetic Association*, **10**(3), 260–263.

POPKOV, M., MAGE, R. G., ALEXANDER, C. B., THUNDIVALAPPIL, S., BARBAS, C. F., & RADER, C. (2003). Rabbit immune repertoires as sources for therapeutic monoclonal antibodies: The impact of kappa allotype-correlated variation in cysteine content on antibody libraries selected by phage display. *Journal of Molecular Biology*, **325**(2), 325–335.

PRINZ, W. A., ÅSLUND, F., HOLMGREN, A., & BECKWITH, J. (1997). The role of the thioredoxin and glutaredoxin pathways in reducing protein disulfide bonds in the Escherichia coli cytoplasm. *Journal of Biological Chemistry*, **272**(25), 15661–15667.

PRITT, B., O'BRIEN, L., & WINN, W. (2007). Mucoid Pseudomonas in cystic fibrosis. *American Journal of Clinical Pathology*, **128**(1), 32–34.

QUINTON, P. M. (2008). Cystic fibrosis: impaired bicarbonate secretion and mucoviscidosis. *The Lancet*, **372**(9636), 415–417.

RAJA, S. (2005). Technology for Automated, Rapid, and Quantitative PCR or Reverse Transcription-PCR Clinical Testing. *Clinical Chemistry*, **51**(5), 882–890.

RAJENDRAN, R., & RAYMAN, G. (2014). Point-of-care blood glucose testing for diabetes care in hospitalized patients: an evidence-based review. *Journal of Diabetes Science and Technology*, **8**(6), 1081–1090.

RAMSEY, B. W., WENTZ, K. R., SMITH, A. L., RICHARDSON, M., WILLIAMS-WARREN, J., HEDGES, D. L., … HARRIS, K. (1991). Predictive value of oropharyngeal cultures for identifying lower airway bacteria in cystic fibrosis patients. *The American Review of Respiratory Disease*, **144**(2), 331–337.

REN, G., KE, N., & BERKMEN, M. (2016). Use of the SHuffle Strains in Production of Proteins. In *Current Protocols in Protein Science* (Vol. 2016, pp. 5.26.1-5.26.21).

RIORDAN, ROMMENS, J., KEREM, B., ALON, N., ROZMAHEL, R., GRZELCZAK, Z., … ET, A. (1989). Identification of the cystic fibrosis gene: cloning and characterization of complementary DNA. *Science*, **245**(4922), 1066–1073.

ROSENFELD, M., EMERSON, J., ACCURSO, F., ARMSTRONG, D., CASTILE, R., GRIMWOOD, K., … WAGENER, J. (1999). Diagnostic accuracy of oropharyngeal cultures in infants and young children with cystic fibrosis. *Pediatric Pulmonology*, **28**(5), 321–328.

RÜDIGER RIDDER, RITA SCHMITZ, F. L. & H. G. (1989). Generation of Rabbit Monoclonal Antibody Fragments from a Combinatorial Phage Display Library and Their Production in the Yeast Pichia pastoris. *Bio/Technology*, **7**(2), 147–153.

RYAN, G., SINGH, M., & DWAN, K. (2011). Inhaled antibiotics for long-term therapy in cystic

fibrosis. *Cochrane Database of Systematic Reviews*, (3), CD001021.

SAJID, M., KAWDE, A. N., & DAUD, M. (2015). Designs, formats and applications of lateral flow assay: A literature review. *Journal of Saudi Chemical Society*, **19**(6), 689–705.

SANDERS, D. B., BITTNER, R. C. L., ROSENFELD, M., HOFFMAN, L. R., REDDING, G. J., & GOSS, C. H. (2010). Failure to Recover to Baseline Pulmonary Function after Cystic Fibrosis Pulmonary Exacerbation. *American Journal of Respiratory and Critical Care Medicine*, **182**(5), 627–632.

SEIDLER, D., GRIFFIN, M., NYMON, A., KOEPPEN, K., & ASHARE, A. (2016). Throat swabs and sputum culture as predictors of P. aeruginosa or S. aureus lung colonization in adult cystic fibrosis patients. *PLoS ONE*, **11**(10), 8–15.

SERRA, R., GRANDE, R., BUTRICO, L., ROSSI, A., SETTIMIO, U. F., CAROLEO, B., … DE FRANCISCIS, S. (2015). Chronic wound infections: The role of Pseudomonas aeruginosa and Staphylococcus aureus. *Expert Review of Anti-Infective Therapy*, **13**(5), 605–613.

SHAND, G. H., PEDERSEN, S. S., BROWN, M. R., & HOIBY, N. (1991). Serum antibodies to Pseudomonas aeruginosa outer-membrane proteins and iron-regulated membrane proteins at different stages of chronic cystic fibrosis lung infection. *J Med Microbiol*, **34**(4), 203–212.

SHEVCHENKO, A., WILM, M., VORM, O., & MANN, M. (1996). Mass Spectrometric Sequencing of Proteins from Silver-Stained Polyacrylamide Gels. *Analytical Chemistry*, **68**(5), 850–858.

SMITH, E. E., BUCKLEY, D. G., WU, Z., SAENPHIMMACHAK, C., HOFFMAN, L. R., D'ARGENIO, D. A., … OLSON, M. V. (2006). Genetic adaptation by Pseudomonas aeruginosa to the airways of cystic fibrosis patients. *Proceedings of the National Academy of Sciences*, **103**(22), 8487–8492.

SMITH, G. P. (1985). Filamentous fusion phage: novel expression vectors that display cloned antigens on the virion surface. *Science (New York, N.Y.)*, **228**(4705), 1315–1317.

SMYTH, A. R., BELL, S. C., BOJCIN, S., BRYON, M., DUFF, A., FLUME, P., … EUROPEAN CYSTIC FIBROSIS SOCIETY. (2014). European Cystic Fibrosis Society Standards of Care: Best Practice guidelines. *Journal of Cystic Fibrosis*, **13**, S23–S42.

SMYTH, A. R., BELL, S. C., BOJCIN, S., BRYON, M., DUFF, A., FLUME, P., … WOLFE, S. (2014). European cystic fibrosis society standards of care: Best practice guidelines. *Journal of Cystic Fibrosis*, **13**(S1), S23–S42.

STAHL, S. J., WATTS, N. R., RADER, C., DIMATTIA, M. A., MAGE, R. G., PALMER, I., … WINGFIELD, P. T. (2010). Generation and Characterization of a Chimeric Rabbit/Human Fab for Co-Crystallization of HIV-1 Rev. *Journal of Molecular Biology*, **397**(3), 697–708.

STUART, B., LIN, J. H., & MOGAYZEL, P. J. (2010). Early Eradication of Pseudomonas aeruginosa in Patients with Cystic Fibrosis. *Paediatric Respiratory Reviews*, **11**(3), 177–184.

SY, A., SRINIVASAN, M., MASCARENHAS, J., LALITHA, P., RAJARAMAN, R., RAVINDRAN, M., … ACHARYA, N. R. (2012). Pseudomonas aeruginosa keratitis: Outcomes and response to corticosteroid treatment. *Investigative Ophthalmology and Visual Science*, **53**(1), 267–272.

TALWALKAR, J. S., & MURRAY, T. S. (2016). The Approach to Pseudomonas aeruginosa in Cystic Fibrosis. *Clinics in Chest Medicine*, **37**(1), 69–81.

TAMURA, Y., SUZUKI, S., KIJIMA, M., TAKAHASHI, T., & NAKAMURA, M. (1992). Effect of proteolytic enzyme on experimental infection of mice with Pseudomonas aeruginosa. *The Journal of Veterinary Medical Science*, **54**(3), 597–599.

TANG, Y., ALI, Z., ZOU, J., JIN, G., ZHU, J., YANG, J., & DAI, J. (2017). Detection methods for Pseudomonas aeruginosa: history and future perspective. *RSC Advances*, **7**(82), 51789–51800.

TANG, Y., ZOU, J., MA, C., ALI, Z., LI, Z., LI, X., … HE, N. (2013). Highly sensitive and rapid detection of pseudomonas aeruginosa based on magnetic enrichment and magnetic separation. *Theranostics*, **3**(2), 85–92.

TRAMPER-STRANDERS, G. A., VAN DER ENT, C. K., SLIEKER, M. G., TERHEGGEN-LAGRO, S. W. J., TEDING VAN BERKHOUT, F., KIMPEN, J. L. L., & WOLFS, T. F. W. (2006). Diagnostic value of serological tests against Pseudomonas aeruginosa in a large cystic fibrosis population. *Thorax*, **61**(8), 689–693.

VALLEJO, L. F., & RINAS, U. (2004). Strategies for the recovery of active proteins through refolding of bacterial inclusion body proteins. *Microbial Cell Factories*, **3**, 1–12.

VAN WEEMEN, B. K., & SCHUURS, A. H. W. M. (1971). Immunoassay using antigen-enzyme conjugates. *FEBS Letters*, **15**(3), 232–236.

VRUBLEVSKAYA, V. V., AFANASYEV, V. N., GRINEVICH, A. A., SKARGA, Y. Y., GLADYSHEV, P. P., IBRAGIMOVA, S. A., … MORENKOV, O. S. (2017). A sensitive and specific lateral flow assay for rapid detection of antibodies against glycoprotein B of Aujeszky's disease virus. *Journal of Virological Methods*, **249**(May), 175–180.

VU, N. X., PRUKSAMETANAN, N., SRILA, W., YUTTAVANICHAKUL, W., TEAMTISONG, K., TEAUMROONG, N., … YAMABHAI, M. (2017). Generation of a rabbit single-chain fragment variable (scFv) antibody for specific detection of Bradyrhizobium sp. DOA9 in both free-living and bacteroid forms. *PLoS ONE*, **12**(6), 1–21.

WEBER, J., PENG, H., & RADER, C. (2017). From rabbit antibody repertoires to rabbit monoclonal antibodies. *Experimental & Molecular Medicine*, **49**(3), e305.

WEST, S. E. H., ZENG, L., LEE, B. L., KOSOROK, M. R., LAXOVA, A., ROCK, M. J., … FARRELL, P. M. (2002). Respiratory Infections With Pseudomonas aeruginosa in Children With Cystic Fibrosis. *Jama*, **287**(22), 2958.

WILDER, C. N., DIGGLE, S. P., & SCHUSTER, M. (2011). Cooperation and cheating in Pseudomonas aeruginosa: The roles of the las, rhl and pqs quorum-sensing systems. *ISME Journal*, **5**(8), 1332–1343.

WONG, R. C., & TSE, H. Y. (2009). *Lateral flow immunoassay*. Springer.

WOO, J. K. K., WEBB, J. S., KIROV, S. M., KJELLEBERG, S., & RICE, S. A. (2012). Biofilm dispersal cells of a cystic fibrosis Pseudomonas aeruginosa isolate exhibit variability in functional traits likely to contribute to persistent infection. *FEMS Immunology and Medical Microbiology*, **66**(2), 251–264.

WORLITZSCH, D., TARRAN, R., ULRICH, M., SCHWAB, U., CEKICI, A., MEYER, K. C., … DöRING, G. (2002). Effects of reduced mucus oxygen concentration in airway *Pseudomonas infections* of cystic fibrosis patients. *The Journal of Clinical Investigation*, **109**(3), 317–325.

WRETLIND, B., & PAVLOVSKIS, O. R. (1983). Pseudomonas aeruginosa elastase and its role in pseudomonas infections. *Reviews of Infectious Diseases*, **5 Suppl 5**(December), S998-1004.

XU, C., ZHANG, C., ZHONG, J., HU, H., LUO, S., LIU, X., … LIU, X. (2017). Construction of an Immunized Rabbit Phage Display Library for Selecting High Activity against Bacillus thuringiensis

Cry1F Toxin Single-Chain Antibodies. *Journal of Agricultural and Food Chemistry*, **65**(29), 6016–6022.

YANG, H., ZHONG, Y., WANG, J., ZHANG, Q., LI, X., LING, S., … WANG, R. (2018). Screening of a ScFv antibody with high affinity for application in human IFN-γ immunoassay. *Frontiers in Microbiology*, **9**(MAR), 1–9.

YANG, J., ZHAO, H. L., RAN, L. Y., LI, C. Y., ZHANG, X. Y., SU, H. N., … ZHANG, Y. Z. (2015). Mechanistic Insights into Elastin Degradation by Pseudolysin, the Major Virulence Factor of the Opportunistic Pathogen Pseudomonas aeruginosa. *Scientific Reports*, **5**, 1–7.

YOON, S. S., HENNIGAN, R. F., HILLIARD, G. M., OCHSNER, U. A., PARVATIYAR, K., KAMANI, M. C., … HASSETT, D. J. (2002). Pseudomonas aeruginosa anaerobic respiration in biofilms: relationships to cystic fibrosis pathogenesis. *Developmental Cell*, **3**(4), 593–603.

YU, H., HE, X., XIE, W., XIONG, J., SHENG, H., GUO, S., … ZHANG, K. (2014). Elastase LasB of Pseudomonas aeruginosa promotes biofilm formation partly through rhamnolipid-mediated regulation. *Canadian Journal of Microbiology*, **60**(4), 227–235.

ZAREI, M. (2018). Infectious Pathogens Meet Point-of-Care Diagnostics. *Biosensors and Bioelectronics*, **106**(February), 193–203.

ZHUANG, X., WATTS, N. R., PALMER, I. W., KAUFMAN, J. D., DEARBORN, A. D., TRENBEATH, J. L., … WINGFIELD, P. T. (2017). Chimeric rabbit/human Fab antibodies against the hepatitis Be-antigen and their potential applications in assays, characterization, and therapy. *Journal of Biological Chemistry*, **292**(40), 16760–16772.

Appendix

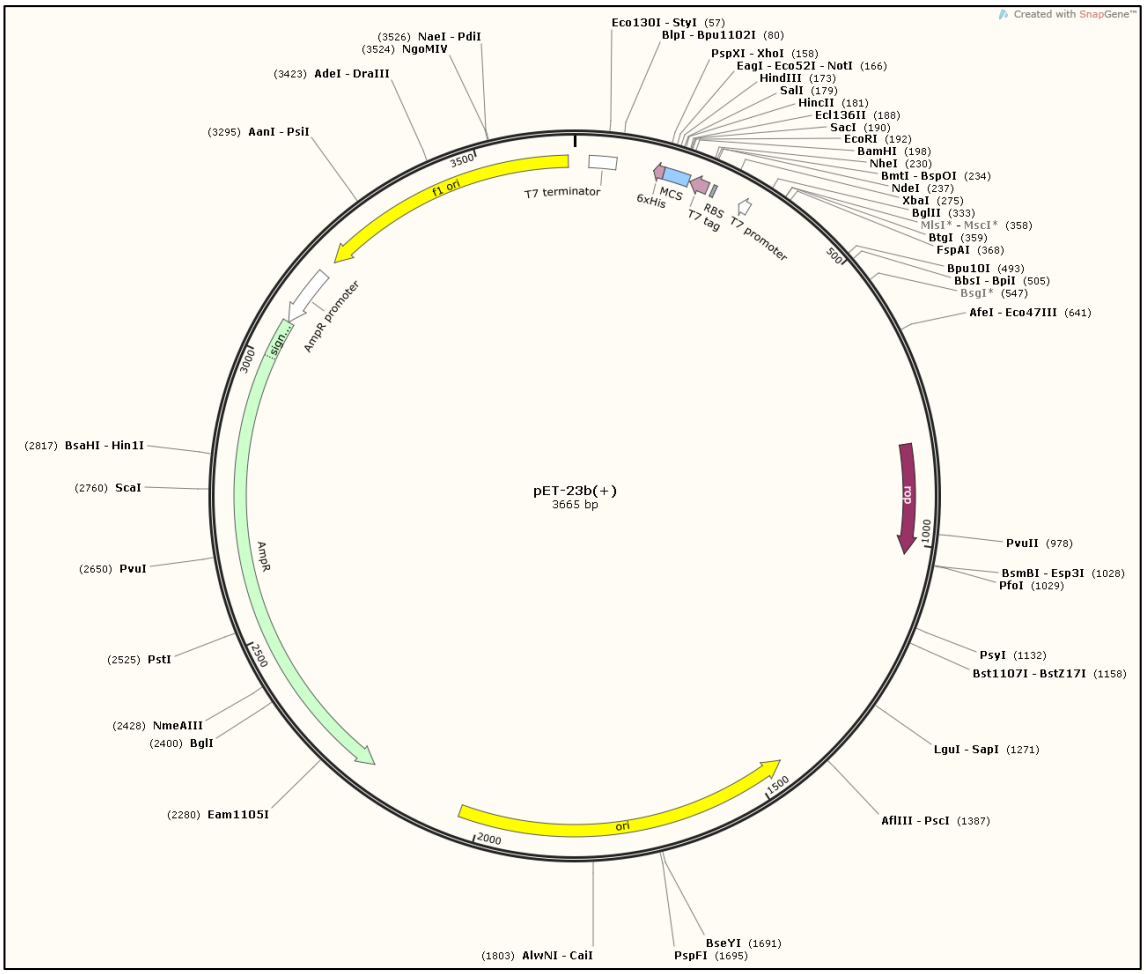

Appendix Figure I | Schematic showing the vector map for the commercially available cloning vector pET 23b (+) (Novagen, Catalogue No.: 69746-3)

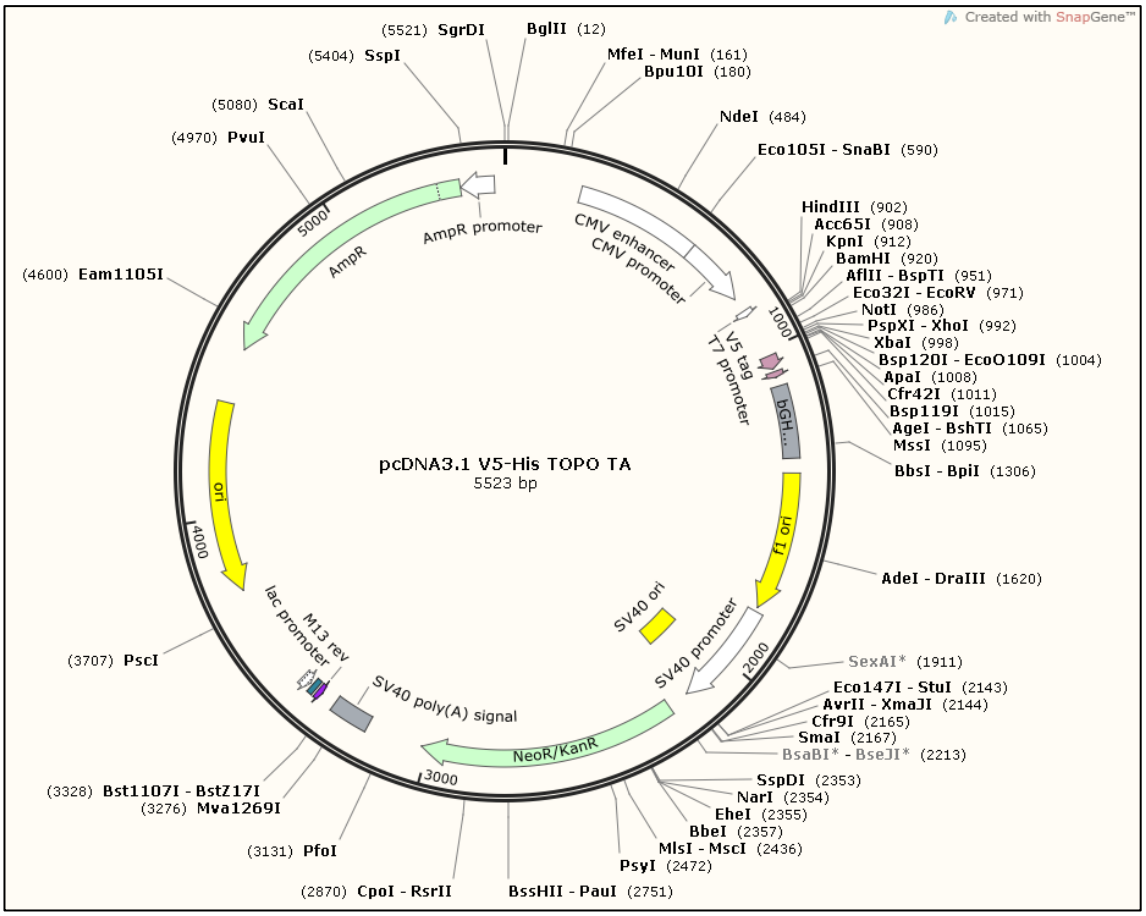

Appendix Figure II | Schematic showing the vector map for the commercially available cloning vector pcDNA™ 3.1/V5-His TOPO® TA (Thermo Scientific™, Catalogue no.: K480040)

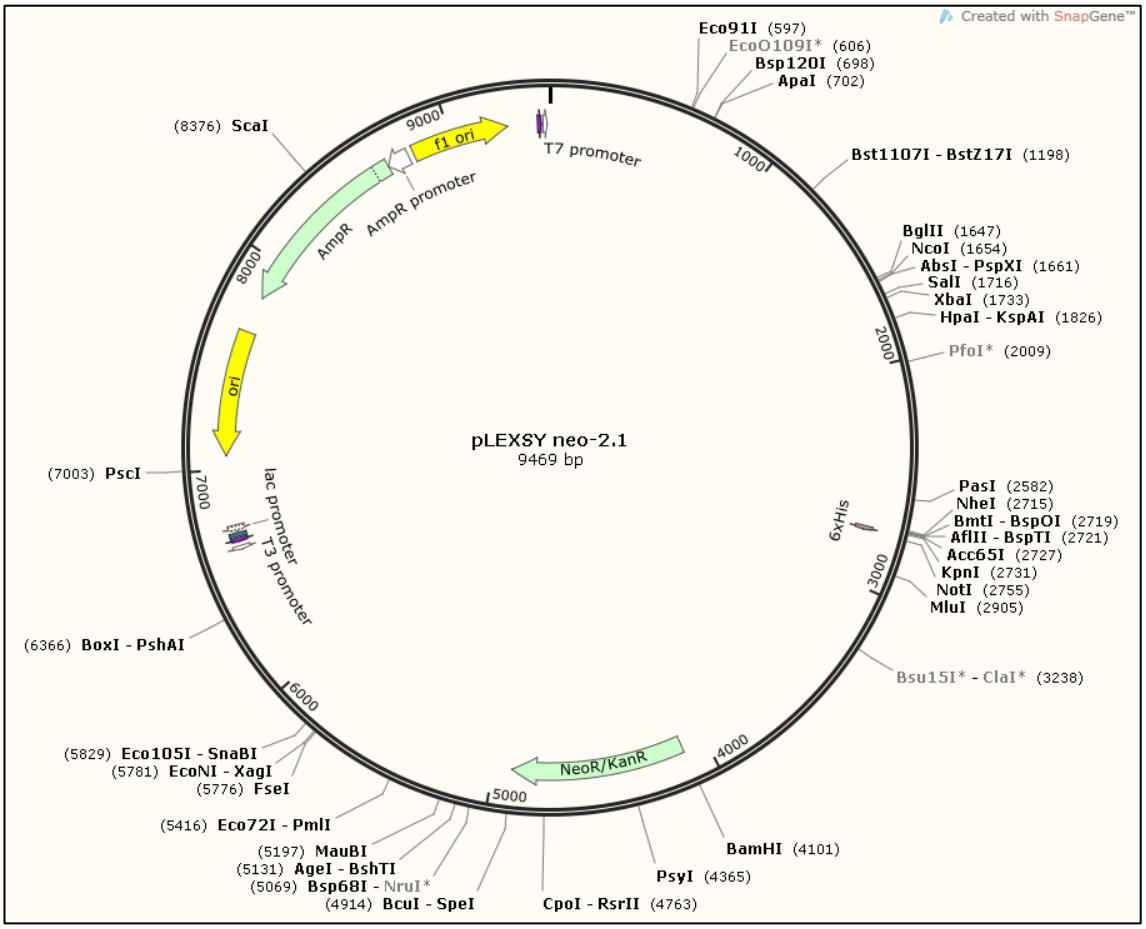

Appendix Figure III | Schematic showing the vector map for the commercially available cloning vector pLEXSY-neo 2.1 (Jena Bioscience, Catalogue no.: EGE-233). The pLEXSY-neo 2.0 vector is no longer commercially available at the time of writing.